

Taxonomic and Functional Analyses of Marine Microbial Polysaccharide Utilisation

Dissertation
zur Erlangung eines Doktor der Naturwissenschaften
-Dr. rer. nat. –

Dem Fachbereich 2 Biologie / Chemie der
Universität Bremen
vorgelegt von

Greta Reintjes

Bremen, April 2017

Die vorliegende Doktorarbeit wurde in der Zeit von August 2013 bis April 2017 im Rahmen des Programms „International Max Planck Research School of Marine Microbiology, MarMic“ in der Abteilung Molekulare Ökologie am Max-Planck-Institute für Marine Mikrobiologie in Bremen angefertigt.

Gutachter: Prof. Dr. Rudolf Amann

Gutachter: Prof. Dr. Carol Arnosti

Tag des Promotionskollegium: 28 April 2017

„ If you can't explain it simply, you don't understand it well enough “
A. Einstein

Summary

Marine primary production accounts for half of the Earth's carbon fixation and therefore has a significant impact on the global carbon cycle. However, although marine primary producers fix such a significant fraction of carbon, their biomass makes up only a small fraction of the total organic carbon pool. This is due to the extremely high turnover of phytoplankton and phytoplankton-derived organic matter within the oceans. This turnover is mediated by marine heterotrophic microorganisms (*Bacteria* and *Archaea*). Marine microorganisms therefore significantly affect the global carbon cycle.

The objectives of this thesis were to investigate how the taxonomic and functional diversity of marine microorganisms affects the bacterially mediated carbon turnover in the Atlantic Ocean.

In chapter 1 and 2 I developed methods which enable a shipboard high-throughput analysis of microbial diversity and abundance. These methods were developed to overcome the time delay between sampling and results and enable a comprehensive interpretation of the microbial community composition even in remote sampling sites. In chapter 3 I explored the biogeographical distribution patterns of the free-living (FL) and particle-associated (PA) bacterial communities across different provinces of the Atlantic Ocean. The FL and PA bacterial community compositions were more similar under copiotrophic condition and more dissimilar under oligotrophic conditions. I could associate these results to the relative age of the available particles as well as the availability of organic matter.

In Chapter 4 I investigated alternative substrate uptake mechanisms in marine bacteria. Using fluorescently labelled polysaccharides (FLA-PS) and super-resolution structured illumination microscopy I could show that a significant fraction of marine bacteria use a “selfish” substrate utilisation mechanism. I combined this analysis with fluorescence in situ hybridization (FISH) to taxonomically identify the organisms as belonging to the *Bacteroidetes*, *Planctomycetes* and *Gammaproteobacteria*. The discovery of a widespread alternative substrate utilisation mechanism significantly affects our global estimates of carbon turnover by marine bacteria.

Finally, in Chapter 5 I investigated the extracellular hydrolysis rates and bacterial community dynamics within fluorescently labelled polysaccharide incubations. These analyses lead to the identification of the dominant microorganisms associated with the hydrolysis of polysaccharides in the marine environment.

The work done in this thesis has furthered our understanding of the activity and distribution patterns of bacterial polysaccharide utilisation mechanisms across the Atlantic Ocean. Additionally, the activity of the individual mechanisms could be associated with specific microbial groups, thereby linking the taxonomy and function of the dominant marine polysaccharide degrading organisms. This study will enable us

Zusammenfassung

to make better predictions of the impact which marine microorganisms have on global biogeochemical cycles.

Zusammenfassung

Die marine Primärproduktion macht die Hälfte der Kohlenstoff-Fixierung der Erde aus und hat daher einen erheblichen Einfluss auf den globalen Kohlenstoffkreislauf. Obwohl marine Primärproduzenten einen signifikanten Anteil an Kohlenstoff fixieren, ergibt ihre Biomasse nur einen Bruchteil des gesamten organischen Kohlenstoff-Pools aus. Dies ist auf den extrem hohen Umsatz von Phytoplankton und Phytoplankton-abgeleiteten organischen Stoffen innerhalb der Ozeane zurückzuführen. Der Abbau geschieht durch marine heterotrophe Mikroorganismen (*Bacteria* und *Archaea*). Marine Mikroorganismen beeinflussen daher den globalen Kohlenstoffkreislauf sehr stark.

Ziel dieser Arbeit war es, zu untersuchen, wie sich die taxonomische und funktionelle Vielfalt mariner Mikroorganismen auf den bakteriellen Kohlenstoffumsatz im Atlantik auswirkt.

In Kapitel 1 und 2 sind die zwei in Rahmen meiner Promotion neuentwickelten Methoden beschrieben, mit denen an Bord eines Forschungsschiffes die Analyse der mikrobiellen Vielfalt deutlich beschleunigt wurde. Diese Methoden wurden entwickelt, um die zeitliche Verzögerung zwischen der Probenentnahme und dem Vorliegen erster Zellzählungen bzw. erster Sequenzdaten so zu verkürzen, dass schon an Bord eine umfassende Interpretation der mikrobiellen Gemeinschaftszusammensetzung möglich ist.

Kapitel 3 befasst sich mit den biogeographischen Verteilungsmustern der freilebender (FL) und Partikelassoziiierter (PA) Bakteriengemeinschaften in verschiedenen Provinzen des Atlantischen Ozeans. Die Zusammensetzung der FL- und PA-Bakteriengemeinschaft waren sich ähnlicher unter nährstoffreichen Bedingungen und sie waren unterschiedlicher bei Nährstoffarmut. Ich konnte diese Ergebnisse dem relativen Alter der verfügbaren Partikel und somit der Verfügbarkeit von organischen Stoffen zuordnen.

In Kapitel 4 untersuchte ich alternative Substrataufnahmemechanismen von marinen Bakterien. Mit fluoreszenzmarkierten Polysacchariden (FLA-PS) konnte ich zeigen, dass ein signifikanter Anteil der marinen Bakterien eine "egoistische" Strategie der Substrataufnahme verwenden. Durch eine Kombination dieser Analyse mit der Fluoreszenz-in-situ-Hybridisierung (FISH) konnten die entsprechenden Mikroorganismen positiv als *Bacteroidetes*, *Planctomycetes* und *Gammaproteobacteria* identifiziert werden. Die Entdeckung dieses alternativen Mechanismus der Polysaccharidverwertung hat weitreichende Auswirkungen für das Verständnis der Rolle der marinen Bakterien im globalen Kohlenstoffkreislauf.

In Kapitel 5 werden extrazelluläre Hydrolyse-Raten von fluoreszenzmarkierten Polysacchariden in Inkubationsversuchen mit Veränderungen in der Bakteriengemeinschaftsdynamik korreliert. Diese Analyse führte zur Identifizierung der dominanten Mikroorganismen, die mit der extrazellulären Hydrolyse von Polysacchariden in diesen Inkubationen verbunden sind.

Zusammenfassung

Diese Doktorarbeit trägt damit dazu bei, die Aktivitäten von marinen Mikroorganismen bei der Polysaccharidverwertung und ihre Verteilungsmuster im Atlantischen Ozean besser zu verstehen. Zusätzlich konnten der bekannte, auf Exoenzyme beruhende Mechanismus und der alternative „egoistische“ Mechanismus mit spezifischen mikrobiellen Gruppen assoziiert werden. Die vorliegende Doktorarbeit trägt damit dazu bei, die Rolle mariner Mikroorganismen im globalen Kohlenstoffkreislauf besser zu verstehen.

Table of Contents

Summary	4
Zusammenfassung.....	6
Table of Contents	9
INTRODUCTION	12
The Global Carbon Cycle.....	12
The Marine Carbon Cycle	13
Marine Microorganisms – Primary Producers	15
Marine Microorganisms – Heterotrophs	17
Phytoplankton Derived Organic Matter	19
Bacterial Polysaccharide Turnover.....	20
Aims	21
Objectives of this Thesis	22
Contribution to Manuscripts and Further Publications	24
CHAPTER 1.....	27
Modification of a High- Throughput Automatic Microbial Cell Enumeration System for Shipboard Analyses	29
CHAPTER 2.....	39
On-site microbial diversity and abundance analysis in the remotest part of the world's oceans, the South Pacific Gyre	41
CHAPTER 3.....	67
Free-living and particle-associated bacteria exist as an interactive assemblage.....	69
CHAPTER 4.....	87
An alternative polysaccharide uptake mechanism of marine bacteria	89
CHAPTER 5.....	101
Tracking bacterial community dynamics in polysaccharide incubations along an Atlantic Meridional Transect.....	103
GENERAL DISCUSSION	125

Acknowledgements	136
APPENDIX	137
Appendix Figures and Table for Chapter 1	138
Appendix Figures and Table for Chapter 2	156
Appendix Figures and Table for Chapter 3	170
Appendix Figures and Table for Chapter 4	174
Appendix Figures and Table for Chapter 5	190
REFERENCES.....	195

Abbreviations

ANOSIM – analysis of similarity	OT2 – one touch 2
CARD–FISH – Catalysed reporter deposition fluorescence <i>in situ</i> hybridisation	PA – particle associated
CAZymes – carbohydrates active enzymes	PCR – polymerase chain reaction
CTD – conductivity temperature depth	PGM – personal genome machine
CV – coefficients of variance	POC – particulate organic carbon
DAPI – 4', 6-diamidino-2- phenylindole	QEDF – quick stack with extended depth of focus
DCM – deep chlorophyll maximum	RDOM – recalcitrant dissolved organic matter
DIC – dissolved inorganic carbon	RT – room temperature
dNTP's – deoxyribose nucleotides triphosphates	SDS – sodium dodecyl sulphate
DOM – dissolved organic matter	SPG – South Pacific Gyre
DOC – dissolved organic carbon	SR-SIM – super resolution structured illumination microscopy
EDF – extended depth of focus	S. Gyre – Southern Gyre
ES – enrichment system	S. Gyre (S) – Southern Gyre (south)
FISH – fluorescence <i>in situ</i> hybridisation	S. Gyre (N) – Southern Gyre (north)
FL –free living	S. Temperate – Southern Temperate
FLA – fluoresceinamine	TCC – total cell counts
FLA-PS – fluorescently labelled polysaccharide	
FOV – field of view	
FQEDF – fast quick stack with extended depth of focus	
HMW – high molecular weight	
ISP – ion sphere particles	
LED – light emitting diode	
LMW – low molecular weight	
NGS – next generation sequencing	
NMDS – non-metric multidimensional scaling	
N. Temperate – Northern Temperate	
N. Gyre – Northern Gyre	
OMZ – oxygen minimum zone	
OTU – operational taxonomic unit	

Introduction

The Global Carbon Cycle

The carbon cycle is one of Earth's most important elemental cycles because carbon is a fundamental molecule which supports all known life on Earth. The carbon cycle describes the sources, sinks, and fluxes (movement) of carbon between its different reservoirs: the oceans, the atmosphere, the terrestrial biosphere (land plants, animals and soils) and the lithosphere (rocks) (Ciais et al 2013). We study the cycling (turnover) of carbon between its reservoirs because the amount of atmospheric carbon affects our climate and therefore our way of life (Falkowski et al 2000).

The turnover of carbon is the time it takes for a carbon atom, for example in an atmospheric CO₂ molecule, to go from being fixed into organic carbon by a plant, to being respired back into CO₂ and returned to the atmosphere. The turnover times between reservoirs vary significantly which results in some reservoirs absorbing and effectively storing large amounts of inactive carbon for long period of time (Ciais et al 2013). This prevents the carbon from getting back into the atmosphere and affecting surface temperatures. For example, although the lithosphere (rocks) holds by far the largest reservoir of carbon (75×10^5 Gt C, $1 \text{ Gt} = 10^{15} \text{ g}$) it is relatively inactive, with turnover times ranging from 10,000 years to longer and carbon fluxes coming only from the weathering of rocks and volcanic eruptions (Ciais et al 2013). In the short-term, it therefore has little to no effect on our current climate. Comparatively the oceans affect the Earth's climate directly because they have quick turnover times and continuously interact with the atmosphere (Raven and Falkowski 1999, Sarmiento and Le Quéré 1996, Volk and Hoffert 1985). Understanding the marine carbon cycle is therefore important as it directly affects our climate.

The Marine Carbon Cycle

The oceans are the Earth's second largest carbon reservoir (38×10^3 Gt C) and their carbon pools (dissolved inorganic carbon (DIC), dissolved organic carbon (DOC) and particulate organic matter (POC)) have turnover times ranging from days to thousands of years (Ciais et al 2013). There are two main processes that influence the flux of carbon from the atmosphere into the oceans; the physical carbon pump and the biological carbon pump (Figure 2) (Legendre et al 2015, Luca et al 2016, Raven and Falkowski 1999, Sarmiento and Le Quéré 1996, Volk and Hoffert 1985). Through the physical carbon pump, CO_2 is continuously exchanged between the atmosphere and the oceans (Figure 1) (Raven and Falkowski 1999). This exchange is a physico-chemical process which is driven by the difference in partial pressure of CO_2 in air and water.

Carbon dioxide from the atmosphere dissolves into the surface oceans and immediately reacts with the water molecules to form carbonic acid, bicarbonate and carbonate ions which are collectively known as dissolved inorganic carbon (DIC) (Figure 1) (Legendre et al 2015, Raven and Falkowski 1999). DIC is the largest pool of carbon in the oceans (37×10^3 Gt C, 97% of total carbon) (Ciais et al 2013). The dissolution of atmospheric CO_2 into the surface oceans is highly dependent on temperature because CO_2 is more soluble in colder waters. The increased solubility in colder waters coupled with the ocean thermohaline circulation, which is the sinking of cold dense surface waters to form deep waters, causes a significant fraction of DIC to be stored in the deep ocean (Broecker 1997, Wunsch 2002). This CO_2 is stored in the oceans because oceanic deep water flows through the ocean basins and can have a transit time of up to 1000 years, during which it has no contact with the atmosphere and therefore no exchange occurs (Maier-Reimer and Hasselmann 1987, Sabine et al 2004).

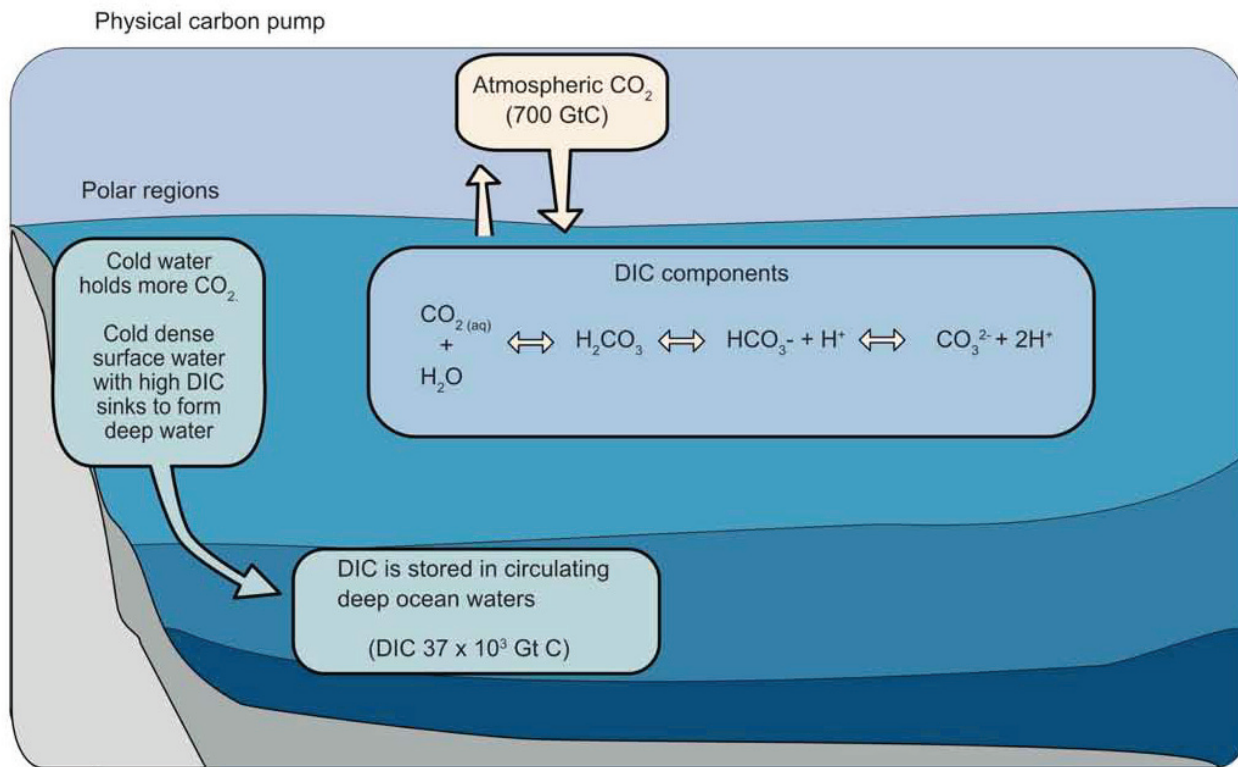


Figure 1 The physical carbon pump. Atmospheric CO₂ dissolves into the water column and interacts with the water molecules to form carbonic acid (H₂CO₃), bicarbonate (HCO₃⁻) and carbonate (CO₃²⁻). These are collectively termed DIC and make up a significant fraction of the oceanic carbon. The dissolution of atmospheric CO₂ is higher in colder water (polar regions). Cold dense water, that is high in DIC, sinks to the deep oceans due to the ocean's thermohaline circulation system. This causes the transport of carbon into the deep oceans where it is stored for up to 1000 of years.

The biological carbon pump is the oceans biologically driven sequestration of carbon from the atmosphere to the deep sea (Figure 2) (reviewed by Turner (2015)). It predominantly occurs in the surface oceans where primary producers fix carbon dioxide (45 - 55 Gt C y⁻¹) through photosynthesis to form DOC and POC (which here includes both living and dead material) (Behrenfeld and Falkowski 1997, Falkowski et al 2000, Field et al 1998, Finkel 2014, Thornton 2014, Westberry et al 2008). Although a large part of the produced POC and DOC is quickly remineralised to CO₂ by marine microorganisms, a small fraction is stored within the oceans for thousands to millions of years. This occurs through the physical sinking of POC into deeper waters (~0.6 – 2.4% of the annually primary production) (Legendre et al 2015, Luca et al 2016, Turner 2015) and from the remineralisation of DOC by marine microorganisms into recalcitrant DOC (RDOC) (~0.5 - 0.6% of the annual primary production) (Jiao et al 2010, Legendre et al 2015). The production of RDOC by

General Introduction

microorganisms is referred to as the microbial carbon pump (Jiao et al 2010, Jiao and Zheng 2011). RDOC is resistant to further degradation and can persist in the oceans for thousands of years (Anderson et al 2015, Osterholz et al 2015).

Although the biological carbon pump contributes yearly to only a small fraction of the stored carbon (~1.1 to 3% of the annual primary production), it plays a significant role in keeping surface DIC concentrations low and allows for the flux of carbon dioxide into the oceans from the atmosphere (Legendre et al 2015). Together the physical and biological carbon pump maintain a vertical gradient of DIC between the surface oceans and deeper water layers and thereby regulate the movement of CO₂ from the atmosphere into the oceans. This has a significant impact on the global carbon cycle and global climate as it reduces the amount of CO₂ in the atmosphere (Ciais et al 2014).

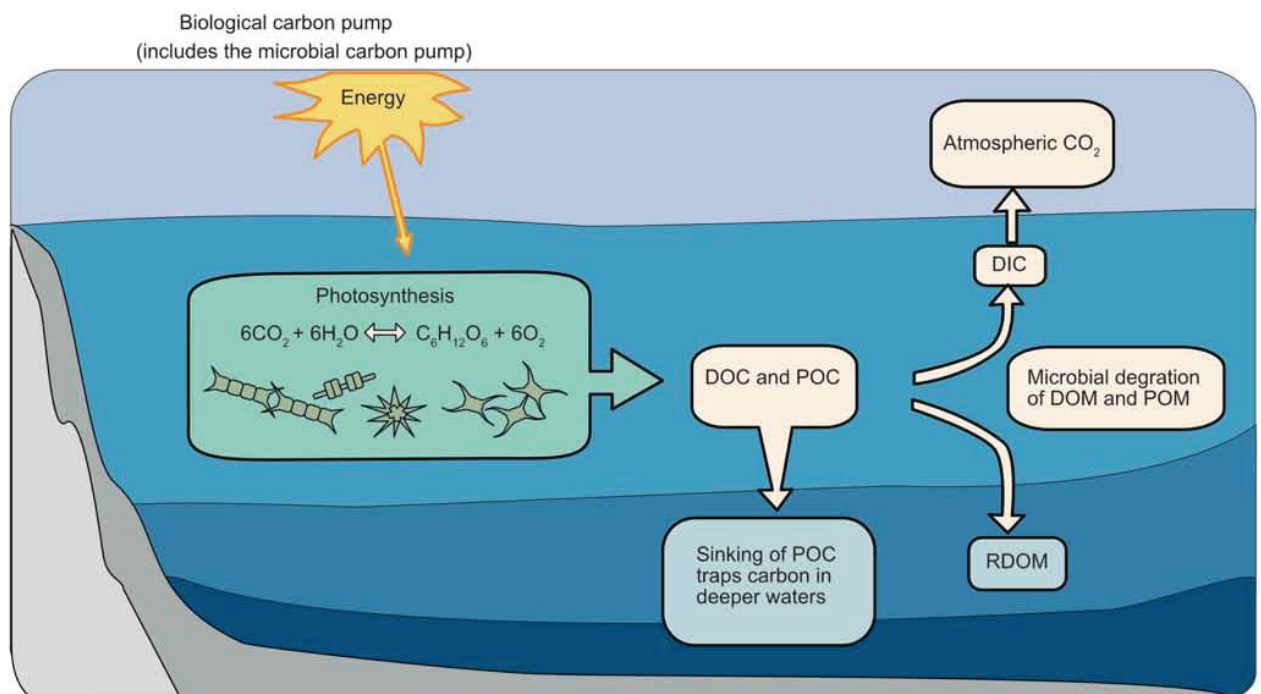


Figure 2 The biological carbon pump refers to the fixation of dissolved inorganic carbon by marine phytoplankton in the surface oceans and the export of the fixed organic material to deeper waters via physical sinking. Additionally, it refers to the remineralisation and transformation of some of the fixed organic matter by marine microorganism into recalcitrant dissolved organic matter (RDOM) via the microbial carbon pump. RDOM is resistant to further degradation and therefore stored in the oceans.

Marine Microorganisms – Primary Producers

Microorganisms are the main constituents of the marine ecosystem both in cellular abundance and biomass (Ciais et al 2013, Whitman et al 1998). They are the dominant

autotrophs (primary producers) and heterotrophs (consumers). Marine microorganisms are generally very small, ranging in size from $0.4\ \mu\text{m}^2$ (picoplankton) to $200\ \mu\text{m}^2$ (microplankton) but are extremely abundant (10^6 cells ml^{-1} seawater) (Levin and Angert 2015, Whitman et al 1998). Due to their small size, they have a high surface to volume ratio, which makes them metabolically very active (Ducklow 1999, Robinson and Williams 2007). Their high abundance and activity drive the biological carbon pump and therefore they directly affect the global carbon cycle (Azam and Malfatti 2007).

Phytoplankton is the collective term used to describe marine primary producers, including phototrophic prokaryotes and phototrophic eukaryotes. Primary producers fix carbon dioxide by using energy from the sun (photolithotrophic) or reduced inorganic compounds (chemolithotrophic). This energy is used to synthesize simple organic molecules from DIC (Figure 2). These simple organic compounds can then be used to synthesize more complex cellular material such as lipids, amino acids, proteins and carbohydrates that often contain other nutrients such as nitrogen, phosphate, sulfur and iron.

The estimated $45 - 55\ \text{Gt C y}^{-1}$ fixed by phytoplankton accounts for about half of the Earth's primary production (Azam and Malfatti 2007, Falkowski et al 2000, Field et al 1998, Finkel 2014, Sarmiento and Gasol 2012, Westberry et al 2008). Phytoplankton make this fixed material available to the marine food web through several processes. Firstly, through the “standard” food web whereby phytoplankton biomass is consumed by primary consumers (zooplankton) which in turn can be consumed by secondary consumers (fish) and thereby the material travels up through the food web (Pomeroy 1974). Alternatively, phytoplankton also actively transport between 10 – 50% of the produced organic matter out of their cells as dissolved organic matter (DOM) (Biddanda and Benner 1997, Teira et al 2001, Teira et al 2003, Thornton 2014). DOM is nearly exclusively available to marine heterotrophic microorganisms and therefore the fate of up to half of the phytoplankton-derived organic matter or a quarter of the global primary production is controlled by marine microorganisms.

Global marine primary production is highly heterogeneous, with large areas of low production and smaller areas of high production (Figure 3). This heterogeneity is due to changes in physico-chemical conditions which regulate and limit phytoplankton growth. These include irradiance (availability of sunlight for energy), temperature and the availability and concentration of essential inorganic nutrients (such as Fe, P, N) (Geider et al 1997, Howarth 1988, Marañón et al 2000, Pedersen and Borum 1996, Raven et al 1999). Limitations in any of these factors restrict primary production and thereby the flux of carbon into the oceans through the biological carbon pump.

The main reason for the high heterogeneity is because vast expanses of surface oceans are oligotrophic, meaning they have very low concentrations of essential nutrients (Fe, P, N) (Morel et al 2007, Polovina et al 2008, Raimbault et al 2008, Smith 1984). The small areas of high primary production are predominantly in coastal regions (Figure 3) where the mixing of water masses or the upwelling of nutrient-rich bottom waters causes pronounced increases in the availability of essential nutrients (Cloern 1996,

General Introduction

Ishizaka et al 1983, Sambrotto et al 1986, Van Dongen-Vogels et al 2012). This results in an increase in primary production and can cause so-called “phytoplankton blooms” (provided irradiance is high). Phytoplankton blooms result in the fixation of a significant amount of carbon dioxide into organic matter thereby driving the biological carbon pump.

Though phytoplankton fix a significant fraction of carbon dioxide, their biomass represents only a small fraction of the total organic carbon pool in the oceans (3 Gt C of a total of ~700 Gt C) (Ciais et al 2013). This uncoupling between carbon fixation and total biomass is due to the extremely high turnover rates of phytoplankton and their derived material in the oceans (Arnosti et al 2011, Kirchman et al 2001, Moran et al 2016, Piontek et al 2010, Piontek et al 2011).

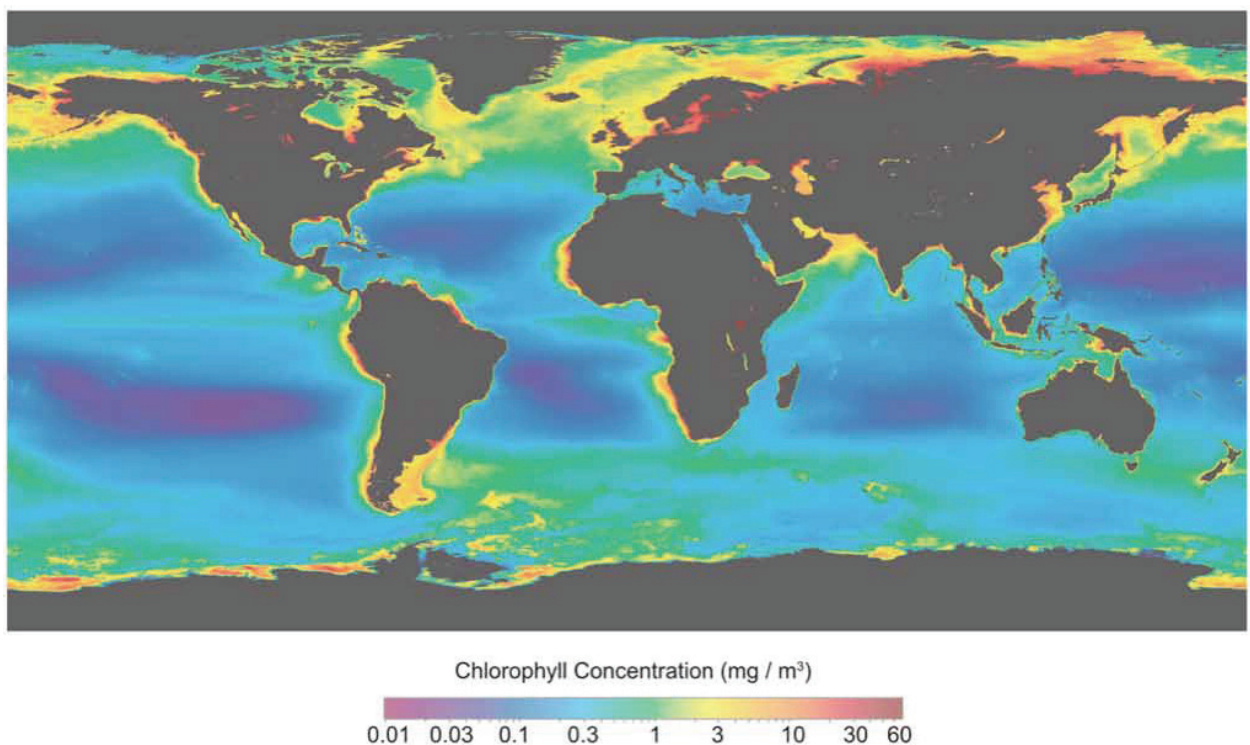


Figure 3 Map showing averaged global chlorophyll a concentrations (primary production) from 04.04.2002-31.10.2015 obtained from MODIS aqua ocean colour data using the algorithm OCI (Ocean Biology Processing Group 2014). The chlorophyll a concentration shows the heterogeneity of global primary production with high concentrations in coastal regions and large areas of low chlorophyll a in open ocean provinces.

Marine Microorganisms – Heterotrophs

Marine heterotrophic microorganisms (*Bacteria* and *Archaea*) turnover between 75 - 95% of the phytoplankton-derived organic matter within days to weeks of its production (Cho and Azam 1988, Moran et al 2016, Piontek et al 2011, Piontek et al

General Introduction

2014). This has a significant effect on the marine carbon cycle because a large part of the fixed carbon is directly respired to CO_2 . However, the remineralisation of DOM does not just influence the carbon cycle but also other biogeochemical cycles because DOM contains many essential nutrients (P, N, Fe) (Moran et al 2016). The remineralisation of DOM releases these nutrients and makes them available to higher levels of the marine food web. This is especially important in the oligotrophic gyres (see above) where phytoplankton growth is limited due to a lack of essential nutrients. In these areas, primary production is dictated by the biological supply of nutrients from the remineralisation of DOM by heterotrophic microorganisms (Letscher et al 2015, Moran et al 2016). The active role heterotrophic microorganisms play in the cycling of DOM is called the microbial loop (Azam et al 1983, Azam 1998) (Figure 4).

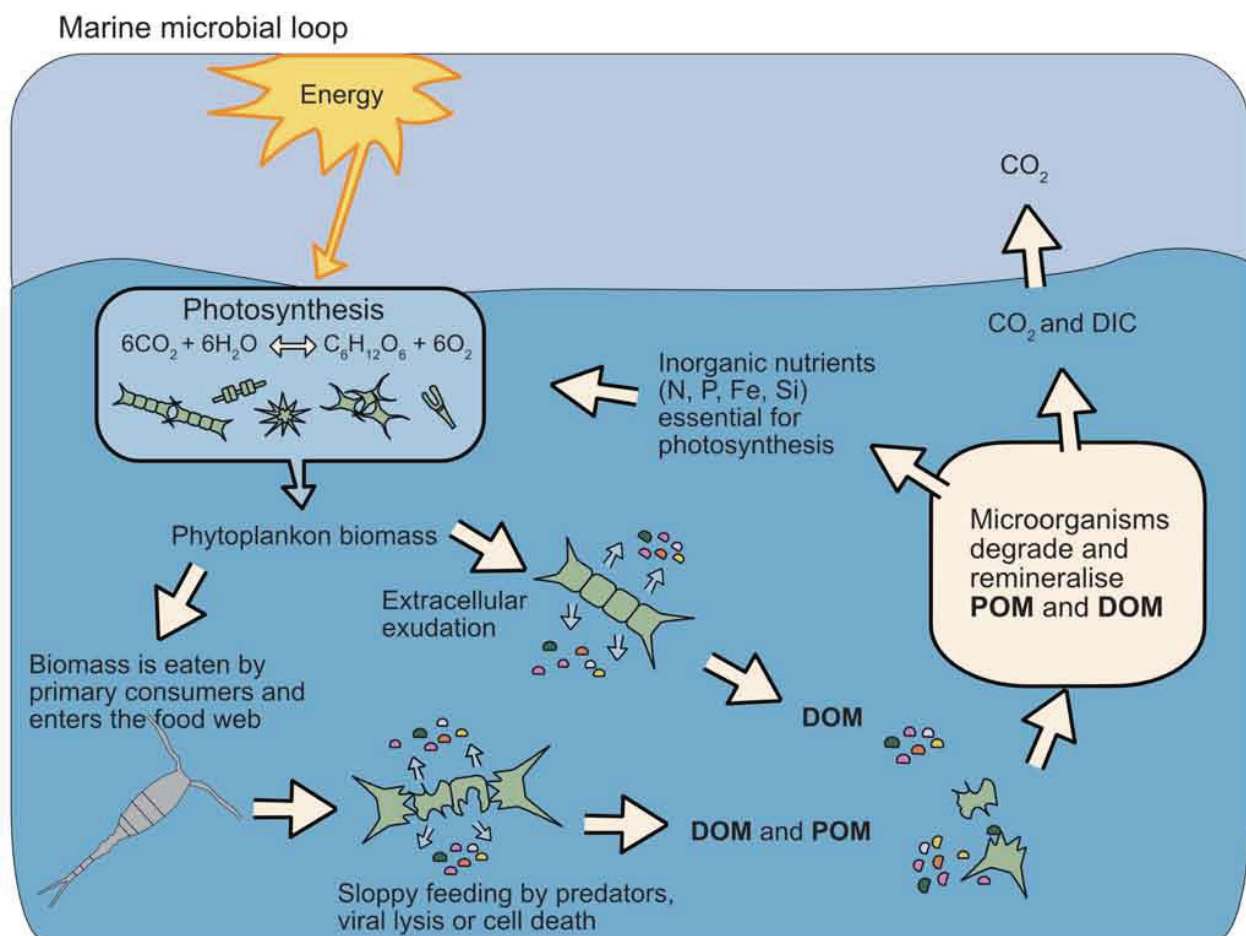


Figure 4 The microbial loop is a representation of the microbially mediated turnover of dissolved organic matter (DOM) and particulate organic matter (POM) in the marine environment. Carbon dioxide is fixed by phytoplankton in the surface oceans. The fixed organic matter is available as dissolved organic matter (DOM) to marine microorganisms and particulate organic matter (POM) to marine microorganisms and marine consumers such as zooplankton. Phytoplankton biomass enters the marine food web via the consumption by marine zooplankton. Additionally, the sloppy grazing of biomass by

consumers, viral lysis and cell death of phytoplankton releases POM and DOM. DOM and POM are degraded and remineralised by marine microorganisms making essential nutrients available for primary production.

Although microorganisms play such an important role in the recycling of organic matter in the marine environment we know relatively little about the processes which they use to do this. This is due primarily to our lack of understanding of how the taxonomic and functional diversity of microorganisms affects carbon turnover in the marine and other ecosystems.

Marine microorganisms are not just highly abundant they are also taxonomically and functionally diverse (Giovannoni and Stingl 2005, Quince et al 2008, Rusch et al 2007, Sunagawa et al 2015, Zinger et al 2011). They exhibit distinct patterns in their distribution as they are selected for by specific environmental conditions (Baldwin et al 2005, Green et al 2008, Hanson et al 2012, Martiny et al 2006, Yilmaz et al 2012). Understanding the individual distribution patterns of microorganisms is important because they have significant impacts on their environment. The focus of this thesis was on the heterotrophic bacteria, which are selected for by phytoplankton-derived organic matter (specifically polysaccharides) and what mechanisms these bacteria use to remineralise organic matter.

Phytoplankton Derived Organic Matter

When conditions are optimal (light, nutrients, temperature) phytoplankton form blooms and produce a high amount of organic matter. As this organic matter becomes available to the microbial community distinct changes in the community composition occur. Specific bacterial groups (for example *Bacteroidetes*, *Gammaproteobacteria*, *Roseobacter*) increase in abundance and other bacterial groups (for example SAR11 and SAR86) decrease in abundance (McCarren et al 2010, Teeling et al 2016). These changes have been repeatedly observed throughout the world's oceans and they occur both on a taxonomic and functional level (Bunse and Pinhassi 2016, Rinta-Kanto et al 2012, Rooney-Varga et al 2005, Sarmiento and Gasol 2012, Sison-Mangus et al 2016, Teeling et al 2012, Wemheuer et al 2015). To fully understand the changes in the bacterial community composition and the role which heterotrophic bacteria play in the turnover of organic matter, we must understand the organic matter itself.

Marine organic matter is broadly classified into three major types, dependent on its residence time within the ocean (Follett et al 2014, Hansell and Carlson 1998, Hansell 2013). Firstly, labile DOM consists of molecules produced by phytoplankton and remineralised within hours to days of their production. Secondly, semi-labile DOM is also produced by phytoplankton but consists of less reactive molecules that can persist in the surface oceans from weeks to years. Finally, refractory DOM (also called recalcitrant - DOM) is produced through photochemical reactions and the metabolic

activity of microorganisms (microbial carbon pump) (Amado et al 2015, Jiao et al 2010, Jiao and Zheng 2011, Osterholz et al 2015). It has the longest residence time, circulating through the major oceanic basins for thousands of years and is therefore the least biologically reactive. All three forms of DOM exist throughout the oceans, although most of the labile and semi-labile DOM is present in a high abundance in the surface oceans as it is produced by phytoplankton. These two type of DOM are of interest in the study of the marine carbon cycle because of their high turnover rates (Legendre et al 2015).

Although current methodological limitations do not allow a full characterisation of the composition of individual constituents of DOM, we do know that it is predominantly produced by marine phytoplankton. Therefore, it must be similar in composition to phytoplankton biomass (25 - 50% proteins, 5 - 50% polysaccharides, 5 - 20% lipids, 3 - 20% pigments, and up to 20% nucleic acids) (Emerson and Hedges 2008).

Further hints of its composition are obtained from bulk seawater analyses which indicate that polysaccharides (> 1000 Da) are a dominant fraction of DOM (Benner et al 1992). Similar results have been obtained from analyses of phytoplankton exudates, which can be comprised of 80 - 90% high molecular weight (HMW) carbohydrates, specifically polysaccharides (Abdullahi et al 2006, Aluwihare and Repeta 1999, Biddanda and Benner 1997, Biersmith and Benner 1998, Myklestad 1995). Polysaccharides, therefore, appear to be an important part of phytoplankton-derived DOM and specifically the actively released DOM.

Polysaccharides are structural and storage compounds of phytoplankton and consist of long sometimes branched chains of monosaccharides bound together by glycosidic bonds. They have a remarkable structural diversity and can consist of varying monosaccharide residues bound by different glycosidic bonds and decorated with different side groups such as sulfate, acetyl or methyl (Dumitriu 2010, Helbert 2017). Analysis of the monosaccharide residues from phytoplankton extracts, using acid hydrolysis, has provided insight into the basic chemical composition of marine polysaccharides. They are primarily composed of the sugar monomers arabinose, xylose, glucose, galactose, mannose, fucose, rhamnose, glucosamine and galactosamine (Aluwihare and Repeta 1999, Aluwihare et al 2002, McCarthy et al 1996). The monomer ratios vary between individual phytoplankton groups, indicating that they produce polysaccharides of different chemical compositions (Abdullahi et al 2006, Aluwihare and Repeta 1999, Myklestad 1995). These monosaccharides are also the dominate sugars found in surface water samples suggesting that phytoplankton polysaccharides are the dominate source of monosaccharides in the marine environment (Aluwihare and Repeta 1999, KerheRvé et al 1995).

Bacterial Polysaccharide Turnover

Marine heterotrophic bacteria degrade polysaccharides using carbohydrate active enzymes (CAZymes), which include glycoside hydrolases (GH), polysaccharide lyases

and carbohydrate esterases. GH's cleave the glycosidic bonds within a polysaccharide (Lombard et al 2014). They can be exo-acting meaning they remove sugars from the end of the polysaccharide chain or endo-acting meaning they hydrolyse bonds within the chain (Driskill et al 1999). GH's are classified into many different families based on their structure and display substrate specificities (Berlemont and Martiny 2016, Lombard et al 2014). The substrate specificity means that a specific GH hydrolyses a limited type of glycosidic bonds and that to degrade a complex polysaccharide several GH's are most likely required. This means that a single bacterial species requires several different GH's or that a consortium of bacteria is required to fully degrade complex polysaccharides (Berlemont and Martiny 2016, Ndeh et al 2017, Xing et al 2015). The high diversity of polysaccharides released by phytoplankton suggests that it is unlikely that a single marine bacterium could contain all the enzymes required to degrade them. Instead, marine bacteria show a specialisation for a specific set or type of polysaccharides (Bauer et al 2006, Teeling et al 2012).

As organic matter becomes available in the marine environment, such as during a phytoplankton bloom, distinct successional patterns in both the diversity and function of heterotrophic bacteria occur. These patterns have been associated to the substrate specialisation of individual heterotrophic bacteria and to the diverse range of polysaccharides that are made available over time by phytoplankton (Bunse and Pinhassi 2016, Landa et al 2016, Teeling et al 2012).

Aims

In this thesis, I set out to investigate how the taxonomic and functional diversity of marine microorganism affects the bacterially mediated carbon turnover in the Atlantic Ocean. I specifically wanted to link the differences in bacterial community compositions to changes in the carbon turnover with a focus on the mechanisms marine microorganisms use to degrade high molecular weight polysaccharides. This will contribute to the understanding of how global patterns in polysaccharide hydrolysis rates are affected by the community composition and distribution patterns of microorganisms. Additionally, it will help us to predict the impact which microbes have on global biogeochemical cycles.

Objectives of this Thesis

The general topic of this doctoral thesis was to investigate the taxonomic and functional diversity of marine microorganisms that significantly contribute to the biological turnover of polysaccharides.

Specific Objectives

I. Develop methods which allow on-site high-throughput analysis of the microbial diversity and abundance.

A major limitation facing microbial ecologists is the need to analyse microbiological samples in a laboratory. Therefore, to enable a direct high-throughput, quantitative and qualitative analysis of a microbial community I sought to modified established laboratory-based techniques for use on-board a research vessel. This would enable a comprehensive analysis of the microbial diversity, total cellular abundance and cellular abundance of specific bacterial groups results, even in remote sampling sites. This direct insight would in turn allow for more well-thought-out on-site research as well as targeted sampling to occur.

II. Analyse the free-living and particle-associated microbial community composition of the Atlantic Ocean with a focus on both diversity and cellular abundance.

I set out to investigate the free-living (FL) and particle-associated (PA) bacterial communities in the surface waters of the Atlantic Ocean. I did this to gain an insight into the biogeographical distribution patterns of the bacteria associated with different lifestyles. Additionally, I wanted to investigate the changes in bacterial community composition between oligotrophic and copiotrophic conditions. This should give us new insights into possible reasons for the previously reported high variability in richness and diversity among the PA and FL communities.

II. Investigate alternative polysaccharide utilisation mechanisms in marine bacteria.

A major objective of this thesis was to investigate if marine bacteria exhibit alternative mechanisms for the uptake of HMW polysaccharides. Recent metagenomics analyses have hinted at the presence of alternative mechanisms of HMW substrate utilisation in marine bacteria. Using a combination of fluorescently labelled polysaccharides (FLA-PS), fluorescence in situ hybridisation (FISH) and super-resolution structured illumination microscopy I wanted to visualise these uptake mechanisms in environmental bacteria.

IV. Analyse the extracellular hydrolysis rate of HMW polysaccharide by marine bacteria and identify the dominant organisms associated with polysaccharide utilisation.

Objectives of Thesis

Previous analyses of the extracellular hydrolysis rate of polysaccharides by marine microbial communities have shown distinct patterns in the rates of hydrolysis across latitudes. However, it is unknown if these patterns are due to the bacterial community composition. Therefore, I set out to investigate the extracellular hydrolysis rates and bacterial community dynamics within fluorescently labelled polysaccharide incubations across the Atlantic Ocean. These analyses should lead to the identification of the microorganisms associated with the hydrolysis of polysaccharides in the marine environment.

Contribution to Manuscripts and Further Publications

Chapter 1 full manuscript published in AEM 2016

Modification of a High- Throughput Automatic Microbial Cell Enumeration System for Shipboard Analyses.

Christin M. Bennke, Greta Reintjes*, Martha Schattenhofer, Andreas Ellrott, Jörg Wulf, Michael Zeder, Bernhard M. Fuchs*

*These authors contributed equally and are joint first authors

Sampling: G.R., J.W. and C.B.; On-board and lab based CARD-FISH experiments: G.R., M.S. and C.B.; Modification of microscope and programming: A.E. and M.Z.; On-board microscopy: G.R. and J.W.; Manual microscopy: G.R. and C.B.; Statistical analysis: G.R., A.E. and C.B.; Data interpretation: G.R., A.E. and C.B.; Designed graphics: G.R., A.E. and C.B.; The manuscript was primarily written by G.R. and C.B. with help from B.F. and M.S.

Chapter 2 full manuscript – in preparation

On-site microbial diversity and abundance analysis in the remotest part of the world's oceans, the South Pacific Gyre

Greta Reintjes, Halina Tegetmeyer, Jörg Wulf, Miriam Bürgisser, Christian Quast, Frank-Oliver Glöckner, Bernhard M. Fuchs, Rudolf Amann

Experimental design: G.R., H.T. and R.A.; Lab based evaluation of individual method steps: G.R.; On-board DNA extraction, PCR, amplicon size selection and quantification: G.R. and H.T.; On-board NGS sequencing: G.R. and H.T.; Bioinformatic analysis: G.R.; Bioinformatic pipeline design: C.Q. and F.O.G.; Total cell counts and CARD-FISH experiments: J.W. and M.B.; Statistical analysis: G.R.; Interpretation of data: G.R. The manuscript was primarily written by G.R. with help from B.F. and R.A.

Chapter 3 full manuscript – in preparation

Free-living and particle-associated bacteria exist as an interactive assemblage.

Greta Reintjes, Cheng Wang, Jörg Wulf, Bernhard Fuchs, Rudolf Amann

Experimental design: G.R. and R.A.; Sampling: G.R. and J.W.; Performed CARD-FISH: G.R. C.W.; Automated and manual cell counting: G.R. and C.W.; DNA extraction, PCR and sequencing on Ion Torrent PGM: G.R.; Statistical analysis: G.R.; Data interpretation: G.R.; Figure preparation: G.R. The manuscript was primarily written by G.R. with help from B.F. and R.A.

Chapter 4 full manuscript published in ISME Journal 2017

An alternative polysaccharide uptake mechanism of marine bacteria

Greta Reintjes, Carol Arnosti, Bernhard M. Fuchs, Rudolf Amann

Experimental design: R.A., C.A., G.R.; Sampling: G.R. and R.A.; Substrate incubations: G.R.; FISH and cell counting, automated microscopy and super-resolution microscopy: G.R.; Fluorescent labelling of polysaccharides: C.A.; Probe design: B.F. The manuscript was written primarily by G.R., C.A. and R.A. with contributions from B.F. G.R. prepared the Figures.

Chapter 5 full manuscript – in preparation

Tracking bacterial community dynamics in polysaccharide incubations along an Atlantic Meridional Transect.

Greta Reintjes, Carol Arnosti, Bernhard M. Fuchs, Rudolf Amann

Experimental design: R.A., C.A., G.R.; Sampling and substrate incubations: G.R.; FISH and cell counting, automated microscopy and super-resolution microscopy: G.R.; fluorescent labelling of polysaccharides: C.A. Data analysis: G.R. and C.A.; Statistical analysis: G.R.; Figure preparation: G.R. The manuscript was written primarily by G.R., C.A. and R.A. with contributions from B.F.

Additional contributions

Determining the bacterial cell biology of Planctomycetes.

Published Nature Communications. March 2017, DOI: 10.1038/ncomms14853

Christian Boedeker, Margarete Schöler, Greta Reintjes, Olga Jeske, Muriel C.F. van Teeseling, Mareike Jogler, Patrick Rast, Daniela Borchert, Damien P. Devos, Martin Kucklick, Miroslava Schaffer, Roberto Kolter, Laura van Niftrik, Susanne Engelmann, Rudolf Amann, Manfred Rohde,

Harald Engelhardt and Christian Jogler

Contribution: *Planctomycetes* cell staining using Nile Red and DAPI, Super-resolution structured illumination microscopy of single cells, 3D image construction from super resolution z-stack images and analysis.

Reoccurring patterns in bacterioplankton dynamics during coastal spring algae blooms. Published in eLife. April 2017, DOI: <http://dx.doi.org/10.7554/eLife.11888>

Hanno Teeling, Bernhard M Fuchs, Christin M Bennke, Karen Krüger, Meghan Chafee, Lennart Kappellmann, Greta Reintjes, Jost Waldmann, Christian Quast, Frank Oliver Glöckner, Judith Lucas, Antje Wichels, Gunnar Gerdt, Karen H Wiltshire, Rudolf Amann

Contribution: Sampling of spring phytoplankton bloom over multiple years, CARD-FISH experiments, Automated cell enumeration of total cell counts and specific bacterial groups.

Ocean-basin wide sampling of copepod reveals a stable associated gut microbiome, dominated by Betaproteobacteria.

Gut symbiosis of *Pleuromamma* copepods with *Limnobacter* is specific at the ocean basin scale.

Manuscript in prep.

Sara J. Cregeen, Greta Reintjes, Nikolaus Leisch, Bernhard M. Fuchs, Rudolf Amann and Mikhail V. Zubkov

Contribution: Sampling of free-living and particle-associated bacterioplankton along the AMT22. DNA extraction, PCR and NGS sequencing. Statistical analysis and data interpretation of bacterioplanktonic communities.

Chapter 1

Modification of a High- Throughput Automatic Microbial Cell Enumeration System for Shipboard Analyses

Christin M. Bennke, Greta Reintjes, Martha Schattenhofer, Andreas Ellrott, Jörg Wulf, Michael Zeder, Bernhard M. Fuchs

Published in Applied and Environmental Microbiology (AEM)
DOI: 10.1128/aem.03931-15



Modification of a High-Throughput Automatic Microbial Cell Enumeration System for Shipboard Analyses

Christin M. Bennke,^{a,*} Greta Reintjes,^a Martha Schattenhofer,^{a,b} Andreas Ellrott,^a Jörg Wulf,^a Michael Zeder,^{a,c} Bernhard M. Fuchs^a

Department of Molecular Ecology, Max Planck Institute for Marine Microbiology, Bremen, Germany^a; Department of Ecology & Genetics, Limnology, Uppsala University, Uppsala, Sweden^b; Technobiology GmbH, Buchrain, Switzerland^c

ABSTRACT

In the age of ever-increasing “-omics” studies, the accurate and statistically robust determination of microbial cell numbers within often-complex samples remains a key task in microbial ecology. Microscopic quantification is still the only method to enumerate specific subgroups of microbial clades within complex communities by, for example, fluorescence *in situ* hybridization (FISH). In this study, we improved an existing automatic image acquisition and cell enumeration system and adapted it for usage at high seas on board an oceanographic research ship. The system was evaluated by testing settings such as minimal pixel area and image exposure times ashore under stable laboratory conditions before being brought on board and tested under various wind and wave conditions. The system was robust enough to produce high-quality images even with ship heaves of up to 3 m and pitch and roll angles of up to 6.3°. On board the research ship, on average, 25% of the images acquired from plankton samples on filter membranes could be used for cell enumeration. Automated enumeration was highly correlated with manual counts ($r^2 > 0.9$). Even the smallest of microbial cells in the open ocean, members of the alphaproteobacterial SAR11 clade, could be confidently detected and enumerated. The automated image acquisition and cell enumeration system developed here enables an accurate and reproducible determination of microbial cell counts in planktonic samples and allows insight into the abundance and distribution of specific microorganisms already on board within a few hours.

IMPORTANCE

In this research article, we report on a new system and software pipeline, which allows for an easy and quick image acquisition and the subsequent enumeration of cells in the acquired images. We put this pipeline through vigorous testing and compared it to manual microscopy counts of microbial cells on membrane filters. Furthermore, we tested this system at sea on board a marine research vessel and counted bacteria on board within a few hours after the retrieval of water samples. The imaging and counting system described here has been successfully applied to a number of laboratory-based studies and allowed the quantification of thousands of samples and FISH preparations (see, e.g., H. Teeling, B. M. Fuchs, D. Becher, C. Klockow, A. Gardebrecht, C. M. Bennke, M. Kassabgy, S. Huang, A. J. Mann, J. Waldmann, M. Weber, A. Klindworth, A. Otto, J. Lange, J. Bernhardt, C. Reinsch, M. Hecker, J. Peplies, F. D. Bockelmann, U. Callies, G. Gerdt, A. Wichels, K. H. Wiltshire, F. O. Glöckner, T. Schweder, and R. Amann, *Science* 336:608–611, 2012, <http://dx.doi.org/10.1126/science.1218344>). We adjusted the standard image acquisition software to withstand ship movements. This system will allow for more targeted sampling of the microbial community, leading to a better understanding of the role of microorganisms in the global oceans.

The exact quantification of cells is fundamental to microbial ecology and hence for understanding the interaction of microorganisms with biotic and abiotic factors. Still, the counting of microbial cells on membrane filters using an epifluorescence microscope remains the method of choice (1–3) for the enumeration of picoplankton cells, although it is rather time-consuming and relies on the experience of the individual person counting. Additionally, manual counting of an entire membrane filter is not practical within a given time frame, and therefore, only a small part is analyzed (usually 12 to 20 fields of view [FOVs]) (3, 4). Consequently, several tools have been developed over the past 2 decades to automatically enumerate microbial cells by means of image acquisition and subsequent image analysis (e.g., references 5–13). Most of these methods automate only the post-image processing; the image acquisition is still done manually. One of the first fully motorized microscope systems for automated image acquisition was presented by Pernthaler and coworkers in 2003 (7). It was applied to several thousands of sample preparations for

Received 8 December 2015 Accepted 18 March 2016

Accepted manuscript posted online 25 March 2016

Citation Bennke CM, Reintjes G, Schattenhofer M, Ellrott A, Wulf J, Zeder M, Fuchs BM. 2016. Modification of a high-throughput automatic microbial cell enumeration system for shipboard analyses. *Appl Environ Microbiol* 82:3289–3296. doi:10.1128/AEM.03931-15.

Editor: A. M. Spormann, Stanford University

Address correspondence to Bernhard M. Fuchs, bfuchs@mpi-bremen.de.

* Present address: Christin M. Bennke, Leibniz Institute for Baltic Sea Research, Warnemünde, Rostock, Germany.

C.M.B. and G.R. contributed equally to this article.

This article is contribution 280 of the AMT program.

Supplemental material for this article may be found at <http://dx.doi.org/10.1128/AEM.03931-15>.

Copyright © 2016, American Society for Microbiology. All Rights Reserved.

Chapter 1 | Modification of a High- Throughput Automatic Microbial Cell Enumeration System for Shipboard Analysis

Bennke et al.

TABLE 1 Oligonucleotide probes used in this study^a

Probe name	Target group	Probe sequence (5'→3')	Length (nt) ^b	FA (%) ^c	Reference
CF319a	<i>Bacteroidetes</i>	TGGTCCGTGTCTCAGTAC	18	35	29
SAR11-152R	SAR11 clade	ATTAGCACAAAGTTTCCYCGTGT	22	25	30
SAR11-441R	SAR11 clade	TACAGTCATTTTCTTCCCGAC	22	25	30
SAR11-441R(modif)	SAR11 clade	TACCGTCATTTTCTTCCCGAC	22	25	31
SAR11-487(modif)	SAR11 clade	CGGACCTTCTTATTCGGG	18	25	31
SAR11-487-H3 ^d	SAR11 clade	CGGCTGCTGGCAAGGTTAGC	22	25	31
SAR11-542R	SAR11 clade	TCCGAACACGCTAGGTC	18	25	30
SAR11-732R	SAR11 clade	GTCAGTAATGATCCAGAAAGYTG	23	25	30
EUB338 I	<i>Bacteria</i>	GCTGCCTCCCGTAGGAGT	18	35	32
EUB338 II	Supplement to EUB338	GCAGCCACCCGTAGGTGT	18	35	33
EUB338 III	Supplement to EUB338	GCTGCCACCCGTAGGTGT	18	35	33

^a All *Bacteria*-specific probes (EUB338 I, EUB338 II, EUB338 III) were applied together as a mix. This applied also to all SAR11-specific probes.

^b nt, nucleotides.

^c FA, formamide concentration (vol/vol) in the hybridization buffer.

^d Unlabeled helper oligonucleotide to probe SAR11-487(modif).

high-throughput analysis of fluorescence *in situ* hybridization (FISH) assays, along a transect across the Atlantic Ocean (14). Further development of this system enabled, for example, the autonomous recognition of the shape of the filter pieces (SamLoc [15]) or sped up the image acquisition time by using light-emitting diode (LED) illumination, which removed the need for manual shutter opening and closing during optical filter changes.

The present study consists of two parts. The first part focuses on the adaptation and further development of the existing counting system of Zeder and Pernthaler (16) to minimize human intervention during the counting process. This system was tested and applied in a stable laboratory environment and compared to manual microscopic counts of microbial cells on membrane filters to verify the quality and reproducibility of the obtained data.

In a next step, we brought this system on board an oceanic research vessel to further develop the automatic microscopy method while being at sea. So far, shipboard cell enumeration has been done either manually with an epifluorescence microscope or by flow cytometry. The flow cytometry method, however, is predominantly used to determine total picoplankton, picoeukaryote, and nanoflagellate abundance. While pigmented microorganisms, like *Synechococcus* and *Prochlorococcus*, can be enumerated separately, heterotrophic nonpigmented microorganisms can be counted only as bulk (17, 18). Bringing microscopy systems to sea on board a research vessel would facilitate the counting of non-pigmented microorganisms that have been specifically labeled with oligonucleotide probes after fluorescence *in situ* hybridization (FISH). This bears some major challenges that need to be overcome. Mass acceleration of the microscope components due to the ship movement up to the meter range results in torsion of the instrument and greatly influences the autofocus and image focus on a nanometer-to-micrometer scale. This is even more true for automated microscope systems with their heavy motorized components, e.g., the stage, which are susceptible to torsional stress. Most of the time, microscopes on board a research vessel are mounted on vibration-free flagstones to minimize the motion of the stage and to reduce unstable focus conditions.

The motivation to develop an onboard automatic microscope counting system is to enable specific picoplankton counts after FISH on-site within a few hours after the retrieval of water samples. So far, the only mention of an automated microscope has been in a grant application in 1989 by Michael Sieracki (NSF,

grant 8813356). In order to use our lab system on board a research vessel, we had to account for the ship's constant motion while at sea. Hence, we improved the stacking and focusing routine developed by Zeder and Pernthaler (16) to obtain high-quality (HQ) images independently of the ship's movement. At first, the quick stack with extended depth of focus (QEDF) was developed and further improved by in-depth focusing (FQEDF). Here, we present the first successful employment of an automatic cell enumeration system on board a research vessel, which was quality checked and verified by manual counts on board, resulting in the first onboard data set of the distribution of the alphaproteobacterial clade SAR11.

MATERIALS AND METHODS

Adaptation of existing counting system and further development. (i) Sampling: land-based image acquisition. Marine surface water samples were collected twice a week from 1 m below the sea surface between 1 January and 31 May 2011 with the research vessel *Ade* at station Kabeltonne, Helgoland Roads, North Sea (54°11'30"N 7°54'00"E). All samples were fixed for 1 h at room temperature by adding a 37% formaldehyde solution (Sigma-Aldrich, Taufkirchen, Germany) to a final concentration of 1%. Filtration was done using a reusable Nalgene bottle top filtration device (catalog no. DS0320-2545), and 10 ml of surface water was filtered through 0.2-μm-pore-size polycarbonate membrane filters (catalog no. WH7060-4702; GE Healthcare, Freiburg, Germany) equipped with cellulose nitrate support filters (pore size, 0.45 μm; model 11306-47-N; Sartorius). Filtration was performed by applying a gentle vacuum of <20 kPa. After drying, filters were stored at -20°C until further analysis.

(ii) Fluorescence *in situ* hybridization and DAPI staining. Filters were cut and subsequently mounted on glass slides using a mixture of glycerol-phosphate-buffered saline (PBS) mounting solutions (CitiFluor AF1 [CitiFluor Ltd., London, United Kingdom] and Vectashield [Vector Laboratories, Inc., Burlingame, CA, USA]) containing the nucleic acid dye DAPI (4',6-diamidino-2-phenylindole; Sigma-Aldrich, Steinheim, Germany) at a final concentration of 1 μg ml⁻¹. The samples that were used for community analysis and the estimation of the minimal object size for bacterial cells were additionally stained by fluorescence *in situ* hybridization and underwent catalyzed reporter deposition (CARD-FISH), according to Thiele et al. (19). The oligonucleotide probes used to target the whole *Bacteria* clade and the *Bacteroidetes* clade are listed in Table 1.

(iii) Refined image acquisition system. Image acquisition was done using a multipurpose fully automated microscope imaging system (MPISYS) (see Fig. S1A to G in the supplemental material) on a Zeiss AxioImager.Z2 microscopic stand (Carl Zeiss MicroImaging GmbH, Göttingen, Germany) with a cooled charged-coupled-device

(CCD) camera (AxioCam MRm; Carl Zeiss) and a Colibri LED light source (Carl Zeiss) with three light-emitting diodes (UV-emitting LED, 365 ± 4.5 nm for DAPI; blue-emitting LED, 470 ± 14 nm for the tyramide Alexa Fluor 488; red-emitting LED, 590 ± 17.5 nm for the tyramide Alexa Fluor 594), combined with the HE-62 multifilter module (Carl Zeiss). This module consists of a triple emission filter TBP 425 (± 25), 527 (± 27), LP615, including a triple beam splitter of TFT 395/495/610.

The imaging software initially acquired an overview image of the microscope stage and object slides in bright-field illumination with a $1\times$ objective (Carl Zeiss) (see Fig. S1B to D in the supplemental material) (SamLoc [15]). Subsequently, the SamLoc software was used to define coordinates for image acquisition based on user-defined grids with FOVs, with a minimum distance of 250 μm between FOVs (see Fig. S1E in the supplemental material). This distance takes into account the frame size (FOV width) of the CCD camera with the $63\times$ objective (Carl Zeiss), which is 141 by 105 μm . To avoid any overlap of FOVs, a minimum distance of one-and-a-half times the diagonal of the CCD camera frame was found to be a reliable distance between two imaged FOVs. After defining the coordinates, an FOV coordinate list was generated, which was subsequently used by the MPISYS software during the automatic image acquisition. This system was evaluated for planktonic samples, in which 55 FOVs were adequate for cell enumeration; however, the number of FOVs needs to be newly evaluated for samples from other habitats.

Next, so-called channels were defined within the MPISYS software according to the fluorescent dyes used (e.g., DAPI, Alexa Fluor 488, and Alexa Fluor 594) (see Fig. S1F in the supplemental material). The channels are user-specified settings for image acquisition (see Fig. S1G in the supplemental material). For each channel, the exposure time (constant or variable), focusing procedure, and number of images per z-stack for the compensation of filter unevenness were selected (20). Notably, for each channel, only one exposure time, either constant or variable, could be selected. If the user requested different exposure times for the same excitation setting, several channels were defined, selecting similar excitation settings but different exposure times.

The algorithm for the focusing routine was adapted from that of Zeder and Pernthaler (16). Focusing was done for each FOV in the first acquired channel and then set as a fixed focal position for the other channels. A z-stack of seven layers per FOV and exposure time was recorded, and subsequently, a single extended depth of field image (EDF) was created (see Fig. S2A in the supplemental material). The EDF was used to compensate for the unevenness of a sample (like, for example, wrinkles on the filter piece) by taking multiple images corresponding to the different focal planes and subsequently creating a single in-focus image (21). For this, the wavelet-based extended-focus functionality of the AxioVision software (Carl Zeiss), which is in compliance with the EDF algorithm, was used.

Images were acquired using a $63\times$ magnification and 1.4 numerical aperture oil immersion plan apochromatic objective (Carl Zeiss). The EDFs were saved in .tiff format and were subsequently loaded into the Automated Cell Measuring and Enumeration tool 2.0 (ACMEtool2.0) program (<http://www.technobiology.ch/index.php?id=acmetool>) (see Fig. S1H to L in the supplemental material). The images obtained using the above-mentioned CCD camera and a $63\times$ oil objective with numerical aperture of 1.4 have a pixel size of $0.1015 \mu\text{m pixel}^{-1}$.

(iv) Image selection and cell determination and enumeration using ACMEtool2.0. All images taken with MPISYS were manually inspected in ACMEtool2.0 (see Fig. S1H in the supplemental material), and low-quality images, such as images with over- or underexposed parts, areas out of focus (unevenness), or too many aggregates, large phytoplankton cells, debris, and particles, were excluded from further analysis to ensure high data quality (see Fig. S3 to S6 in the supplemental material) (20). In a second step, a so-called metafile was calculated from the remaining HQ images for faster image processing (see Fig. S1I in the supplemental material). This metafile contained the coordinates of all recognized objects of each image of all channels and stored parameter values, like object area,

circularity, mean gray value, and signal-to-background ratio. These parameters were used to define logical selection rules and stored in "set" and "subset" definitions. To enumerate FISH-positive cells, the following sets were defined. One set was defined to identify all blue fluorescent DAPI-stained cells under UV illumination. A second set was defined to determine which cells show green fluorescence (the FISH signal) under blue excitation. The third set was defined to detect all red-emitting objects under green excitation (see Fig. S3A to F in the supplemental material). Due to the high productivity of the sampling site at Helgoland Roads, this was needed to discriminate against autofluorescence signals of debris and small algae (sample image material is provided in Fig. S4A and B and S5A and B in the supplemental material). Consequently, FISH-positive cells were identified as the logical combination of the three sets: blue positive, green positive, and red negative.

Finally, after optimal selection of parameters and manual cross-checks, cells were counted automatically by the program (see Fig. S1J in the supplemental material), and cell numbers were exported in a tab-delimited report file (see Fig. S1K in the supplemental material). Furthermore, ACMEtool2.0 provides a summary file in which the number of analyzed FOVs per sample and total counted cells were given. For a detailed overview, an FOV report of the numbers of counted cells per FOV was provided. This report also gives a detailed overview of the cell distribution on the filter.

Onboard automatic counting system. (i) Sampling and sample preparation on board. Planktonic seawater samples were taken during the Atlantic Meridional Transect (AMT) 22 on the research vessel RRV *James Cook* (Southampton, United Kingdom, to Punta Arenas, Chile, 10 October to 24 November 2012). Samples were taken using a Sea Bird CTD with carousel water sampler (Sea Bird Electronics, Inc., USA), which was deployed twice daily at predawn and solar noon intervals. A total of 50 stations were sampled at a 20-m water depth. From each sample, 100 ml of seawater was fixed with 37% formaldehyde in a final concentration of 1% for 1 to 2 h at room temperature. Subsequently, triplicate 20-ml subsamples were filtered onto 47-mm polycarbonate membrane filters with a $0.2\text{-}\mu\text{m}$ pore size using a vacuum of 20 kPa. These filters were dried and stored at -20°C until further analysis.

All stations were analyzed using CARD-FISH directly on board the research ship within a few hours after the retrieval of samples. The filters were processed according to the method of Thiele et al. (19) and subsequently mounted on glass slides using a DAPI-amended mixture of Citi-Fluor AF1 and Vectashield. The oligonucleotide probes used to target the alphaproteobacterial clade SAR11 are listed in Table 1. Cell enumeration and community analyses were done directly on board using a fully motorized Axioplan 2 microscope (Carl Zeiss) for automatic image acquisition and the ACMEtool2.0 software for image analysis. Manual verification of the automatically obtained cell counts was done after completion of automated image acquisition to prevent bleaching of the stained cells. The typical manual inspection period is in the range of seconds to minutes, which affects the signal strength of the stained cells. In contrast, exposure times in the range of milliseconds do not negatively influence the signal intensities (data not shown).

(ii) Automated image acquisition on board. The Axioplan 2 microscope was equipped with a $63\times/1.4$ oil plan apochromatic objective lens, a four-slide scanning stage (Märzhäuser, Wetzlar, Germany), LED epifluorescence illumination of 365 nm, $470 - 5/15$ nm, and 590 ± 10 nm (KSL 70; Rapp Optoelectronic, Wedel, Germany), a multiband optical filter with beam splitter HC395/495/610, and emission filter HC425 (± 25), 527 (± 25), LP615 (AHF Analysentechnik, Tübingen, Germany), and a cooled CCD camera (Orca C4742-95-12NR; Hamamatsu Photonics, Hamamatsu City, Japan). The pixel size of this microscope and the associated objectives was $0.1068 \mu\text{m pixel}^{-1}$. The acquisition of overview images was done via webcam and using the SamLoc software (15). The previously described automated image acquisition software MPISYS was modified for the different hardware requirements and was extended with new functionality to account for the ship's movements. We developed a

new quick-stack method with an extended depth of field (QEDF) routine. In comparison to the original stack image acquisition with EDF (see Fig. S2A in the supplemental material), in which positioning and image acquisition were done subsequently for every single image of the stack, QEDF used a live video stream approach (see Fig. S2B in the supplemental material). A video stream was recorded, while the microscopic stage moved from first to last stack position. The image frames of the live stream, which fit the needed stack positions best, were taken for the EDF calculation that followed. However, the time-consuming EDF calculation was postponed until all stacks from all channels were recorded to avoid a focus shift between alterations of channels. Using QEDF, it was possible to acquire multichannel multilayer images on board, but the yield of good-quality images was still low. This is because QEDF is still a pure image acquisition method and relies on the initially found focal position. In order to increase the amount of HQ images, we combined the QEDF stacking algorithm with in-depth focusing, and this was called focused QEDF (FQEDF) (see Fig. S2C in the supplemental material). The live stream image acquisition was done over a distance of 3 times the required stack size. The focal position of the live stream was calculated and represents the center of the required stack. Around this position, image frames were taken, and the FQEDF file was calculated, similar to the procedure with QEDF and EDF. The frame rate for QEDF and FQEDF is nearly exclusively dependent on the exposure time, because live imaging needs to be done in full frame at full resolution. In QEDF and FQEDF, there is continuous movement of the stage during image acquisition but in a range of 1 to 3 $\mu\text{m s}^{-1}$; therefore, it is slow enough that axial motion blur does not pose a problem.

RESULTS

Adaptation of existing counting system and further development. (i) Influence of exposure time on counting accuracy. The first step in our automated cell counting routine is the image acquisition of the stained microorganisms. The influence of exposure times on subsequent cell detection and enumeration was tested. We acquired images with various measured exposure times by the autoexposure function of the AxioVision software for every FOV. Here, this variable measured exposure time is called DAPI-auto. The automatically measured exposure times ranged from a minimum of 49 ms to maximum of 255 ms, with a mean exposure time of 74 ± 22 ms. Additionally, from the same set of samples, images were acquired with constant exposure times of 50 ms (termed DAPI-50ms) and 25 ms (DAPI-25ms). Fifty milliseconds was selected as a reference exposure time at the lower limit of DAPI-auto, and 25 ms was randomly chosen to see if the acquisition time could be reduced.

In total, 44 marine DAPI-stained planktonic samples were imaged by using the three different channel definitions. From each sample, 55 FOVs were recorded, and after manual image inspection, $>50\%$ (30 ± 10) high-quality FOVs per sample were obtained. These were then processed further for cell enumeration. The two fixed exposure times (DAPI-25ms and DAPI-50ms) resulted in similar cell numbers per FOV ($P = 0.685$, t test), but the cell numbers differed slightly from the ones derived from various exposure times from the DAPI-auto channel ($P = 0.006$) (Fig. 1). The DAPI-auto channel occasionally resulted in an overestimation of the cells per FOV, which originated from elevated background fluorescence leading to a low signal-to-noise-ratio. Therefore, two closely located cells appeared to be merged and were consequently counted as one by the algorithm. However, the automatically measured exposure times still often resulted in similar numbers of cells per volume as fixed exposure times, although the conditions of image acquisition differed for each FOV. Additionally, the image acquisition time for 55 FOVs using DAPI-auto

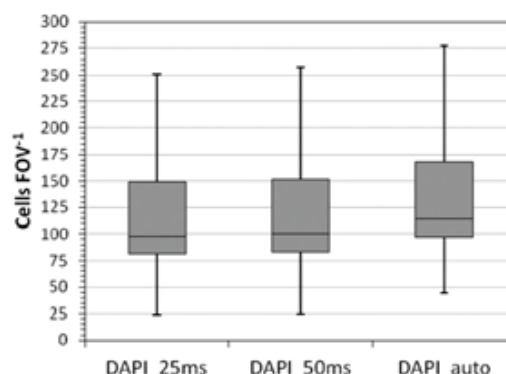


FIG 1 Number of cells per FOV obtained with different exposure time settings. Two constant exposure times (DAPI-25ms and DAPI-50ms) and one varying exposure time (DAPI-auto) were selected.

settings exceeded those from DAPI-50ms and DAPI-25ms settings by >1 h. Hence, the exposure time was set to 50 ms under stable laboratory conditions but had to be newly evaluated for samples from different habitats. Using fixed exposure times results in faster and standardized image acquisition for all samples from one habitat, leading to high reproducibility and comparability of images. The exposure time of 25 ms was rejected, and 50 ms was chosen instead, since 25 ms was at the lower limit of the image acquisition time with respect to signal-to-background ratio and was not considerably faster than 50 ms.

(ii) Estimation of the minimal object size for bacterial cells. One major aspect of cell detection using the ACMETool2.0 software is to define the set and subset definitions, which heavily rely on the signal-to-background ratio and on the size (in pixels) of the objects. A specific threshold in the object size is necessary to be able to distinguish between bacterial cells and other objects, like viruses and autofluorescent particles, which tend to be smaller (22, 23). To determine the minimal object size needed for the accurate detection of only bacterial cells, 33 marine planktonic samples were DAPI stained to determine the total object abundance and hybridized with probes specific for *Bacteria* (EUB I to III) and *Bacteroidetes* (CF319a). The bacterial probe mixture of EUB I to III was used, since it detects mainly all bacterial cells in planktonic waters, assuming a 100% detection rate.

After image acquisition and quality checking, various thresholds of 10 to 50 pixels (equivalent to 0.1 to 0.5 μm^2) for the object size were tested (Fig. 2A and B). The lowest area consisting of 10 pixels (0.1 μm^2) was assumed to detect 100% of the objects stained by DAPI. Increasing thresholds (>15 pixels, $>0.15 \mu\text{m}^2$) for the object size logically resulted in decreased numbers of detected objects. This decrease in numbers represents a fraction of smaller particles, such as virus-like or other particles, which are picked up when using lower thresholds (<15 pixels, $<0.15 \mu\text{m}^2$). By removing these particles from the total object counts, the accuracy of the number of bacterial cells, defined as an object containing both a DAPI and an EUB I to III (*Bacteria*-specific probe) signal, increased. Small objects (e.g., viruses) that contained only a DAPI but no FISH signals were no longer included.

If, however, the threshold was set too high, for example, at ≥ 30 pixels, there was a decreased detection rate of both total cells (DAPI, 10%) and hybridized cells (EUB I to III and CF319a, 19%

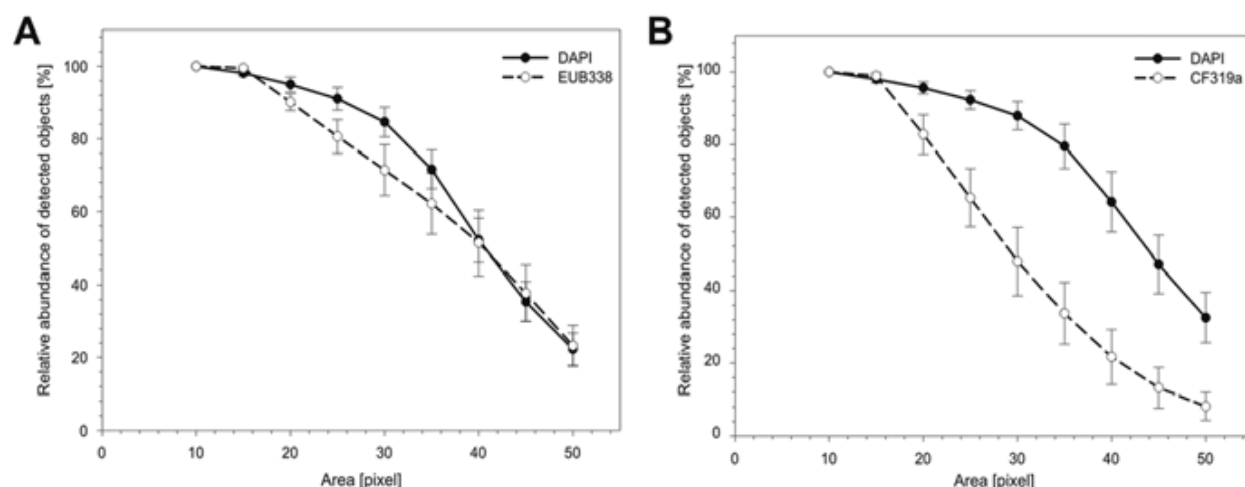


FIG 2 Estimation of the minimal object area size in pixels for the accurate enumeration of bacterial cells. Relative object counts of (A) DAPI-stained (30 ms) and EUB I- to III-stained (100 ms) and (B) DAPI-stained (30 ms) and CF319a-stained (150 ms) cells as the percentage of total counts from the smallest pixel area measured (10 pixels). The optimal pixel area size was determined by testing fixed object area sizes from 10 to 50 pixels from DAPI- and FISH-stained cells. Error bars indicate standard deviations ($n = 33$).

[Fig. 2A] and 35% [Fig. 2B], respectively). For the automated detection of bacterial cells, the optimum object size for our samples was found to be in the range of 17 to 20 pixels or 0.18 to 0.21 μm^2 .

(iii) **Comparison of manual versus automated cell counting.** To further evaluate the automated counting process, bacterial cells in a subset of 22 of the above-mentioned 44 stained and hybridized water samples were enumerated both manually and automatically. Student's two-sample t test was used to compare the distribution of bacterial counts done by manual analysis with the distribution of bacterial counts done by automatic analysis. The obtained P value was >0.05 , revealing that the distribution of bacterial counts does not differ between manual and automatic analyses. Additionally, regression analysis of the obtained manual and automatic counts revealed r^2 values of >0.98 (Fig. 3A and B), indicating a slight underestimation by automated counting. However, the coefficients of variation (CVs) for automatic and manual counts differed greatly. The CV per sample is determined by dividing the standard deviation by the

mean of cell counts from all fields of view per sample, whereas the average CV is defined by the mean of CVs across all 22 samples. Student's two-sample t test was used to compare the CVs per sample across all 22 samples done by manual analysis with the CVs per sample across all 22 samples done by automatic analysis. The obtained P value was 0.000234, thus being smaller than the significance level of 0.001, revealing significant differences between the CVs per sample across all 22 samples acquired by automatic counting compared to manual analysis. This means that the average CV was higher for manual counting ($19\% \pm 7\%$) than for automatic counting ($12\% \pm 3\%$). Hence, with the automatic system, the lowest CV per sample accounted for a minimum of 7% variance within one sample. In contrast, 10% variance per sample was received with manual analysis. Moreover, the highest CV per sample obtained by manual counting was 35%, whereas the automatic analysis resulted in the highest CV per sample of about 24%.

Onboard automatic counting system. (i) Modifications in focusing routine for onboard usage. Based on the promising results of part I, in which we successfully established the automatic

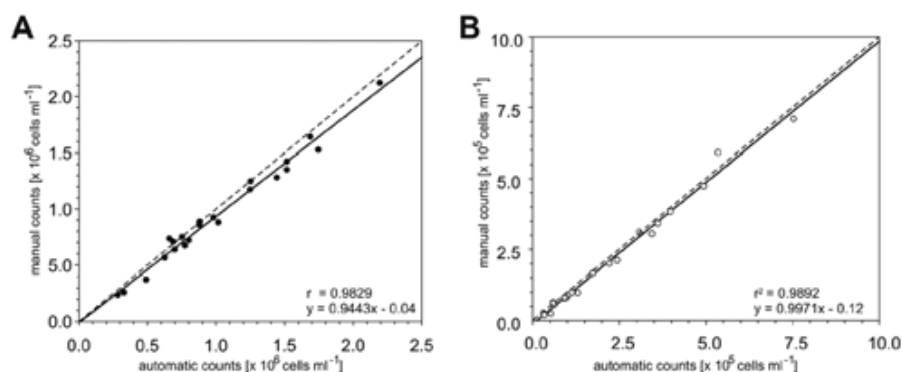


FIG 3 Manual versus automatic cell counts ashore. Cell enumeration was done after CARD-FISH with the oligonucleotide probe CF319a. (A) DAPI counts per volume. (B) FISH-positive cell counts per volume. The regression coefficient (r^2) and formula are depicted at the lower right side of each graph.

Chapter 1 | Modification of a High- Throughput Automatic Microbial Cell Enumeration System for Shipboard Analysis

Bennke et al.

TABLE 2 Overview of improvements in stacking and focusing routines to obtain HQ images on board a research vessel

Method	High-quality image yield (%)	Criteria fulfilled (minimum 10 high-quality images) (%)
EDF	0–25	19
QEDF	4–26	62
FQEDF	11–35	97

counting system inside a stable laboratory environment, an adaptation for shipboard usage was addressed. To address the complexity of the ship's constant motions while being at sea, the stacking and focusing routine to obtain high-quality images was improved. At first, the quick stack with extended depth of focus (QEDF) was developed and further improved by in-depth focusing (FQEDF) (Table 2).

On board, the average performance of using standard stacking (stacking seven z-layers) and the EDF method yielded, on average, only 10% HQ images, with a range from 0 to 25%. In contrast, in the laboratory, an average of >50% HQ images was generated. It was reported previously (4), consistent with our own experience, that a minimum of 10 HQ images is required to obtain statistically relevant counts of the bacterial cell abundance in the downstream image analysis. By using the standard stacking and EDF method, this criterion was fulfilled on board in only 19% of the cases ($n = 32$; see Table S1 in the supplemental material).

QEDF enabled faster stacking of images than the EDF stacking. This increased the total number of FOVs per sample and yielded an average of 13% (4 to 26%) HQ images, slightly more than that with EDF. Additionally, the number of samples with ≥ 10 HQ images was much higher (62% compared to 19%, $n = 21$; see Table S2 in the supplemental material). However, QEDF is still a pure-image acquisition method and depends on the initially found focal position. FQEDF, however, combines the fast image stacking acquisition with a refocusing approach; it can to an extent follow the movement caused by the ship. For example, FQEDF produced up to 20% HQ images for DAPI and the specific FISH probe, with a maximum roll angle of 6.3° , a maximum pitch angle of 5° , and a maximum ship heave of 3 m. In contrast, QEDF yielded only 10% HQ DAPI images and 20% HQ FISH images, with maximum pitch and roll angles of 5° and 3.8° , respectively,

and a ship heave of 2.3 m. With the regular EDF calculation algorithm, 13% HQ DAPI images and 5% HQ FISH images were acquired, with maximum pitch and roll angles of 4.2° and 8.8° , as well as a heave of up to 2.5 m (see Table S1 in the supplemental material).

The FQEDF stacking and imaging algorithm allowed for onboard automated multichannel and multilayer image acquisition. On average, the FQEDF stacking and imaging algorithm yielded 24% (range, 11% to 53%) HQ images. The statistical criteria for ≥ 10 HQ images per sample and channel were achieved in 97% of all cases ($n = 58$; see Table S1 in the supplemental material).

(ii) **Onboard automated and manual microscopy.** Water samples from >50 stations were processed directly after sampling with CARD-FISH, using a mix of six oligonucleotide probes specific for the SAR11 clade (Table 1). All samples were analyzed on board using the FQEDF algorithm of the automatic microscope and the cell enumeration system ACMEtool2.0. Subsequently, manual counts were obtained on board directly after the image acquisition and compared to the automatically produced counts. Image acquisition was done using fixed exposure times, as described in part I, to keep the analyses comparable. The optimal exposure time for DAPI in the oligotrophic open ocean waters could be set to 30 ms and for SAR11 to 150 ms.

The automatically obtained total cell abundances and SAR11-specific cell counts were manually validated directly on board and were in good agreement with the automatic counts (Fig. 4A and B). Regression analysis revealed r^2 values of >0.90 for all analyses. Student's two-tailed test provided P values of >0.05 (DAPI, $P = 0.679$; SAR11, $P = 0.317$), indicating that there were no differences between the onboard manual and automatic cell enumeration methods.

DISCUSSION

In this study, we evaluated and further improved an automated image acquisition and counting system for the enumeration of microbial cells in plankton samples on board a research ship.

The imaging and counting system described here has been successfully applied to a number of laboratory-based studies and allowed the quantification of thousands of samples and FISH preparations (see, e.g., reference 24). The newly developed onboard

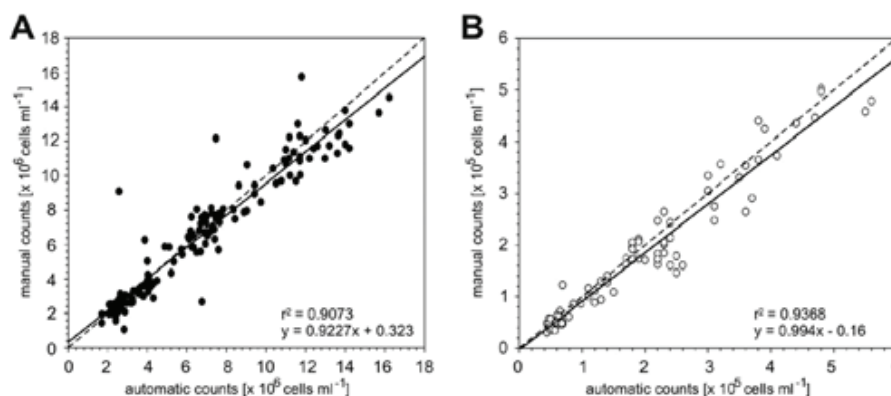


FIG 4 Manual versus automatic cell counts obtained onboard. Cell enumeration was done after CARD-FISH with the oligonucleotide probe SAR11. (A) DAPI counts per volume. (B) FISH-positive cell counts per volume. The regression coefficient (r^2) and formula are depicted at the lower right side of each graph.

focusing routine allows for a detailed on-site analysis of the microbial community. We improved the standard image acquisition algorithm to withstand ship movements (pitch and roll angles up to 6.3° and ship heaves of up to 3 m). Onboard, the focal position is not stable; therefore, a fast method was needed in order to acquire the image stacks for the extended depth of field method before the focus is lost: QEDF. However, QEDF is still a pure image acquisition method, relying on the initially found focal position. FQEDF combines the fast image stack acquisition with a refocusing approach. It not only tries to be faster than focus loss, but it can follow the focus within certain limits. The frame rate for QEDF or FQEDF is nearly exclusively dependent on the exposure time, because for this, the live imaging needs to be done in full frame at full resolution. For the initial focus routine, we can go with subframes and pixel binning up to 32 frames per second. For EDF, the stage is not in motion during image acquisition. It moves to a certain stack position and stops, the image is acquired, and it moves on. In QEDF and FQEDF, the stage moves continuously during live image acquisition but in the range of 1 to 3 $\mu\text{m s}^{-1}$, which is slow enough that axial motion blur is not a problem.

With the FQEDF routine, one in four images was suitable for further quantification with the ACMEtool2.0. Since the system can run autonomously for many hours, the output is sufficient to have an in-depth analysis of the samples on site. The ability to quickly receive an insight into both the total cell count and relative abundance of specific microbial groups (FISH) at a precise location can lead to more targeted sampling approaches. This will enable more hypothesis-driven analyses of the microbial community, which is particularly relevant for sampling done at sites that are not or that cannot be sampled regularly. Furthermore, this system could outcompete the routinely used aquatic cell enumeration system of flow cytometry. Flow cytometry is not well suited for the quantification of a large number of samples after FISH, for several reasons. FISH is best done on filters; however, flow cytometry requires cells to be suspended in a liquid. The transfer of cells from filter into liquid is feasible but always at the cost of cell loss (25). Additionally, FISH in suspension is not applicable to marine planktonic samples containing small cells, like those of SAR11, since the centrifugation steps involved in the protocol with standard benchtop centrifuges are insufficient for the sedimentation of these tiny cell types.

As a general recommendation, the automated microscope should ideally be located at or near the center of the ship's movement to minimize the influence of pitch, roll, and heave. In modern research ships, this often would be where the labs used for gravimetric analyses are located. For future use on board, we would propose also a lightweight slide scanning stage, which would be less susceptible to ship movements and mass acceleration, hence increasing the yield of high-quality images suitable for ACME analysis. Additionally, it is important to test the optimum exposure times for each sample type, as differences in staining or sample preparation might interfere with optimal image quality for downstream ACME analyses.

Under optimal shipboard and sea weather conditions, the system has the capacity to acquire images from a single filter piece consisting of 55 FOVs and two fluorescent channels (DAPI and FISH) in approximately 15 min, which adds up to a potential throughput of around 50 filters in 12 h. The subsequent manual inspection and ACME tool analysis take up another 2 to 3 h for the 50 filters. The final results can be obtained after ~15 h from 50

filters, while manual counting of the same amount of 55 FOVs on only a single filter takes a minimum of about 2 h. Naturally, under bad weather conditions, these performance values will deteriorate with increasing wave impact.

The bottleneck and critical step in our workflow is the image quality assessment, which needs manual inspection of thousands of individual images. This is necessary to weed out low-quality images, like out-of-focus images, images with over- or underexposed parts, or images with too many aggregates, large phytoplankton cells, or debris (see Fig. S4 to S6 in the supplemental material). This process cannot yet be automated in a confident manner. Although the manual image control step is still quite laborious, the entire workflow is considerably faster and more objective than manual microscopic counting.

The cell counts obtained from the automated enumeration program ACMEtool2.0 were not significantly different from manually obtained cell counts. Furthermore, with our automated system, a larger number of FOVs are processed, and consequently, more cells are examined, leading to more statistically significant cell quantifications. Ultimately, human errors during counting are minimized, and hence, the standardized counting routine allows for a direct comparison of different sampling campaigns. Original image files can be archived and reanalyzed anytime with improved or different image analysis tools.

In principle, this pipeline can be applied to a wide range of microbial habitats and environments, not just planktonic samples. In the case of sediments, cells have to be detached from the substratum by sonication or other methods and diluted in buffer before being brought onto a filter (26, 27). Additionally, Bižić-Ionescu and coworkers (28) successfully adapted the autonomous cell enumeration system to quantify specific cell types after FISH in aggregate samples. Many samples are characterized by intense autofluorescence, which may render fluorescent staining of cells impossible. One solution in the future might be to use multispectral imaging to distinguish between specific signals and background. It should be technically feasible to implement this step into our imaging and counting pipeline. Our system consists of a two-component pipeline, the autonomous image acquisition followed by cell enumeration with ACMEtool, and these components can also be used independently. For example, ACMEtool has the potential to be used to enumerate objects from high-quality confocal laser scanning or even superresolution structured illumination micrographs, as it works with standard image file formats as input (e.g., 8-bit .tiff).

In summary, the system and software pipeline we present here generates fast and reliable cell counts both in the laboratory and on board a research vessel. This system will allow for more targeted sampling of the microbial community, leading to a better understanding of the role of microorganisms in difficult-to-assess sites.

ACKNOWLEDGMENTS

This study was supported by the Max Planck Society, the Helmholtz Society, and the Natural Environment Research Council (NERC). The German Federal Ministry of Education and Research (BMBF) supported this study by funding the Microbial Interactions in Marine Systems project (MIMAS, project 03F0480A; <http://www.mimas-project.de>).

We thank the captain and crew of the *Ade* for help with sampling at the island Helgoland. We are also grateful to the captain and crew of the RRS *James Cook* for assistance in sampling during the AMT 22 cruise. We

Chapter 1 | Modification of a High- Throughput Automatic Microbial Cell Enumeration System for Shipboard Analysis

Bennke et al.

greatly appreciate the substantial contribution of Marcus Blohs (University of Applied Sciences Lausitz, Germany) for microscopy. We are also grateful to Rudolf Amann from the Max Planck Institute for Marine Microbiology, Bremen, Germany, for many fruitful discussions.

This study is a contribution to the international IMBER project and was supported by the United Kingdom Natural Environment Research Council National Capability funding to Plymouth Marine Laboratory and the National Oceanography Centre, Southampton, United Kingdom.

FUNDING INFORMATION

This work, including the efforts of Bernhard M. Fuchs and Christin M. Bennke, was funded by Federal Ministry of Education and Research, Germany (BMBF) (03F0480A).

REFERENCES

- Porter FG, Feig YS. 1980. The use of DAPI for identifying and counting aquatic microflora. *Limnol Oceanogr* 25:943–948.
- Hobbie JE, Daley RJ, Jasper S. 1977. Use of nucleopore filters for counting bacteria by fluorescence microscopy. *Appl Environ Microbiol* 33:1225–1228.
- Kepner RL, Pratt JR. 1994. Use of fluorochromes for direct enumeration of total bacteria in environmental samples: past and present. *Microbiol Rev* 58:603–615.
- Seo EY, Ahn TS, Zo YG. 2010. Agreement, precision, and accuracy of epifluorescence microscopy methods for enumeration of total bacterial numbers. *Appl Environ Microbiol* 76:1981–1991. <http://dx.doi.org/10.1128/AEM.01724-09>.
- Bloem J, Veninga M, Shepherd J. 1995. Fully automatic determination of soil bacterium numbers, cell volumes, and frequencies of dividing cells by confocal laser scanning microscopy and image analysis. *Appl Environ Microbiol* 61:926–936.
- Singleton S, Cahill JG, Watson GK, Allison C, Cummins D, Thurnheer T, Guggenheim B, Gmür R. 2001. A fully automated microscope bacterial enumeration system for studies of oral microbial ecology. *J Immunoassay Immunochem* 22:253–274. <http://dx.doi.org/10.1081/IAS-100104710>.
- Pernthaler J, Pernthaler A, Amann R. 2003. Automated enumeration of groups of marine picoplankton after fluorescence *in situ* hybridization. *Appl Environ Microbiol* 69:2631–2637. <http://dx.doi.org/10.1128/AEM.69.5.2631-2637.2003>.
- Abramoff MD, Magelhaes PJ, Ram S. 2004. Image processing with ImageJ. *Biophotonics Int* 11:36–42.
- Selinummi J, Seppälä J, Yli-Harja O, Puhakka JA. 2005. Software for quantification of labeled bacteria from digital microscope images by automated image analysis. *Biotechniques* 39:859–863. <http://dx.doi.org/10.2144/000112018>.
- Thiel R, Blaut M. 2005. An improved method for the automated enumeration of fluorescently labelled bacteria in human faeces. *J Microbiol Methods* 61:369–379. <http://dx.doi.org/10.1016/j.mimet.2004.12.014>.
- Zhou Z, Pons MN, Raskin L, Zilles JL. 2007. Automated image analysis for quantitative fluorescence *in situ* hybridization with environmental samples. *Appl Environ Microbiol* 73:2956–2962. <http://dx.doi.org/10.1128/AEM.02954-06>.
- Daims H. 2009. Use of fluorescence *in situ* hybridization and the daime image analysis program for the cultivation-independent quantification of microorganisms in environmental and medical samples. *Cold Spring Harb Protoc* 2009:dbp.p02523. <http://dx.doi.org/10.1101/pdb.p02523>.
- Morono Y, Terada T, Masui N, Inagaki F. 2009. Discriminative detection and enumeration of microbial life in marine subsurface sediments. *ISME J* 3:503–511. <http://dx.doi.org/10.1038/ismej.2009.1>.
- Schattenhofer M, Fuchs BM, Amann R, Zubkov MV, Tarran GA, Pernthaler J. 2009. Latitudinal distribution of prokaryotic picoplankton populations in the Atlantic Ocean. *Environ Microbiol* 11:2078–2093. <http://dx.doi.org/10.1111/j.1462-2920.2009.01929.x>.
- Zeder M, Ellrott A, Amann R. 2011. Automated sample area definition for high-throughput microscopy. *Cytometry A* 79:306–310. <http://dx.doi.org/10.1002/cyto.a.21034>.
- Zeder M, Pernthaler J. 2009. Multispot live-image autofocus for high-throughput microscopy of fluorescently stained bacteria. *Cytometry A* 75:781–788. <http://dx.doi.org/10.1002/cyto.a.20770>.
- Zubkov MV, Burkill PH, Topping JN. 2006. Flow cytometric enumeration of DNA-stained oceanic planktonic protists. *J Plankton Res* 29:79–86. <http://dx.doi.org/10.1093/plankt/fbl059>.
- Hill PG, Heywood JL, Holland RJ, Purdie DA, Fuchs BM, Zubkov MV. 2012. Internal and external influences on near-surface microbial community structure in the vicinity of the Cape Verde islands. *Microb Ecol* 63:139–148. <http://dx.doi.org/10.1007/s00248-011-9952-2>.
- Thiele S, Fuchs B, Amann R. 2011. Identification of microorganisms using the ribosomal RNA approach and fluorescence *in situ* hybridization, p 171–189. *In* Wilderer P (ed), *Treatise on water science*. Academic Press, Oxford, United Kingdom.
- Zeder M, Kohler E, Pernthaler J. 2010. Automated quality assessment of autonomously acquired microscopic images of fluorescently stained bacteria. *Cytometry A* 77:76–85. <http://dx.doi.org/10.1002/cyto.a.20810>.
- Forster B, Van de Ville D, Berent J, Sage D, Unser M. 2004. Complex wavelets for extended depth-of-field: a new method for the fusion of multichannel microscopy images. *Microsc Res Tech* 65:33–42. <http://dx.doi.org/10.1002/jemt.20092>.
- Fuhrman JA. 1999. Marine viruses and their biogeochemical and ecological effects. *Nature* 399:541–548. <http://dx.doi.org/10.1038/21119>.
- Levin PA, Angert ER. 2015. Small but mighty: cell size and bacteria. *Cold Spring Harb Perspect Biol* 7:a019216. <http://dx.doi.org/10.1101/cshperspect.a019216>.
- Teeling H, Fuchs BM, Becher D, Klockow C, Gardebrecht A, Bennke CM, Kassabgy M, Huang S, Mann AJ, Waldmann J, Weber M, Klindworth A, Otto A, Lange J, Bernhardt J, Reinsch C, Hecker M, Peplies J, Bockelmann FD, Callies U, Gerds G, Wichels A, Wiltshire KH, Glöckner FO, Schweder T, Amann R. 2012. Substrate-controlled succession of marine bacterioplankton populations induced by a phytoplankton bloom. *Science* 336:608–611. <http://dx.doi.org/10.1126/science.1218344>.
- Sekar R, Fuchs BM, Amann R, Pernthaler J. 2004. Flow sorting of marine bacterioplankton after fluorescence *in situ* hybridization. *Appl Environ Microbiol* 70:6210–6219. <http://dx.doi.org/10.1128/AEM.70.10.6210-6219.2004>.
- Velji MI, Albright LJ. 1986. Microscopic enumeration of attached marine bacteria of seawater, marine sediment, fecal matter, and kelp blade samples following pyrophosphate and ultrasound treatments. *Can J Microbiol* 32:121–126. <http://dx.doi.org/10.1139/m86-024>.
- Tischer K, Zeder M, Klug R, Pernthaler J, Schattenhofer M, Harms H, Wendeberg A. 2012. Fluorescence *in situ* hybridization (CARD-FISH) of microorganisms in hydrocarbon contaminated aquifer sediment samples. *Syst Appl Microbiol* 35:526–532. <http://dx.doi.org/10.1016/j.syapm.2012.01.004>.
- Bizić-Ionescu M, Zeder M, Ionescu D, Orlic S, Fuchs BM, Grossart H, Amann R. 2014. Comparison of bacterial communities on limnic versus coastal marine particles reveals profound differences in colonization. *Environ Microbiol* 17:3500–3514. <http://dx.doi.org/10.1111/1462-2920.12466>.
- Manz W, Amann R, Ludwig W, Vancanneyt M, Schleifer KH. 1996. Application of a suite of 16S rRNA-specific oligonucleotide probes designed to investigate bacteria of the phylum *Cytophaga-Flavobacter-Bacteroides* in the natural environment. *Microbiology* 142:1097–1106. <http://dx.doi.org/10.1099/13500872-142-5-1097>.
- Rappé MS, Connon SA, Vergin KL, Giovannoni SJ. 2002. Cultivation of the ubiquitous SAR11 marine bacterioplankton clade. *Nature* 418:630–633. <http://dx.doi.org/10.1038/nature00917>.
- Gómez-Pereira PR, Hartmann M, Grob C, Tarran GA, Martin AP, Fuchs BM, Scanlan DJ, Zubkov MV. 2013. Comparable light stimulation of organic nutrient uptake by SAR11 and *Prochlorococcus* in the North Atlantic subtropical gyre. *ISME J* 7:603–614. <http://dx.doi.org/10.1038/ismej.2012.126>.
- Amann RI, Binder BJ, Olson RJ, Chisholm SW, Devereux R, Stahl DA. 1990. Combination of 16S rRNA-targeted oligonucleotide probes with flow cytometry for analyzing mixed microbial populations. *Appl Environ Microbiol* 56:1919–1925.
- Daims H, Brühl A, Amann R, Schleifer KH, Wagner M. 1999. The domain-specific probe EUB338 is insufficient for the detection of all *Bacteria*: development and evaluation of a more comprehensive probe set. *Syst Appl Microbiol* 22:434–444. [http://dx.doi.org/10.1016/S0723-2020\(99\)80053-8](http://dx.doi.org/10.1016/S0723-2020(99)80053-8).

Chapter 2

On-site microbial diversity and abundance analysis in the remotest part of the world's oceans, the South Pacific Gyre

Greta Reintjes, Halina Tegetmeyer, Jörg Wulf, Miriam Bürgisser, Christian Quast, Frank-Oliver Glöckner, Bernhard M. Fuchs, Rudolf Amann

Manuscript in prep.

Abstract

The field of microbial ecology has increased immensely in recent years due primarily to advances in culture-independent methodologies. Specifically, the advances in DNA sequencing technologies have enabled a more in-depth analysis of the taxonomy and functional potential of the microbial communities. To still further our understanding of the diversity and metabolic capabilities of microorganism's microbial ecologist analyse remote and extreme environments like hypersaline lakes, acid mine drains or hydrothermal vents

A major limitation in the current culture-independent methodologies is that they are predominantly laboratory based and cannot be used to gain direct results in the field. To overcome this limitation, we modified a laboratory based culture independent sequencing pipeline to function on-board a research vessel. This allowed us to obtain a detailed overview of the microbial community composition within 48 hours of sampling.

Using our on-board sequencing pipeline, we analysed the microbial community of the South Pacific Gyre (SPG), which is one of the most remote parts of the world's oceans. The surface waters of the SPG had extremely low nutrient and chlorophyll *a* concentrations and were dominated by oligotrophic organisms such as SAR86, *Candidatus Actinomarina*, SAR11 surface 4, SAR116 and *Prochlorococcus*. The deep chlorophyll maximum (DCM) was at a depth of 200 - 250 m and had a chlorophyll *a* concentration which was comparable to other oceanic gyres (0.47 mg m⁻³). It had a diverse microbial community composition partially consisting of organisms associated with organic matter degradation such as *Bacteroidetes*. Below the DCM and in the aphotic zone the dominant organisms were the SAR406 clade, SAR234 clade, SAR202 clade and the Sva0996 clade.

By developing an on-board sequencing pipeline, we could obtain “direct” results of the microbial diversity even in the remotest part of the world's oceans. This further enabled us to do more targeted sampling and hypothesis-driven research during our research expedition into the SPG.

Introduction

The field of microbial ecology has grown immensely in recent years due primarily to methodological advances in culture-independent techniques (DeLong 2009, Franzosa et al 2015, Giovannoni and Stingl 2005, Mardis 2008, Pace 1997, Rappé and

Giovannoni 2003, Riesenfeld et al 2004, Wagner and Haider 2012). Specifically, advances in high-throughput DNA sequencing technologies have allowed for the identification of the uncultured majority of microorganisms (Gilbert et al 2010, Mardis 2008, Mardis 2013, Sogin et al 2006). DNA sequencing of a biological sample can provide both a taxonomic profile (“Who is there?”) and a functional profile (“What can they do?”) of the microbial community (De Vargas et al 2015, Faust et al 2015, Ghai et al 2013, Iverson et al 2012, Riesenfeld et al 2004, Rusch et al 2007, Sunagawa et al 2015, Venter et al 2004). These profiles, as well as the efficiency and ease of their replication, have moved microbial ecology into a new era and allowed for significant breakthroughs in our understanding of the microbial world. They have enabled microbial ecologists to identify the “unseen majority” and highlighted new metabolic potentials of microorganisms, which in turn have advanced our understanding of the origin and evolution of life on Earth as well as processes such as global nutrient cycles, energy production, the human microbiome, and infectious diseases (Cho and Blaser 2012, Dabney et al 2013, DeLong 2009, Hansel 2017, Moran et al 2016, Novelli et al 2010).

To further our understanding of the diversity and metabolic capabilities of microorganisms it is essential to sample unique and previously unknown microorganisms from novel or extreme environments such as like hypersaline lakes, acid mine drains or hydrothermal vents (Antranikian et al 2005, Baker and Banfield 2003, Litchfield 1998, Martin et al 2008, van den Burg 2003). However, remote and unique environments can be difficult to sample and unlike direct measurements such as temperature, DNA samples for microbial ecology analysis are predominantly preserved for later analysis in the lab. The analysis does not occur directly but rather weeks to months later. Further targeted sampling efforts and follow-up studies therefore rarely occur immediately after sampling but rather must wait for future sampling efforts. These can in turn be hindered due to site accessibility or project funding limitations. The absence of direct analysis of the microbial community is one of the major challenges still facing the advancement of microbial ecology, especially in remote sampling sites.

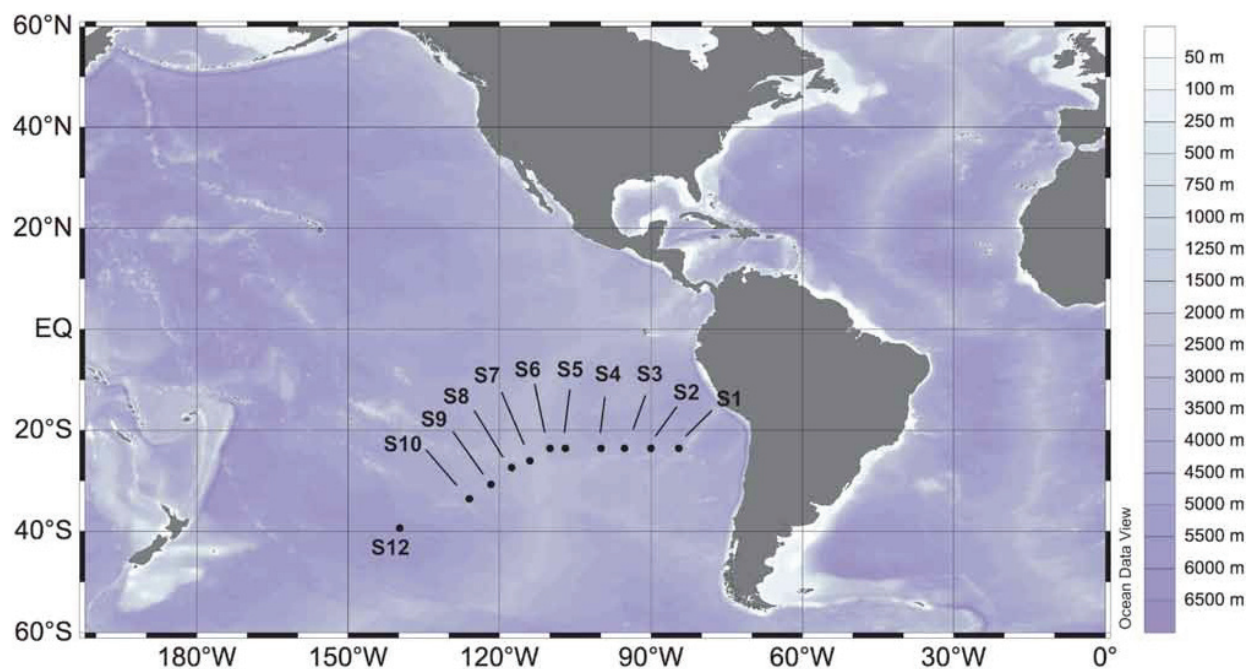
An example of a remote sampling site with limited previous research is the South Pacific Gyre (SPG). The SPG is one of the most remote parts of the world's oceans and is the furthest distance from any continent. It contains the oceans most oligotrophic waters, the lowest sea surface chlorophyll *a* concentrations and has been described as a marine biological dessert (Morel et al 2007, Raimbault et al 2008, Ras et al 2008). Although there are limited data available, recent studies have indicated that while these waters are ultra-oligotrophic there is still microbial activity, specifically carbon and nutrient cycling (Halm et al 2012, Van Wambeke et al 2008, Walsh et al 2015). The SPG may contain the last ultra-oligotrophic microbial community, which has not received (or received only limited) exposure to anthropogenic nutrient loading and may therefore hold unique metabolic potentials.

We set out to analyse the ultra-oligotrophic microbial community of the SPG directly on-board the RV Sonne. We designed and optimised a high-throughput sequencing and data analysis pipeline for on-board use and combined this with an established on-board automated image acquisition and cell enumeration pipeline (Chapter 1). The combination of these pipelines enabled the analysis of both the microbial diversity and bacterial cellular abundances on-site. This gave us a detailed insight into the microbial community of the SPG within hours of sampling allowing for further targeted sampling and focused hypothesis-driven research.

Methods

Sampling

Seawater samples were collected aboard the RV Sonne SO-245 „UltraPac“ cruise from Antofagasta, Chile (17.12.2015) to Wellington, New Zealand (28.01.2016) (Chapter 2 Figure 1). Water samples were taken from a total of 11 stations (Chapter 2 Figure 1) using a Seabird sbe911+ CTD (Seabird Scientific, WA, USA) with a Niskin rosette. Two types of stations were sampled: main stations and intermediate stations. On main stations, the CTD was cast through the entire water column to 50-100 m above the seafloor and samples were taken at various depths throughout the water column (Chapter 2 Supplementary Table 1). Generally, 4 to 5 CTDs were cast to reduce the time between sampling at depth and processing of the samples. Intermediate stations consisted of a single CTD cast down to 500 m and samples were taken from variable depths (Chapter 2 Supplementary Table 1). For diversity analysis, a total of 1 L of seawater was sampled for each depth at each station. The water was directly filtered onto 47 mm polycarbonate filter (0.2 µm pore size) using a bottle top Nalgene filter holder (Thermo Fisher, MA, USA) and a vacuum pump. After filtration samples were used directly for DNA extraction.



Chapter 2 Figure 1 Sampling sites in the South Pacific Gyre indicated by black dots. Latitudes and longitudes of individual stations are shown in Supplementary Table 1.

Physico-chemical Data

Physico-chemical characteristics of the water column of every station along the “UltraPac” cruise were examined using a CTD. Salinity and depth were calculated from pressure values and temperature was corrected to ITS-90. The CTD was also equipped with additional sensors for turbidity, fluorescence, oxygen, and PAR. All CTD data was obtained from and is available on Pangaea (www.pangaea.de), (Zielinski et al 2017). The physico-chemical data were analysed using the ODV4 software (www.odv.awi.de). The most significant changes in the physico-chemical parameters occurred in the top 500 m of the water column, therefore both the total depth (0 to 5000 m) and only the top 500 m were analysed independently.

DNA Extraction

Microbial DNA extractions were done using the MoBio Power Water DNA Extraction Kit (MoBio Laboratories, Inc., CA, USA) as recommended by the manufacturer. The MoBio Power Water kit was chosen because it is specially designed for DNA extraction from filters and there is a significant reduction in the amount of

hands-on time in comparison to other extraction methods such as SDS-chloroform extraction (Fuhrman et al 1988). DNA extraction using silica absorption in comparison to liquid phase extraction facilitates DNA extraction even during rough sea conditions. Additionally, a kit is transport friendly and reduces the amount of lab equipment and dangerous reagents required on-board.

Polymerase Chain Reaction (PCR)

PCR was carried out using the Platinum PCR SuperMix High Fidelity polymerase kit (Thermo Fisher). It is a ready-made PCR master-mix containing polymerase, salts, magnesium, and dNTPs. It requires only the addition of primers and DNA and has a high-quality yield even from low DNA concentrations. PCR was carried out using the primers S-D-Bact-0341-b-S-17 (5'-CCTACGGGNGGCWGCAG-3') and S-D-Bact-0785-a-A-21 (5'-GACTACHVGGGTATCTAATCC-3') targeting the V3-V4 variable region of the 16S rRNA, evaluated by (Klindworth et al 2013). Both primers were fusion primers with additional adaptor and barcode sequences at the 3' end to allow sequencing and separation of samples in down-stream analyses. The reverse primers contained the Ion tr-P1 adaptor at the 5' end of the primer (5'-CCTCTCTATGGGCAGTCGGTGAT-3'). The forward primers contained both the Ion A adaptor (5'-CCATCTCATCCCTGCGTGTCTCCGACTCAG-3') and one of 40 IonXpress barcodes (Ion Xpress 1 - 40) as well as the key sequence (GAT) before the primer.

Reverse fusion primer sequence:

(5'-CCTCTCTATGGGCAGTCGGTGAT GACTACHVGGGTATCTAATCC-3')

Forward fusion primer sequence:

(5'-CCATCTCATCCCTGCGTGTCTCCGACTCAGCTAAGGTAACGAT
CCTACGGGNGGCWGCAG-3')

DNA and PCR Product Quantification

A successful sequencing reaction requires precise quantities of the template library to ensure a clonal amplification on individual Ion Sphere Particles (ISPs) (see below). A fragment analyser (AATI) was used to check the quality and quantity of the PCR products and final sequencing pools. All template libraries and final sequencing pools were analysed using the DNF - 472 standard sensitivity NGS kit sizing DNA (AATI, size range from 25 bp – 5,000 bp and up to a minimum of 0.1 ng μl^{-1}) as recommended by the manufacturer. The fragment analyser is a very robust system, which allows automatic processing of multiple samples. It was adapted to ship movements by adding magnets to the individual sample trays, thereby preventing the accidental dropping of a sampling tray caused by ship pitches, during plate movement

or at the “on hold” position inside the tray drawers. The internal plate lift was mechanically stabilised from ship movement and vibration by the installation of an additional guide rail on the upper side connected via rubber mounts. Additionally, a specialised stand with transport handles and attachments was applied for easy manual transport and to allow for secure attachment to a surface (Chapter 2 Supplementary Figure 1).

Size Selection

PCR amplicons were size selected using Agencourt AMPure XP (BeckmanCoulter, Krefeld, Germany). The size selection and clean-up of amplicons is an essential part of a 16S rRNA sequencing pipeline (Head et al 2014). Several methods were tested prior to and on-board the RV Sonne to ensure a high yield of size specific amplicons. These included Ampure XP beads (BeckmanCoulter), E-Gel SizeSelect Agarose Gels (Thermo Fisher), the QIAquick PCR purification kit (Qiagen, Hilden, Germany), the QIAquick Gel Extraction Kit (Qiagen) and the QiagenMinElute kit (Qiagen). For each kit, all procedures were done as recommended by the manufacturers.

In addition to using each kit individually, we also tested combinations of kits. For example, we used the E-Gel SizeSelect Agarose Gels (Thermo Fisher) to extract amplicon bands of a specific size and then cleaned and concentrated the extracted amplicons using the QIAquick PCR purification kit (Qiagen).

For direct gel extraction, the amplicons were run on a 1% LE agarose gel (Biozyme, Oldendorf, Germany), and bands were visualised using a transilluminator DR-45M (Clare Chemical Research, Göttingen, Germany) and cut out with a sterile scalpel. The cut-out gel slices were purified using the QiagenMinElute kit (Qiagen). The same amount of PCR product was individually added to each size selection method and the obtained amplicons were compared for purity, yield and amplicon size using a fragment analyser (Advanced Analytical Technologies, Inc (AATI), Ankeny, USA). After testing the Agencourt AMPure XP beads (BeckmanCoulter) were chosen for on-board size selection. Although direct gel extraction had the highest yield of size specific amplicons, it is an impractical method for on-board use as gel pouring and electrophoresis are movement sensitive methods. The second highest DNA yields were obtained using the Agencourt AMPure XP beads (BeckmanCoulter) and it is an easy procedure with limited methodological steps and appropriate for on-board use.

Ion Torrent Sequencing and Raw Sequence

Processing

The Ion Torrent PGM (Thermo Fisher) was chosen for on-board sequencing because it is the most physically robust of the well-established sequencing platforms. It has compact dimensions and is not overly sensitive to physical movement even during sequencing reactions. It also enables user interaction with software and hardware components, allowing the user to do repairs and fix technical issues without the need for specialised personnel. The Ion Torrent PGM was adapted for on-board use by securing it to a 2 cm thick polyethylene base plate and the internal hard drives were replaced by SSDs. The base was equipped with handles that could be used for manual transportation of the sequencer and to fasten it to a surface (Chapter 2 Supplementary Figure 1). A similar base was fastened to the Ion OneTouch 2 Instrument (Thermo Fisher) and Ion OneTouch ES instrument (Thermo Fisher). The Torrent Server (Thermo Fisher) was also adapted to withstand ship-board vibration and transport by placing it in a custom-made metal frame using rubber mounts (Chapter 2 Supplementary Figure 1).

Sequencing was carried out as recommended by the manufacturer using an Ion Torrent PGM sequencer (Thermo Fisher). Emulsion PCR and enrichment of template-positive ion sphere particles (ISP) was done using the Ion PGM Hi-Q OT2 Kit (Thermo Fisher) on the Ion OneTouch 2 Instrument (Thermo Fisher) and Ion OneTouch ES instrument (Thermo Fisher) following the Ion Torrent user manual. Subsequently, the ISP were sequenced using the Ion PGM Hi-Q Sequencing Kit (Thermo Fisher) following the user manual on an Ion PGM system (Thermo Fisher). Sequencing was done on Ion 314, 316 and 318 chip Kit v2 (Thermo Fisher) with a total of 1200 flows. The chips vary in their capacity (number of sensors) and therefore total output, run time and processing time. Specifically, the Ion 314 chip has 1.2 M sensors, a total output of up to 100 Mb and a run time of 2 - 4 h. The Ion 316 chip has 6.1 M sensors, an output of up to 1 Gb and runs for 3 - 5 hours. The Ion 318 chip has 11 M sensors, a total output of up to 2 Gb and runs from 4 - 7 hours.

The Torrent Suite software, which converts the raw signals (raw pH values) into incorporation measurements and ultimately into basecalls for each read, was used for initial quality trimming. The standard Torrent suite settings and more stringent settings were applied. The standard settings and stringent setting were defined in the basecaller arguments of the Torrent Suite Software. Standard: BaseCaller --barcode-filter 0.01 --barcode-filter-minreads 20 --barcode-mode 1 --barcode-cutoff 3 --trim-qual-cutoff 10 --trim-qual-window-size 20 --trim-min-read-len 100. Stringent: Basecaller --barcode-mode 1 --barcode-cutoff 0 --trim-qual-cutoff 15 --trim-qual-window-size 10 --trim-min-read-len 250. Finally the reads were exported as .sff files

using the file exporter plugin in the Torrent suite software. The .sff files were split into individual sample FASTA files using mothur version 1.35.1 (Schloss et al 2009) (sffinfo()) and analysed using the Offline SilvaNGS Pipeline called “Lab on a ship” (see below).

Offline SilvaNGS Pipeline “Lab on a ship”

The computer cluster “lab on a ship” was developed to facilitate offline 16S rRNA sequence classification using the SilvaNGS pipeline. Previously this was only available using the online platform (Quast et al 2013). The benefit of having an offline version is the potential to use it on-board a research vessel. The online platform of this classification system is run on a highly efficient computing cluster with 36 nodes. This is required due to the complexity of the software and its associated required computing power. To ensure a similarly quick classification system an efficient computer cluster was obtained for the offline analysis (Supermicro, CA, USA). The complete pipeline can be run using a single command line argument. Alternatively, the user can run each region of the pipeline individually and analyse each section of the processing pipeline (Chapter 2 Supplementary Table 2).

Both the offline and online pipeline were run using the SILVA SSU database release SSU Ref 119. The pipelines are highly similar and varied only in the quality trimming steps (specifically trimming of ambiguous bases and homopolymers). These were omitted in the offline version of the server due to their high computing requirements. Quality trimming was instead performed prior to analysis on the SILVA offline server using the Torrent suite software. To test the “Lab on a ship” server and ensure that similar community composition results are obtained using different quality trimming methods a mock community analysis was done. The output from the two servers was then compared using cluster analysis.

Statistical Analysis

Reads were classified to genus level and statistical analysis was carried out using normalised read abundances. Community dissimilarity analyses were calculated using Bray-Curtis index (Bray and Curtis 1957). Non-metric multidimensional scaling (NMDS) plots were created using the Vegan package (Oksanen et al 2013) of R project (R Development Core Team, Vienna, Austria). Analyses of similarity (ANOSIM) tests were carried out using the Vegan package in the R Project (R Development Core Team). Depth profiles of individual bacterial clades were analysed by sorting all samples based on depth and then plotting the most abundance clades in bubble plots.

Total Cell Counts (TCC) and FISH

TCC and FISH were carried out as described in Chapter 1. DAPI and FISH stained cells were visualised and counted automatically using a fully automated image acquisition and cell enumeration system (Chapter 1). For FISH the probe PRO405 was used to target the *Prochlorococcus* (West et al 2001). The *Prochlorococcus* were enumerated because they are one of the most abundance primary producers in oligotrophic open ocean gyres (Malmstrom et al 2013, Vaulot et al 1995, West et al 2001).

Results

On-Board Next Generation Sequencing and Data Analysis

DNA could be extracted from every sample, with an average concentration of $4.36 \mu\text{g ml}^{-1}$ of seawater (Chapter 2 Table 1). The overall yield was within the range of the kit standards (Kit Manual: Ocean water sample (coastal) of 100 ml should yield 3 – 11 $\mu\text{g ml}^{-1}$). The DNA extraction efficiency was proportional to the total cell counts within the SPG (Chapter 2 Table 1). Lower DNA yields were obtained from deeper waters which had lower cell counts (3000 – 5000 m; $2.14 \times 10^4 \text{ cells ml}^{-1}$ – yield $0.45 \mu\text{g ml}^{-1}$) and the highest DNA yields were obtained around the deep chlorophyll maximum (DCM), which had the highest cell counts $5.95 \times 10^5 \text{ cells ml}^{-1}$ (Chapter 2 Table 1).

Chapter 2 | On-site microbial diversity and abundance analysis in the remotest part of the world's oceans, the South Pacific Gyre

Chapter 2 Table 1 Averaged total cell counts (TCC) and DNA yield ($\mu\text{g ml}^{-1}$) with standard deviations over different depths ranges of the SPG. The n value specifies the number of samples per depth range.

Depth (m)	$\mu\text{g ml}^{-1}$	Standard deviation	TCC	n
20	4.82	1.95	5.25E+05	8
40-60	5.84	2.84	5.93E+05	11
75-100	7.37	2.85	5.95E+05	12
125-150	7.70	3.61	4.57E+05	16
160-175	6.94	4.71	3.41E+05	11
200-250	4.88	3.11	1.91E+05	22
300-500	2.18	1.30	1.17E+05	21
750-1500	0.92	0.72	4.14E+04	10
2000-3000	0.40	0.15	2.22E+04	7
3500-5000	0.45	0.21	2.14E+04	7

In total, 1983 Mbp were sequenced directly on board the RV Sonne on the “Ultracpac” cruise using an Ion Torrent PGM. Before processing this equated to 7.26 million reads with a median read length of 290 bases. Sequencing was done on three sequencing chip types (Ion 314, Ion 316, Ion 318) with two analysis strategies (default and stringent). The difference in yield per chip type and analysis method is shown in Chapter 2 Table 1. There was no major variability in the sequencing quality between chip types except total yield and overall processing time. The more stringent quality trimming settings decreased the total number of bases and total reads by 30% and the total number of reads by up to 52%. The lower read abundance between chip types was also due to the total ISP loading of the individual chips, which varied from 71% (314) to 50% (318). With more stringent quality trimming the mean read length increased from 278 bp to 368 bp and the median read length increased from 290 bp to 411 bp. Results from the higher stringency settings were used to analyse the bacterial community because they were of higher quality and better read length.

Chapter 2 Table 2 Torrent Suite sequencing results of raw sequencing data using three different sequencing chip types and two analysis methods (default and stringent). Loading refers to the percentage of wells of each sequencing chip which are filled with ISPs.

Settings	Chip type	Number of runs	Total bases (Mbp)	Total number of reads (Q20)	Loading (%)	Mean length (bp)	Median (bp)	Mode (bp)
Default	314	5	83	3.06E+05	72	265	258	446
Stringent			56	1.48E+05		379	439	446
Difference			-33%	-52%		43%	70%	0%
Default	316	1	465	1.49E+06	52	312	364	440
Stringent			322	8.47E+05		380	433	440
Difference			-31%	-43%		22%	19%	0%
Default	318	2	551	2.12E+06	50	259	248	440
Stringent			404	1.17E+06		345	362	440
Difference			-27%	-45%		33%	46%	0%

To validate the “lab on a ship” server two mock community data were analysed on both the SilvaNGS online and the SilvaNGS offline „lab on a ship“ server using the same SILVA database SSU REF 119 (Quast et al 2013). Cluster analysis showed that the same samples analysed on different pipelines were highly similar (Chapter 2 Supplementary Figure 2). Mantel tests showed no significant difference between the community compositions of the online and offline servers (Run 1: Mantel statistic $R = 0.996$, $P = 0.001$ based on 1000 permutations).

A total of 200 samples were processed on the SilvaNGS offline server on-board the RV Sonne, which equated to a total of 32 million reads and an average of 160,921 reads per sequencing project (after stringent quality trimming). The average read length was 399 bp, with a maximum of 538 bp.

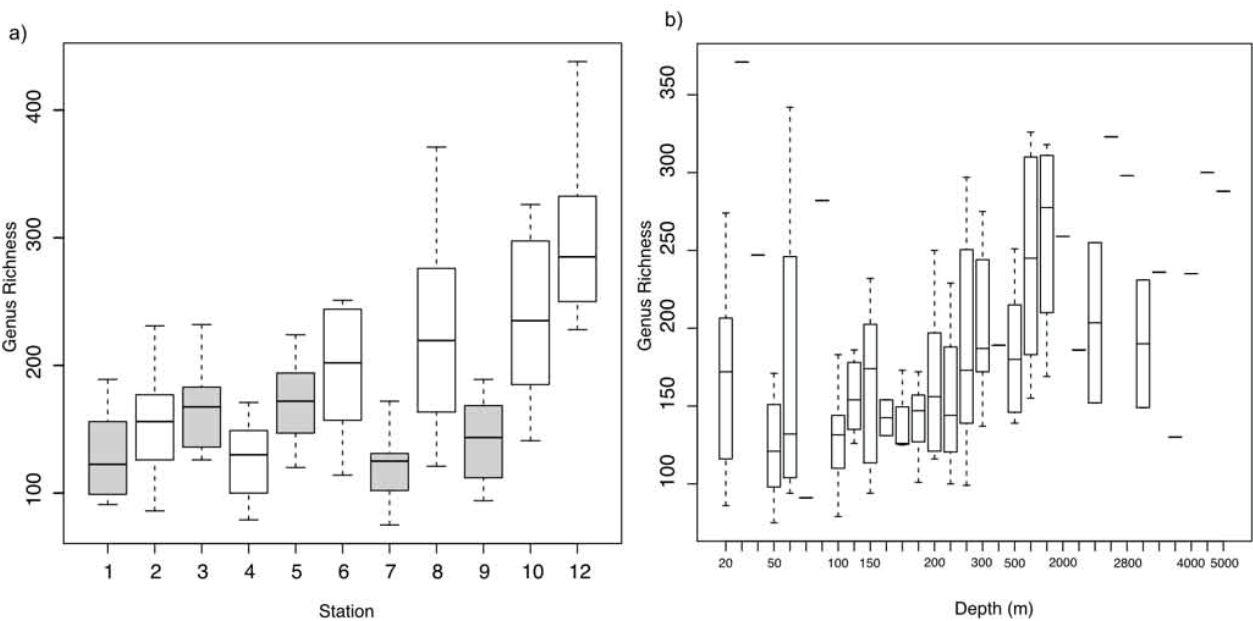
For all stations, a minimum of 3500 reads per samples were obtained. The median read abundance for main stations was ~24,000 and intermediate stations had ~8800 reads (Chapter 2 Table 3). A higher sequencing depth was obtained for the main stations to allow for a more in-depth analysis of the rare community. This was done by adding different amounts of PCR product to the library pools.

Chapter 2 Table 3 Sequencing read abundances values for all stations and within different station types (main and intermediate) within the SPG.

	All stations	Main	Intermediate
Average	18630	23247	10274
Median	13051	24035	8809
Mode	9321	8531	9321
Minimum	3454	5433	3454
Maximum	61928	61928	34095

Microbial Diversity of the SPG

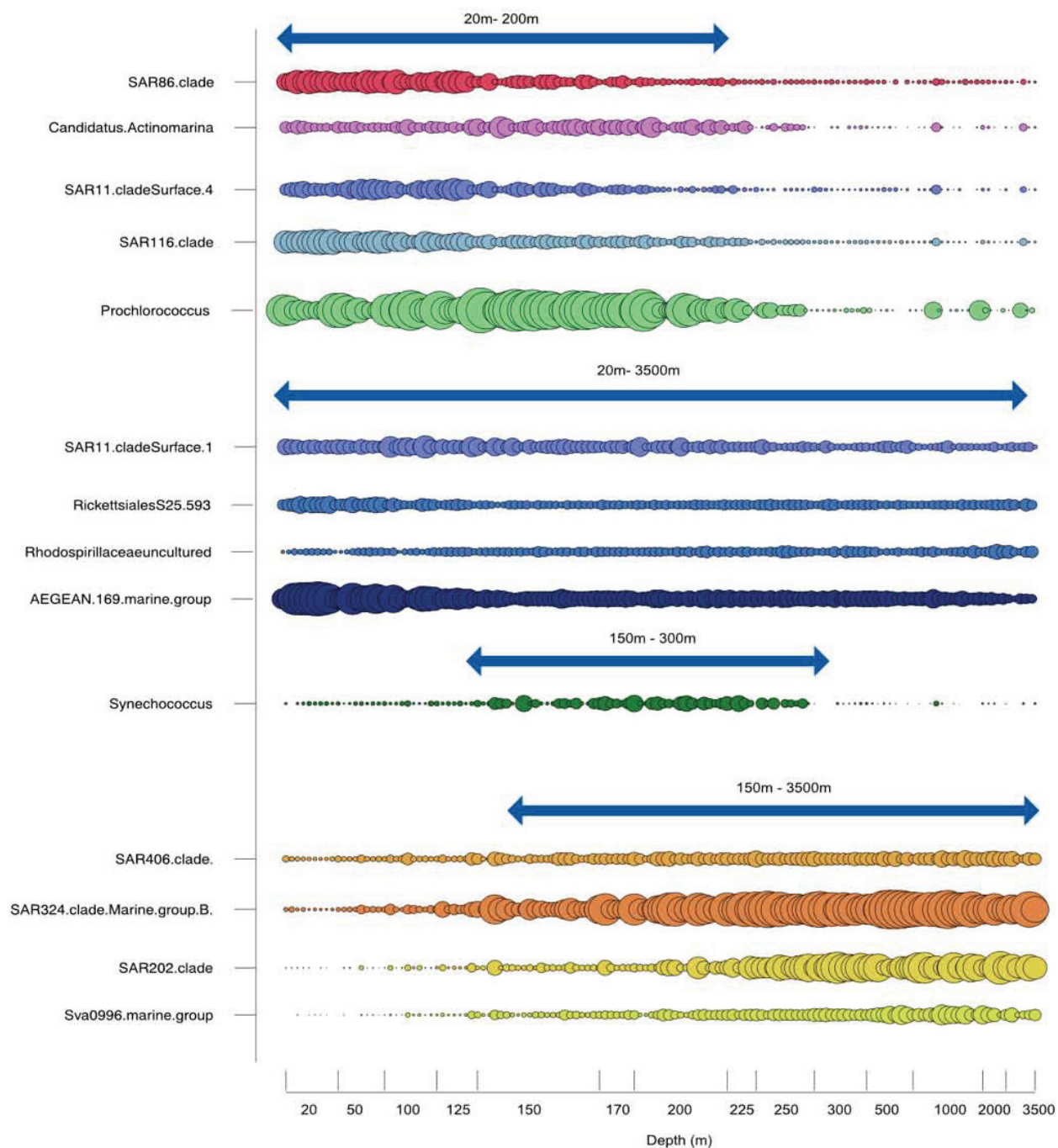
There was an increase in bacterial richness and diversity (Shannon Index) with depth at all stations of the SPG (Chapter 2 Figure 1). Additionally, there was an increase in richness from east (80°W) to west (160°W) (Chapter 2 Figure 1). The lower diversity in the samples from stations 7 and 9 was because they were intermediate stations (shown in grey) that were only sampled to a depth of 500 m.



Chapter 2 Figure 1 Genus richness across different stations (east to west) (a) and with depth (20 -5000 m) (b) as sampled in the SPG. The boxes coloured in grey highlight the intermediate stations, which were only sampled to 500m depth

There were 14 genera with a high read abundance throughout the SPG. These groups showed a distinct distribution with depth, having a higher abundance either in the photic zone or below the photic zone (Chapter 2 Figure 2). In the surface waters from 20 – 200 m depth the SAR86, *Candidatus Actinomarina*, SAR11 surface 4, SAR116 and *Prochlorococcus* were dominant. *Synechococcus* was also abundant in the photic zone but present at a lower depth of 150 – 300 m. Below the DCM and in the aphotic zone SAR406, SAR234, SAR202 and the Sva0996 marine group were dominant. The SAR11 surface 1, *Rickettsiales* S25 953, *Rhodospirillaceae* and AEGEAN 169 marine group were abundant throughout the water column from 20 – 3500 m depth.

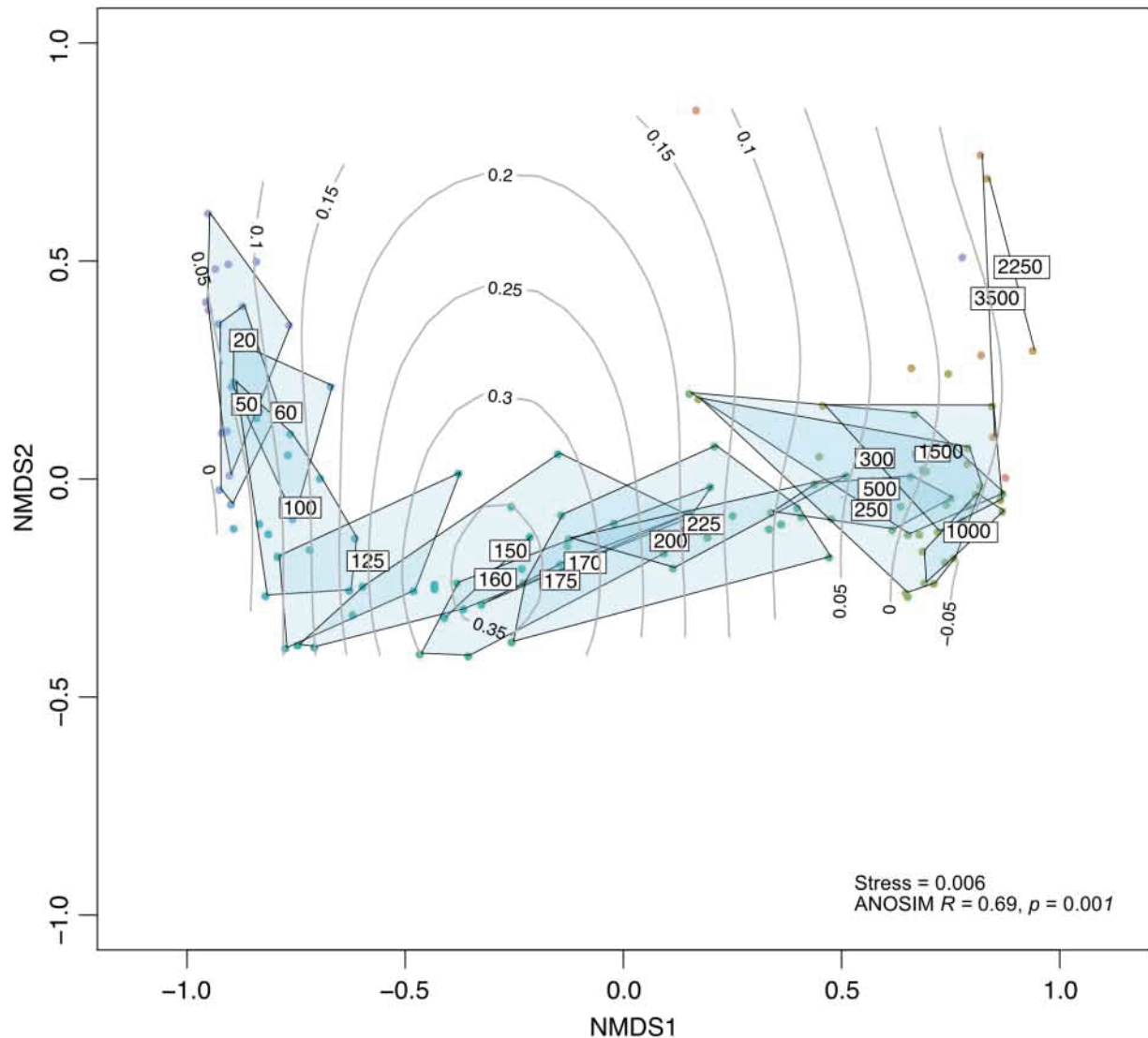
In addition to the dominant genera there was also a high number of rare genera throughout the SPG (read abundance < 0.1%). There were 550 genera that had both a low abundance and were present in a low number of sites (3 or less) and there were 120 genera that were present in nearly all sites but had a low overall abundance. These ubiquitous but rare genera were predominantly from the *Verrucromicrobia* (*Puniceicoccaceae*), *Planctomycetes*, *Deltaproteobacteria* and the *Bacteroidetes* (*Flavobacteriaceae*).



Chapter 2 Figure 2 Bubble plot showing the depth distribution of dominant microbial groups in the SPG. All samples were sorted by depth before plotting.

The microbial community across the SPG varied significantly with depth, but not across geographic distances (Chapter 2 Figure 2, Chapter 2 Figure 3). Samples from the same depth, throughout the SPG, had a highly similar microbial community

composition as indicated in the non-metric multidimensional scaling (NMDS) plot showing the Bray-Curtis dissimilarity between sites (Chapter 2 Figure 3). ANOSIM showed a significant difference with depth ($R = 0.6906$, $P = 0.001$). The highest variability among individual communities of the same depth was seen in the DCM (125 - 250 m).



*Chapter 2 Figure 3 NMDS plot showing the dissimilarity among the microbial communities between individual samples of the SPG. ANOSIM analysis showed a significant difference between microbial communities with depth. Point colour and blue boxes group all samples of a specific depth and highlight dissimilarity at specific depths. Chlorophyll *a* is represented in grey isoclines and shows the depth of the DCM (160 -150 m).*

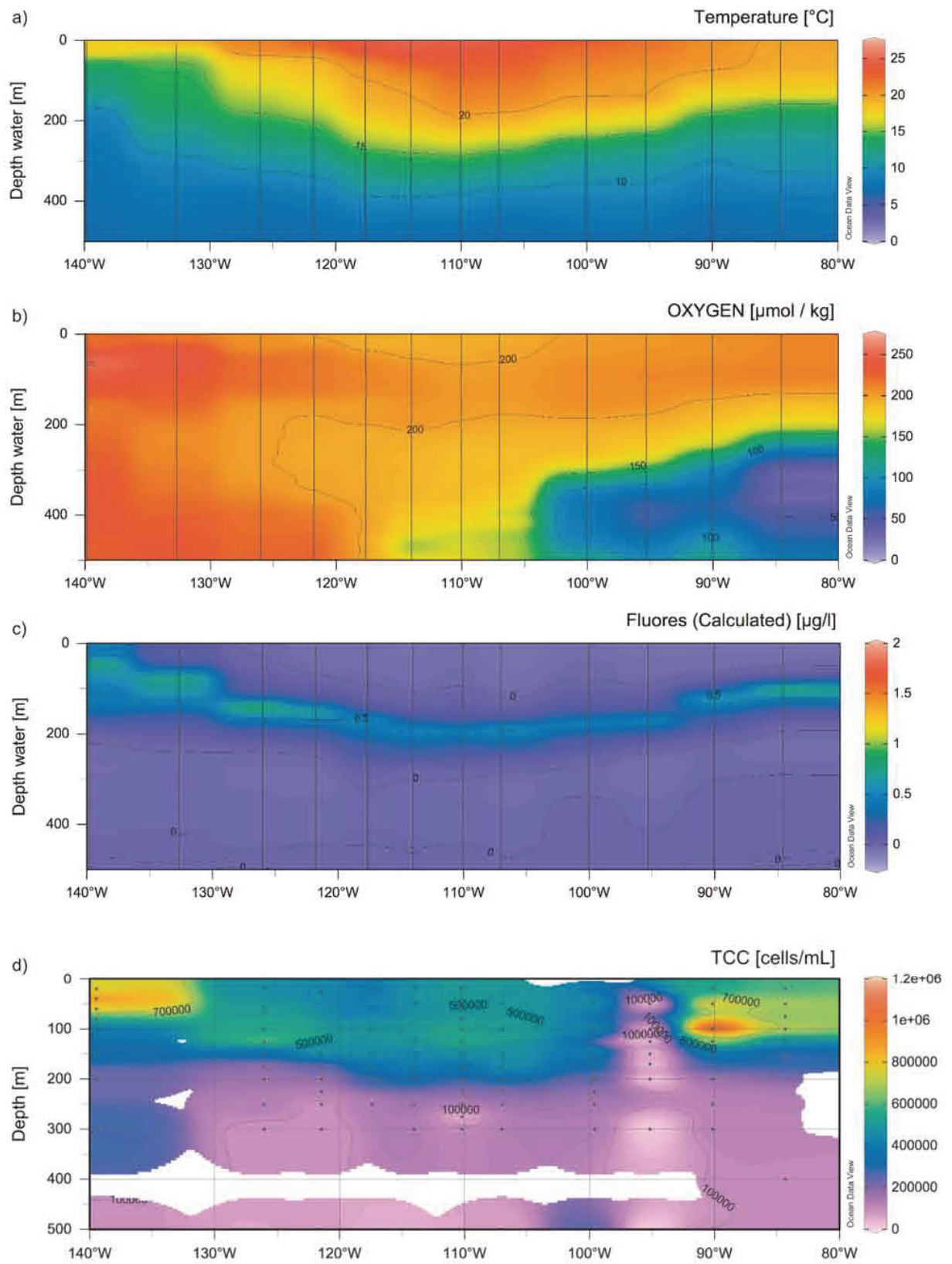
Total Cell Counts and Physico-chemical Analysis of the SPG

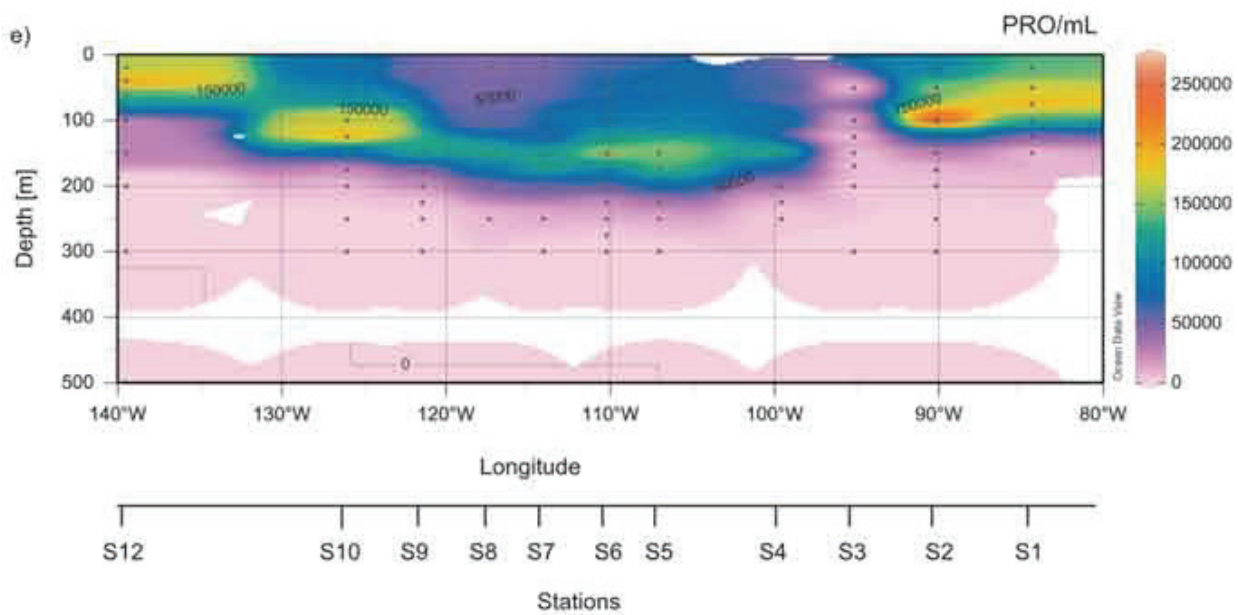
The top 500 m of the SPG exhibited the most variable change in conditions (Chapter 2 Figure 5a-c). The central gyre (100°W – 120°W) had characteristically high temperatures of 20 - 25°C which extended to a depth of 300 m (Chapter 2 Figure 5a). The oxygen concentration increased slightly at the surface towards the New Zealand Coast (140°W) and showed a distinct decrease from 200 to 50 $\mu\text{mol kg}^{-1}$ between 200 - 500 m depth from 80°W to 100°W (Chapter 2 Figure 5b). This is the location of a well-documented oxygen minimum zone (OMZ), where oxygen is depleted due to higher microbial respiration rates in the water column (Canfield et al 2010, Lam et al 2009, Pinti 2014). Fluorescence was highest in the surface waters at 140°W indicating high primary productivity (Chapter 2 Figure 5c). Throughout the SPG there was a detectable band of fluorescence, which descended to a depth of 200 – 250 m within the central SPG (110°W). The physico-chemical profile of the entire water column highlighted that under the top 500 m the physico-chemical parameters stayed relatively consistent (Chapter 2 Figure 5f-h).

Similar results could be seen in the TCC and abundance of *Prochlorococcus* (enumerated using the PRO406 FISH probe). The highest variability in TCC was found in the top 250 m and below 250 m they stayed relatively constant throughout the water column (10^4 cell ml^{-1}) (Chapter 2 Figure 5i). The highest abundance of cells was found at 50 m between 135°W and 140°W and at 100 m depth at 90°W (Chapter 2 Figure 5d). In the central gyre, the TCC were highest at 100 m depth (6×10^4 cell ml^{-1}), although they were also high in the surface waters (5×10^4 cell ml^{-1}).

The *Prochlorococcus* were only present in the top 250 m (Chapter 2 Figure 5e and 8j). Their distribution pattern mimicked that of the DCM. *Prochlorococcus* had a higher abundance in the surface waters (top 100 m) outside of the gyre (80 – 90°W and 130 – 140°W), whereas the gyre the abundance of *Prochlorococcus* was highest at 150 – 200 m.

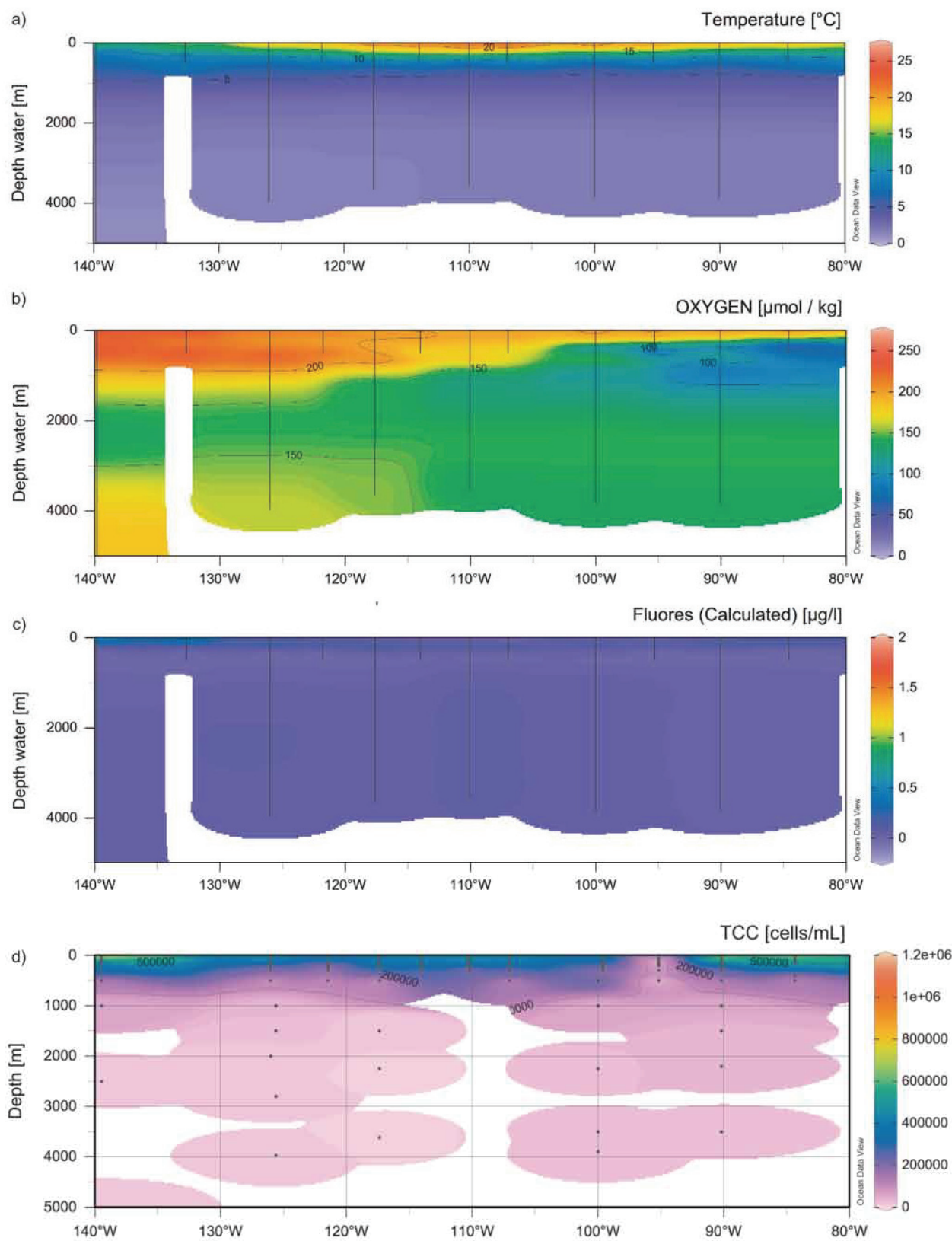
Chapter 2 | On-site microbial diversity and abundance analysis in the remotest part of the world's oceans, the South Pacific Gyre

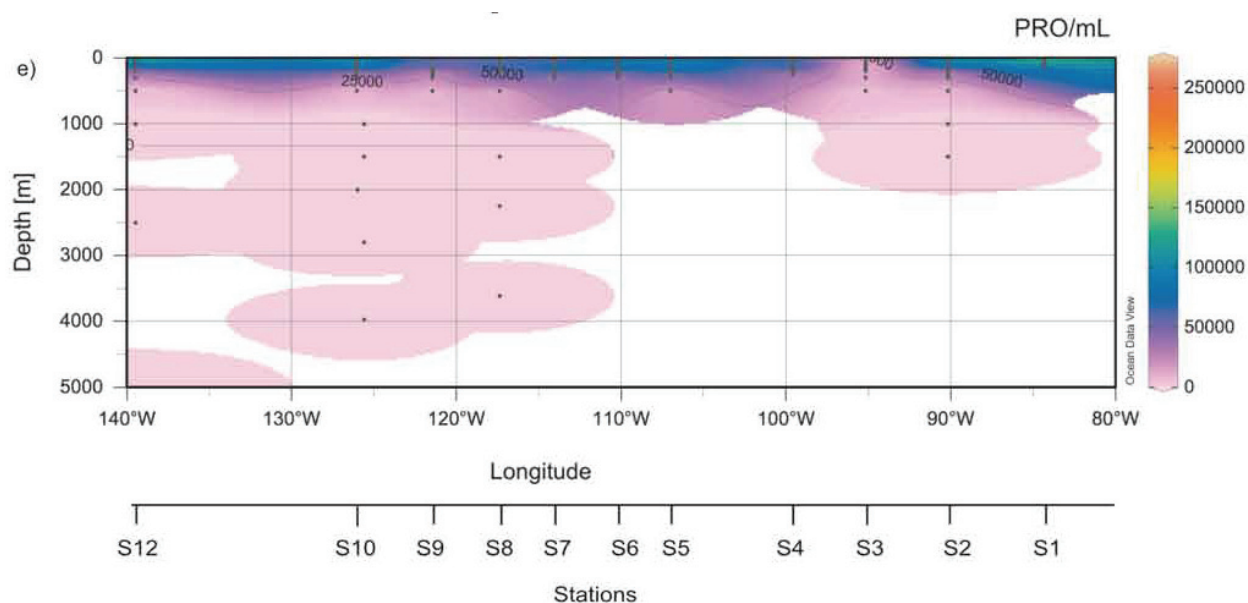




Chapter 2 Figure 4 Contour plots derived from CTD measurements at all stations during the SO245. The plots show physico-chemical data from 0-500 m from stations sampled across the SPG. a) Temperature with depth ($^{\circ}\text{C}$). b) Oxygen concentration with depth ($\mu\text{mol kg}^{-1}$). c) Calculated fluorescence ($\mu\text{g L}^{-1}$). d) Total cellular abundance enumerated by DAPI staining (cell mL^{-1}). e) Total abundance of *Prochlorococcus* enumerated using the FISH probe PRO405 (cell mL^{-1}). The sampling stations are indicated on the axis below the plots.

Chapter 2 | On-site microbial diversity and abundance analysis in the remotest part of the world's oceans, the South Pacific Gyre





*Chapter 2 Figure 5 Contour plots derived from CTD measurements at all stations during the SO245. The plots show physico-chemical data from 0-5000 m from stations sampled across the SPG. a) Temperature with depth ($^{\circ}\text{C}$). b) Oxygen concentration with depth ($\mu\text{mol kg}^{-1}$). c) Calculated fluorescence ($\mu\text{g L}^{-1}$). d) Total cellular abundance enumerated by DAPI staining (cell mL^{-1}). e) Total abundance of *Prochlorococcus* enumerated using the FISH probe PRO405 (cell mL^{-1}). The sampling stations are indicated on the axis below the plots*

Discussion and Conclusion

On-site Analysis of the Microbial Community

We developed a functioning on-board sequencing and data analysis pipeline, which enables the analysis of a microbial community's taxonomic profile ("Who is there") within hours of sampling even in remote locations.

A next generation sequencing platform and all required lab procedures were adjusted to work even under challenging conditions, such as ship-board pitch and roll movements. There was a positive correlation between the absolute cellular abundance and the extracted DNA concentration. The minimum sampling effort required for an in-depth diversity profile of a community using this pipeline required a minimum of 10^4 cells mL^{-1} or for our samples 100 ml – 1 L of seawater. It took a maximum of 48 h (Chapter 2 Supplementary Table 4) from the time of sampling to obtaining a detailed insight into the microbial diversity of the entire water column (20 - 5000 m depth) at a

given station. This pipeline enables the on-site analysis of microbial diversity and drastically minimises the time between sampling and analysis of standard microbial samples.

The pipeline can be combined with other high-throughput methods, such as automated cell enumeration, to obtain both microbial diversity and abundance results on-site (Chapter 1). For example, the pipeline presented here yields an in-depth analysis of microbial diversity. These results can then be used to select group specific FISH probes and enable the enumeration of target microbial clades via automated microscopy (Chapter 1) (Amann et al 2001). Knowing, on-site, if a target organism is present or absent and its absolute cellular abundance allows microbial ecologist to improve and adjust their sampling efforts and experimentation particularly for cultivation efforts, single cell analysis or metagenomics (DeLong 2009, Iverson et al 2012). Additionally, the combined analysis of diversity and abundance has recently been shown to be essential in achieving a comprehensive interpretation of a community, as sequencing data alone is only semi-quantitative (Pros et al 2017).

Alternatively, when combined with flow cytometry, our pipeline allows for the on-site analysis of a sorted population as well as determining the sorting efficiency and pureness of specific sorted cell populations. The ability to obtain a direct insight into the microbial diversity accelerates hypothesis-driven research allowing microbial ecology to move away from sampling just under the premise of understanding “who is there?” and begin to further our understanding of “why they are there?”.

Picoplankton community of the SPG

Using our newly established on-site pipeline we could gain a detailed insight into the ultra-oligotrophic microbial community of the most remote part of the world's ocean. The SPG's microbial community showed a significant change with depth. This trend has also been shown in the North Pacific, South Atlantic and Northern Atlantic Gyres (Agogue et al 2011, Cram et al 2015, DeLong et al 2006, Friedline et al 2012, Hewson et al 2006, Schattenhofer et al 2009). The distinct vertical distribution of microorganisms in the marine environment is linked to the significant changes in the physico-chemical conditions across depths, for example, the change in temperature, oxygen and nutrient concentrations. Additionally, the decrease in the availability of light, with depth, limits photosynthetic primary production and therefore also the availability of labile organic matter (Moran et al 2016, Osterholz et al 2015, Pakulski and Benner 1994).

The low bacterial richness found in the surface waters of the SPG (specifically at 20 – 50 m) is likely due to the extreme nutrient (nitrogen) limited nature of these waters (direct measurements from surface waters (5 m) NO_x $0.041 \mu\text{mol l}^{-1}$, NO_3 $0.038 \mu\text{mol l}^{-1}$, unpublished data). Previous measurements of the surface nitrate showed similarly extremely N-limiting conditions in the top 160 m (Letscher et al 2015, Raimbault et al

2008). Although the surface waters are extremely oligotrophic, we found high cellular abundances (4×10^5 cells ml^{-1}) indicating that specialised oligotrophic organisms do persist. The sequencing results showed that these organisms were predominantly *Prochlorococcus*, SAR11, SAR116, SAR86 and AEGEAN 169 marine group. Specifically, for the SAR11 and SAR86 it is well documented that both are optimised for an oligotrophic lifestyle (Brown et al 2014, Giovannoni and Stingl 2005, Molloy 2012, Swan et al 2013). Single cell analyses of these groups have highlighted genomic streamlining, resource specialisation and heightened resource acquisition abilities (Dupont et al 2012, Gómez-Pereira et al 2012a, Luo and Moran 2015, Molloy 2012, Tripp 2013). Additionally, they are equipped with proteorhodopsins which enable enhanced nutrient uptake via photoheterotrophy (Béjà et al 2000, Giovannoni et al 2005). The dominant organisms in the surface of the SPG are therefore oligotrophic organisms, classifiable as K-strategists, which have adapted to thrive under nutrient-depleted conditions.

The primary autotrophic organisms within the SPG, *Prochlorococcus*, showed higher read and cellular abundances in deeper waters (100 – 150 m). Its lower abundance in surface waters indicated that the nutrient poor conditions may limit its growth or the high irradiance causes inhibited growth (Moore et al 1998, Partensky et al 1993).

The surface water of the SPG had extremely low fluorescence which was below the detection limit in our study but previously measured at 0.017 mg m^{-3} (Ras et al 2008, Zielinski et al 2017). This increased to 0.47 mg m^{-3} in the DCM and could be measured down to nearly 300 m depth, which is remarkably deep. Comparatively measurement taken in the North and South Atlantic Gyres show similar fluorescence concentrations in surface waters and the DCM, although the depth of the DCM in the Atlantic is higher in the water column (North Atlantic Gyre surface: 0.11 mg m^{-3} , DCM (120 m): 0.52 mg m^{-3} and South Atlantic Gyre surface: 0.06 mg m^{-3} , DCM (165 m): 0.66 mg m^{-3}) (Reintjes et al. unpublished – Chapter 3). The previous classification of the SPG as “ultra-oligotrophic” from predictive modelling of primary production using ocean colour data underestimated the total activity due to the extreme depth of the DCM (Ras et al 2008).

In the mesopelagic zone of the SPG, where light becomes limiting, there was a distinct change in the microbial community from SAR11 surface clade 1, SAR86 and *Prochlorococcus* dominated to SAR324, SAR406, and SAR202 dominated. Although there are currently no cultured representatives of these three bacterial groups, metagenomic analyses have revealed some insight into their possible metabolic capabilities. SAR202 and SAR324 have been associated with carbon and sulphur oxidation (Biers et al 2009, Morris et al 2004, Sheik et al 2014, Swan et al 2011) and are likely chemolithoautotrophs ubiquitous in the dark oceans. In particular, SAR324 has also been associated with the degradation of the lipid chains of chlorophyll *a* which may explain its heightened abundance under the DCM (Chitsaz et al 2011). It is possible that the upper mesopelagic community is specialised in recycling the labile

organic matter sinking from the photic zone (Anderson and Tang 2010, Hewson et al 2006, Letscher et al 2015).

In addition to an increase in richness with depth, there was also an increase in richness from the east (Chile) to west (New Zealand). This increase is also linked to changes in the physico-chemical parameters. Specifically, the decrease in surface water temperatures and high increase in fluorescence close to the New Zealand coast indicated higher primary production and labile organic matter input. This was confirmed by the increase in read abundance of the phylum *Bacteroidetes* (*Fluviicola*, *Formosa*, NS9, NS5, NS4) and *Gammaproteobacteria* (SAR92) which are often associated with the hydrolysis of labile organic matter (Buchan et al 2014, Gómez-Pereira 2010, Neumann et al 2015, Teeling et al 2012).

Conclusion

We designed and optimised an on-board sequencing and data analysis pipeline that enabled us to obtain on-site diversity results of the microbial community of the SPG. It gave us a detailed insight into the microbial diversity within 48 hours of sampling. The community composition indicated a dominance of a few key oligotrophic organisms in surface waters, which are adapted to the extreme physico-chemical conditions. The DCM was at a remarkably deep depth but indicated primary productivity similar to that of other oceanic gyres. The ability to obtain “direct” results of the microbial diversity, even in extremely remote sampling sites, will allow microbial ecologists to do more targeted sampling and hypothesis-driven research and further our understanding of the diversity and metabolic capabilities of microorganisms.

Outlook

During the SO245 cruise on board the RV Sonne we did not just develop and test a high-throughput NGS sequencing pipeline. We also used it to perform targeted sampling of unique microbial groups within the SPG. Additionally, we used it to develop further methods to analyse specific microbial communities. These analyses are currently still in-progress and are therefore only discussed here in the outlook.

The obtained read abundance data was used to select FISH probes and enumerate the abundance of specific microbial groups. This was done directly on-board with a fully automated high-throughput image acquisition and cell enumeration system (Chapter 1). Although FISH can be performed without knowing the microbial community composition, it is both time and cost-effective to have prior knowledge of the

bacterial diversity. This enables a more precise selection of FISH probes and prevents unnecessary laboratory work.

Furthermore, we used the NGS pipeline in combination with flow cytometry to sort specific microbial cells and analysed their diversity. Initially, we flow sorted the easily identifiable *Prochlorococcus* and *Synechococcus*, using their fluorescence signal. The sorted populations of *Prochlorococcus* and *Synechococcus* (10,000 cells) were then sequenced using our on-board pipeline. The obtained relative read abundance data was used to analyse the sorting efficiency and purity. If the flow sorted samples showed a high diversity the sorting was repeated with a more stringent sorting gate to obtain a higher purity.

The selected sorting of populations of interest based on their pigment content, cell size or DNA content, in combinations with an on-board NGS pipeline, allows for the taxonomic identification of unusual bacterial groups (size, shape, pigments). This, furthermore, allows for the selected sorting of known populations for single cell genomics or metagenomics analyses.

Acknowledgements

We thank the captain and crew of the RS Sonne for assistance at sea. We also thank Tim Ferdelman the principle scientist of the Ultrapac cruise. Additional thanks go to Andreas Ellrott, Sandi Orlic and Jörg Wulf for technical assistance in the lab and at sea. Thank you to Anke Meyerdirk for helpful discussions about the project. This project was funded by the Max Planck Society.

Chapter 3

Free-living and particle-associated bacteria exist as an interactive assemblage.

Greta Reintjes, Cheng Wang, Jörg Wulf, Bernhard Fuchs, Rudolf Amann

Manuscript in prep.

Abstract

Marine bacteria are categorised into two distinct lifestyles free-living (FL) and aggregate or particle-associated (PA). This categorisation is due to their selective attachment to particulate organic matter (POM), which is a source of nutrients in an otherwise limiting environment. The categorisation of marine bacteria into different lifestyles is often accompanied with a categorisation into different size fractions. This is owing to the method used to separate different fractions of POM; the sequential filtration through filters of varying pore sizes.

We argue here that although bacteria do exhibit distinct lifestyles, the classification of bacteria into size fractions does not necessarily reflect biological relevant categories. We tested this hypothesis by comparing the bacterial community composition and cellular abundance of three size fractions (FL ($> 0.2 \mu\text{m} < 3 \mu\text{m}$), small PA ($> 3 \mu\text{m} < 10 \mu\text{m}$), large PA ($> 10 \mu\text{m}$)) across five oceanic provinces of the Atlantic Ocean. Samples were taken from a wide range of physico-chemical conditions to analyse a diverse range of particles. These included samples from a phytoplankton bloom, where fresh POM was actively being produced and samples from two oligotrophic gyres that had low nutrient conditions and low primary production.

We found that the total cellular abundance of the FL fraction was \sim three orders of magnitude higher than that of the PA fractions ($1 \times 10^6 \text{ cell ml}^{-1}$, $1 \times 10^3 \text{ cell ml}^{-1}$ in the FL and PA, respectively). Diversity analyses showed both differences and similarities in the community composition of each size fraction and we could associate these contradictory results to the relative age of the available particles. From the present study, we suggest that given variations in particle chemistry and the complexity of colonisation and succession patterns on particles, the categorisation of individual bacteria into different “size fractions” is not a biologically meaningful method to categorise the community variations. The method of size fractionation should rather be seen as a tool to analysing the total community composition, as it enables the enrichment and analysis of the low abundant PA community.

Introduction

Vast expanses of the world's oceans are predominantly nutrient limited (Millero 1996, Pilson 2012, Smith 1984) but the seasonal input of high amounts of organic matter, mainly from phytoplankton blooms, prompt significant changes in substrate availability (Biddanda and Benner 1997, Biersmith and Benner 1998, Finkel 2014). Phytoplankton derived organic matter is present in two forms; dissolved organic matter (DOM) and particulate organic matter (POM) (Anderson et al 2015, He et al 2016, Thornton 2014). POM is often viscid (sticky) which leads to the formation of aggregates (Kjørboe et al 1990). Due to their sticky nature, aggregates often bind

further material such as living and dead marine phytoplankton or zooplankton cells, transparent exopolymeric particles, faecal pellets and inorganic minerals (Grossart and Simon 1993, Turner 2015). They range in size from $< 1 \mu\text{m}$ to 10 cm and can be present to an abundance of < 1 to 10^8 L^{-1} (Alldredge et al 1993, Logan et al 1995, Pilska et al 1998, Wells and Goldberg 1991). Aggregates are a source of organic matter in an otherwise largely limiting environment and are therefore rapidly colonised by selective marine bacteria from the surrounding water column (Datta et al 2016). These bacteria remineralise the aggregates, which has a significant impact on global nutrient and carbon cycling (Huston and Deming 2002, Lyons and Dobbs 2012, Simon et al 2002).

The attachment of selective groups of bacteria to aggregates has resulted in a general categorisation of marine bacteria into two distinct lifestyles; free-living (FL) and aggregate- or particle-associated (PA). The PA fraction is often further categorised into different size fractions owing to the method used to separate them; sequential filtration through filters of varying pore sizes (Mestre et al 2017, Padilla et al 2015). The distinction between size fractions is drawn because FL and PA bacteria are exposed to different selective forces (e.g. nutrient availability) which are assumed to gradually drive the organisms to become phylogenetically and functionally distinct (Luo and Moran 2015, Rösler et al 2012, Zhang et al 2007).

FL bacteria are defined as pelagic bacteria adapted for growth in low nutrient and substrate levels, such as the SAR11, SAR86 or *Prochlorococcus* (Flombaum et al 2013, Luo and Moran 2015, Malmstrom et al 2013, Morris et al 2002, Partensky et al 1999, Tripp 2013). FL cells often have smaller genomes with fewer gene copies, lower metabolic potential and fewer genes encoding transcription and signal transduction (Dupont et al 2012, Morris et al 2012, Swan et al 2013). Additionally, they often contain high numbers of transporter genes with high affinities (Tripp 2013).

Contrastingly PA bacteria typically have a high metabolic versatility, high hydrolysis activity and large genomes with an array of substrate utilisation and uptake genes (Lyons and Dobbs 2012, Simon et al 2014). These organisms are predominantly heterotrophic, with specialisations for complex organic molecule degradation, such as those found in aggregates (Grossart and Simon 1993, Simon et al 2002).

Diversity analyses between different size fractions show clear distinctions between the microbial assemblages (Mestre et al 2017, Milici et al 2017, Rieck et al 2015, Rösler et al 2012, Suzuki et al 2017). However, there is also contrasting evidence showing similarities among the communities across all size fractions (Crespo et al 2013, Hollibaugh et al 2000, Rieck et al 2015). In fact, some bacteria are known to be able to switch between lifestyles depending on chemical triggers and substrate availability (Grossart 2010, Pruzzo et al 2005). Additionally, a large fraction of marine bacteria are motile and show chemotaxis toward substrate hotspots and could therefore exist both as FL and PA (Grossart et al 2001, Kjørboe et al 2002, Seymour et al 2009).

Bacteria exhibit distinct lifestyles, however, we hypothesise that the distinction between multiple different “size fractions” is arbitrary and that they do not reflect

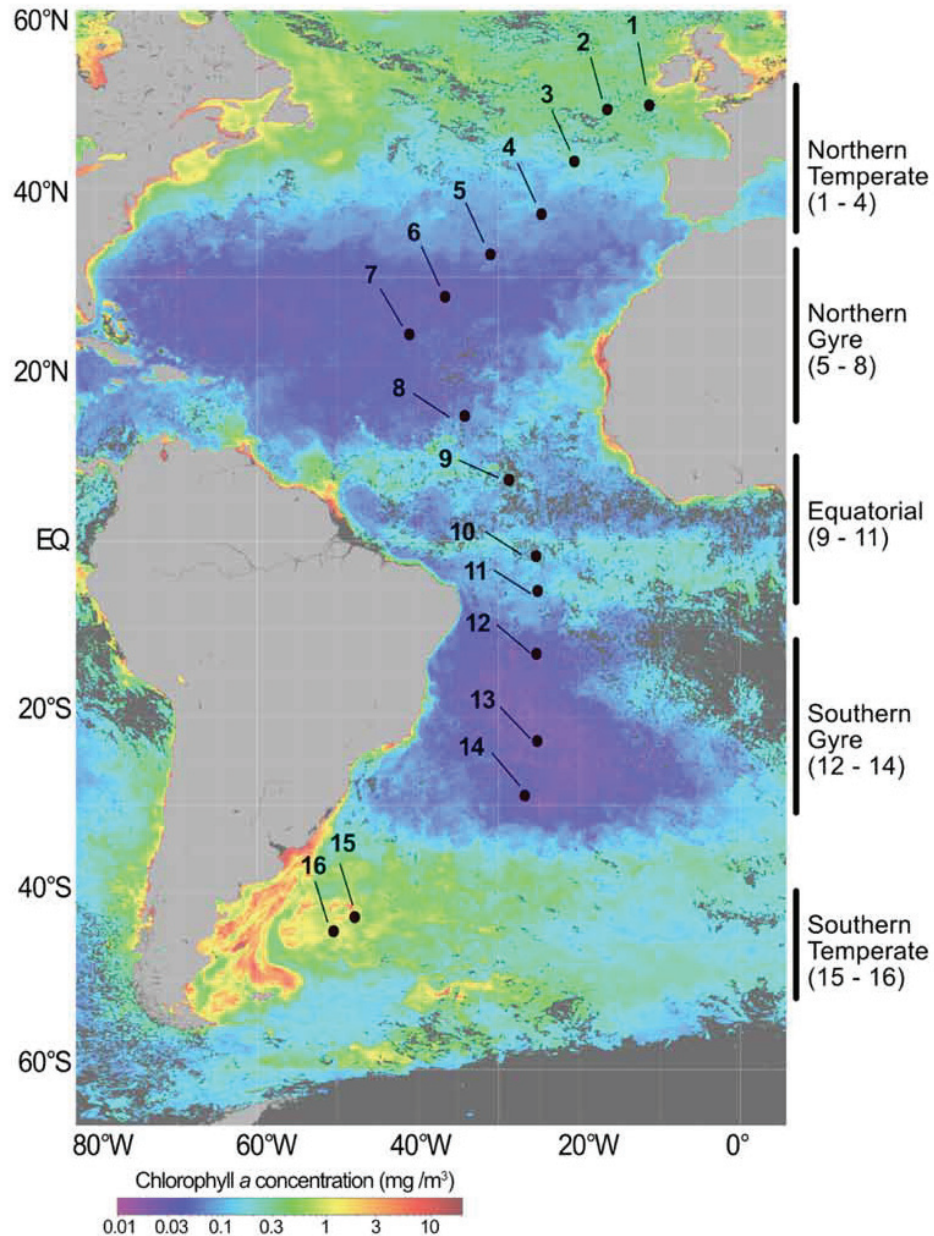
biological entities. Rather bacteria are specialised to FL, PA or intermediate lifestyles and are therefore part of an interacting assemblage. Additionally, we hypothesise that variations in the PA community are not due to the individual size of particles but due to variations in the chemical composition and age of the particles. We tested these hypotheses by analysing the community composition between different microbial lifestyles using 16S rRNA sequencing and combining this with fluorescence *in situ* hybridisation (FISH) to visualise and enumerating the abundance of phylogenetically distinct bacterial groups. We did this across five distinct oceanic provinces of the Atlantic Ocean, in one of which a phytoplankton bloom was actively progressing resulting in increased organic matter production. The distinct variability between the physico-chemical parameters and level of organic matter input in the provinces should allow for a detailed comparison between the microbial assemblages.

Methods

Sampling

Planktonic seawater samples were taken during the Atlantic Meridional Transect (AMT) 22 cruise, on the RRS James Cook (Southampton, UK, to Punta Arenas, Chile, 10 Oct to 24 Nov 2012). Samples were taken using a rosette of 20 L Niskin bottles with an attached Sea Bird CTD (Sea Bird Scientific). A total of 16 stations were sampled at 20 m water depth at solar noon for microbial community analysis (Chapter 3 Figure 1). From each sampling site between 15 L to 45 L of seawater was sequentially filtered onto 142 mm diameter polycarbonate filters with pore sizes of 10 μ m (Large-PA), 3 μ m (Small-PA) and 0.2 μ m (FL). Different volumes of seawater were sampled to prevent filter clogging. Specifically, at sites where previous studies have shown high cell counts, lower volume of water was filtered (Schattenhofer et al 2009, Tarran et al 2006, Zubkov et al 2000). These filters were stored at -80°C until further analysis. For FISH analysis of the FL fraction 1 L of seawater was sampled from 37 stations at 20 m depth at solar noon. The samples were fixed using formaldehyde to a final concentration of 1% for 1 h at RT. Triplicate 20 ml subsamples were filtered through a 47 mm diameter polycarbonate filters with a pore size of 0.2 μ m, applying a

gentle vacuum of < 200 mbar. These filters were left to air dry and stored at -20°C until further analysis.



Chapter 3 Figure 1 Sampling sites across different oceanic regions in the Atlantic Ocean during the AMT 22 cruise. Sampling sites (1 – 16) are indicated by black dots and oceanic regions with corresponding stations are shown on the side of the map. Map colouring shows the productivity of the regions using chlorophyll concentrations (map obtained from MODIS, (Ocean Biology Processing Group 2014))

Physico-chemical Data

The AMT22 passed through several oceanic provinces (Longhurst 2007), which for this study, were classification into the Northern Temperate, Northern Gyre, Equatorial, Southern Gyre and Southern Temperate. The biogeographical provinces were identified using their physical, chemical and biological characteristics (Chapter 3 Figure 2). These were measured at every CTD sampling station from 0 m to 500 m depth. Temperature ($^{\circ}\text{C}$) was measured using a Sea-Bird 3 premium temperature sensor (Sea Bird Scientific). Dissolved oxygen (ml L^{-1}) was measured using the Sea-Bird 43 dissolved oxygen sensor (Sea Bird Scientific) and calibrated against Winkler titration measurements from 9 samples collected at the pre-dawn CTD. Conductivity (S m^{-1}) was measured using a Sea-Bird4 conductivity sensor (Sea Bird Scientific). Fluorescence (mg m^{-3}) was measured using a CTG FAST track Fast Repetition Rate fluorometer (Chelsea Technologies Group, UK) and calibrated against extracted chlorophyll-*a* measurements made on seawater samples collected from 9 depths at each station. Pressure (mbar) was measured using a Digiquartz pressure sensor (Paroscientific, Inc., WA, USA) suspended below the CTD. Salinity (PSU) was measured using a Guideline Autosol 8400B salinometer (OSIL, UK) and calibrated against bench salinometer measurements from 4 samples collected from each cast (all metadata is available via the BODC website <https://www.bodc.ac.uk/data/documents/cruise/11427/>). The physico-chemical data were analysed using the ODV4 software (www.odv.awi.de).

DNA Extraction

Microbial DNA was extracted using the MoBio Ultra Clean Soil DNA Extraction Kit (MoBio Laboratories) as recommended by the manufacturer with the following alterations. Instead of soil a fixed size (150 mm x 250 mm) polycarbonate filter piece was directly added to the Bead Solution Tubes.

Sequencing

Sequencing was carried out on a 454 Titanium FLX (ROCHE, CT, USA) and Ion Torrent PGM (Thermo Fisher). Two sequencing platforms were used to reduce possible biases between the two methods and PCR biases. The 454 Titanium FLX is a pyrosequencing method whereas the Ion Torrent PGM measures pH changes from the release of a proton during the incorporation of a dNTP into a DNA polymer. Where possible samples were sequenced on both platforms to increase the accuracy (reduce sequencing bias) and yield per sample. Sequencing reads were analysed using

the SilvaNGS pipeline and results were pooled for total community analysis per sample.

PCR and Sequencing on 454 Titanium FLX

PCR was carried out in a total volume of 50 µl using the primers S-D-Bact-0341-b-S-17 (5'-CCTACGGGNGGCWGCAG-3') and S-D-Bact-0785-a-A-21 (5'-GACTACHVGGGTATCTAATCC-3) targeting the V3 - V4 variable region of the 16S rRNA, evaluated by (Klindworth et al 2013). The master mix components and concentrations are shown in Chapter 3 Supplementary Table 1. The master mix and DNA was incubated in a thermocycler (Mastercycler Tm gradient, Eppendorf, Hamburg, Germany) with the program indicated in Chapter 3 Supplementary Table 1. Subsequently, the PCR products were visualised by gel electrophoresis (1% LE agarose, Biozyme). Amplicon bands were visualised using a transilluminator DR - 45M (Clare Chemical Research) and cut out with a sterile scalpel. The gel slices were purified using the QiagenMinElute kit (Qiagen). After purification, the PCR products were pooled into libraries with a minimum DNA concentration of 1 µg DNA as measured using a Qubit assay (Invitrogen, Darmstadt, Germany). The libraries were then sent to the Max-Planck Institute for Plant Genomics in Cologne, for sequencing on a ROCHE 454 titanium FLX (ROCHE).

PCR and Sequencing on Ion Torrent PGM

PCR was carried out as described in detail in (see Chapter 2: Polymerase chain reaction (PCR)).

Size Selection

After PCR the amplicons were size selected on 2% E-Gel size select gels using the E-Gel iBase Power System and E-Gel Safe Imager Real Time Transilluminator (Thermo Fisher). Amplicons were run on a gel for 17 - 18 min using a Low Range DNA Ladder (Thermo Fisher) as a reference. Amplicons were extracted directly from the gel by adding 20 µl of low TE buffer to the extraction well. The extraction was repeated 5 times for each sample to increase the yield. Subsequently, the size-selected amplicons were cleaned up and concentrated over silica column using the Qiagen QIAquick PCR purification kit (Qiagen).

The amplicon concentration and quality were quantified using a Fragment Analyser (AATI) and the DNF - 472 standard sensitivity NGS fragment analysis kit (1 bp – 6,000 bp). After quantification, the amplicons were pooled as described in the Ion Amplicon Library Preparation (Fusion Method) Manual.

Ion Torrent Sequencing

Ion Torrent sequencing was carried out as recommended by the manufacturer and as described in detail in Chapter 2 (Ion Torrent Sequencing). Sequencing was undertaken on ION 314 v2 chips (Thermo Fisher) and the Torrent Suite software was used for all initial quality trimming and analysis.

Sequence Processing using SilvaNGS

The sequence reads from the Ion Torrent PGM (Thermo Fisher) and 454 Titanium FLX (Roche) were further processed using the bioinformatics pipeline of the SilvaNGS project (Quast et al 2013). This involved quality controls for sequence length (> 200 bp) and the presences of ambiguities ($< 2\%$) and homopolymers ($< 2\%$). The remaining reads were aligned against the SSU rRNA seed of the SILVA database release 115 (Quast et al 2013). The classification was done by a local BLAST search against the SILVA SSURef 115 NR database using `blast -2.2.22 +` with standard settings.

Statistical Analysis and Diversity Analyses

Statistical analyses were carried out using normalised read abundances and a classification to genus level. Community dissimilarity was calculated using Bray-Curtis and subsequently plotted using NMDS in the Vegan (Oksanen et al 2013) package of R project (R Development Core Team). Significance tests, analyses of site-specific community composition differences and correlations to environmental factors, were done using ANOSIM and Mantel tests in the Vegan package.

Total Cell Counts (TCC), FISH and Microscopy

All sample filters were analysed using CARD-FISH. Total bacterial abundance (EUBI-III (Amann et al 1990)) and the cellular abundance of three major phyla were enumerated using phylum specific FISH probes (*Bacteroidetes* (CF319a (Manz et al 1996)), *Gammaproteobacteria* (GAM42, (Manz et al 1992)) and *Cyanobacteria* (CYA664 (Schönhuber et al 1999))). The filters were processed as described in Chapter 1. After CARD-FISH the filters were counterstained with DAPI and mounted using a Citifluor (EMS, USA) Vectashield (Vector Laboratories, UK) (v/v) (4 : 1) mounting solution. CARD-FISH and DAPI stained cells were visualised and manually enumerated on a Zeiss Axioskop 2 motplus fluorescence microscope. In addition to manual analysis, the filters were also counted automatically using a fully automated

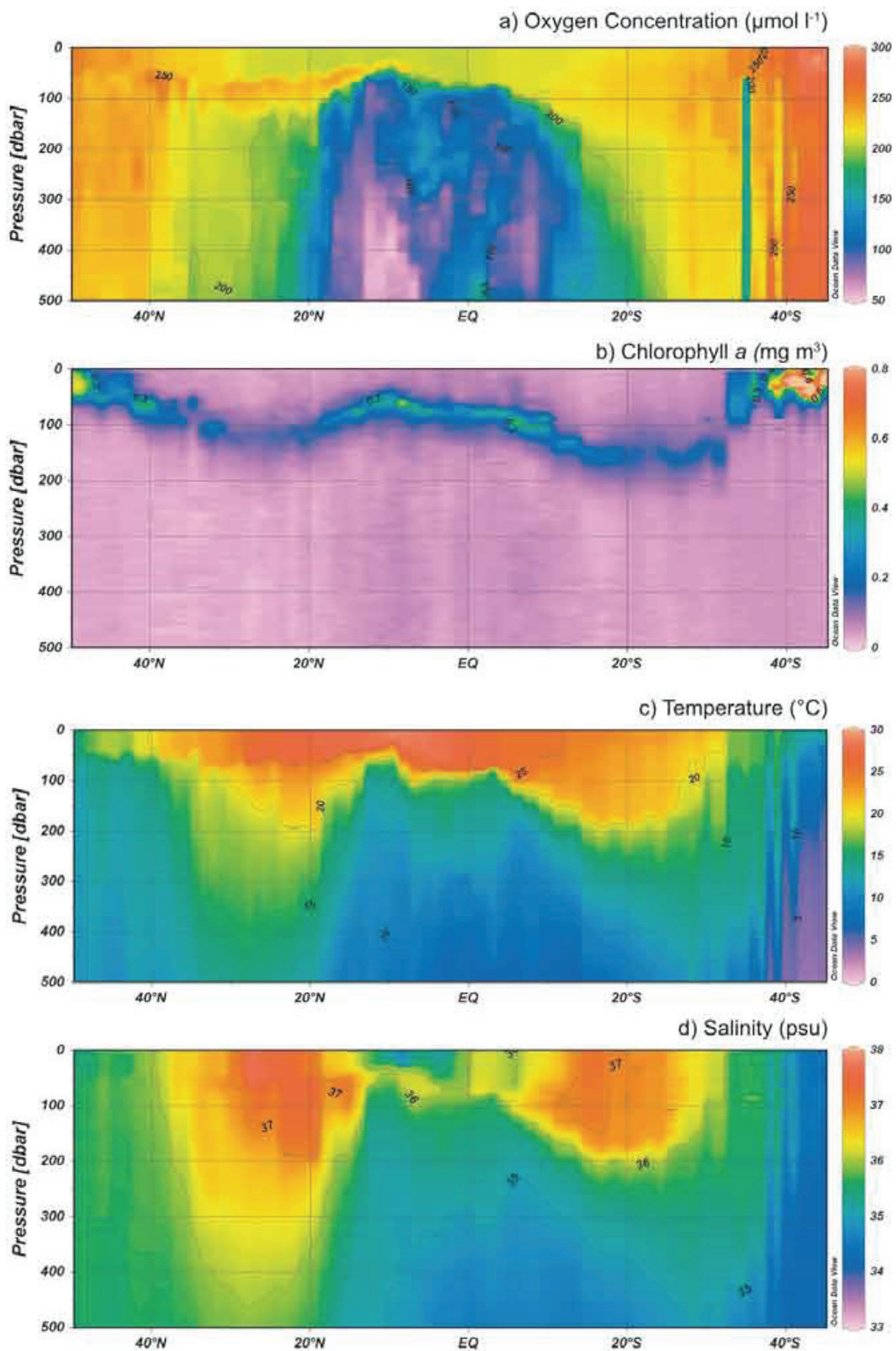
image acquisition and cell enumeration system described in detail in Chapter 1. For our evaluation FISH positive signals for each probe were determined by an overlapping (30% minimum overlap) signal of both DAPI (360 nm) and FISH (488 nm), with a minimum area of 17 (DAPI) or 30 (FISH) pixels (0.17 - 0.3 μm^2) and minimal signal background ratio of 1 (DAPI) or 2.5 (FISH).

Results and Discussion

Physico-chemical Characteristics of the Atlantic Ocean

The Atlantic Ocean can be separated into several distinct provinces with varying physico-chemical conditions, which select for adapted microbial communities (Chapter 3 Figure 2). There are two oligotrophic gyres characterised by high surface temperatures (20 – 25°C), high salinity (37 psu) and low nutrient availability (specifically nitrate and phosphate (Chapter 3 Supplementary Figure 1)). The high temperatures and salinity of the surface waters cause the formation of a thermocline resulting in nutrient depletion. This reduces primary production and organic matter availability in the surface waters. In the central equatorial province, however, there are high surface temperatures but low salinity due to high precipitation rates. Finally, there are two temperate provinces that experience the seasonal mixing of water masses and high nutrient concentrations. Consequently, there are seasonal phytoplankton blooms and high organic matter production in surface waters. During our sampling campaign, the S. Temperate province had particularly low surface water temperatures (10 – 7°C) and high nitrate and phosphate concentrations indicating mixing with cold nutrient rich bottom waters (Chapter 3 Figure 2, Chapter 3 Supplementary Figure 1). Due to the high nutrient availability, there was high surface chlorophyll *a* concentrations (4 mg m^{-3}) indicating high primary production.

Chapter 3 | Free living and particle associated bacteria exist as an interactive assemblage



Chapter 3 Figure 2 Contour plots derived from CTD measurements from 0 to 500 m depth (shown as pressure) at all stations during the AMT22 research cruise (shown as latitude on the x-axis). a) Oxygen concentration ($\mu\text{mol L}^{-1}$). b) Chlorophyll a concentrations (mg m^{-3}). c) Seawater temperature ($^{\circ}\text{C}$). d) Salinity (psu).

Sequencing Statistics and Diversity Indices

An average of 10,000 reads per samples were obtained using an Ion Torrent and Roche 454 sequencing platform (median 9,400). The highest richness was found in the FL size fraction and the lowest richness was found in the large PA size fraction (Chapter 3 Table 1). Similar results have previously been found by Acinas et al (1999), Ghiglione et al (2007), and Hollibaugh et al (2000). However, these results contradict other studies that have highlighted higher richness in large PA size fractions (Mestre et al 2017, Rieck et al 2015, Suzuki et al 2017).

Chapter 3 Table 1 Statistical analysis of bacterial richness and diversity calculated from relative read abundances. Samples were taken from three size fractions along the AMT22 (free-living – FL, small particle-associate (3 μm filter pore size) – small PA and large particle-associated (10 μm filter pore size) – large PA)

	Richness	Shannon Index	Simpsons Index	Evenness
Total average	229	3.46	0.93	0.64
FL	246	3.34	0.92	0.61
Small PA	236	3.72	0.95	0.69
Large PA	196	3.26	0.9	0.62

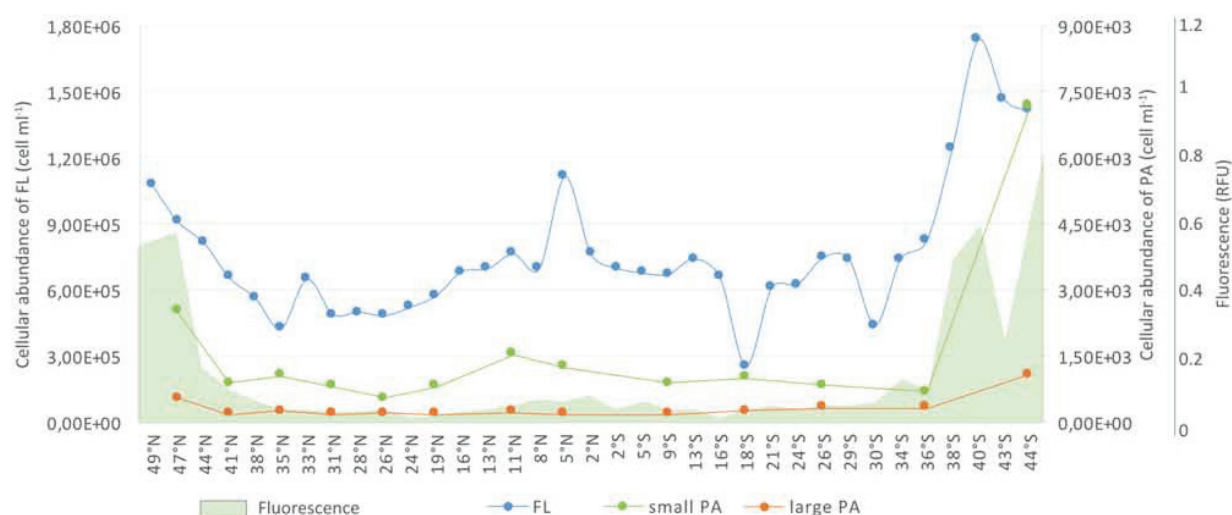
Cellular Abundance

The total cellular abundance of bacteria (enumerated using the FISH probes EUB I-III) in the FL fraction was ~three orders of magnitude higher than in the PA fractions (average abundance: $1 \times 10^6 \text{ cell ml}^{-1}$, $1 \times 10^3 \text{ cell ml}^{-1}$, $3 \times 10^2 \text{ cell ml}^{-1}$, in the FL, small PA and large PA, respectively) (Chapter 3 Figure 3). The absolute abundance of *Bacteroidetes*, *Gammaproteobacteria* and *Cyanobacteria* showed the same trend with higher cellular abundance in the FL in comparison to the PA size fraction (Chapter 3 Supplementary Table 2). The extremely low abundance of individual bacterial groups

Chapter 3 | Free living and particle associated bacteria exist as an interactive assemblage

on particles throughout the Atlantic Ocean suggests that there is a high number of selective niches on particles and that PA bacteria are part of the “rare” biosphere (Sogin et al 2006). The rare biosphere is often associated with heightened metabolic activity and potential, which is also true for many PA bacteria (Campbell et al 2011, Kellogg and Deming 2014, Lyons and Dobbs 2012, Shade et al 2014, Simon et al 2014). Their high metabolic potential means that PA bacteria play an important role in organic matter turnover as well as nutrient cycling, particularly of POM (Arnosti et al 2012, Kellogg and Deming 2014, López-Pérez et al 2016). As POM is remineralised and solubilised it becomes available as DOM for other organisms fuelling biochemical cycling (Milici et al 2017).

There was a significant increase in the TCC of all size fractions in the Southern Temperate stations. This increase was positively correlated to the total fluorescence ($r = 0.77$, $r = 0.92$, $r = 0.95$ for FL, small PA and large PA respectively). In the Southern Temperate stations, bacterial growth was stimulated in all size fractions by the increase in available nutrient and organic matter due to higher primary production.



Chapter 3 Figure 3 Plot showing the total cell counts (enumerated by DAPI staining) within each size fraction (FL (blue), small PA (green), large PA (orange)) at sampling stations along the AMT22 (latitude along the x-axis). The left y-axis shows the cellular abundance of the FL size fraction. The right y-axis shows the cellular abundance of the two PA size fractions. The light green background overlay shows the average surface fluorescence at each sampling site.

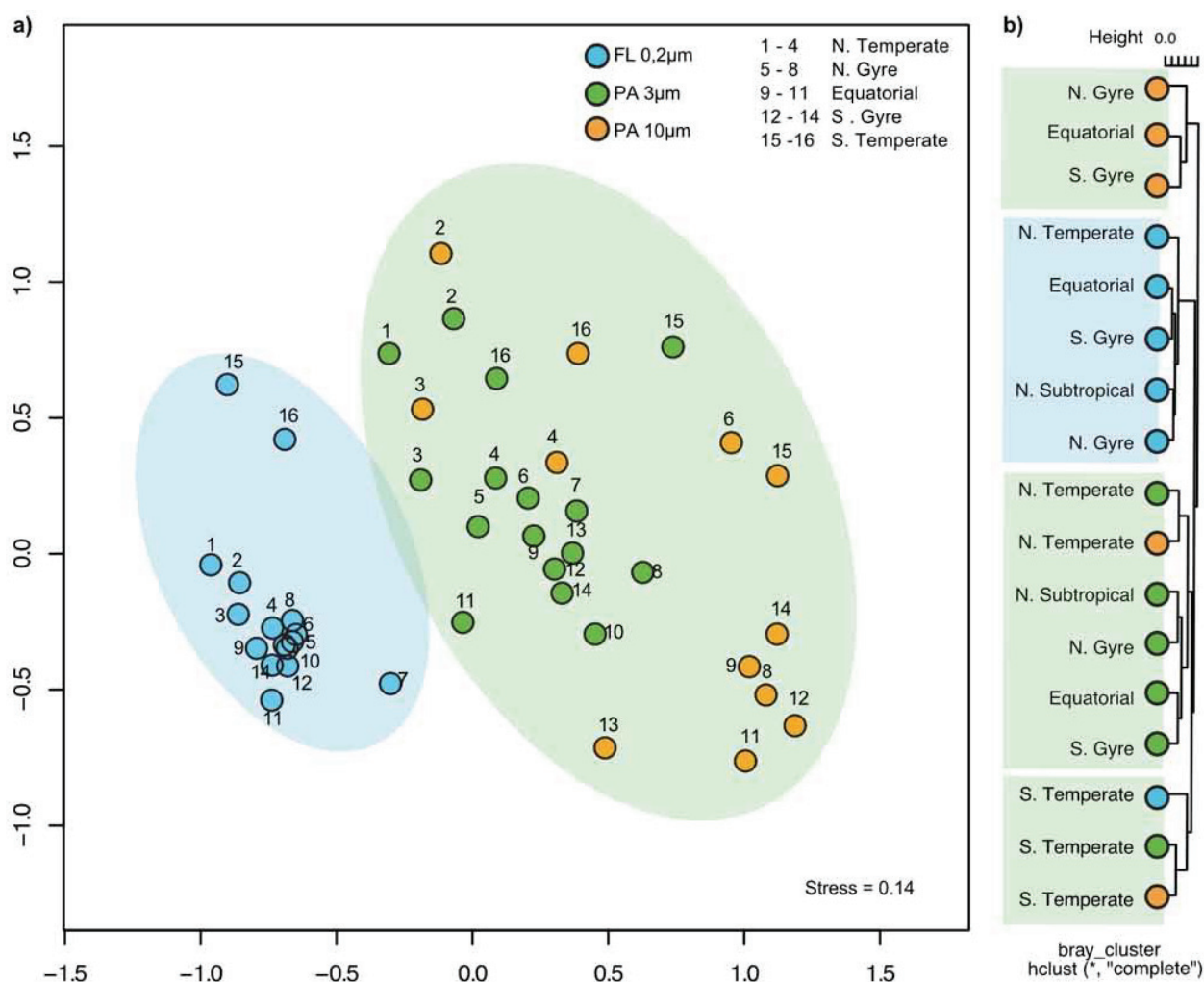
Bacterial Community Composition Based on Sequencing Data

The bacterial community of the Atlantic Ocean was dominated by a few key phyla, specifically the *Proteobacteria*, *Cyanobacteria*, *Actinobacteria* and *Bacteroidetes*. Similar results have previously been shown by (Friedline et al 2012, Yilmaz et al 2012, Zinger et al 2011). The FL community consisted of predominately oligotrophic organisms (SAR86, SAR11, SAR116, AEGEAN 169, *Prochlorococcus* and Candidatus *Actinomarina*), which were present in high read abundances (Chapter 3 Figure 5). These organisms are known for their specialisation in resource acquisition in low-nutrient environments such as the open ocean gyres (Molloy 2012, Morris et al 2012, Rappe' et al 2002, Yang et al 2016). The FL community showed no biogeographical distribution pattern, except in the S. Temperate stations where a pronounced change in the FL community composition could be seen. The abundance of the previously dominant groups SAR11, SAR116, *Prochlorococcus* and Candidatus *Actinomarina* decreased while *Formosa*, *Polaribacter*, uncultured *Flavobacteria*, *Rhodobacteraceae* and SAR92 increased (Chapter 3 Figure 5). Cluster analysis and NMDS showed that all FL samples had a high degree of similarity and clustered closely together, except for the FL sample from the S. Temperate stations (Chapter 3 Figure 4) in this region. The pronounced changes in physico-chemical parameters (increased primary production and nutrient availability) in the S. Temperate stations caused significant changes within the FL bacterial community. The change from dominantly oligotrophic to dominantly copiotrophic organisms indicated that the community composition of the FL size fraction can change significantly depending on the physico-chemical conditions. Previous studies have shown similar pronounced changes in the FL community particularly during algal blooms where there is a change in the DOM and POM abundance and composition (El-Swais et al 2014, Tada et al 2011, Teeling et al 2012, Teeling et al 2016).

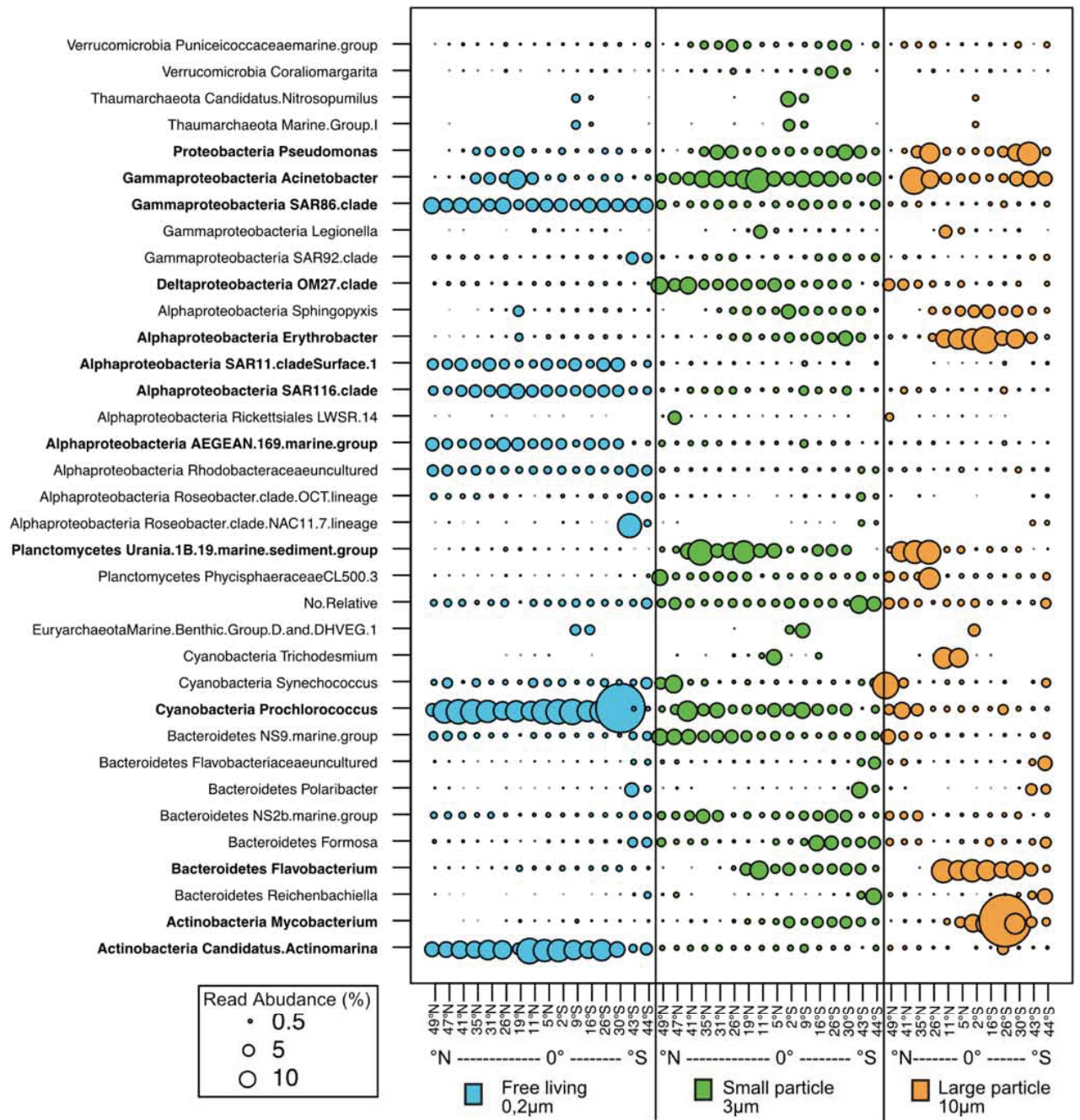
The PA communities were dominated by *Verrucomicrobia*, *Planctomycetes*, *Deltaproteobacteria*, *Gammaproteobacteria* and *Bacteroidetes* (Chapter 3 Figure 5). There was a high degree of dissimilarity between the PA communities (Chapter 3 Figure 4). They consisted predominantly of organisms associated with attachment or organic matter degradation which has also been shown in previous analyses of the PA size fraction (Buchan et al 2014, Lage and Bondoso 2014, Milici et al 2017). A distinct change in the PA community was observed in the S. Temperate stations (Chapter 3 Figure 5). There was an increase in the abundance of *Bacteroidetes* and *Rhodobacteraceae* and a decrease in the abundance of *Deltaproteobacteria* and *Planctomycetes*. Cluster analysis of all stations indicated that the FL, small PA and large PA bacterial communities of the S. Temperate stations were highly similar to each other (Chapter 3 Figure 4).

Chapter 3 | Free living and particle associated bacteria exist as an interactive assemblage

At the time of sampling, the S. Temperate stations were experiencing a phytoplankton bloom during which organic matter (DOM and POM) is released into the water column. This increase in available organic matter prompted a significant increase in the TCC (Chapter 3 Figure 3) and a change in the community composition of both the FL and PA size fractions to organisms with a specialisation in complex organic matter degradation, particularly the *Bacteroidetes* (Chapter 3 Figure 5).



Chapter 3 Figure 4 a) NMDS plot (stress 0.14) showing the dissimilarity between the microbial communities of different sampling stations. The dot colours represent the size fraction of each sample (blue = FL, green = small PA, orange = large PA). The ellipsoids represent the clustering of the samples within a size fraction (blue = FL, green = PA). The numbers beside the dots indicate the sample locations 1-4 N. Temperate, 5-8 N Gyre, 9-11 Equatorial, 12-14 S. Gyre and 15-16 S. Temperate stations. b) Bray-Curtis cluster analysis of the microbial community between size fraction and stations (the colour scheme is the same as used in the NMDS plot).



Chapter 3 Figure 5 Bubble plot of genera with a minimum normalised relative read abundance of 0.5%. The size of the bubbles indicates the average relative abundances (%) of each genus in each sample. The plot is separated and coloured by size fraction: blue = FL, green = small PA, orange = large PA. Samples within each size fraction are shown across latitude (49°N – 44°S).

The overall ANOSIM results show a significant difference between the FL and PA community compositions ($r^2 = 0.667$, $P = 0.0009$). However, there was also a high degree of overlap between each size fraction, especially under specific physico-chemical conditions such as in the S. Temperate station. The increased similarity among the size fractions in this region indicated that there were similar selection forces acting on all size fractions or that there was an active exchange between the size fractions in the S. Temperate stations.

Any particles in the water column, including live (phytoplankton) cells, are colonised initially by motile or non-motile FL bacteria (Bennke et al 2013, Dang and Lovell 2000, Datta et al 2016). Therefore, the POM produced in the S. Temperate station was colonised by FL bacteria, explaining their increased abundance in the PA size fraction. Equally, PA bacteria are not necessarily fixed to a particle but can exhibit hop-on, hop-off behaviour and therefore be present in multiple size fractions (Kjørboe et al 2003, McCarter 1999). In fact, for some *Bacteroidetes* species (*Polaribacter dokdonensis* (MED 134) and *Leeuwenhoekiella blandensis* (MED217)) alternated between lifestyles. They can attach to surfaces and use complex organic matter such as polysaccharides and proteins (Fernández-Gómez et al 2013) and during times of organic matter limitation, they can switch to a free-living lifestyle using proteorhodopsins to obtain energy from light (Béjà et al 2000, Fernández-Gómez et al 2013, González et al 2008). The apparent interchangeability of bacteria between different size fractions would explain the high overlap in community composition between different size fractions found in our study and multiple others (Crespo et al 2013, Hollibaugh et al 2000, Mestre et al 2017, Milici et al 2017).

An additional factor that should be considered is the particles' chemical composition. López-Pérez et al (2016) found that different types of particles (diatomaceous earth, sand, chitin and cellulose) are colonised by different communities of bacteria. The “new” particles produced in the S. Temperate station are predominantly phytoplankton-derived organic matter and select for specific heterotrophs in both the FL and PA fraction. Specifically, there was an increase in the abundance of *Bacteroidetes* which are often associated with phytoplankton-derived organic matter (Teeling et al 2012). The high dissimilarity between the S. Temperate PA community and the PA communities of the other stations indicated that particles in different oceanic provinces may vary in chemical composition and therefore select for different bacterial groups.

Another reason for the high variability between the PA communities could be due to succession patterns occurring during particle colonisation (Datta et al 2016). Analysis of bacterial colonisation of chitin particles demonstrated that PA bacteria undergo rapid succession patterns (Datta et al 2016). Motile bacteria that can use the particles as a resource are the initial colonisers. Subsequently, secondary consumers colonise the particle, likely because they are attracted by the metabolites produced by the primary colonisers rather than the particle composition (Datta et al 2016). The colonisation of “new” particles in the S. Temperate station by predominantly

Bacteroidetes may represent an initial colonisation by organisms using the particle as a resource (i.e. polysaccharides, proteins). The communities of particles in other regions, such as in the Gyres, represent a more established but variable community of secondary colonisers. Sampling different size fractions at a specific point in time give only a snapshot of the current part of a continuous succession pattern. To fully comprehend the differences in the community composition between different PA size fractions it is necessary to also understand chemical composition and age of the particles.

Conclusions

The selective attachment of marine bacterial to particulate organic matter has resulted in their categorization into different size fractions. However, this is likely too simple a categorisation given the complexity of colonisation and succession patterns on particles, as well as the variations in particle biochemistry and the potential for lifestyle interchangeability of bacteria. Additionally, the physical size of a particle is unlikely to determine the attachment of a bacterium to a particle. The method of size fractionation should rather be seen as a means of “enriching” the rare but active PA community allowing for an in-depth analysis of the full metabolic capability and potential of a microbial assemblage.

Outlook

This manuscript has not been submitted for peer review, as further work is currently underway to address some of the questions highlighted in the discussion. Specifically, we are currently attempting to classify the chemical composition of the particles using lectin staining (Bennke et al 2013). Lectins are carbohydrate-binding proteins that bind to extracellular polymeric substrates and glycoconjugates. They are commercially available as fluorescently labelled lectins and can be combined with super-resolution structured illumination microscopy to visualise the substrates and glycoconjugates of a particle. In a previous study, Bennke et al (2013) tested seventy-seven commercially available lectins for their binding efficiency and sensitivity to marine phytoplankton cells and macro aggregates. Twelve of these showed specific binding to marine particles and their specificity covered several substrates, specifically galactose, sialic acid, N-acetyl-galactosamine, fucose and mannose. Using these lectins the chemical composition of the particles across the Atlantic Ocean is being analysed. This analysis will give us a spatial distribution pattern of the carbohydrate content of particles and may help us understand why specific bacteria are found on particles in one oceanic province but not in another. Additionally, it can potential give us a better

understanding of the spatial distribution of different particle-associated carbohydrates across the Atlantic Ocean.

Additionally, using meta-genomics we are analysing the genetic potential of the PA organisms, which should yield further insight into their specific distribution patterns. The functional potential of the PA community can be used to form hypotheses about their possible activities on the particles. To date, there have only been a few metagenomics studies of PA microbial communities (Allen et al 2012, Ganesh et al 2014, Smith et al 2013). These studies have shown differences between the PA and FL communities as well as distinctions between different size fractions. However, there is often a high proportion of eukaryotic, and phylogenetically unclassified sequences in the PA community metagenomes making them difficult to analyse (Simon et al 2014).

We are currently analysing the PA bacterial community of the S. Temperate stations, which were directly correlated to the increase in chlorophyll *a* and appeared to respond to the addition of fresh organic matter. Of interest in these analyses are the genes encoding the proteins which are involved in the utilisation of dissolved organic matter as well as the specific carbohydrate active enzymes. These can also be used to predict the carbohydrate content of the particles, assuming they are actively expressed. Similar predictions were made from the analyses of FL communities during phytoplankton blooms (Teeling et al 2012). Metagenomics potentials and substrate predictions could be combined with the results of the lectin staining and may yield new insight into the hydrolysis of POM in the marine environment.

A parallel analysis of the metagenomics potential of the PA community from oligotrophic open ocean particles would also be interesting, as these varied considerably in the community composition to their FL counterparts. The high taxonomic variation should be reflected in the functional potential and further our limited understanding of the different bacterial lifestyles (Allen et al 2012).

Acknowledgements

We thank Jörg Wulf and Andreas Ellrott for technical assistance and helpful discussions. We thank the captain and crew of the RRS James Cook, as well as the principle scientist Glen Tarran (Plymouth Marine Laboratories) for assistance at sea. This work was supported by the Max Planck Society. This study is a contribution to the international IMBER project and was also supported by the UK Natural Environment Research Council National Capability funding to Plymouth Marine Laboratory and the National Oceanography Centre, Southampton.

Chapter 4

An alternative polysaccharide uptake mechanism of marine bacteria

Greta Reintjes, Carol Arnosti, Bernhard M. Fuchs, Rudolf Amann

Manuscript published: ISME Journal March 2017
DOI: 10.1038/ismej.2017.26

ORIGINAL ARTICLE

An alternative polysaccharide uptake mechanism of marine bacteria

Greta Reintjes¹, Carol Arnosti², Bernhard M Fuchs¹ and Rudolf Amann¹¹Department of Molecular Ecology, Max Planck Institute for Marine Microbiology, Bremen, Germany and²Department of Marine Sciences, University of North Carolina-Chapel Hill, Chapel Hill, NC, USA

Heterotrophic microbial communities process much of the carbon fixed by phytoplankton in the ocean, thus having a critical role in the global carbon cycle. A major fraction of the phytoplankton-derived substrates are high-molecular-weight (HMW) polysaccharides. For bacterial uptake, these substrates must initially be hydrolysed to smaller sizes by extracellular enzymes. We investigated polysaccharide hydrolysis by microbial communities during a transect of the Atlantic Ocean, and serendipitously discovered—using super-resolution structured illumination microscopy—that up to 26% of total cells showed uptake of fluorescently labelled polysaccharides (FLA-PS). Fluorescence *in situ* hybridisation identified these organisms as members of the bacterial phyla *Bacteroidetes* and *Planctomycetes* and the gammaproteobacterial genus *Catenovulum*. Simultaneous membrane staining with Nile red indicated that the FLA-PS labelling occurred in the cell but not in the cytoplasm. The dynamics of FLA-PS staining was further investigated in pure culture experiments using *Gramella forsetii*, a marine member of *Bacteroidetes*. The staining patterns observed in environmental samples and pure culture tests are consistent with a ‘selfish’ uptake mechanisms of larger oligosaccharides (>600 Da), as demonstrated for gut *Bacteroidetes*. Ecologically, this alternative polysaccharide uptake mechanism secures substantial quantities of substrate in the periplasmic space, where further processing can occur without diffusive loss. Such a mechanism challenges the paradigm that hydrolysis of HMW substrates inevitably yields low-molecular-weight fragments that are available to the surrounding community and demonstrates the importance of an alternative mechanism of polysaccharide uptake in marine bacteria.

The ISME Journal advance online publication, 21 March 2017; doi:10.1038/ismej.2017.26

Introduction

Marine microbial communities are responsible for processing an estimated half of the organic carbon annually produced in the ocean (Azam and Malfatti, 2007). It is generally assumed that the high-molecular-weight (HMW) fraction of this organic matter is hydrolysed initially by extracellular enzymes to sizes <600 Da (Weiss *et al.*, 1991) for transport into the cell (Arnosti, 2011). The conditions under which the production of an extracellular enzyme might be energetically beneficial, the extent to which diffusive loss of hydrolysed products limits the utility of extracellular enzyme production and scenarios under which non-enzyme-producing

organisms may benefit from the activities of enzyme producers have been considered in recent models (for example, Vetter *et al.*, 1998; Allison, 2005; Traving *et al.*, 2015). These models assume that hydrolysis occurs in the extracellular environment and that hydrolysis products therefore are available to the wider microbial community. Models consequently typically express substrate availability in terms of monomer production and transport. Field measurements have likewise measured carbohydrate metabolism by microbial communities in the ocean via production and uptake of monosaccharides (for example, Rich *et al.*, 1996). With few exceptions, moreover, investigations of carbohydrate dynamics have focussed primarily on enzymatic hydrolysis of glucose-containing substrate proxies (MUF- α - and β -glucose; Zacccone *et al.*, 2012; Kellogg and Deming, 2014); glucose dynamics have also been used as a representation of polysaccharide metabolism in general (Christian and Karl, 1995; Piontek *et al.*, 2014).

Different marine heterotrophs, however, specialise in uptake of low-molecular-weight and HMW substrates (for example, Cottrell and Kirchman, 2000; Elifantz *et al.*, 2005, 2007). Natural microbial

Correspondence: C Arnosti, Department of Marine Sciences, University of North Carolina-Chapel Hill, Chapel Hill, NC 27599-3300, USA.

E-mail: arnosti@email.unc.edu

or R Amann, Department of Molecular Ecology, Max Planck Institute for Marine Microbiology, Celsiusstrasse 1, Bremen D-28359, Germany.

E-mail: ramann@mpi-bremen.de

Received 30 September 2016; revised 6 December 2016; accepted 22 January 2017

communities in surface ocean waters also exhibit substrate preferences. Differences in the spectrum of polysaccharides hydrolysed (Arnosti *et al.*, 2005, 2012) and a latitudinal gradient in enzyme activities (Arnosti *et al.*, 2011) that parallels large-scale patterns in microbial biogeography have been demonstrated (for example, Baldwin *et al.*, 2005; Fuhrman *et al.*, 2008; Wietz *et al.*, 2010). The importance in marine systems of an alternative substrate uptake mechanism, known for gut bacteria (*Bacteroidetes*), has been suggested by metagenomic data from coastal ocean waters (Teeling *et al.*, 2012, 2016) and oceanic provinces in the North Atlantic (Gómez-Pereira *et al.*, 2012). With this mechanism, polysaccharides are bound to the outer membrane, partially hydrolysed, and transported as larger oligosaccharides (> 600 Da) into the periplasm using TonB-dependent outer membrane receptors/transporters (Cho and Salyers, 2001), a mechanism homologous to the starch utilisation system (sus-like) (D'Elia and Salyers, 1996). Direct evidence of the manner in which individual bacteria in the ocean take up HMW polysaccharides, however, is still lacking.

To examine the links between activities and communities across broad spatial scales, we incubated natural microbial communities of five distinct oceanic provinces—Northern Temperate, Northern Gyre, Equatorial, Southern Gyre and Southern Temperate (Longhurst *et al.*, 1995)—of the Atlantic Ocean (Supplementary Figure S1) with specific fluorescently labelled polysaccharides (FLA-PS). These polysaccharides, laminarin, xylan and chondroitin sulphate, were selected because they are present in large quantities in the ocean and/or enzymes that hydrolyse these polysaccharides are widely distributed among marine bacteria. For example, the production of laminarin, an energy storage product of diatoms, has been estimated at 5–15 billion metric tons annually (Alderikamp *et al.*, 2007). Xylan is a major component of red and green algae (Lahaye *et al.*, 1993; Usov, 2011) and thus widely present in the ocean, and chondroitin sulphate, which is commercially derived from shark cartilage, is rapidly and readily hydrolysed across broad ranges of ocean waters (Arnosti, 2011) and by a diverse array of marine bacterial isolates (Wegner *et al.*, 2013; Xing *et al.*, 2015). These polysaccharides also differ in chemical composition: laminarin is a glucose polysaccharide, xylan a polymer of xylose (a pentose rather than hexose sugar), and chondroitin sulphate is a sulphated polymer of *N*-acetylgalactosamine and glucuronic acid. These substrates thus provide the opportunity to probe the activities of a wider range of enzymes (Arnosti, 2003).

We subsampled the incubations at sea and serendipitously observed, using epifluorescence microscopy, that up to 26% of the individual bacterial cells bound the FLA-PS. Pursuing these observations, we combined FLA-PS staining with single-cell identification by fluorescence *in situ* hybridisation (FISH) (Amann *et al.*, 1995) and

super-resolution light microscopy to visualise the uptake of FLA-PS by individual bacterial cells in natural communities in surface ocean waters.

Materials and methods

Sampling and substrate incubations

Seawater samples were collected aboard the RRV *James Cook* during the Atlantic Meridional Transect 22 cruise from Southampton, UK, to Punta Arenas, Chile, from 10 October to 24 November 2012. In five different oceanic provinces (Supplementary Figure S1) at solar noon, triplicate 20 litre seawater samples were collected from 20 m depth using a Niskin rosette with an attached Sea Bird CTD (Sea Bird Electronics Inc., Bellevue, WA, USA). From each triplicate, subsamples of 500 ml were added to sterile glass bottles and incubated with one of the three FLA-PS, laminarin, chondroitin sulphate and xylan (nine bottles in total), for a total of 12–18 days. In addition, a treatment control, consisting of 500 ml seawater in a sterile glass bottle without a FLA-PS, as well as killed controls, consisting of 50 ml autoclaved seawater with one of the three FLA-PS, were incubated under the same conditions. All bottles were incubated at room temperature (RT) in the dark and sampled at regular time points (typically at 30 min, 1, 3, 6, 12 and 18 days). At each time point, samples for FISH analysis, measurement of extracellular enzyme activities and DNA analysis were collected. For FISH, 20 ml of water was filtered through a 47 mm (0.2 µm pore size) polycarbonate filter, applying a gentle vacuum of <200 mbar. After drying, the filters were stored at –20 °C until further analysis. For DNA analysis, 10 ml was filtered through a 0.2 µm pore size polycarbonate filter using a Whatman 420200 Swin-Lok reusable filter holder (Sigma-Aldrich Chemie GmbH, Munich, Germany).

FLA-PS synthesis and measurement of extracellular enzymatic activity

Three polysaccharides (laminarin, xylan, chondroitin sulphate) obtained from Sigma-Aldrich (Munich, Germany) were fluorescently labelled with fluorescein amine (Sigma-Aldrich; isomer II) as described in Arnosti (2003). The FLA-PS solutions are free of monosaccharides or oligosaccharides, due to the fact that they are repeatedly injected onto standardised gel permeation chromatography systems as part of the labelling procedure; any low-molecular-weight carbohydrates are thereby removed during purification. Average-molecular weights of fluorescently labelled laminarin, xylan and chondroitin sulphate are 6000, 9000 and >50 000 daltons, respectively. A single polysaccharide was added at a concentration of 1.75 µmol monomer-equivalent to each 500 ml water sample; each polysaccharide was incubated in triplicate, plus one killed control, as described above.

Substrate staining, FISH and epifluorescence microscopy

For all the time points, the cells were filtered as described and counter-stained with 4',6-diamidino-2-phenylindole (DAPI) and Nile red and subsequently mounted using a Citifluor/VectaShield (4:1) mounting solution. Substrate-stained cells were visualised and enumerated using a fully automated microscope imaging system, described in detail by Bennke *et al.* (2016), on a Zeiss AxioImager.Z2 microscope stand (Carl Zeiss MicroImaging GmbH, Göttingen, Germany) with a cooled charged-coupled-device (CCD) camera (AxioCam MRm; Carl Zeiss) and a Colibri LED light source (Carl Zeiss) with three light-emitting diodes (UV-emitting LED, 365 ± 4.5 nm for DAPI; blue emitting LED, 470 ± 14 nm for FLA-PS 488; red-emitting LED, 590 ± 17.5 nm for the tyramide Alexa 594, FISH), combined with the HE-62 multifilter module (Carl Zeiss). This module consists of a triple emission filter TBP 425 (± 25), 527 (± 27), LP 615, including a triple beam splitter of TFT 395/495/610. All automatic cell counts were validated using manual cell counting. Briefly automated cell counting was carried out by initially acquiring images (using a $63\times$ magnification and 1.4 numerical aperture oil immersion plan apochromatic objective (Carl Zeiss)), at selected wavelengths (DAPI, FLA-PS, FISH), of a previously defined set of coordinates consisting of a minimum of 46 fields of view on each sample filter (Bennke *et al.*, 2016). Subsequently, the images were imported into the ACMETOOL2.0 (<http://www.technobiology.ch/index.php?id=acmetool>) image analysis software. From the images, cells were deemed 'substrate stained' if they showed a positive signal in both the DAPI and FLA-PS (488) images. Additionally, these signals had to have a minimum overlap of 30%, a minimum area of 17 or 30 pixel ($0.17\text{--}0.3\ \mu\text{m}^2$) (DAPI signal and FLA-PS signal, respectively) and a minimum signal background ratio of 1 or 2.5 (DAPI and FLA-PS signals, respectively) (Bennke *et al.* 2016).

FISH was carried out with slight alterations of the protocol by Manz *et al.* (1992). The hybridisation buffer contained 900 mM NaCl, 20 mM Tris-HCl (pH 7.5), 0.02% sodium dodecyl sulphate, 10% dextran sulphate (wt/vol) and 1% (wt/vol) blocking reagent (Boehringer; Mannheim, Germany) with a formamide concentration optimised for individual probes (Supplementary Table S1). All hybridisations were carried out at 46°C in a humidity chamber for 3 h, with a subsequent wash in a buffer containing 14–900 mM NaCl (dependent on formamide concentration in the hybridisation buffer), 20 mM Tris-HCl (pH 8), 5 mM EDTA (pH 8) and 0.01% sodium dodecyl sulphate at 48°C . For super-resolution structured illumination microscopy (SR-SIM), the cells were initially scraped from the filter using a sterile scalpel and heat fixed to coverslips at 46°C . After heat fixation, FISH was carried out as described above.

Super-resolution structured illumination microscopy

Substrate incubation samples were visualised on a Zeiss ELYRA PS.1 (Carl Zeiss) using 561, 488 and 405 nm lasers and BP 573-613, BP 502-538 and BP 420-480+LP 750 optical filters. Z-stack images were taken with a Plan-Apochromat $63\times/1.4$ Oil objective and processed with the software ZEN2011 (Carl Zeiss). SR-SIM images are taken by exciting the sample using non-uniform wide-field illumination. The laser light passes through an optical grating, generating a striped-shaped sinusoidal interference pattern. This pattern then combines with the sample information originating from structures below the diffraction limit to generate moiré fringes. The image is detected by a CCD camera and contains high spatial frequency sample information shifted to a lower spatial frequency band that is transmitted through the objective. Mathematical reconstructions from raw image slices then allow for a reconstruction of a high-resolution image with doubled resolution in the *xy* plane (Schermerle *et al.*, 2010). Intensity line profiles of individual cells were carried out using the ZEN black software (Carl Zeiss).

Medium preparation

HaHa medium was prepared as described in detail by Hahnke and Harder (2013) and Hahnke *et al.* (2015). The basic HaHa medium was supplemented with $0.2\ \mu\text{m}$ sterile filtered carbon sources (glucose, cellobiose, yeast extract, peptone, casamino acids (Hahnke and Harder, 2013), laminarin (Sigma-Aldrich) and FLA-laminarin) to make different carbon source media (Supplementary Table S2).

Pure culture FLA-PS incubations

FLA-PS incubations were performed using a pure culture of *Gramella forsetii* strain KT0803 (DSM 17595), a marine member of *Bacteroidetes*. All growth experiments were carried out in biological duplicates. For all incubations and sampling time points (see below), cell growth and FLA-substrate uptake was analysed by fixing 1 ml of culture using 2% sterile filtered formaldehyde for 1 h at RT. Subsequently, the sample was filtered through a $25\ \text{mm}$ polycarbonate filter ($0.2\ \mu\text{m}$ pore size), applying a gentle vacuum of $<200\ \text{mbar}$, and the cells were visualised using microscopy (see 'Substrate staining, FISH and epifluorescence microscopy' section above). Cell fluorescence due to FLA-substrate uptake was quantified using an Accuri C6 flow cytometer (BD Accuri Cytometers, Ann Arbor, MI, USA).

G. forsetii was grown in HaHa high carbon medium (Supplementary Table S2) until it reached the stationary phase (48 h) and a cell count of $10^7\ \text{cells ml}^{-1}$. Subsequently, *G. forsetii* was inoculated (1:10) into HaHa minimal medium and grown for 48 h; this was repeated twice to starve the culture and mimic a minimal carbon environment. To track

the uptake of FLA-laminarin by *G. forsetii*, in a low carbon environment, this starved culture was inoculated (1:10) into HaHa FLA-laminarin 35 μM medium and sampled every 3 h.

To allow for the upregulation of gene expression and production of enzymes capable of laminarin uptake (induction), the starved *G. forsetii* culture was inoculated into HaHa laminarin medium

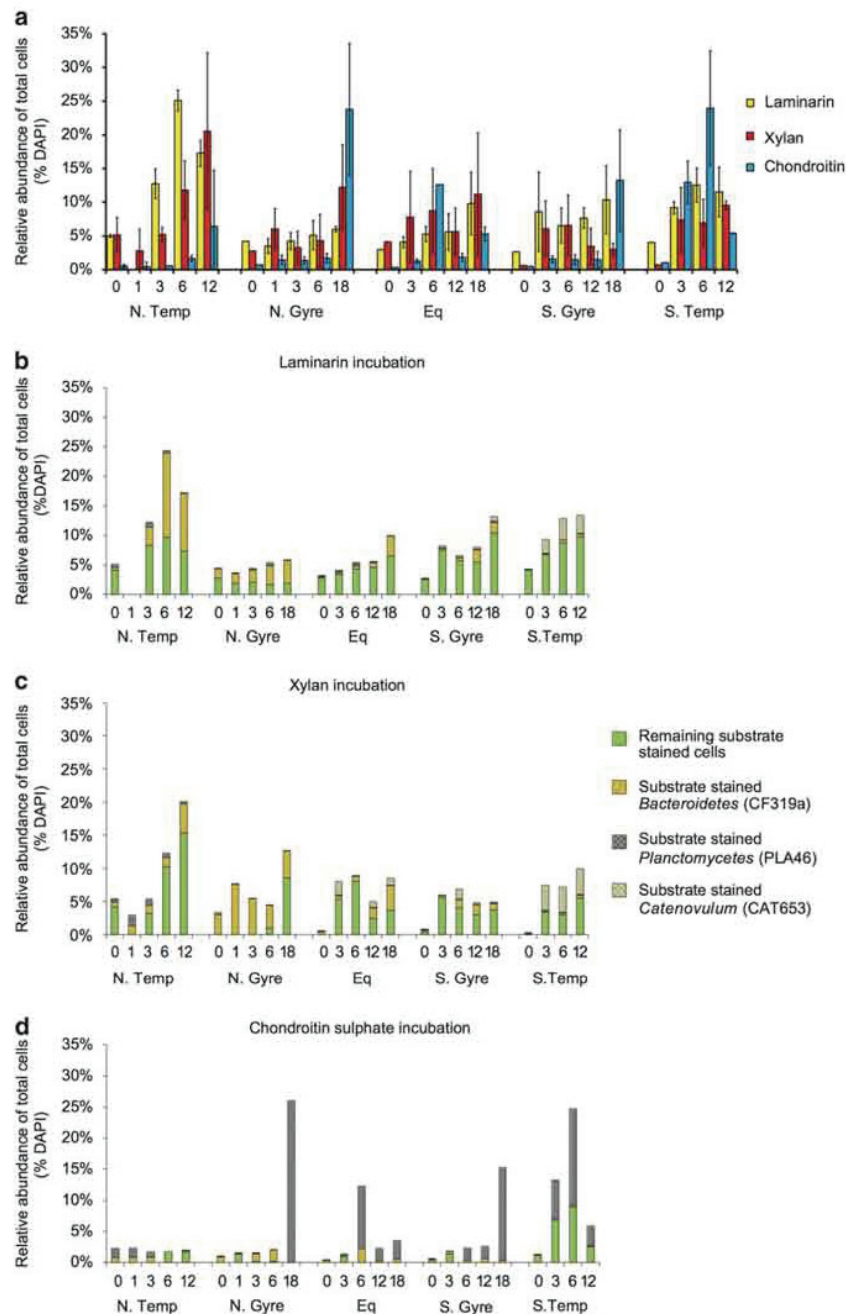


Figure 1 Relative abundance of substrate-stained cells and FISH identification of substrate-stained cells in incubations of seawater from five stations of different provinces of the Atlantic Ocean (see Supplementary Figure S1 for station locations). (a) relative abundance of cells stained by laminarin (yellow), xylan (red) and chondroitin sulphate (blue). Incubation time is indicated by 'T' (0–18 days). T0 refers to samples taken approximately 30 min after addition of the FLA-PS. (b) Relative abundance of laminarin-stained cells and fraction stained by FISH probes for *Bacteroidetes* (CF319a), *Planctomycetes* (PLA46) and *Catenovulum* (CAT653). (c) Relative abundance of xylan-stained cells and fraction stained by FISH probes for *Bacteroidetes* (CF319a), *Planctomycetes* (PLA46) and *Catenovulum* (CAT653). (d) Relative abundance of chondroitin-stained cells and fraction stained by FISH probes for *Bacteroidetes* (CF319a), *Planctomycetes* (PLA46) and *Catenovulum* (CAT653).

for 48 h (1×10^6 cells ml^{-1}). This was also carried out to test whether the uptake of FLA-laminarin increased after induction of the cells, mimicking an environment where laminarin is already available. Induced *G. forsetii* was inoculated (1:10) in both HaHa FLA-laminarin $35 \mu\text{M}$ medium and HaHa FLA-laminarin $3.5 \mu\text{M}$ medium. Substrate staining was tracked by sampling at 5, 20, 40, 60, 80 and 100 min.

To further analyse the FLA-substrate uptake by the cells and to determine whether the FLA tag can be excreted, after 100 min incubation in HaHa FLA-laminarin $35 \mu\text{M}$ medium, the substrate-stained cells were inoculated (1:10) in HaHa laminarin. The decrease in FLA signal was analysed by sampling at 20, 40, 60, 80, 100 min and 1 day after inoculation.

All growth experiments without FLA-laminarin were sampled regularly to check for autofluorescence or other sources of fluorescence that could be mistaken for substrate signals. Additionally, to ensure that there was no unspecific binding of FLA-laminarin to cells, cells grown in HaHa high carbon medium and HaHa laminarin medium were fixed using 2% sterile filtered formaldehyde for 1 h at RT and subsequently incubated with $35 \mu\text{M}$ FLA-laminarin for 4 h. The cells were then filtered through a 25 mm ($0.2 \mu\text{m}$ pore size) polycarbonate filter, applying a gentle vacuum of $<200 \text{ mbar}$ and visualised using microscopy. There was no unspecific binding of substrate to fixed cells.

Flow cytometry and fluorescence quantification

Cell fluorescence due to FLA-substrate uptake was quantified in all *G. forsetii* growth cultures using an Accuri C6 flow cytometer (BD Accuri Cytometers). Initially, the cells were fixed in 37% sterile filtered formaldehyde (final concentration 2%) for 1 h at RT. The 8- and 6-peak validation bead suspensions (Spherotech, Lake Forest, IL, USA) were used as internal references. The cells were analysed under laser excitation at 488 nm from a blue-green diode laser and the green fluorescence was collected in the FL1 channel ($530 \pm 30 \text{ nm}$). An electronic threshold of 10 000 FSC-H was set to reduce background noise. All samples were analysed at the same flow rate (slow) and a total of 20 000 events per sample were acquired. Bacteria were detected from the signature plot of SSC-H vs green fluorescence (FL1-H). The FCM output was analysed using the BD Accuri software. Cells were assumed to give a positive signal if their associated mean fluorescence intensity was greater than the FL1-H of a culture not incubated in FLA-laminarin. As *G. forsetii* can form aggregates over time, a subset of data was defined using gates that represented single cells. For these gates, comparative fluorescence intensity was carried out by comparison of the mean fluorescence intensity to that of non-FLA-laminarin-stained cells.

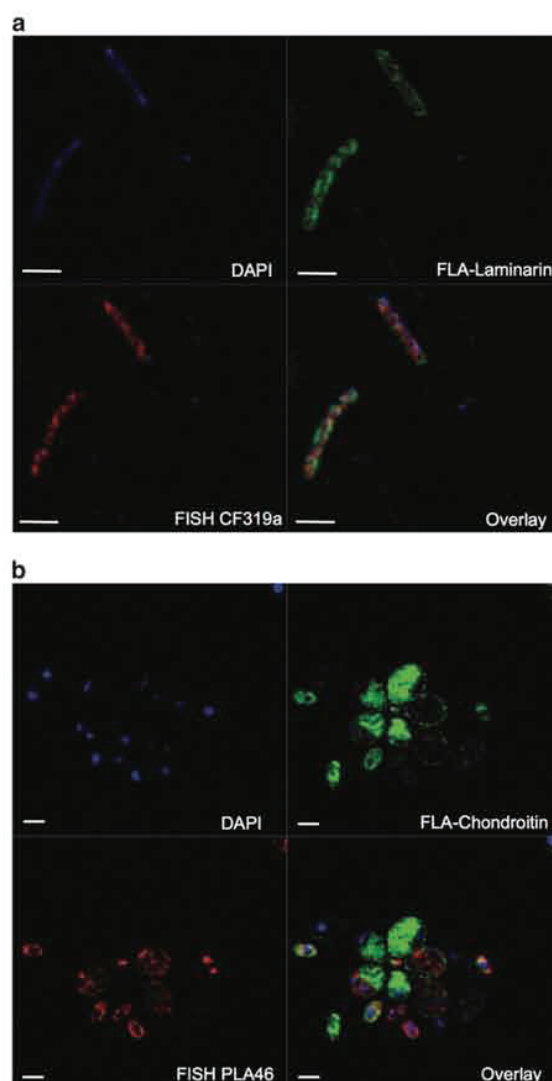


Figure 2 SR-SIM of cells stained by (a) DAPI (blue), FLA-laminarin (green) and *Bacteroidetes*-specific FISH probe (CF319a, red); (b) DAPI (blue), FLA-chondroitin sulphate (green) and *Planctomycetes*-specific FISH probe (PLA46, red). Scale bar = $1 \mu\text{m}$.

Results and discussion

We incubated sea water from five distinct oceanic provinces with three FLA-PS and observed by epifluorescence microscopy that a considerable fraction of the bacterial community—up to 26% of total cells (Figure 1a)—bound detectable amounts of substrate (Figure 2, Supplementary Figure S2). Fluorescent staining was seen in all incubations but varied considerably with substrate and station (Figure 1a). The highest overall abundance and most rapid staining of cells was usually seen in the laminarin incubations. For example, in the Northern Temperate province 5% of cells show staining after just

30 min (T_0) and the abundance increased to 25% after 6 days. Xylan staining of cells was also seen quickly (5% at T_0) in the Northern Temperate, Northern Gyre and Equatorial stations but not in the Southern Gyre or Southern Temperate stations. The highest abundance of xylan-stained cells was in the Northern Temperate station after 12 days (20%). In the chondroitin sulphate incubations, the increase of substrate-stained cells occurred more slowly. High abundances of $22 \pm 3\%$ were nonetheless observed at later time points (T_{18}) in the gyre stations. At the Southern Temperate station, a high percentage of cells were stained already at T_6 . Many different cell morphologies were observed among substrate-stained cells—cocci, rod shaped and ovoid; the rate of staining of the different cell types varied (Figure 2, Supplementary Figure S2). A diverse range of bacteria thus were binding FLA-PS.

Examination of individual cells using SR-SIM, which enables visualisation of prokaryotic cell compartments, showed that the initial association of cells with substrates occurred in the cell periphery within 30 min (Supplementary Figure S4a). Such rapid direct staining was surprising, as polysaccharide additions were moderate (ca. $21 \mu\text{M}$ C) and the average number of fluorophores per molecule of polysaccharide (the labelling density) was low (between 0.5 and 1.3 per polysaccharide molecule; Arnosti (2003). Currently, it is not possible to measure the absolute number of fluorophores taken up over time by individual cells in an environmental sample. However, a comparison of the FLA-PS signal and the FISH signal resulting from a $4 \times$ labelled rRNA targets oligonucleotide of the same cell (Figure 2) suggests that thousands of FLA-PS molecules have been bound by individual cells.

Rapid staining was also observed in pure cultures of *G. forsetii* incubated with FLA-laminarin (Supplementary Figure S3 and Supplementary Table S3). When *G. forsetii* cells grown on a minimal carbon medium with no polysaccharide were inoculated into a medium containing FLA-laminarin ($35 \mu\text{M}$ monomer l^{-1}), it took up to 12 h for substrate-specific staining to be observed. However, when *G. forsetii* was grown on a laminarin medium and subsequently inoculated into FLA-laminarin ($3.5 \mu\text{M}$ monomer l^{-1}) containing media, staining could be seen within minutes (Supplementary Figure S3 and Supplementary Table S3). This result not only shows the high affinity of induced *G. forsetii* towards laminarin but also demonstrates that a fraction of the environmental bacteria were likely induced or specialised for the immediate uptake of polysaccharides, as seen by staining at T_0 (Figure 1a and Supplementary Figure S4).

Live *G. forsetii* lost much of the substrate signal from FLA-laminarin within 24 h (Supplementary Table S3). Specifically, when *G. forsetii* was transferred from HaHa FLA-laminarin medium into HaHa laminarin medium, cells continued growing and

simultaneously lost the FLA-laminarin signal over time. The slow removal of FLA from the cell indicates that the substrate was not unspecifically bound to the cell surface but instead taken up into the cell. Moreover, the loss of signal in *G. forsetii* over time cannot be solely related to dilution through cell division, as the signal decreased more rapidly than average doubling times of *G. forsetii*.

In environmental samples, the overall abundance of substrate-stained cells increased with time in all incubations ($R^2 = 0.0823$, $P\text{-value} = 0.0153$) (Figure 1a), despite the fact that (with a single exception) the absolute cellular abundances within the incubations did not increase significantly (Supplementary Figure S5). Although the abundance of stained cells increased, this relationship varied by station and substrate. At the Equatorial station (xylan and chondroitin sulphate incubations) and the Southern Gyre station (laminarin and xylan incubations), moreover, there was a decrease in the abundance of substrate-stained cells between day 3 and day 6. No substrate staining was detected in heat-killed or formaldehyde-fixed cell controls, indicating that staining was due to biological activity (Supplementary Figure S6).

The ability to use polysaccharides has been confirmed for many marine bacterial phyla, including *Bacteroidetes*, *Planctomycetes*, *Verrucomicrobia* and *Proteobacteria* (Martinez-Garcia *et al.*, 2012; Teeling *et al.*, 2012; Kabisch *et al.*, 2014; Lage and Bondoso, 2014; Wietz *et al.*, 2015). Based on the literature (Schattenhoffer *et al.*, 2009; Teeling *et al.*, 2012; Lage and Bondoso, 2014; Wietz *et al.*, 2015) and cell morphologies, a selection of group-specific FISH probes (Supplementary Table S1) was used to identify and enumerate specific bacterial group abundances at each time point and station. The combination of FISH with substrate staining allowed for the identification of organisms directly taking up a specific substrate (Figures 2a and b). Using this probe set (CF319a, PLA46 and CAT653 targeting the *Bacteroidetes*, *Planctomycetes* and *Catenovulum*, respectively), an average of $48\% \pm 49\%$ (median of 55%) of the substrate-stained cells could be identified (Figures 1b–d). Future analysis using 16S rRNA sequencing is currently being pursued to supplement this probe set in future and further increase the fraction of identified cells.

The FISH counts of the substrate incubations of the Atlantic Ocean showed an increase in abundance of the selected clades. For example, FISH counts of the laminarin incubation at the Northern Temperate station showed a nearly fivefold increase in *Bacteroidetes* abundance over 6 days (from 7.2×10^4 to 3.3×10^5 cells ml^{-1} at day 6), with 80% of these cells showing substrate-specific staining (Figure 1b and Supplementary Figure S9). In the other regions, *Bacteroidetes* did not increase as strongly in abundance, possibly due to lower initial cell numbers, but the percentage of substrate stained *Bacteroidetes* increased from 5% to $72 \pm 28\%$ in 12–18 days.

Planctomycetes cellular abundances likewise increased, particularly in the chondroitin sulphate incubation of the Southern Temperate station, from

2.3×10^3 to 2.5×10^5 cell ml⁻¹ over 6 days; 84% of these cells showed substrate staining (Figure 1d and Supplementary Figure S9). The substrate-stained

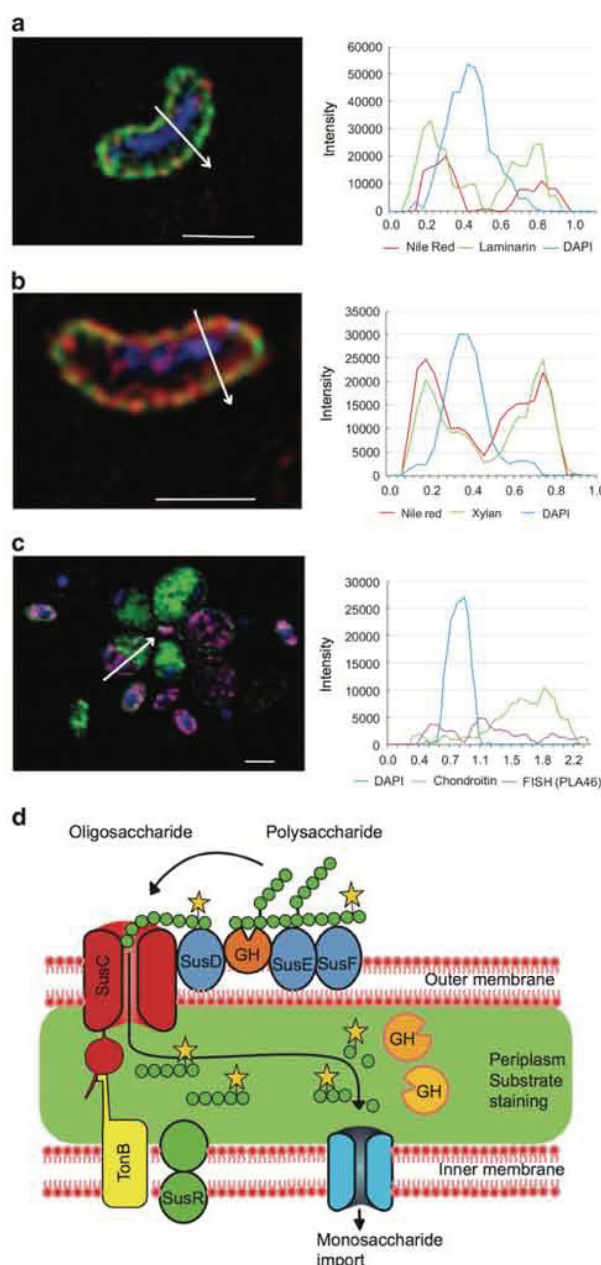


Figure 3 SR-SIM images showing Sus-like uptake of FLA-PS and fluorescence intensity line profiles localising substrate-specific staining after 6 days of incubation. (a and b) Cells stained with FLA-PS (green), Nile red (red; membrane) and DAPI (blue; DNA). White arrows indicate sections along which the fluorescence intensity line profiles were recorded. Scale bars = 1 μm. Corresponding profiles indicating co-localisation of substrate and membrane are shown on the right. (a) *Bacteroidetes* cell from the Northern Temperate station stained with FLA-laminarin. (b) *Bacteroidetes* cell from the Southern Temperate station stained with FLA-xylan. (c) *Planctomycetes* cells from the Southern Temperate station stained with FLA-chondroitin. Cells were identified using the FISH probe PLA46 (magenta), which labels the riboplasm; the substrate staining is in the periplasm. (d) Conceptual model of sus-like bacterial uptake of FLA-PS into the periplasm via TonB-dependent outer membrane transporters, causing halo-like staining in periplasm (green). The large oligosaccharides are further hydrolysed within the periplasm to monosaccharides, disaccharides or trisaccharides, which are subsequently transported into the cytoplasm. Modified after Koropatkin *et al.* (2012). 'GH' represents glycoside hydrolases.

cells in the chondroitin sulphate incubations of other regions exhibited distinctive *Planctomycetes*-like cell morphologies but were only partially identified as *Planctomycetes* with FISH probe PLA46, perhaps due to difficulty of permeabilising *Planctomycetes* cells (Pizzetti *et al.*, 2011). In addition to the *Bacteroidetes* and *Planctomycetes*, the gammaproteobacterial genus *Catenovulum* also showed substrate-specific staining. *Catenovulum* increased in abundance in the laminarin and xylan incubations at the Equatorial, Southern Gyre and Southern Temperate stations and constituted 1–4% of the total stained cells.

Substrate-stained cells predominantly exhibited a halo-like staining that was restricted to the cell periphery (Figures 3a and b, Supplementary Figure S8). Fluorescence intensity line profiles of individual cells in combination with Nile red membrane counterstaining showed a co-localisation of the substrate signal with the cell membranes (Figures 3a and b). However, in cells <0.5 µm in width, for example, some *Bacteroidetes*, the halo-like staining could not, due to limits of optical resolution, definitively be shown to be within the periplasmic space between the membranes. In contrast, for the larger cells of *Planctomycetes* uptake of FLA-chondroitin sulphate across the outer membrane could be seen (Figure 3c and Supplementary Figure S7). SR-SIM revealed that FLA-chondroitin sulphate had been transported into the periplasm but not into the riboplasm (Figure 3c and Supplementary Figure S7). Similar to the periplasm of Gram-negative bacteria, the periplasm is a cell compartment located between an inner and an outer membrane that does not contain ribosomes (Fuerst and Sagulenko, 2011).

Genomic analyses of marine strains from *Bacteroidetes* and *Planctomycetes* have shown that they have the potential to express carbohydrate transporters for the uptake of large oligosaccharides through the outer membrane (Fuerst and Sagulenko, 2011; Teeling *et al.*, 2012; Paparoditis *et al.*, 2014). Intestinal *Bacteroidetes* in particular are known for sus-like polysaccharide utilisation loci (Koropatkin *et al.*, 2012). When expressed, the proteins encoded in these loci are principally located in the outer membrane and the periplasm. They sequentially bind and hydrolyse polysaccharides, transporting large oligosaccharides into the periplasm, where further degradation occurs in a protected space (Figure 3d; Koropatkin *et al.*, 2012). Our observations of the staining patterns of marine *Bacteroidetes* cells are consistent with this mode of substrate processing. Previous research on *G. forsetii* has shown that, in laminarin-amended cultures, the expression of proteins required for its binding, transport and utilisation of laminarin is induced (Kabisch *et al.*, 2014). Here we show that induced *G. forsetii* cells are stained with FLA-laminarin in minutes (Supplementary Figure S3), whereas cells that were not induced required hours before

staining can be detected. Up to 5% of open ocean bacteria are readily stained with FLA-laminarin, showing detectable staining after just 30 min (T0), which indicates that for these bacteria no induction is required: they are primed for rapid uptake of laminarin into the periplasm. (Supplementary Figure S4a).

Based on our microscopic examination of *Bacteroidetes* from the surface ocean, data from pure cultures of *G. forsetii* and genomic information (Koropatkin *et al.*, 2012; Teeling *et al.*, 2012; Kabisch *et al.*, 2014), we hypothesise that the substrate uptake we observed is homologous to the sus-like mechanism of gut *Bacteroidetes*. This mechanism has recently been referred to as 'selfish' by Cuskin *et al.* (2015) owing to the fact that, after uptake of large oligosaccharides, further degradation occurs in the protected periplasmic space. Selfish substrate uptake confers a distinct ecological benefit by minimising formation of monosaccharides, disaccharides and trisaccharides in the external environment and avoiding diffusive loss of enzymes (Figure 3d; Cuskin *et al.*, 2015). The uptake of chondroitin sulphate by *Planctomycetes* likely occurs via an analogous but unknown mechanism.

As demonstrated by the substantial fraction of the natural microbial community that was stained by just three distinct substrates (Figure 1a), this substrate utilisation strategy is important not only in the anaerobic and organic-carbon rich environment of the human gut (Cuskin *et al.*, 2015) but also in the oxic, dilute and comparatively organic-carbon-poor surface waters of the Atlantic Ocean. Although these experiments were carried out in bottle incubations that may well have led to changes in the microbial community from its initial composition, the organisms growing later in the incubations must ultimately have originated from the seawater sample we collected. The activity seen later in the incubations thus may not reflect the exact dynamics that occur in the ocean, but nonetheless highlight the selfish uptake capabilities that these microorganisms possess. Moreover, the observation that FLA-PS were bound by organisms in both the early (initial 30 min) and late (up to 18 days) phases of the incubations suggest that this strategy of substrate acquisition competes well with alternative strategies of substrate utilisation in complex microbial communities. These observations imply that a re-evaluation of models of bacterial substrate utilisation in natural environments will be necessary. Current models typically encompass two classes of organisms, those that produce enzymes that release low-molecular-weight substrates to the environment and those that use the hydrolysis products but do not produce enzymes themselves (for example, Allison, 2005; Kaiser *et al.*, 2015; Traving *et al.*, 2015). These two-player models will need to be expanded to consider organisms that have evolved mechanisms to minimise substrate sharing.

Conclusions

Measurements and models of the manner in which the most abundant products of photosynthesis, polysaccharides, are channelled into the microbial food chain need to account for the varying ecological strategies of heterotrophic marine bacteria. Most field measurements of enzyme activities rely on substrate proxies containing monomers (Zaccone *et al.*, 2012; Kellogg and Deming, 2014); carbohydrate uptake measurements in ocean waters likewise are made most frequently with monosaccharides (Rich *et al.*, 1996). These measurements do not account for bacteria that quickly capture and process HMW polysaccharides. The speed and extent of selfish substrate uptake by phylogenetically distinct bacteria at five widely spaced stations in the Atlantic Ocean demonstrate that this is an important mechanism of carbon utilisation that previously has been overlooked. Future models as well as measurements will need to account for this mode of substrate acquisition as part of microbially driven carbon cycling in the ocean.

The FLA-PS staining method, in combination with FISH, allows for direct identification of polysaccharide-degrading bacteria in environmental samples. Based on this new method, future studies can specifically measure the types and quantities of phytoplankton-produced polysaccharides that are processed by this mechanism, as well as explore other locations and conditions under which selfish substrate utilisation may predominate.

Conflict of Interest

The authors declare no conflict of interest.

Acknowledgements

We thank the captain and crew of the RRV *James Cook*, as well as the principle scientist Glen Tarran (Plymouth Marine Laboratories), for assistance at sea. We also thank Jörg Wulf, David Probandt, Marion Stagars, Andreas Ellrott and Sherif Ghobrial for technical assistance and Ian Head, Cindy Lee and Andreas Teske for helpful discussions. This work was supported by the Max Planck Society and by the U.S. National Science Foundation (OCE-1332881 to CA). CA was additionally supported in part by a fellowship from the Hanse Institute for Advanced Study (Delmenhorst, Germany). This study is a contribution to the international IMBER project and was also supported by the UK Natural Environment Research Council National Capability funding to Plymouth Marine Laboratory and the National Oceanography Centre, Southampton. This is contribution number 281 of the AMT program.

Author contributions

Experimental design: RA, CA, and GR; sampling: GR and RA; FISH and cell counting, automated microscopy and super-resolution microscopy: GR;

fluorescent labelling of polysaccharides: CA; probe design: BF. The manuscript was written primarily by GR, CA and RA with contributions from BF. GR prepared the figures.

References

- Alderkamp A-C, Van Rijssel M, Bolhuis H. (2007). Characterization of marine bacteria and the activity of their enzyme systems involved in degradation of the algal storage glucan laminarin. *FEMS Microbiol Ecol* **59**: 108–117.
- Allison SD. (2005). Cheaters, diffusion and nutrients constrain decomposition by microbial enzymes in spatially structured environments. *Ecol Lett* **8**: 626–635.
- Amann RI, Ludwig W, Schleifer KH. (1995). Phylogenetic identification and *in situ* detection of individual microbial cells without cultivation. *Microbiol Rev* **59**: 143–169.
- Arnosti C. (2003). Fluorescent derivatization of polysaccharides and carbohydrate-containing biopolymers for measurement of enzyme activities in complex media. *J Chromatogr B* **793**: 181–191.
- Arnosti C, Durkin S, Jeffrey WH. (2005). Patterns of extracellular enzyme activities among pelagic marine microbial communities: implications for cycling of dissolved organic carbon. *Aquat Microb Ecol* **38**: 135–145.
- Arnosti C. (2011). Microbial extracellular enzymes and the marine carbon cycle. *Annu Rev Mar Sci* **3**: 401–425.
- Arnosti C, Steen AD, Ziervogel K, Ghobrial S, Jeffrey WH. (2011). Latitudinal gradients in degradation of marine dissolved organic carbon. *PLoS One* **6**: e28900.
- Arnosti C, Fuchs BM, Amann R, Passow U. (2012). Contrasting extracellular enzyme activities of particle-associated bacteria from distinct provinces of the North Atlantic Ocean. *Front Microbiol* **3**: 425.
- Azam F, Malfatti F. (2007). Microbial structuring of marine ecosystems. *Nat Rev Microbiol* **5**: 782–791.
- Baldwin AJ, Moss JA, Pakulski JD, Catala P, Joux F, Jeffrey WH. (2005). Microbial diversity in a Pacific Ocean transect from the Arctic to Antarctic circles. *Aquat Microb Ecol* **41**: 91–102.
- Bennke CM, Reintjes G, Schattenhofer M, Ellrott A, Wulf J, Zeder M *et al.* (2016). Modification of a high-throughput automatic microbial cell enumeration system for ship board analyses. *Appl Environ Microbiol* **82**: 3289–3296.
- Cho KH, Salyers AA. (2001). Biochemical analysis of interactions between outer membrane proteins that contribute to starch utilization by *Bacteroides thetaio-*
taomicron. *J Bacteriol* **183**: 7224–7230.
- Christian JR, Karl DM. (1995). Bacterial ectoenzymes in marine waters: activity ratios and temperature responses in three oceanographic provinces. *Limnol Oceanogr* **40**: 1042–1049.
- Cottrell MT, Kirchman DL. (2000). Natural assemblages of marine Proteobacteria and members of the Cytophaga-Flavobacter cluster consuming low- and high-molecular-weight dissolved organic matter. *Appl Environ Microbiol* **66**: 1692–1697.

- Cuskin F, Lowe EC, Temple MJ, Zhu Y, Cameron EA, Pudlo NA *et al.* (2015). Human gut *Bacteroidetes* can utilize yeast mannan through a selfish mechanism. *Nature* **517**: 165–169.
- D'Elia JN, Salyers AA. (1996). Effect of regulatory protein levels on utilization of starch by *Bacteroides thetaiotaomicron*. *J Bacteriol* **178**: 7180–7186.
- Elifantz H, Malmstrom RR, Cottrell MT, Kirchman DL. (2005). Assimilation of polysaccharides and glucose by major bacterial groups in the Delaware estuary. *Appl Environ Microbiol* **71**: 7799–7805.
- Elifantz H, Dittel AI, Cottrell MT, Kirchman DL. (2007). Dissolved organic matter assimilation by heterotrophic bacterial groups in the western Arctic Ocean. *Aquat Microb Ecol* **50**: 39–49.
- Fuerst JA, Sagulenko E. (2011). Beyond the bacterium: *planctomycetes* challenge our concepts of microbial structure and function. *Nat Rev Microbiol* **9**: 403–413.
- Fuhrman JA, Steele JA, Hewson I, Schwalbach MS, Brown MV, Green JL *et al.* (2008). A latitudinal diversity gradient in planktonic marine bacteria. *Proc Natl Acad Sci* **105**: 7774–7778.
- Gómez-Pereira PR, Schüller M, Fuchs BM, Bennke C, Teeling H, Waldmann J *et al.* (2012). Genomic content of uncultured *Bacteroidetes* from contrasting oceanic provinces in the North Atlantic Ocean. *Environ Microbiol* **14**: 52–66.
- Hahnke RL, Harder J. (2013). Phylogenetic diversity of Flavobacteria isolated from the North Sea on solid media. *Syst Appl Microbiol* **36**: 497–504.
- Hahnke RL, Bennke CM, Fuchs BM, Mann AJ, Rhiel E, Teeling H *et al.* (2015). Dilution cultivation of marine heterotrophic bacteria abundant after a spring phytoplankton bloom in the North Sea. *Environ Microbiol* **17**: 3515–3526.
- Kabisch A, Otto A, König S, Becher D, Albrecht D, Schüller M *et al.* (2014). Functional characterization of polysaccharide utilization loci in the marine Bacteroidetes '*Gramella forsetii*' KT0803. *ISME J* **8**: 1492–1502.
- Kaiser C, Franklin O, Richter A, Dieckmann U. (2015). Social dynamics within decomposer communities lead to nitrogen retention and organic matter build-up in soils. *Nat Commun* **6**: 8960.
- Kellogg CTE, Deming JW. (2014). Particle-associated extracellular enzyme activity and bacterial community composition across the Canadian Arctic Ocean. *FEMS Microbiol Ecol* **89**: 360–375.
- Koropatkin NM, Cameron EA, Martens EC. (2012). How glycan metabolism shapes the human gut microbiota. *Nat Rev Microbiol* **10**: 323–335.
- Lage OM, Bondoso J. (2014). Planctomycetes and macroalgae, a striking association. *Front Microbiol* **5**: 133.
- Lahaye M, Michel C, Barry JL. (1993). Chemical, physico-chemical and *in-vitro* fermentation characteristics of dietary fibres from *Palmaria palmata* (L.) Kuntze. *Food Chem* **47**: 29–36.
- Longhurst A, Sathyendranath S, Platt T, Caverhill C. (1995). An estimate of global primary production in the ocean from satellite radiometer data. *J Plankton Res* **17**: 1245–1271.
- Manz W, Amann R, Ludwig W, Wagner M, Schleifer K-H. (1992). Phylogenetic oligodeoxynucleotide probes for the major subclasses of proteobacteria: problems and solutions. *Syst Appl Microbiol* **15**: 593–600.
- Martinez-Garcia M, Brazel DM, Swan BK, Arnosti C, Chain PSG, Reitenga KG *et al.* (2012). Capturing single cell genomes of active polysaccharide degraders: an unexpected contribution of *Verrucomicrobia*. *PLoS One* **7**: e35314.
- Papadimitis P, Västermark Å, Le AJ, Fuerst JA, Saier MH Jr. (2014). Bioinformatic analyses of integral membrane transport proteins encoded within the genome of the planctomycetes species, *Rhodopirellula baltica*. *Biochim Biophys Acta* **1838**: 193–215.
- Piontek J, Sperling M, Nöthig E-M, Engel A. (2014). Regulation of bacterioplankton activity in Fram Strait (Arctic Ocean) during early summer: the role of organic matter supply and temperature. *J Mar Syst* **132**: 83–94.
- Pizzetti I, Fuchs BM, Gerdt G, Wichels A, Wiltshire KH, Amann R. (2011). Temporal variability of coastal planctomycetes clades at kabeltonne station, North Sea. *Appl Environ Microbiol* **77**: 5009–5017.
- Rich JH, Ducklow HW, Kirchman DL. (1996). Concentrations and uptake of neutral monosaccharides along 14° W in the equatorial Pacific: contribution of glucose to heterotrophic bacterial activity and the DOM flux. *Limnol Oceanogr* **41**: 595–604.
- Schattenhofer M, Fuchs BM, Amann R, Zubkov MV, Tarran GA, Pernthaler J. (2009). Latitudinal distribution of prokaryotic picoplankton populations in the Atlantic Ocean. *Environ Microbiol* **11**: 2078–2093.
- Schermelleh L, Heintzmann R, Leonhardt H. (2010). A guide to super-resolution fluorescence microscopy. *J Cell Biol* **190**: 165–175.
- Teeling H, Fuchs BM, Becher D, Klockow C, Gardebrecht A, Bennke CM *et al.* (2012). Substrate-controlled succession of marine bacterioplankton populations induced by a phytoplankton bloom. *Science* **336**: 608–611.
- Teeling H, Fuchs BM, Bennke CM, Krüger K, Chafee M, Kappelmann L *et al.* (2016). Recurring patterns in bacterioplankton dynamics during coastal spring algae blooms. *eLife* **5**: e11888.
- Traving SJ, Thygesen UH, Riemann L, Stedmon CA. (2015). A model of extracellular enzymes in free-living microbes: which strategy pays off? *Appl Environ Microbiol* **81**: 7385–7393.
- Usov AI. (2011). Chapter 4—Polysaccharides of the red algae. In: Horton D (ed). *Advances in Carbohydrate Chemistry and Biochemistry*. Academic Press, pp 115–217.
- Vetter YA, Deming JW, Jumars PA, Krieger-Brockett BB. (1998). A predictive model of bacterial foraging by means of freely released extracellular enzymes. *Microb Ecol* **36**: 75–92.
- Wegner C-E, Richter-Heitmann T, Klindworth A, Klockow C, Richter M, Achstetter T *et al.* (2013). Expression of sulfatases in *Rhodopirellula baltica* and the diversity of sulfatases in the genus *Rhodopirellula*. *Mar Genomics* **9**: 51–61.
- Weiss M, Abele U, Weckesser J, Welte W, Schiltz E, Schulz G. (1991). Molecular architecture and electrostatic properties of a bacterial porin. *Science* **254**: 1627–1630.
- Wietz M, Gram L, Jørgensen B, Schramm A. (2010). Latitudinal patterns in the abundance of major marine bacterioplankton groups. *Aquat Microb Ecol* **61**: 179.
- Wietz M, Wemheuer B, Simon H, Giebel H-A, Seibt MA, Daniel R *et al.* (2015). Bacterial community dynamics during polysaccharide degradation at contrasting sites

- in the Southern and Atlantic Oceans. *Environ Microbiol* **17**: 3822–3831.
- Xing P, Hahnke RL, Unfried F, Markert S, Huang S, Barbeyron T *et al.* (2015). Niches of two polysaccharide-degrading *Polaribacter* isolates from the North Sea during a spring diatom bloom. *ISME J* **9**: 1410–1422.
- Zaccone R, Boldrin A, Caruso G, La Ferla R, Maimone G, Santinelli C *et al.* (2012). Enzymatic activities and prokaryotic abundance in relation to organic matter along a West–East Mediterranean Transect (TRANSMED Cruise). *Microb Ecol* **64**: 54–66.



This work is licensed under a Creative Commons Attribution 4.0 International License. The images or other third party material in this article are included in the article's Creative Commons license, unless indicated otherwise in the credit line; if the material is not included under the Creative Commons license, users will need to obtain permission from the license holder to reproduce the material. To view a copy of this license, visit <http://creativecommons.org/licenses/by/4.0/>

© The Author(s) 2017

Supplementary Information accompanies this paper on The ISME Journal website (<http://www.nature.com/ismej>)

Chapter 5

Tracking bacterial community dynamics in polysaccharide incubations along an Atlantic Meridional Transect.

Greta Reintjes, Carol Arnosti, Bernhard M. Fuchs, Rudolf Amann

Manuscript: In preparation

Abstract

We recently reported an alternative “selfish” polysaccharide uptake mechanism of marine bacteria which significantly impacted our understanding of the global turnover of organic matter. Here we report on the extracellular hydrolysis rates of polysaccharides and the change in microbial community composition based on 16S rRNA tag sequencing and fluorescence *in situ* hybridisation (FISH) within the same experiments. These new analyses gave us an insight into the activity of other polysaccharide utilisation mechanisms within the same experiments and allowed us to qualitative and quantitative access the changing in microbial community composition during the incubations.

Five of the six tested polysaccharides were hydrolysed at every station but the rates and spectrum of hydrolysis varied across the Atlantic Ocean. The highest rates of hydrolysis were seen in the laminarin and xylan incubations (22 nmol monomer L⁻¹ h⁻¹ and 17 nmol monomer L⁻¹ h⁻¹ for laminarin and xylan, respectively). We found distinct patterns in the rates and spectrum of hydrolysis of individual polysaccharide and could associate these to variations in the community composition between stations. In our previous study, we discovered that the *Bacteroidetes*, *Planctomycetes* and *Catenovulum* were using an alternative substrate uptake mechanism and now using 16s rRNA sequencing we could further classify these into specific genera. Additionally, we could show that *Alteromonas* was potentially a dominant external degrader within the Atlantic Ocean. The combined analysis of the activity of different substrate utilisation mechanisms and changes in the community composition enabled us to link specific bacterial groups to specific functions and identify the potentially dominant polysaccharide degrading organisms in the Atlantic Ocean. Using these data, we can begin to hypothesise on how differences in the global distribution patterns of specific microorganism effect the turnover of organic matter in the marine environment.

Introduction

Marine phytoplankton fix an estimated 44 to 67 Gt of carbon per year which accounts for half of the global carbon fixation (Ciais et al 2013, Field et al 1998, Finkel 2014, Westberry et al 2008). The primary mediators of the decomposition and remineralisation of up to 90% of this fixed carbon are heterotrophic microorganisms (Cho and Azam 1988, Elifantz et al 2007, Hedges 1992, Moran et al 2016, Piontek et al 2011). Phytoplankton derived carbon is available to microorganisms largely in the form of dissolved organic matter (DOM) and it is degraded within hours to days of its production (Arnosti 2004, Bunse and Pinhassi 2016, Elifantz et al 2005, Elifantz et al 2007, Kirchman et al 2001). The high turnover of organic matter by marine microorganisms has a significant impact on global carbon and nutrient cycling (Landa et al 2016, Legendre et al 2015, Piontek et al 2011, Teira et al 2008).

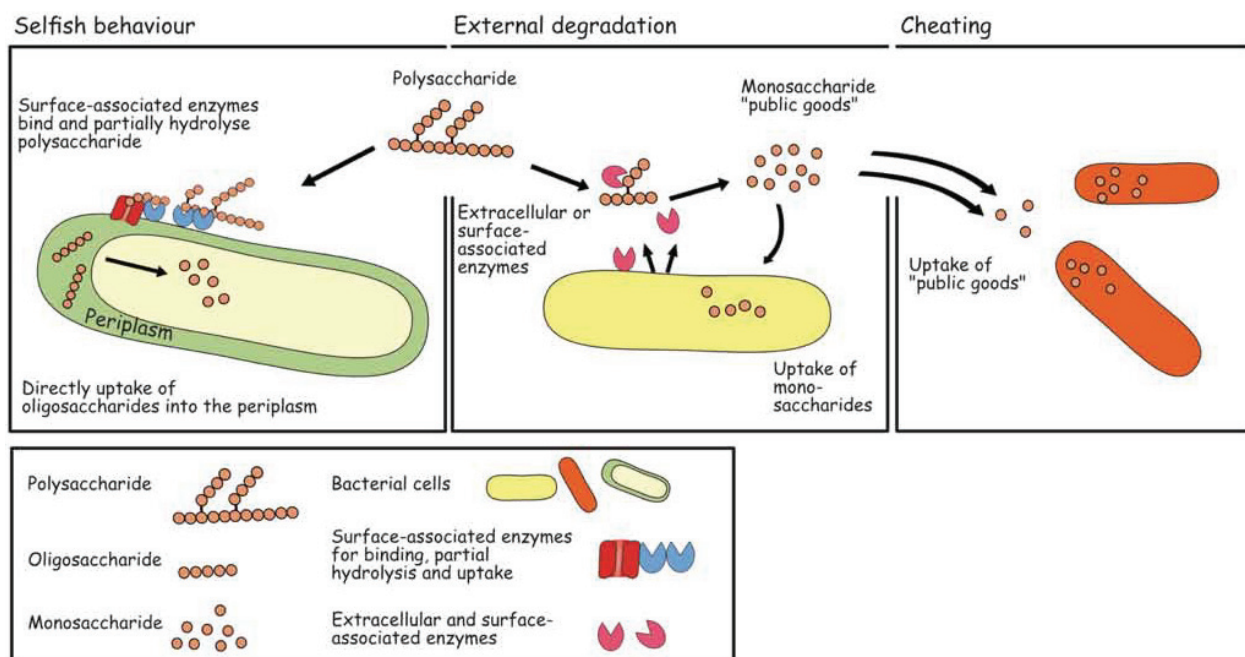
Phytoplankton derived organic matter consists of low molecular weight (LMW) compounds, such as amino acids and sugars, and high molecular weight (HMW) components, such as proteins, polysaccharides, lipids and nucleic acids (Alderkamp et al 2007, Benner et al 1992, Biddanda and Benner 1997, Biersmith and Benner 1998, Mykkestad 1995). Polysaccharides can account for as much as 50% of the total dissolved organic carbon (DOC) in surface oceans (Benner et al 1992). Whereas microorganisms can directly transport the LMW components across their cell membranes, a major fraction of HMW substrates must first be extracellularly enzymatically hydrolysed (Arnosti 2011, Decad and Nikaido 1976, Weiss et al 1996). The remineralisation of a significant fraction of marine organic matter is, therefore, dependent on the enzymatic activity of microorganisms.

Environmental enzymatic activity rates are determined by measuring the change in concentration of a substrate or the rate of product production over time (Arnosti 2003, Chróst 1992). However, it is currently not or only partially possible to fully characterise and measure the concentrations of specific polysaccharides within an environmental sample (reviewed in detail by Thornton (2014)), (Becker et al 2017). Without knowing the concentration of a polysaccharide, we cannot determine its rate of hydrolysis or estimate the impact its turnover has on the global carbon cycle.

We can, however, calculate the potential hydrolysis rates by using fluorescently-labelled polysaccharide (FLA-PS) incubations (Arnosti 2003). FLA-PS incubations allow for the quantification of the change in the molecular mass distribution of a specific polysaccharide as it is enzymatically hydrolysed to smaller sizes over time. Previous analyses using FLA-PS have highlighted distinct patterns both in the spectrum and rates of polysaccharide hydrolysis across latitudes (Arnosti et al 2011). It is unknown however if these patterns are dependent on differences in the microbial community composition and to what extent functional differences between communities affect the activity rates.

Chapter 5 | Tracking bacterial community dynamics in polysaccharide incubations along an Atlantic Meridional Transect

Marine microorganisms have three main mechanisms of accessing HMW substrate; external degradation, cheating and selfish behaviour (Chapter 5 Figure 1) (Allison 2005, Cuskin et al 2015, Kaiser et al 2015, Reintjes et al 2017). Selfish organisms use surface-associated enzymes to bind and partially degrade HMW substrates on the cell surface and then directly transport the produced oligomers into the cell. These are further hydrolysed within the protective space of the periplasm (Cuskin et al 2015, Kabisch et al 2014, Reintjes et al 2017). External degraders (aka. decomposers, cooperative microbes) produce extracellular or surface-associated enzymes to externally degrade HMW substrates to sizes suitable for uptake (Kaiser et al 2015, West et al 2007). The extracellular degradation of a substrate causes the release of hydrolysis products into the environment; collectively called “public goods” (Cordero et al 2012, West et al 2007). “Public goods” are freely available LMW substrates that can be taken up by other organisms such as “cheaters” and scavengers (Allison 2005, West et al 2007). Cheaters do not produce extracellular enzymes but profit from the enzymatic activity of other organisms (Allison 2005, Kaiser et al 2015). These functional differences between microorganisms may also influence the hydrolysis patterns previously observed in the marine environment.



Chapter 5 Figure 1 Schematic diagram of the three main mechanisms of HMW substrate utilisation of marine bacteria. Selfish behaviour: cells use surface associated enzymes to bind and partially degrade polysaccharides. These are directly taken up into the periplasm for further degradation with no production of extracellular hydrolysis products. External degradation: cells use surface-associated or extracellular enzymes to degrade polysaccharide to sizes suitable for uptake. This causes the production of extracellular hydrolysis products termed “public goods”. Cheating: cells do not / cannot produce enzymes

for the hydrolysis of polysaccharides but take up the hydrolysis products produced by the activity of other organisms.

We investigated both the taxonomic and functional diversity of microorganisms associated with the hydrolysis of HMW polysaccharides to increase our understanding of why there are differences in the patterns of extracellular hydrolysis rates across oceanic provinces. We did this by analysing the activity of external degraders using FLA-PS incubations and identifying the active external degraders using 16S rRNA sequencing and fluorescence *in situ* hybridisation (FISH). We combined these results with our previous finding of the taxonomy and activity of selfish behaviour within in the Atlantic Ocean (Reintjes et al 2017). These combined analyses allowed us to further our understanding of the patterns in polysaccharide utilisation on a functional and taxonomic level across the Atlantic Ocean.

Methods

Sampling and Substrate Incubations

During the Atlantic Meridional Transect (AMT) 22 cruise from Southampton, UK, to Punta Arenas, Chile, from 10.10.2012 to 24.11.2012 seawater samples were taken from five sites in four different oceanic provinces (Chapter 4 Supplementary Figure 1). These included the Northern Temperate, Northern Gyre, Equatorial and Southern Gyre province. The Southern Gyre was sampled twice, once in the north and once in the south. The samples were collected at solar noon using a Niskin bottle rosette with an attached Sea Bird CTD (Sea Bird Scientific). Triplicate 20 L samples were taken at each station from 20 m depth. Six 500 ml subsamples of each triplicate were added to acid washed sterile glass bottles (18 in total) and incubated with one of six fluorescently labelled polysaccharides (FLA-PS) for a total of 12 to 18 days. The polysaccharides were laminarin, xylan, chondroitin sulphate, arabinogalactan, fucoidan, pullulan and they were added at a concentration of 1.75 μ M monomer equivalent to each 500 ml incubation mimicking a natural low input of organic matter. Two types of control samples were taken. Firstly, an additional 500 ml subsample was incubated in a sterile glass bottle, without a polysaccharide; this served as a treatment control. Secondly, six 50 ml subsamples of seawater were placed in sterile glass bottles and autoclaved. Subsequently, one of each of the 6 polysaccharides was added to a bottle and incubated under the same conditions; these served as killed controls.

All bottles (18 incubation, 1 treatment control, 6 kill control) were kept at room temperature in the dark. Subsamples for microscopy, FISH analysis, extracellular

enzymatic activity and microbial diversity were collected at regular time points (typically 30 min, 1, 3, 6, 12, and 18 days). For microscopy and FISH, 20 ml of water was filtered through a 47 mm (0.2 μ m pore size) polycarbonate filter, applying a gentle vacuum of < 200 mbar. After drying, the filters were stored at -20°C until further analysis. For microbial diversity analyses, 10 ml of water was filtered through a 0.2 μ m pore size polycarbonate filter using a Whatman 420200 Swin-Lok filter holder (Sigma-Aldrich, Munich, Germany). Two ml of the filtrate from the microbial diversity sample was collected and stored at -80°C for measurement of extracellular enzyme activity.

DNA Extraction

Microbial DNA was extracted using the MoBio Power Water DNA Extraction Kit (MoBio Laboratories, Inc) as recommended by the manufacturer.

PCR and Sequencing

PCR was carried out using the primers S-D-Bact-0341-b-S-17 (5'-CCTACGGGNGGCWGCAG-3') and S-D-Bact-0785-a-A-21 (5'-GACTACHVGGGTATCTAATCC-3) targeting the V3-V4 variable region of the 16S rRNA (Klindworth et al 2013) and Phusion High-Fidelity DNA polymerase as recommended by the manufacturer (Thermo Fisher). Subsequently, the PCR products were visualised and amplicon bands were cut out with a sterile scalpel. The excised gel slices were purified using the QiagenMiniElute kit (Qiagen). After purification, the PCR products were pooled into libraries with a minimum DNA concentration of 1 μ g, measured using a Qubit assay (Invitrogen). The libraries were paired-end sequenced using the 300 bp chemistry on an Illumina Miseq (Illumina, CA, USA).

Processing of Sequencing Data

The sequence reads from the Illumina Miseq were further processed using the bioinformatics pipeline of the SilvaNGS project (Quast 2013). Processing involved quality controls for sequence length (> 200 bp) and the presences of ambiguities (< 2%) and homopolymers (< 2%). The remaining reads were aligned against the SSU rRNA seed of the SILVA database release 119 (Quast et al 2013). The classification was done by a local BLAST search against the SILVA SSURef 119.1 NR database using blast -2.2.22+ with standard settings.

Microbial Diversity Analysis and Evaluation of Sequencing Triplicates

The interpretation and visualisation of the microbial diversity analyses were done using normalised species abundance to site matrices using the R software with the packages Vegan (community ecology package (Oksanen et al 2013)) and Rioja (Analysis of Quaternary Science Data (Juggins 2016-07-13)). Specifically, the Vegan package was used to calculate diversity indices, community ordination, ANOSIM and dissimilarity analysis.

All substrate incubations were performed in biological triplicates and the community within each triplet showed similar changes in diversity (Chapter 5 Supplementary Figure 1Chapter 5 Supplementary Figure 2). The similarity was calculated by first obtaining the mean variance of the triplicate read abundance from each genus and then calculating the mean variance in each sample (all genera). The standard deviation was calculated by taking the square root of the mean variance of each sample. Subsequently, the confidence intervals were calculated. The mean variance of all triplicate incubations was 1.62×10^{-5} with a mean standard deviation of 3.6×10^{-3} and 95% confidence interval of 2.37×10^{-4} ; 79% of the samples fell within the confidence intervals. A treatment control bottle with no substrate addition was run in parallel at all stations (as mentioned above).

The change in community composition over the course of each incubation was investigated using the percentage change in abundance of each genus over time (minimum read abundance of 0.5%). The percentage change in abundance is calculated by analysing the change in normalised read abundance of each bacterial genus over time compared to the initial community (T0). The percentage change in abundance highlights both the positive and negative responses of each genus to the substrate addition.

Extracellular Enzymatic Activity

Six polysaccharides (laminarin, xylan, chondroitin sulphate, arabinogalactan, pullulan, fucoidan) obtained from Sigma-Aldrich (Germany) were fluorescently labelled with fluoresceinamine (Sigma-Aldrich; isomer II) as described in Arnosti (2003). The fluorescently labelled polysaccharide solutions are free of mono- or oligosaccharides because they are repeatedly injected onto standardised gel permeation chromatography systems as part of the labelling procedure; any lower molecular weight carbohydrates are thereby removed during purification. A single polysaccharide was added at a concentration of $1.75 \mu\text{mol}$ monomer-equivalent to each 500 ml water sample; each polysaccharide was incubated in triplicate, plus one killed control, as

described above. Activities of enzymes that hydrolyse each polysaccharide were determined by monitoring the changes in molecular weight of the fluorescently labelled polysaccharides over the time course of the incubations, as described in detail in Arnosti (2003). In brief, a sub-sample of each sample was injected into a gel permeation chromatography / HPLC system with two Sephadex columns (G-50 and G-75 gel) connected in sequence, with the column outflow passing through a Hitachi fluorescence detector set to excitation and emission maxima of 490 and 530 nm, respectively. Columns were standardised using a series of FITC-labelled dextrans, and free fluorescent tags (Sigma-Aldrich). Changes in substrate molecular weight distribution relative to the time-zero samples were determined at each time point, and hydrolysis rates were calculated from the changes in molecular weight distribution with time. Note that added polysaccharides would be in competition with naturally present substrates for the enzyme active sites; hydrolysis rates reported here are potential rates. Since the added substrate represents a ~25% increase in total DOC typical for surface ocean waters of the North Atlantic (Longhurst 2007), however, the added substrate is likely at saturating concentrations for specific enzymes.

Substrate Staining, FISH and Automated Microscopy

A selection of groups specific FISH probes was chosen based on the bacterial groups that showed changes in read abundance during the incubations (see Results, Microbial Diversity). This selection included probes for the *Bacteroidetes* (CF319a), *Planctomycetes* (PLA46), *Alteromonadales* (ALT1314) and *Catenovulum* (CAT653) (Chapter 4 Supplementary Table 1).

All cell staining and microscopy was done as described in detail in Chapter 4. Briefly, for the enumeration of substrate stained cells all samples were counterstained with DAPI and subsequently mounted using a Citifluor (EMS) Vectashield (Vector Laboratories) (v/v) (4 : 1) mounting solution. The samples were then visualised and enumerated on a fully automated microscope imaging system, as described in detail in Chapter 1. FISH was carried out as described in Chapter 4 with the FISH probes shown in Chapter 4 Supplementary Table 1. To test for relationships between the total cellular abundance of specific bacterial clades enumerated by FISH and the change in extracellular hydrolysis activity over time Pearson correlations were performed using the R software package.

Results

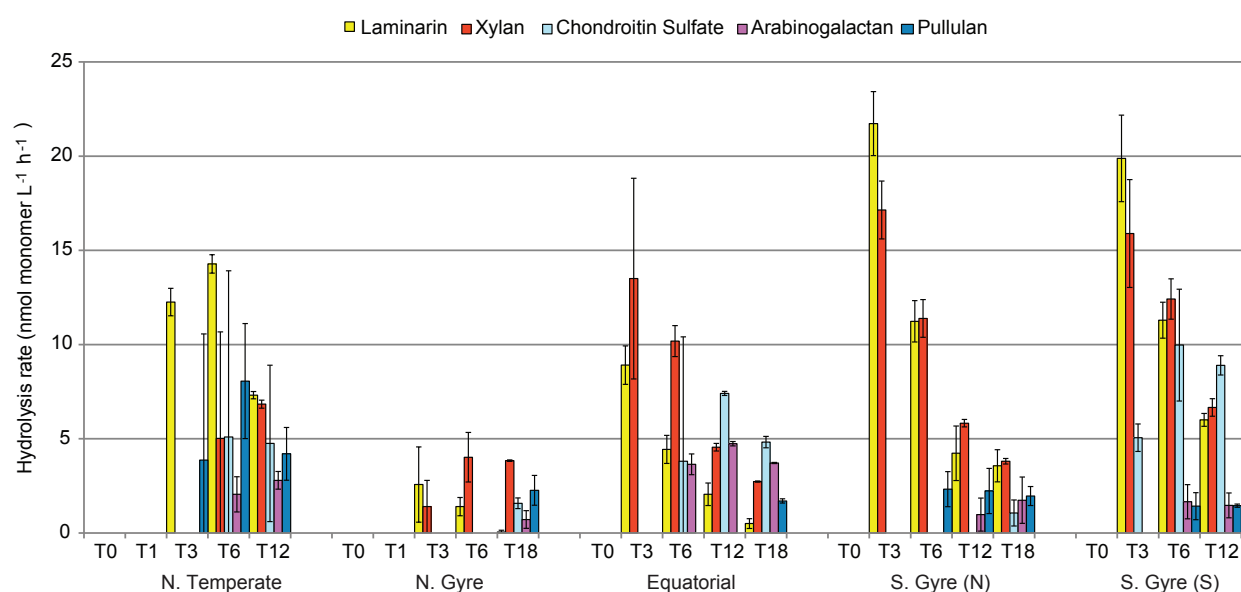
Extracellular Hydrolysis Rates

Five of the six polysaccharides were hydrolysed at every station, although the rates varied considerably by station and substrate (Chapter 5 Figure 1). Fucoidan was not measurably hydrolysed in any incubation. Laminarin and xylan had the highest overall hydrolysis rates and were rapidly hydrolysed in all stations. The highest rate of hydrolysis of these two substrates occurred in the S. Gyre (N) (22 nmol monomer L⁻¹ h⁻¹ and 17 nmol monomer L⁻¹ h⁻¹ for laminarin and xylan, respectively) and the S. Gyre (S) (20 nmol monomer L⁻¹ h⁻¹ and 16 nmol monomer L⁻¹ h⁻¹ respectively) (Chapter 5 Figure 2). In all stations, except the N. Temperate and N. Gyre, laminarin and xylan followed a similar hydrolysis pattern with the highest hydrolysis rates at day three. The subsequent decrease in calculated hydrolysis rate is primarily because most of the substrate was hydrolysed to small size classes by day 3, such that longer incubation times yielded lower calculated rates (see Methods).

The N. Temperate had the most distinct hydrolysis patterns, with only laminarin and pullulan being hydrolysed at day three, whereby pullulan hydrolysis could only be measured in one of the triplicates (Chapter 5 Figure 2). All five substrates were actively hydrolysed at day 6 but again there was high variability between the triplicates. This high variability between the biological triplicates was only seen in the N. Temperate station.

The N. Gyre had the lowest overall hydrolysis rates with only two of the six substrates (laminarin and xylan) being hydrolysed at low rates at day 3 (Chapter 5 Figure 2). Only after 18 days of incubation could low rates of hydrolysis of five substrates be detected. Contrastingly both S. Gyre stations had high hydrolysis rates of laminarin and xylan within 3 days in both stations and high hydrolysis rates of chondroitin sulphate in the S. Gyre (S) station.

Chondroitin sulphate hydrolysis could be measured earlier in the N. Temperate, Equatorial and S. Gyre (S); with the highest and earliest rate seen in the Southern Gyre (S) (10 nmol monomer L⁻¹ h⁻¹; T6) (Chapter 5 Figure 2). By comparison, hydrolysis rates of chondroitin sulphate were very low (1 nmol monomer L⁻¹ h⁻¹) and could only be measured on day 18 in the N. Gyre and S. Gyre (N). Arabinogalactan showed a hydrolysis pattern similar to chondroitin sulphate. The highest hydrolysis of arabinogalactan was at the Equatorial station (5 nmol monomer L⁻¹ h⁻¹; T12). Pullulan was hydrolysed fastest in the N. Temperate and S. Gyre (N) (T6), but overall the rates were low (average; 2 nmol monomer L⁻¹ h⁻¹) at all stations.



Chapter 5 Figure 2 Hydrolysis rates (nmol monomer L⁻¹ h⁻¹) of laminarin (yellow), xylan (red), chondroitin sulfate (light blue), arabinogalactan (purple) and pullulan (dark blue) in different oceanic provinces (N. Temperate, N. Gyre, Equatorial, S. Gyre (N), S. Gyre (S)) with incubation time (T0, T1, T3, T6, T12, T18 days). Error bars indicate a difference in rates among biological triplicate bottles

Microbial Diversity

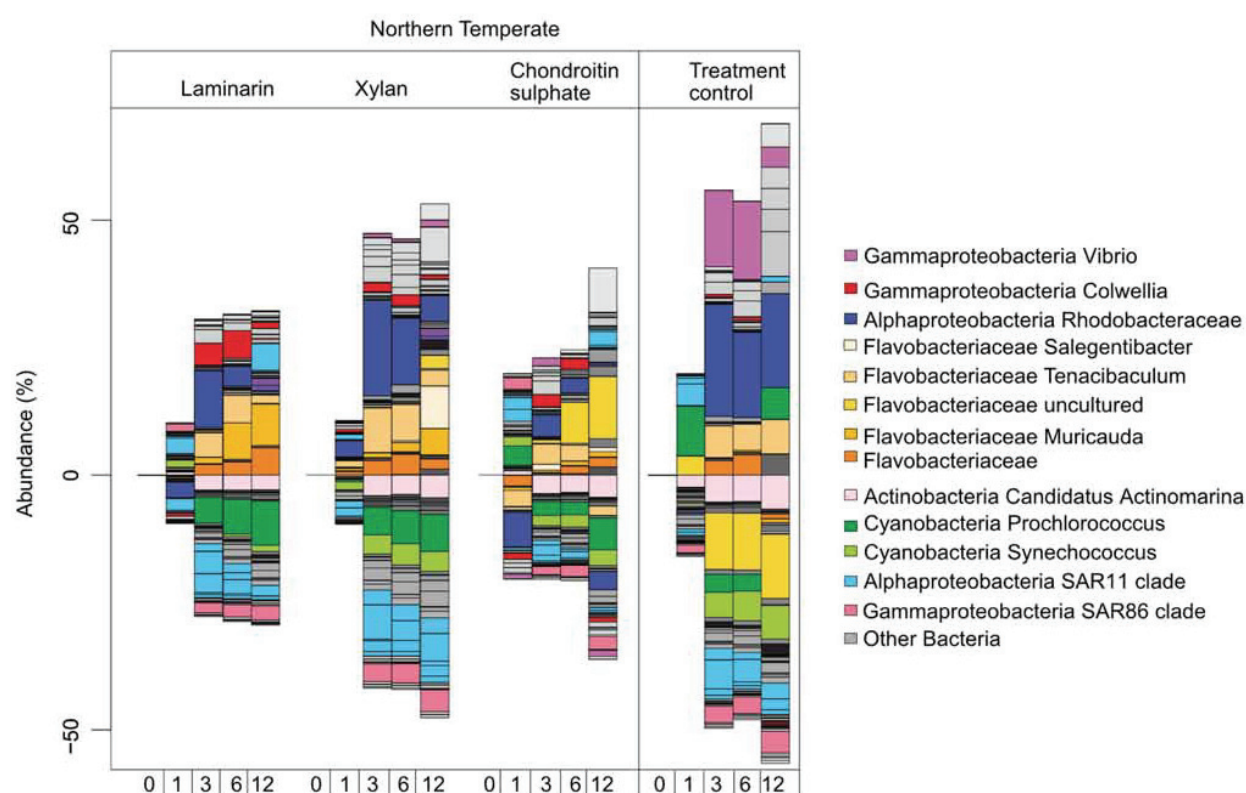
The change in microbial diversity was only analysed in the laminarin, xylan and chondroitin sulphate incubations. We deliberately chose to sequence a selected set of incubations because we wanted to analyse each biological triplicate from these incubations. Although it is not yet common practice to analyse biological replicates using NGS, we sequenced and analysed replicates to statistically show that there is a reproducible change in community composition. The analysis of biological replicates is essential because it determines to what extent results are representative of the environment (Prosser 2010). However, owing to the high volume of data produced from analysis replicates we reduced our analyses set by examining only the incubations with the highest activity rates (Chapter 5 Figure 2).

ANOSIM of the initial communities (T0) showed a slight difference between the stations ($R = 0.48$, $p = 0.0009$) (Chapter 5 Supplementary Figure 3). In all stations, the dominant genera were SAR86, *Alteromonas*, SAR11, SAR116, AEGEAN-169 marine group, *Rhodobacteraceae*, *Prochlorococcus*, NS5, NS4, Candidatus *Actinomarina* (Chapter 5 Supplementary Figure 4). These results are consistent with previous findings of surface ocean waters showing that the same groups dominate across large oceanic regions (Friedline et al 2012, Giovannoni and Stingl 2005, Giovannoni and Vergin

2012, Yilmaz et al 2012). Differences in the total community composition were most apparent in the N. Temperate and N. Gyre. The N. Gyre had a higher abundance of *Gammaproteobacteria* and *Alphaproteobacteria*, whereas the N. Temperate exhibited a high abundance of *Flavobacteriaceae*, *Alphaproteobacteria* and a lower abundance of *Gammaproteobacteria* (Chapter 5 Supplementary Figure 4).

Microbial community composition changes during the course of each incubation showed both a substrate-specific changes - enrichment of *Planctomycetes* in nearly all chondroitin sulphate incubations - and site-specific changes with an increase of different organisms (*Bacteroidetes*, *Alteromonas* and *Catenovulum*) in the laminarin and xylan incubations (Chapter 5 Figure 3, Chapter 5 Figure 4, Chapter 5 Figure 5, Chapter 5 Figure 6, Chapter 5 Figure 7). All incubations showed a decrease in *Cyanobacteria*, specifically *Prochlorococcus* and *Synechococcus*. This corresponds to their phototrophic lifestyle as incubations were kept in the dark.

In the N. Temperate, there was an increase in *Bacteroidetes* in all incubations (Chapter 5 Figure 3) specifically, the family *Flavobacteriaceae* and the genera *Muricauda*, *Salegentibacter*, *Tenacibaculum* and uncultured *Flavobacteriaceae*. There was also an increase in the alphaproteobacterial genus *Shimia* and the gammaproteobacterial genus *Colwellia*. The treatment control had a similar increase of the genera *Shimia* and *Tenacibaculum* but also a marked increase in *Vibrio*, which was not seen in the substrate incubations.

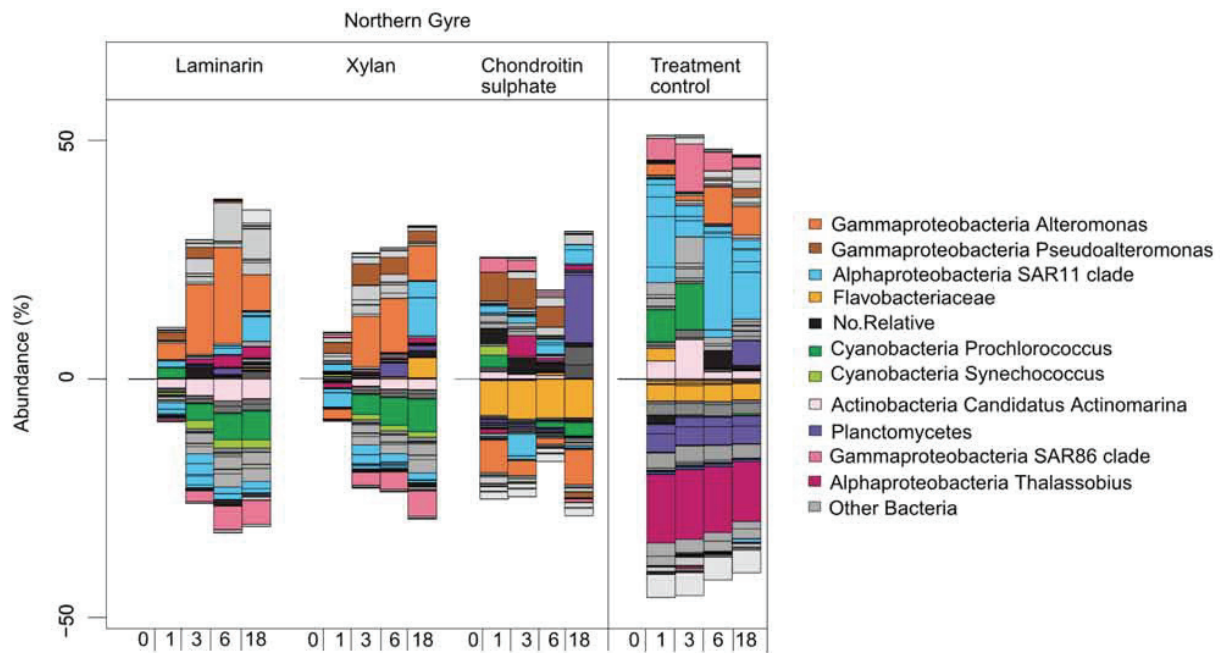


Chapter 5 Figure 3 Percentage change in relative read abundance of bacterial genera within substrate incubations (laminarin, xylan, chondroitin sulphate) and treatment control of the N. Temperate station. Substrate incubations were sampled at T0, 1, 3, 6, and 12 days.

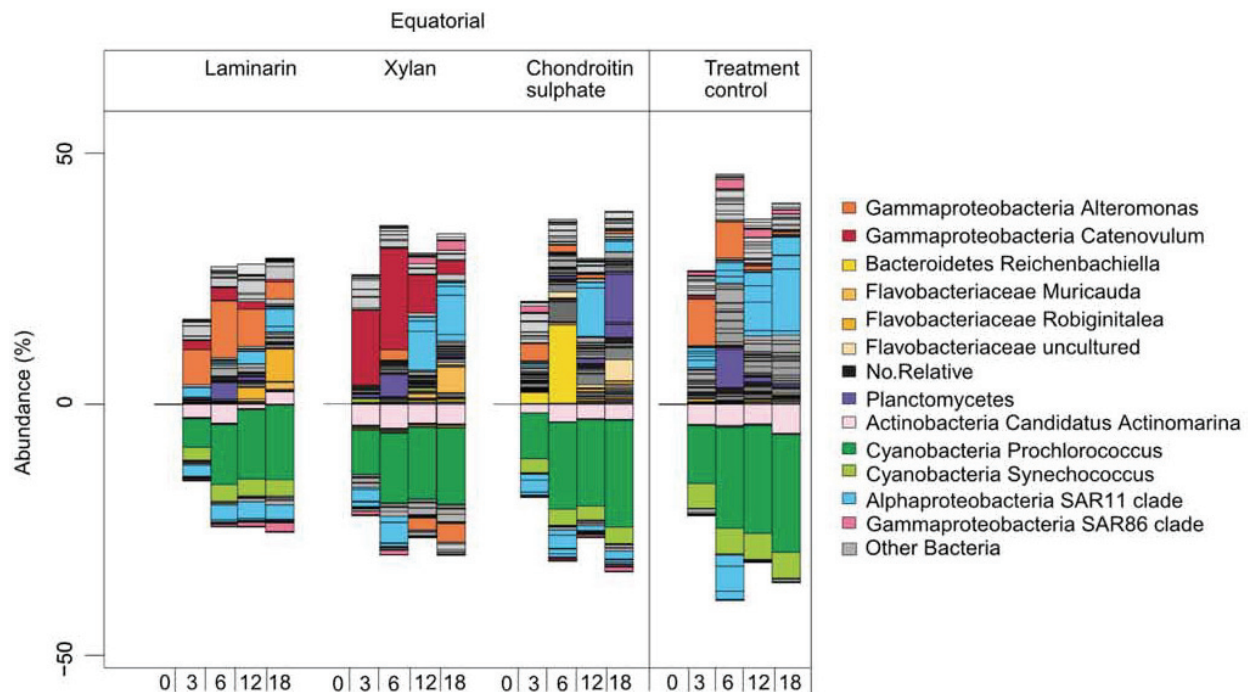
In the laminarin and xylan incubations of all other stations, there was an increase of predominantly *Gammaproteobacteria* specifically the genus *Alteromonas*, *Catenovulum* and other *Alteromonadaceae*. whereas in the chondroitin sulphate incubations there was an increase of *Planctomycetes*, specifically the *Rhodopirellula* and *Planctomyces*. The *Planctomycetes* increased after 12 to 18 days in the N. Gyre, Equatorial and S. Gyre (N) and after 3 days in the S. Gyre (S) (Chapter 5 Figure 4, Chapter 5 Figure 5, Chapter 5 Figure 6, Chapter 5 Figure 7). In addition to the *Planctomycetes* there was an increase in *Flavobacteriaceae* in the Equatorial and S. Gyre (S) chondroitin sulfate incubations, specifically the genus *Reichenbachiella* and *Tamlana* respectively. The S. Gyre (N) also showed an increase in *Verrucomicrobia* late in the chondroitin sulphate incubation.

In all stations, there was a decrease in the abundance of the initial (T0) dominant groups of SAR86 and Candidatus *Actinomarina* as well as *Prochlorococcus* and *Synechococcus*. Similarly, SAR11 showed an initial decrease in all incubations but increased in abundance late (T12 - T18) in the N. Gyre, Equatorial and S. Gyre (N). The treatment controls generally showed different changes in composition in comparison to the incubations although slight similarities could be seen.

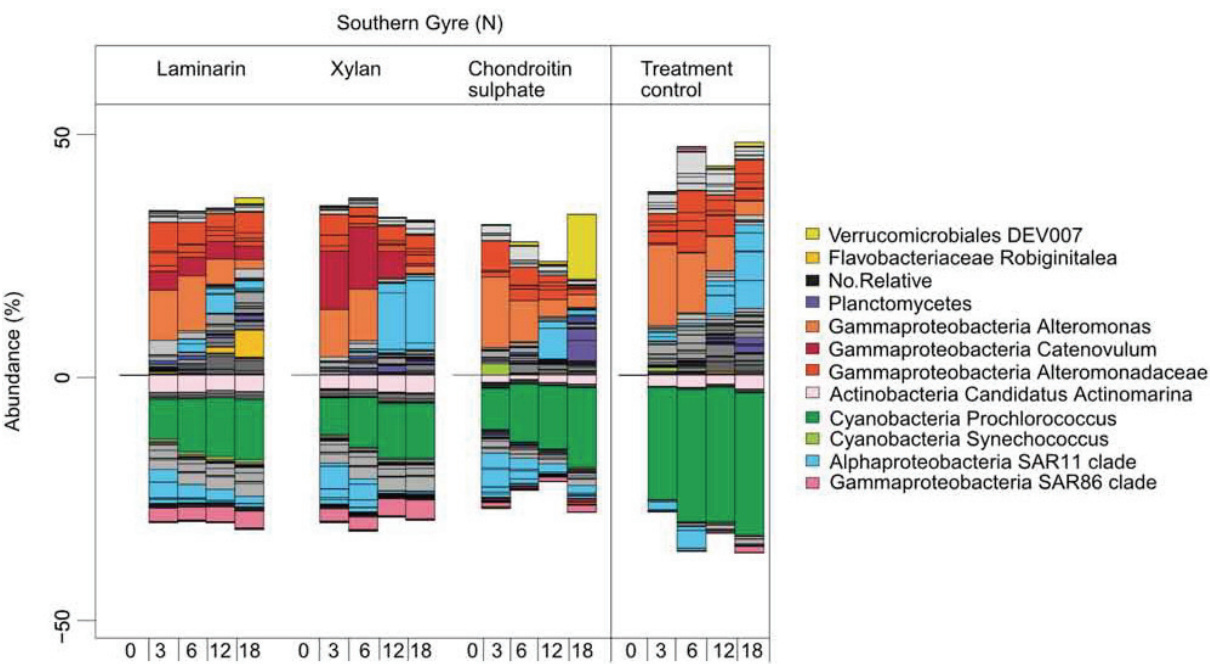
Chapter 5 | Tracking bacterial community dynamics in polysaccharide incubations along an Atlantic Meridional Transect



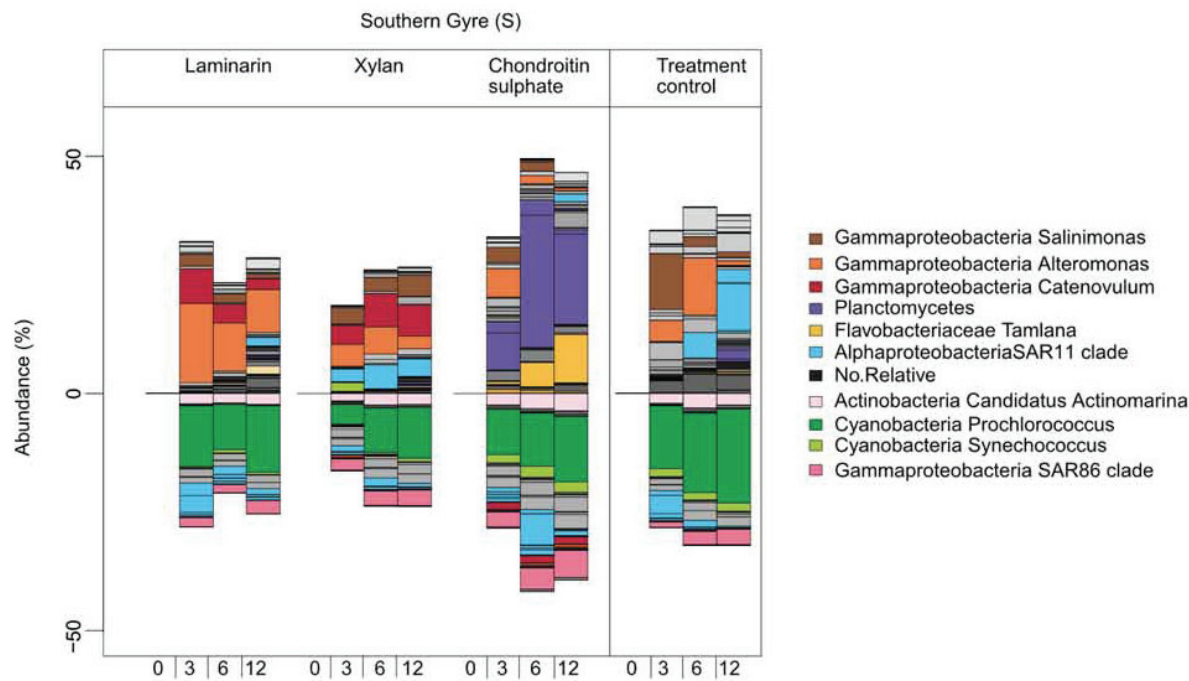
Chapter 5 Figure 4 Percentage change in relative read abundance of bacterial genera within substrate incubations (laminarin, xylan, chondroitin sulphate) and treatment control of the N. Gyre station. Substrate incubations were sampled at T0, 1, 3, 6, and 18 days.



Chapter 5 Figure 5 Percentage change in relative read abundance of bacterial genera within substrate incubations (laminarin, xylan, chondroitin sulphate) and treatment control of the Equatorial station. Substrate incubations were sampled at T0, 3, 6, 12, and 18 days.



Chapter 5 Figure 6 Percentage change in relative read abundance of bacterial genera within substrate incubations (laminarin, xylan, chondroitin sulphate) and treatment control of the S. Gyre (N) station. Substrate incubations were sampled at T0, 3, 6, 12, and 18 days.



Chapter 5 Figure 7 Percentage change in relative read abundance of bacterial genera within substrate incubations (laminarin, xylan, chondroitin sulphate) and treatment control of the S. Gyre (S) station. Substrate incubations were sampled at T0, 3, 6, 12 days.

Total Cellular Abundance

The total cellular abundance did not change significantly during the incubations (with a single exception, Chapter 4 Supplementary Figure 5). The percentage change in abundance of specific groups accompanied by low changes in bulk abundance indicated a community level response to the substrate addition. Although a bottle effect is inevitable within such incubations, the data obtained reflects the potential of the *in situ* organisms as the bacteria within the bottles were certainly from the original water sample.

Relative Abundance of Specific Bacterial Groups (Enumerated by FISH)

In the laminarin incubation, there was an increase in the abundance of *Bacteroidetes* in the N. Temperate, N. Gyre and S. Gyre (S) (Chapter 5 Figure 8a). In addition to the *Bacteroidetes*, there was an increase in abundance of *Alteromonas* in all laminarin incubations. They increased significantly at day 3 in all stations, with an average increase from 8.12×10^3 cells ml⁻¹ to 1.07×10^5 cells ml⁻¹. Additionally, the gammaproteobacterial genus *Catenovulum* increased in abundance in the laminarin incubation of the S. Gyre (N) and S. Gyre (S).

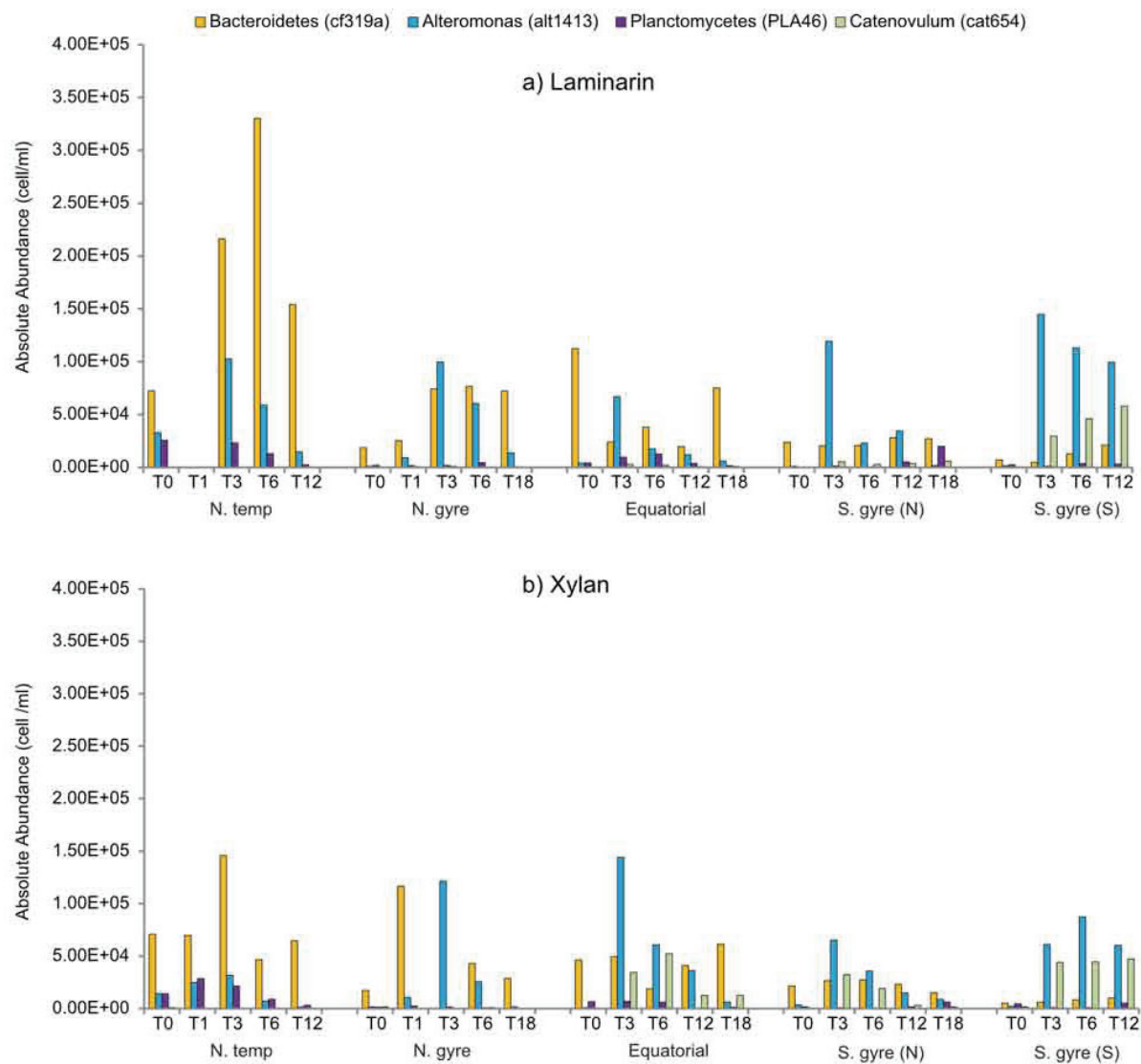
In the xylan incubations, there was a significant increase in the abundance of *Bacteroidetes* in the N. Temperate and N. Gyre (Chapter 5 Figure 8b). In the Equatorial region, their abundance increased only slightly after 12 - 18 days. *Alteromonas* increased in abundance by day 3 in all stations of the xylan incubation. Similar to the laminarin incubations there was an increase in *Catenovulum* in the Equatorial, S. Gyre (N) and S. Gyre (S) stations.

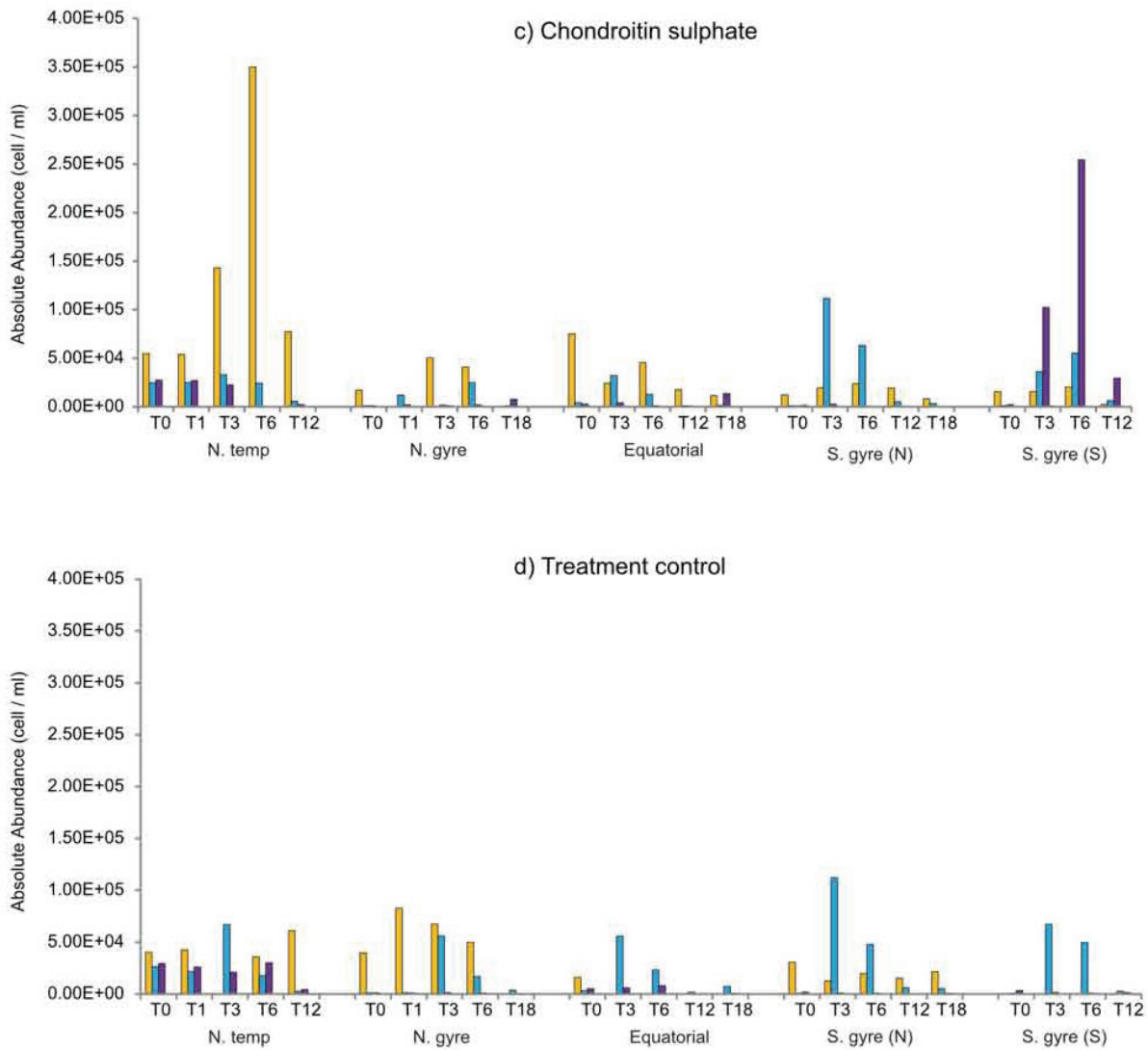
In the chondroitin sulphate incubations, the highest increase in cellular abundance was seen in the *Planctomycetes*. They increased in abundance in the N. Gyre, Equatorial, S. Gyre (N), and S. Gyre (S) stations (Chapter 5 Figure 8c). In the N. and S. Gyre (N), *Planctomycetes* only increased in abundance after 18 days, whereas in the Equatorial and S. Gyre (S) stations they increased after 6 days. In addition to the *Planctomycetes*, the *Alteromonas* increased in the Equatorial, S. Gyre (N) and S. Gyre (S) station at day 3. In the chondroitin sulphate incubation of the N. Temperate station there was no increase in *Planctomycetes*, however, there was an increase in *Bacteroidetes* from 5.48×10^4 cells ml⁻¹ to 3.60×10^5 cells ml⁻¹ after 6 days (Chapter 5 Figure 8c).

The treatment controls showed no increase in abundance of *Bacteroidetes* (except in the N. Gyre), *Catenovulum* or *Planctomycetes* (Chapter 5 Figure 8d). There was an increase in the abundance of *Alteromonas* in all treatment control bottles but it was not as high as in the substrate incubations (except in the S. Gyre (S)). Slight changes in the

Chapter 5 | Tracking bacterial community dynamics in polysaccharide incubations along an Atlantic Meridional Transect

community composition of the treatment control were expected as experiments were done in bottles and the seawater used in the experiments would have a natural abundance of DOM which can also cause community composition changes.





Chapter 5 Figure 8 Absolute abundances of specific bacterial groups during substrate incubations and treatment control in the N. Temperate, N. Gyre, Equatorial, S. Gyre (N), S. Gyre (S). The absolute abundance was determined by using group-specific FISH probes CF319a (orange), PLA46 (purple) and CAT653 (green), ALT1413 (blue) for *Bacteroidetes*, *Planctomycetes*, *Catenovulum* and *Alteromonas* respectively. Panels: (a) laminarin, (b) xylan, (c) chondroitin sulphate and (d) treatment control.

Correlation of Extracellular Hydrolysis Activity with Cellular Increase of Specific Microbial Groups (Enumerated by FISH)

Pearson correlations between the increase in cellular abundance of specific microbial groups (enumerated by FISH) and the extracellular hydrolysis activity were performed. A significant correlation between the increase in abundance of *Alteromonas* cells and the increase in extracellular hydrolysis activity was seen in the laminarin ($R = 0.59$, P -value = 0.002) and xylan ($R = 0.56$, P -value = 0.005) incubations. Additionally, there was a negative correlation between the increase in *Bacteroidetes* abundance and extracellular hydrolysis activity in the laminarin incubation ($R = -0.43$, P -value = 0.035) and a positive relationship between the increase of *Catenovulum* and extracellular hydrolysis of xylan ($R = 0.52$, p -value = 0.015).

Discussion

The microbial community composition throughout the Atlantic Ocean had the potential to quickly hydrolyse laminarin. The high potential to degrade laminarin has also been shown across a broad latitudinal range (Arnosti et al 2011). Laminarin has been identified as one of the major storage compounds of marine phytoplankton and its global production is estimated at 5 to 15 billion tons per year (Alderikamp et al 2007, Hecky et al 1973). The seemingly global potential to degrade laminarin indicates that it could be highly available and a common substrate for marine microorganisms. The most distinct hydrolysis patterns occurred in the N. Temperate station. Consistent with these distinct patterns there was also a distinctive change in the community composition compared to the other stations. All substrate incubations of the N. Temperate stations had an increase in both the cellular and read abundance of *Bacteroidetes*, specifically the family *Flavobacteriaceae* and the genera *Muricauda*, *Salegentibacter*, *Tenacibaculum*. Many *Flavobacteriaceae* are HMW specialists and have been repeatedly reported to contain a specific genetic repertoire for the degradation of polysaccharides (Bauer et al 2006, Buchan et al 2014, Fernández-Gómez et al 2013, Gómez-Pereira 2010, Teeling et al 2012). Within our incubations, they showed the ability to use three distinct polysaccharides further highlighting the metabolic versatility of the family. In the N. Temperate station the *Flavobacteriaceae* had a higher initial (T0) abundance which appeared to give them a competitive advantage over other organisms in the substrate incubations. Comparatively, *Flavobacteriaceae* had a

lower initial abundance and did not significantly increase in the incubations in all other stations.

All other stations (N. Gyre, Equatorial, S. Gyre (N) and S. Gyre (S)) showed highly similar patterns of hydrolysis particularly in the laminarin and xylan incubations, although the rates varied and were particularly low in the N. Gyre. All stations showed an increase in cellular and read abundance of *Gammaproteobacteria*, specifically the genus *Alteromonas* and *Catenovulum*, except the N. Gyre where only *Alteromonas* increased. The initial read abundance of *Alteromonas* and *Catenovulum* was higher in the Equatorial, S. Gyre (N) and S. Gyre (S), specifically when compared to the N. Temperate stations. Although the cellular abundance of *Alteromonas* and *Catenovulum* was low in all incubations they increased in abundance and responded to the substrate addition.

In the chondroitin sulfate incubations of the N. Gyre, Equatorial, S. Gyre (N) and S. Gyre (S) there was a substrate-specific selection of *Planctomycetes*, specifically the genera *Rhodopirellula* and *Planctomyces*. This selection was substrate-specific as no other organisms appeared to hydrolyse chondroitin sulfate (except *Bacteroidetes* in the N. Temperate station). Hydrolysis could only be measured after there was an increase in *Planctomycetes*. Throughout the Atlantic Ocean there is a lower potential to use chondroitin sulfate and the *Planctomycetes* and *Bacteroidetes* were the only organisms that degraded this high sulphated marine polysaccharide. Both phyla have been shown to contain sulfatases which would enable them to degrade chondroitin sulfate (Bondoso et al 2017, Gómez-Pereira 2010, Gómez-Pereira et al 2012b, Grondin et al 2017, Wegner et al 2013).

Our results show that differences in the microbial community composition among stations result in different patterns in the rates of hydrolysis. Consequently, the global distribution patterns of marine microorganisms have an impact on the rate of bacterially mediated carbon turnover.

An important limitation of our study is the necessity to do incubations in bottles, this inevitably leads to changes in the bacterial community composition due to the “bottle effect” (Calvo-Díaz et al 2011, Hammes et al 2010, Lee and Fuhrman 1991, Massana et al 2001). However, we addressed this issue by adding only a low amount of substrate and running a treatment control in parallel to each incubation. The lack of any significant increase or decrease (“boom and bust”, (Alonso-Sáez et al 2015, Calvo-Díaz et al 2011)) in cellular abundance within the incubations suggested that there was a continuous predator-prey relationship and/or the effects of viral lysis kept the microbial abundance constant. The water samples were not prefiltered to mimic natural conditions and allowing for grazing and viral lysis to occur as in a natural environment. We focused on the dominant changes in community composition because all incubations were done directly in seawater and contained a natural concentration of DOM and polysaccharides which may have caused additional minor changes.

Relationship Between Taxonomy and Function

Taxonomic variations in the community composition corresponded to differences in the hydrolysis patterns. In the following, we argue that based on correlations between total abundance and hydrolysis rates, bacterial group specific substrate utilisation mechanisms can be identified.

We make this argument to link taxonomy and function and to formulate a hypothesis on the distribution of individual substrate utilisation mechanisms across the Atlantic Ocean. We identified the dominant external degraders by correlating the increase in extracellular hydrolysis rates with the increase in cellular abundance. This was done under the assumption that the extracellular hydrolysis of a substrate yields resources for growth resulting in increased abundance. The *Alteromonas* were significantly correlated with the increase in hydrolysis rates in the laminarin and xylan incubations. Although their initial abundance was always very low they increased significantly during the incubations in all provinces except the N. Temperate. *Alteromonas* have previously been shown to respond to the addition of phytoplankton derived polysaccharides and DOC (Allers et al 2007, Neumann et al 2015, Sarmento and Gasol 2012, Tada et al 2011, Taylor and Cunliffe 2017, Teeling et al 2016, Wietz et al 2015). For example, Taylor and Cunliffe (2017) could show that *Alteromonas* assimilated phytoplankton-derived exopolymers and increased in abundance within 18 hours of incubation. Additionally, both in pure culture analyses and environmental transcriptomic analyses the *Alteromonas* showed the metabolic capacity to degrade complex polysaccharides (McCarren et al 2010, Neumann et al 2015). Our results indicate that *Alteromonas* extracellularly hydrolyse HMW polysaccharides and can quickly respond to changes in substrate availability. However, their substrate range may be limited as they did not degrade chondroitin sulphate. Our study agrees with the theory that *Alteromonas* are r-strategists which can quickly make use of available substrates (Allers et al 2007, McCarren et al 2010, Neumann et al 2015, Sarmento and Gasol 2012, Taylor and Cunliffe 2017, Wietz et al 2015).

Potential cheaters were identified by analysing the latent changes in the microbial composition after the hydrolysis rates reached a peak at day 3 – 6. The read abundance of SAR11 increased late in the incubations, mostly where *Alteromonas* had previously shown high abundance. We took this as an indication of possible scavenging of the “public goods” produced by *Alteromonas* or other sharing organisms. Genetic information of SAR11 has shown that they lack the ability to actively degrade HWM substrates, but have a high abundance of ABC transporters for both amino acids and sugars (Elifantz et al 2005, Morris et al 2012, Tang et al 2012, Tripp 2013). The increase in available hydrolysis products, caused by the extracellular hydrolysis of the HMW substrate, may be scavenged by the SAR11 explaining their increase in abundance late in the incubations where essentially all the HMW substrate is degraded.

Within the N. Temperate province there was an increase in *Bacteroidetes* in all substrate incubations. However, the *Bacteroidetes* were negatively correlated to the extracellular hydrolysis rates. In a previous study, we could show that they use an alternative, “selfish”, mechanism for substrate utilisation which does not result in the production of extracellular hydrolysis products and therefore no measurable extracellular hydrolysis rates (Reintjes et al 2017). The *Bacteroidetes* are HMW specialists that take up HMW substrate directly (Buchan et al 2014, Elifantz et al 2007, Fernández-Gómez et al 2013, Gómez-Pereira 2010, Kabisch et al 2014). Their initial high abundance in the N. Temperate province may have enabled them to quickly use the HMW substrates and effectively reduce the substrate available for other organisms such as external degraders.

Catenovulum and *Planctomycetes* were also identified as selfish organisms (Reintjes et al 2017) and increased in abundance in the N. Gyre, Equatorial, S. Gyre and S. Temperate. *Catenovulum* and *Planctomycetes* both exhibited selfish substrate uptake (of xylan and chondroitin sulphate, respectively) but showed significant differences in the increase in total cellular abundance during the incubations. The *Planctomycetes* used chondroitin sulphate almost exclusively and significantly increased in abundance. Comparatively, *Catenovulum* showed selfish uptake of xylan but did not increase significantly in abundance. The simultaneous increase of external degraders, such as *Alteromonas*, in the xylan incubations caused a competition for the substrate. This competition may have restricted the growth of *Catenovulum* and caused the observed variation in growth between the two selfish organisms.

Finally, the S. Gyre had the highest extracellular hydrolysis rates of laminarin and xylan. Additionally, there was a very low abundance of selfish organisms (Reintjes et al 2017). The rapid hydrolysis of HMW substrate by external degraders decreased its availability of HMW substrates and resulted in a limited growth of selfish organisms. This resulted in external degraders outcompeting selfish organisms in the S. Gyre. Similarly, in all stations, where high rapid hydrolysis activity for laminarin and xylan was seen (Equatorial and S. Gyre stations), a generally low selfish behaviour was observed.

Conclusion

In the marine environment, there is a high abundance of HMW polysaccharides, which are available almost exclusively to heterotrophic microorganisms. The current methods of analysing and modelling organic matter turnover rates in the marine environment are limited because they rarely account for the differences in functionality between microorganisms. Using our combined analyses of selfish substrate uptake, extracellular hydrolysis rates and the qualitative and quantitative changes in bacterial community composition we could link the taxonomy and function of marine microorganisms. By associating individual mechanisms with

specific bacterial groups, we can begin to understand how global variations in the distribution patterns of microorganism affect the turnover rates of organic matter in the marine environment.

Acknowledgements

We thank Jörg Wulf, Andreas Ellrott and Sherif Ghobrial for technical assistance. We thank the captain and crew of the RRS James Cook, as well as the principle scientist Glen Tarran (Plymouth Marine Laboratories) for assistance at sea. This work was supported by the Max Planck Society and by the U.S. National Science Foundation (OCE-1332881 to C.A.). C.A. was additionally supported in part by a fellowship from the Hanse Institute for Advanced Study (Delmenhorst, Germany). This study is a contribution to the international IMBER project and was also supported by the UK Natural Environment Research Council National Capability funding to Plymouth Marine Laboratory and the National Oceanography Centre, Southampton.

General Discussion

Discussion

In this part of my thesis, I will summarise the major achievements of the research that was done during this thesis and discuss them in a broader context. Moreover, I will present open research questions and suggest approaches to address these questions. I will not discuss the results of the methodological chapters 2 and 3 again since these two chapters represent ongoing research. The respective outlooks have, therefore, been solely stated as part of each chapter's conclusion.

I. Three-player models of marine polysaccharide utilisation

The work done in this thesis has significantly changed our understanding of how marine bacteria interact with and degrade HMW organic matter. Prior to this study, it was assumed that marine bacteria can only access HMW substrate using extracellular enzymes (Arnosti 2004, Sinsabaugh 1994, Vetter et al 1998). This inevitably leads to the production of smaller hydrolysis products which are also available to scavenging organisms, which do not produce enzymes (Allison 2005, Trivisano and Velicer 2004, West et al 2007). This hypothesis resulted in the formations of a two-player model of substrate acquisition in marine bacteria, consisting of bacteria capable of degradation and others that profit from the scavenging of degradation products. The results presented in this study expand this two-player model to include an additional substrate uptake mechanism (Figure 5). This alternative mechanism is homologous to that gut bacteria, which have been shown to take up HMW substrates in a selfish manner. The mechanism is specialised for the uptake of HMW compounds and minimises the production of freely diffused extracellular enzymes and hydrolysis products (Chapter 4) (Cuskin et al 2015). Furthermore, the work of this thesis enabled the identification of the dominant organisms associated with each of the three substrate utilisation mechanisms (Figure 5, Chapter 4 and 5).

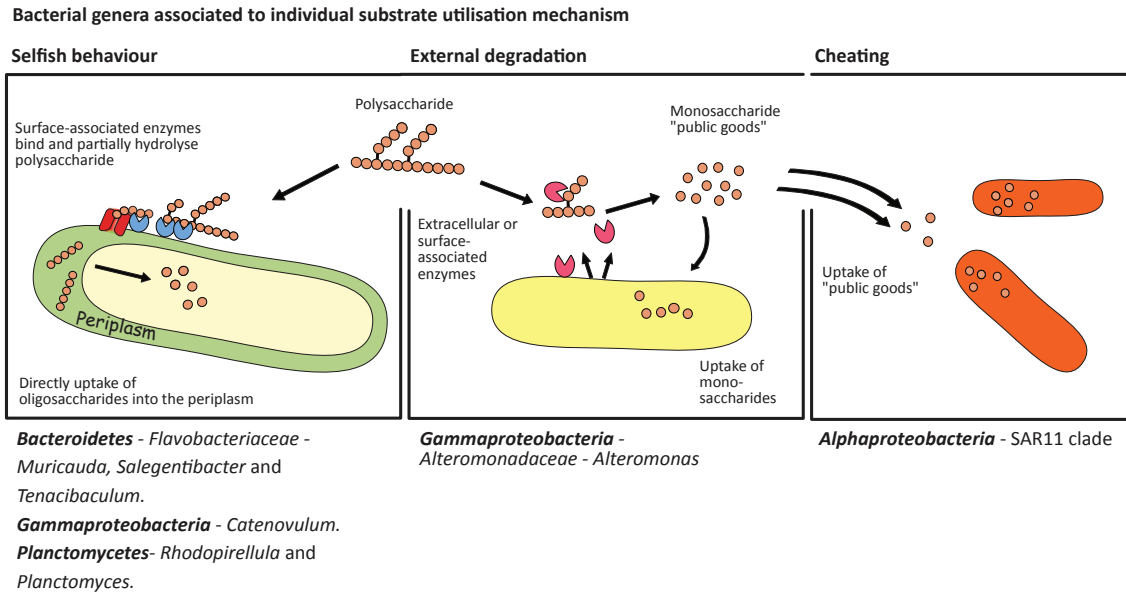


Figure 5 Proposed three-player model of substrate acquisition in marine bacteria. The Schematic diagram shows the mechanisms of HMW substrate utilisation of marine bacteria and the bacterial genera associated with each mechanism (above). Selfish behaviour (*Bacteroidetes*, *Gammaproteobacteria*, *Planctomycetes*): cells use surface associated enzymes to bind and partially degrade polysaccharides. These are directly taken up into the periplasm for further degradation with no production of extracellular hydrolysis products. External degradation (*Gammaproteobacteria*): cells use surface-associated or extracellular enzymes to degrade polysaccharides to sizes suitable for uptake. This causes the production of extracellular hydrolysis products termed "public goods". Cheating (*Alphaproteobacteria*): cells do not / cannot produce enzymes for the hydrolysis of polysaccharides but take up the hydrolysis products produced by the activity of other organisms.

II. Culture-independent analysis of HMW substrate uptake in *Bacteroidetes* and other marine bacteria

Prior to this study, it was not possible to analyse the activity of selfish bacteria in environmental samples. The widespread presence and activity of this alternative uptake mechanism, in the marine environment, could only be shown using the newly developed culture-independent technique (Chapter 4). Using fluorescently labelled polysaccharide (FLA-PS) incubations the uptake of polysaccharides into the periplasm of individual environmental bacterial cells, could be visualised (Figure 6). Furthermore, we combined the newly developed substrate staining technique with FISH to identify the organisms showing substrate uptake. The results, obtained from these two techniques, were analysed using a high-throughput automated image acquisition and enumeration system (Chapter 1). This enable the statistically relevant analyse of ~2000 samples taken from FLA-PS incubations of different provinces of the Atlantic Ocean.

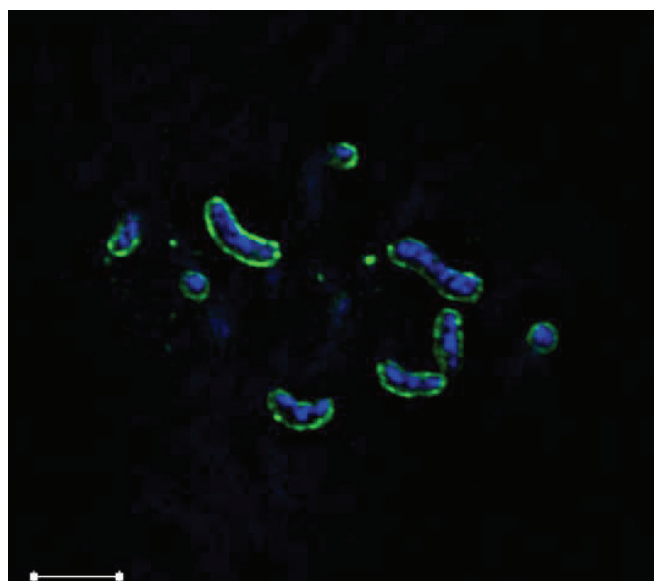


Figure 6 Super-resolution structured illumination microscopy image showing uptake of fluorescently labelled substrate in an environmental sample. Cells were stained with DAPI to visualise the DNA (blue), while the FLA- laminarin can be seen in green in the periplasm of the cells. The figure shows the incubation experiment after 6 days, done on the AMT22 research cruise from a station sampled in the Northern Temperate region (described in chapter 4 and 5). Scale bar = 2 μm

This high-throughput culture independent-technique enabled the identification of a high abundance of the cells, showing substrate specific staining, as *Bacteroidetes*. Based on the cell-specific staining patterns, I hypothesised that these cells were selfishly taking up polysaccharides through the activity of sus-like systems (Chapter 4) (D'Elia and Salyers 1996, Martens et al 2009, Reeves et al 1997). This hypothesis agrees with the metagenomics findings of high abundances of sus-like systems in marine *Bacteroidetes* (Cuskin et al 2015, D'Elia and Salyers 1996, Gómez-Pereira et al 2012b, Kabisch et al 2014, Teeling et al 2012, Wemheuer et al 2015). This study thereby provides robust evidence that marine *Bacteroidetes* use a selfish mechanism to take up and degrade polysaccharides.

I also showed that the gammaproteobacterial genus *Catenovulum* and the *Planctomycetes* affiliated with the genera *Planctomyces* and *Rhodopirellula* took up FLA-PS into their periplasm (Chapter 4). Neither *Catenovulum* nor *Planctomycetes* have been found to contain canonical sus-like systems and therefore likely use yet other methods to transport FLA-PS into their periplasmic space.

Currently, there are only two available isolates (Li et al 2015, Yan et al 2011) and two draft genomes (Shan et al 2014) of the gammaproteobacterial genus *Catenovulum*. Protein predictions of *Catenovulum agarivorans* YM01 (accession no. PRJNA158387) and *Catenovulum agarivorans* DS-2 (accession no. PRJNA200359) genomes reveal the presence of several tonB dependent receptors and hypothetical proteins of outer

membrane SusC/RagB and susD/RagA. Additionally, both genomes contain predicted glycoside hydrolases associated with the families 3 and 43 indicating potential xylanases. These protein predictions indicate a potential to use xylan and the presence of a mechanism that could be similar to the *Bacteroidetes* sus-like system. These prediction are in agreement with the selfish xylan staining observed during this study. Further detailed studies with isolates of *Catenovulum* would enable the biochemical charateristion of their potentially selfish polysaccharide utilisation mechanism.

Planctomycetes is a well-studied phylum with a wide range of genetic potentials (reviewed by Fuerst and Sagulenko 2011). Marine *Planctomycetes* have frequently been associated with macroalgae and the degradation of organic matter (Bengtsson and Øvreås 2010, Berlemont and Martiny 2016, Bondoso et al 2017, Lage and Bondoso 2014). Genetic analyses have shown that they are uniquely equipped to degrade marine sulphated polysaccharides due to a high abundance of sulfatase genes (Glöckner et al 2003, Paparoditis et al 2014, Wegner et al 2013). This may also have been the reason why *Planctomycetes* increased so strongly in the chondroitin sulfate incubations, of this study. Further analysis are required to understand the mechanism with which *Planctomycetes* take up chondroitin sulfate into their periplasm.

III. *Substrate specific staining of Bacteroidetes*

The *Bacteroidetes* are widely distributed and present in a broad range of environments including, terrestrial soils, marine waters and sediments, as well as in human and animal gut systems (review by Gupta and Lorenzini 2007, and Thomas et al 2011). They are specialised for the degradation of polymers, such as proteins and polysaccharides, because they have unique substrate acquisition systems (Thomas et al 2011). These systems are called sus-like systems and encoded by co-localised and co-regulated genes that coordinate the recognition, binding, enzymatic degradation and uptake of polysaccharides (reviewed in detail by Foley et al 2016 and, Grondin et al 2017). The gene clusters encoding these systems are termed polysaccharide utilisation loci (PULs) (Bjursell et al 2006, Foley et al 2016, Grondin et al 2017).

Although many other bacteria have been shown to contain several of the genes encoded in PULs (Neugebauer et al 2005, Neumann et al 2015), there is one gene unique to the *Bacteroidetes*. This gene encodes the susD protein, which is responsible for the cell surface carbohydrate binding (Bjursell et al 2006, Cameron et al 2014). The susD forms together with the outer membrane pore formed by susC subunits a complex which enables the binding and transport of large oligosaccharides into the cell. The activity of the susC and susD proteins accounts for up to 70% of the binding capacity of sus-like systems and therefore play a central role in the uptake of polysaccharides by *Bacteroidetes* (Bjursell et al 2006, Cameron et al 2014, Reeves et al 1997). Additionally, they are also likely responsible for the uptake of FLA-PS into the periplasm resulting in the substrate specific staining which was observe in this study.

A recent X-ray crystallography study has provided further detail on the structure of the susC-susD protein complex (Glenwright et al 2017). The authors described the protein complex as a “pedal bin” structure, whereby each susC pore is capped by a susD binding protein. This structural description is relevant for the work done in this thesis because it allows for a theoretical size and abundance prediction of the complex on a cell. This, in turn, enables us to evaluate whether the level of staining, observed in environmental and cultured *Bacteroidetes* of this study, is feasible (thousands of FLA, Chapter 4) and can give us an indication of selfish uptake rates.

The susCD protein complex exists of dimers that have a maximum length of 14 nm and a width of 6.4 nm, which corresponds to a surface area of $\sim 90 \text{ nm}^2$. As much as 50% of the outer membrane of gram negative bacteria can consist of proteins (Koebnik et al 2000). Therefore, assuming an average cell surface area of $2.52 \mu\text{m}^2$ (calculated from the average cell size of *G. forsetii* ($2 \mu\text{m} \times 0.5 \mu\text{m}$) using an ellipsoid calculation for surface area) and that one-tenth of the outer membrane proteins are susCD complexes (under highly induced condition), a total of 1,400 susCD complexes could be present in the outer membrane. These high abundance would agree with proteomics studies that have shown that the complex can be highly expressed (Glenwright et al 2017, Kabisch et al 2014, Reeves et al 1997, Teeling et al 2012) and can make up as much as 13% of the total identified proteins of an environmental meta-proteome (Teeling et al 2012). Additionally, they agree with primary-labelled fluorescence antibody experiments which show high abundance of susD on the cell surface under induced conditions (Rogers et al 2013).

The calculations presented here are no doubt highly speculative and we cannot yet calculate the absolute abundance of susCD complexes in the outer membrane of a cell. However, if the susCD complex is present at the hypothesised or a similar abundance it would explain the high level of substrate staining which was observed in the induced culture of *G. forsetii* within the short time of 5 min (Chapter 4). The signal intensity of the substrate staining requires that thousands of FLA-PS were transported into the cell within these few minutes. Data obtained in this study also suggest that some marine *Bacteroidetes* are expressing notable levels of the susCD complex in their marine habitat, as staining in environmental samples was observed within 30 min of substrate incubations. (Chapter 4). Further analyses of the activity and expression of susCD complexes in marine *Bacteroidetes* would significantly impact our understanding of the turnover of polysaccharide in the marine environment.

IV. Outlook

As demonstrated in this study, selfish substrate uptake is present throughout the marine environment and likely has as a significant impact on global carbon cycling. To determine the extent of this impact, further research efforts should focus on developing methods to measure the rates of FLA-PS uptake by selfish organisms in environmental samples. In the following I present four possible culture-independent methods of measuring selfish uptake rates.

- Measurements of the rates of selfish uptake can be achieved by quantifying the fluorescence intensity of the FLA-PS signal within cells over time. Currently, it is not possible to measure the absolute number of fluorophores taken-up over time by individual cells in an environmental sample. However, by comparing the FLA-PS signal intensities to a known standard set of signal intensities, the rate of polysaccharide uptake can be measured. For this the average number of fluorophores per molecule of polysaccharide (the labelling density relative to the sugar monomers) must be known which is often in the range of 0.5 to 1.3 fluorescein molecules per polysaccharide molecule (Arnosti (2003)). This can then be used to estimate the number of polysaccharides taken up by individual cells, assuming that the whole polysaccharide is taken up. These analyses would be possible with microscopy or flow cytometry.
- Alternatively, selfish uptake rates can be calculated using “fluorescence housekeeping”. By precisely tracking the amount of FLA within an incubation the abundance of intracellular FLA could be calculated. Here, one needs to assume that selfish organisms take up 100% of the FLA-PS thereby fully removing the fluorescein from the medium. Other bacteria degrading FLA-PS by exoenzymes would, in contrast, move the fluorescein label from higher molecular weight to lower molecular weight compounds but leave it to 100% in the medium. Specifically, when selfish organisms take up FLA-PS they remove FLA from the supernatant. Therefore, if the FLA signal intensity of the supernatant of a FLA-PS incubation is directly compared to the FLA signal intensity of a parallel negative control, then the difference in signal intensities corresponds to the amount of intracellular FLA. This could then be used to calculate the uptake of FLA-PS into the periplasm and thereby the uptake rate of FLA-PS by selfish organisms.
- Extracellular hydrolysis rates of FLA-PS are calculated by analysing the change in molecular weight of the added polysaccharide over time using liquid chromatography coupled with fluorescence detection (Arnosti 2003). The same method could potentially be used for the calculation of selfish uptake rates of FLA-PS, as well as, characterising the size of the periplasmic oligosaccharides. By analysing not just the supernatant of an incubation but also the cells (or cell lysate), the intracellular fraction of FLA-PS could be measured. Ideally this method should be developed using pure cultures. It requires the gentle separation of the cells from the medium, without compromising the membrane integrity. Subsequently the cells are fully and rapidly lysed to release the FLA from intracellular pools. Later this method could also be applied to environmental incubations to obtain the average selfish uptake rates of a bacterial community.

- Finally, by using alternative polysaccharide labelling methods and more sensitive measuring techniques, a precise quantification of the selfish uptake rates in environmental samples could be achieved. In particular, fluorine labelling of polysaccharides for analyses by nanoSIMS or Nanogold labelling of polysaccharides for subsequent analysis by electron microscopy seem to be promising options (Behrens et al 2008, Hainfeld and Powell 2000, Montesano-Roditis et al 2001, Musat et al 2012). However, it is important that the alternative labels are stable and small enough to be readily taken up by the cells like FLA. Additionally, it is important that the label is not actively hydrolysed by the cell because then the activity cannot be traced back to selfish uptake. For example, radioactively labelled polysaccharides (^{14}C) would enable the quantification of uptake rates of polysaccharides but would not be concentrated within the periplasm and could therefore not be conclusively linked to selfish uptake.

In the following I will outline future research projects that would enable us to analyse and advance our understanding of the organisms exhibiting selfish behaviour in environmental samples, are highlighted.

- To fully understand the extent of selfish substrate uptake, the mechanisms distribution in marine and other environments should be analysed. This could be achieved by performing additional FLA-PS incubations in other samples. Preliminary results from incubations in the South Pacific Gyre, mesopelagic waters and during a coastal phytoplankton bloom indicate that selfish substrate uptake is indeed widespread throughout marine waters and likely actively contributes significantly to the global carbon turnover. Additionally, the preliminary results indicated that the rates of selfish activity vary under different environmental condition.
- Furthermore, although we have a good understanding of the sus-like-system of *Bacteroidetes*, we know relatively little about other “selfish” uptake mechanisms in marine bacteria. The substrate specific staining of *Catenovulum* and *Planctomycetes*, which was observed in this study, was hypothesised to be a selfish uptake mechanism but further analyses are required to prove this. Additionally, although combining the FLA-PS incubations with FISH allowed us to identify a large fraction of the substrate stained cells (Chapter 4), there were substrate stained cells that were not target by our FISH probes.

To enable a more comprehensive analysis of the taxonomy and function of selfish organisms FLA-PS incubations could be combined with flow cytometry and cell sorting. By fluorescence activated sorting, the cells showing substrate specific signals could be retrieved for a more detailed analysis of the active polysaccharide degrading community. The flow-sorted cells could then be analysed by 16S rRNA sequencing, metagenomics or

single cell genomics to gain a detailed insight into their diversity and metabolic potentials. This combination of methods could enable the selective “tagging and sorting” of heterotrophic communities specialised in the uptake and degradation of specific polysaccharides.

- Finally, recent analyses have indicated that some gut *Bacteroidetes* perform “leaky” selfish behaviour (Grondin et al 2017, Rakoff-Nahoum et al 2014, Rakoff-Nahoum et al 2016). Leaky selfish behaviour occurs when a substrate is bound to the cell, partially degraded but not or only partially transported. This causes the production of partially degraded oligosaccharides that are available to other organisms (Rakoff-Nahoum et al 2016). Additionally, it is possible that the susCD complex is only “moderately” specific and consequently takes up oligosaccharides that contain glycosidic bonds that the bacterium is not capable of degrading. This was partially confirmed by the unspecific transport of FLA during our substrate incubations. The subsequent release of these “un-degraded” oligosaccharides would result pseudo-leaky behaviour. The extent of “leaky” selfish behaviour could be tested in culture experiments using FLA-PS, by simultaneously analysing both the rate of selfish staining and the change in molecular weight of the polysaccharides over time.

V. *Marine polysaccharide utilisation mechanisms across the Atlantic Ocean*

In the present study, using FLA-PS incubations potential extracellular hydrolysis rates of polysaccharides were determined across different oceanic provinces of the Atlantic Ocean. For the first time, such measurements were combined with detailed analyses of the changes of bacterial community composition within FLA-PS incubations using both 16S rRNA sequencing and FISH. This enabled the identification of the potentially dominant polysaccharide degrading microorganisms (see chapter 5).

A major aim of this study was to analyse how the taxonomy and function diversity of microorganisms affect the bacterially mediated carbon turnover in the Atlantic Ocean. This study could show, that differences in the microbial community composition, among provinces of the Atlantic Ocean, caused difference in the rate of extracellular hydrolysis of polysaccharides (Chapter 5). However, this was not due to differences in the functional potentials of the external degraders among sites, in fact *Alteromonas* was found to be the dominate external degrader in nearly every site, but rather due to the competition between different substrate utilisation mechanisms.

Using the combine results of the activity of external degraders and selfish organisms within the Atlantic Ocean I evaluate, here, under which conditions a specific substrate utilisation strategy out-competed the other. I focus on the patterns within the laminarin and xylan incubations because they showed both high selfish and high extracellular hydrolysis activities (Chapter 5).

Selfish substrate uptake was measurable prior to the activity of external degraders (extracellular hydrolysis rates). These “early” selfish organisms were identified, in this study, as belonging to the *Bacteroidetes*. The *Bacteroidetes* continuously produce sus-like systems at a low concentration, so-called “surveillance levels” (Cameron et al 2014, Karunatilaka et al 2014, Martens et al 2014). They are, therefore, directly equipped to take up HMW substrates. As substrate becomes available, it is bound to the cell surface, partially degraded and taken up into the periplasm via susCD complexes. The presence of oligosaccharide in the periplasm cause the up-regulation of the sus-like system which, due to its co-localisation and co-regulation, results in a rapid response (Cameron et al 2014, Karunatilaka et al 2014, Martens et al 2014). In cultured *Bacteroidetes* this up-regulation occurs within minutes (5 – 40 min) of the substrate addition (Rogers et al 2013). These findings indicate that the quick (30 min) substrate specific staining, observed in this study, maybe due to the presence of “surveillance level” amounts of sus-like systems in marine *Bacteroidetes*, which results in quick recognition and up-regulation of the required genetic machinery.

However, although *Bacteroidetes* responded quicker to the FLA-PS addition they did not always increase significantly in abundance (Chapter 5). In this study, we could associate this to differences in the initial abundance of *Bacteroidetes* and external degraders (*Alteromonas*) within the incubations (Chapter 5). The results indicated that selfish organisms needed to have a specific threshold-abundance to out-complete external degraders. However, the polysaccharides which were used in this study were relatively “simple” (laminarin and xylan). Comparatively, marine *Bacteroidetes* rather show a high amount of specialisation for complex polysaccharides (Berlemont and Martiny 2016, Fernández-Gómez et al 2013, Gómez-Pereira 2010, Gómez-Pereira et al 2012b). It is therefore possible that this threshold-abundance is only required when they are in competition for simple polysaccharides. Alternatively, they may only face high levels of competition for simpler polysaccharide.

In the present study, we could show when external degraders showed high activity, selfish activity was low. External degraders are social foraging organisms because their activity causes the production of “public goods” which are freely available (Allison 2005, West et al 2007). “public goods” causes the induction of further social foragers resulting in increased hydrolysis rates (Allers et al 2007, Allison 2005, McCarren et al 2010, West et al 2007). Additionally, it is possible that external degraders preferentially produce specific molecules that are selective for other social foragers. For example, the selfish uptake mechanism of *Bacteroidetes* is induced and up-regulated by oligosaccharides (Cameron et al 2014, Karunatilaka et al 2014, Martens et al 2009). However, if social foragers directly degrade the FLA-PS to small molecular, such as monosaccharides, they would prevent the induction of selfish organisms.

Recent models of extracellular enzyme dynamics have indicated that the production of extracellular enzymes is only feasible with a minimum substrate concentration in the μM range (Traving et al 2015). Our substrate incubations were performed using μM substrate ranges and, due to their enclosed nature, may preferentially select for external degraders. Comparatively, the production of cell associated enzymes is

feasible down to a nM range of substrate (Traving et al 2015). Therefore, a potential future research project could include performing incubation with varying concentration of FLA-PS to identify under which conditions the various substrate utilisation mechanism are selected for.

Concluding Remarks

The research that was done in this doctoral thesis has resulted in the development of methods which enable the fast and reliable analysis of the abundance and diversity of microbial communities on-board a research vessel. Additionally, it has furthered our understanding of the community composition of different bacterial lifestyles across the Atlantic Ocean.

Furthermore, the work presented in this thesis has significantly furthered our understanding of the activity and distribution patterns of bacterial polysaccharide utilisation mechanisms and enabled the association of these substrate utilisation mechanisms with specific bacterial groups. Using the information presented in this thesis we can begin to understand how global variations in the distribution patterns of microorganisms affect the turnover rates of organic matter in the marine environment. This study will enable us to make better predictions of the impact which marine microorganisms have on global biogeochemical cycles.

Acknowledgements

Thank you to ...

- PD. Dr. Bernhard Fuchs, for all your support during my doctoral thesis. I am very fortunate to have had such a great supervisor. Thank you for always having an open door and for leading my ever-curious mind in the right direction when it wandered of track.
- Prof. Dr. Rudolf Amann, for encouraging me to have a look at everything under the microscope and for always taking the time to have a look yourself. Thank you for giving me the opportunity to do my doctoral thesis in the department of molecular ecology and for creating an amazing working atmosphere in your group.
- Prof. Dr. Carol Arnosti, for supervising my doctoral thesis and all the great advice. Thank you also for your amazing writing tips and teaching me how to improve my own writing skills.
- Prof. Dr. Ulrich Fischer, for being my thesis committee member.
- Greta Giljan, for being my thesis committee member and being the greatest office buddy.
- Sebastian Miksck, for being my thesis committee member.
- Jörg Wulf, Kathrin Büttner and Andreas Ellrott, for your continued help and technical support.
- David Probandt, Clara Martinez, Brandon Kwee Boon Seah, Lennart Kappelmann and Beatriz Noriega Ortega for being yourselves and a source of sunshine through out my studies.
- Sara Cregeen, for the last-minute proof reading of my thesis, you're the best.
- The Molecular Ecology Department, for your support and making every working day fun and exciting. For the great group seminars and the continuous input and helpful discussions.
- All former members of the Molecular ecology department and other scientists whom I forgot to mention but helped me in my studies.
- My parents, word cannot express how grateful I am for having such loving parents. Thank you for encouraging me to live my own life and accepting every opportunity.
- Mein Schwesterherz, for always being herself and always being honest.
- Philipp, for your patience, your kindness and of course for waking me up in the morning.

Appendix

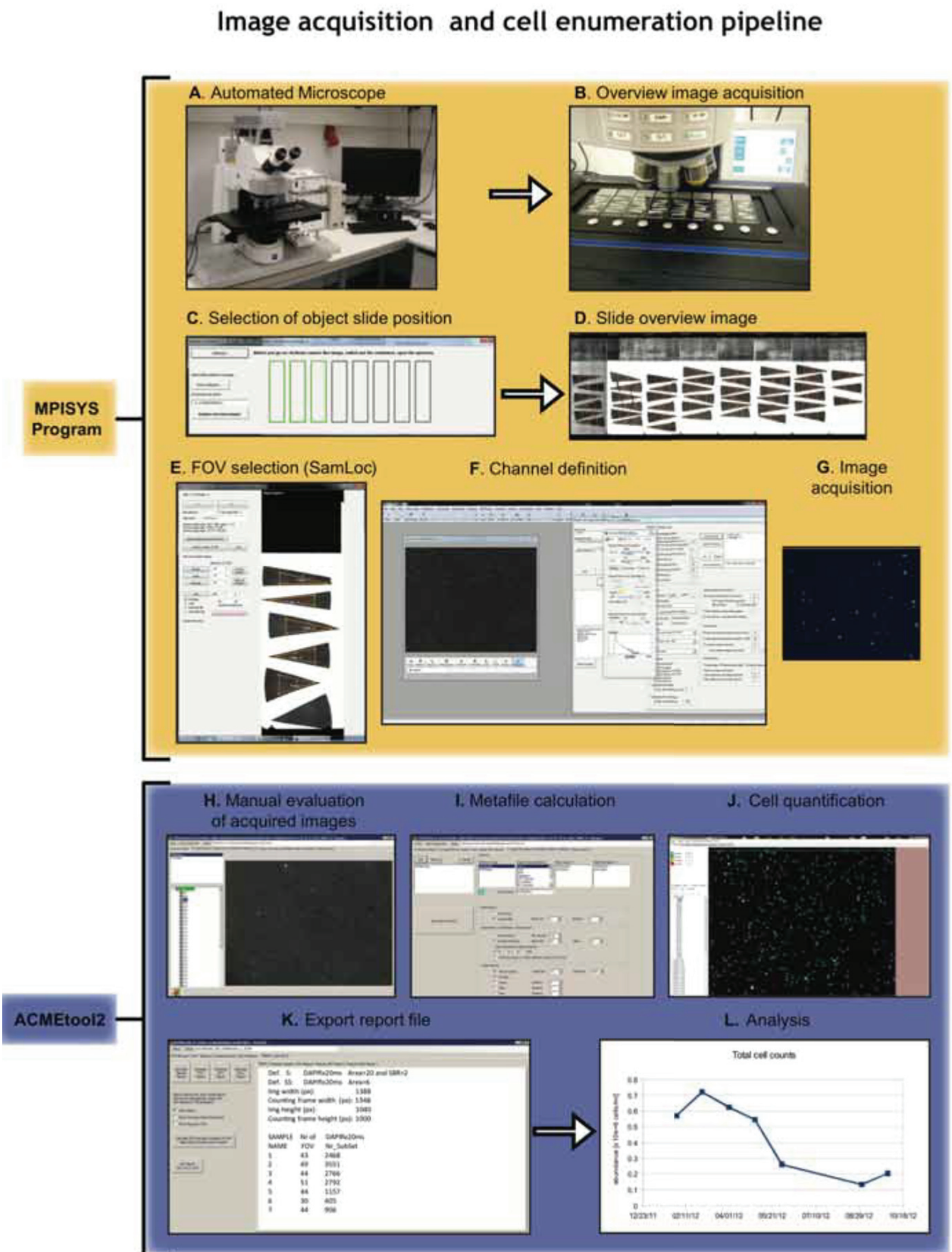
Appendix Figures and Table for Chapter 1

Modification of a High- Throughput Automatic Microbial Cell Enumeration System for Shipboard Analyses

Christin M. Bennke, Greta Reintjes, Martha Schattenhofer, Andreas Ellrott,
Jörg Wulf, Michael Zeder, Bernhard M. Fuchs

Published in Applied and Environmental Microbiology (AEM)

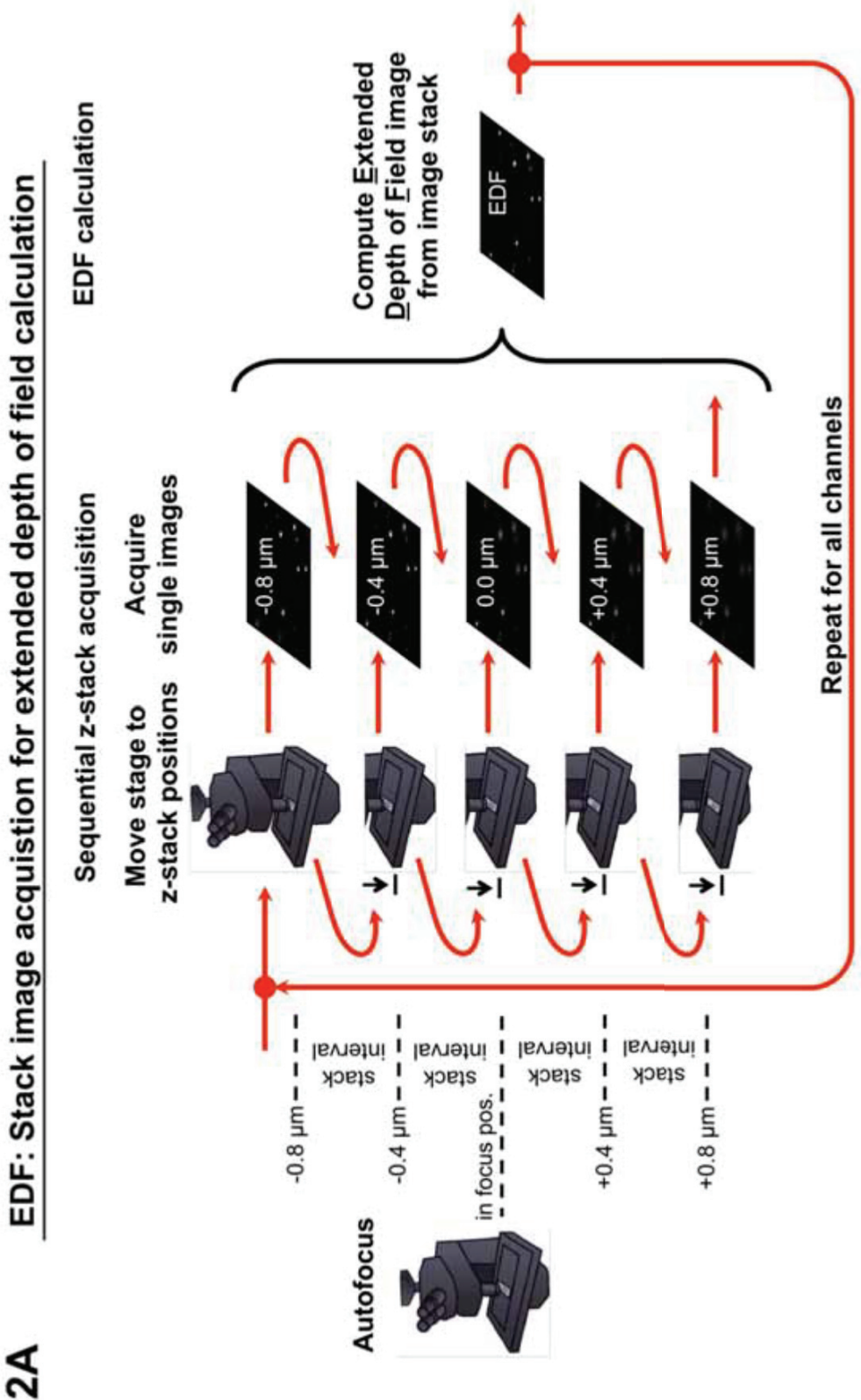
DOI: 10.1128/aem.03931-15



Chapter 1 Supplementary Figure 1 Flow chart of automatic image acquisition and cell enumeration pipeline. At first, the MPISYS program (A-G) is used, which is then flowed by

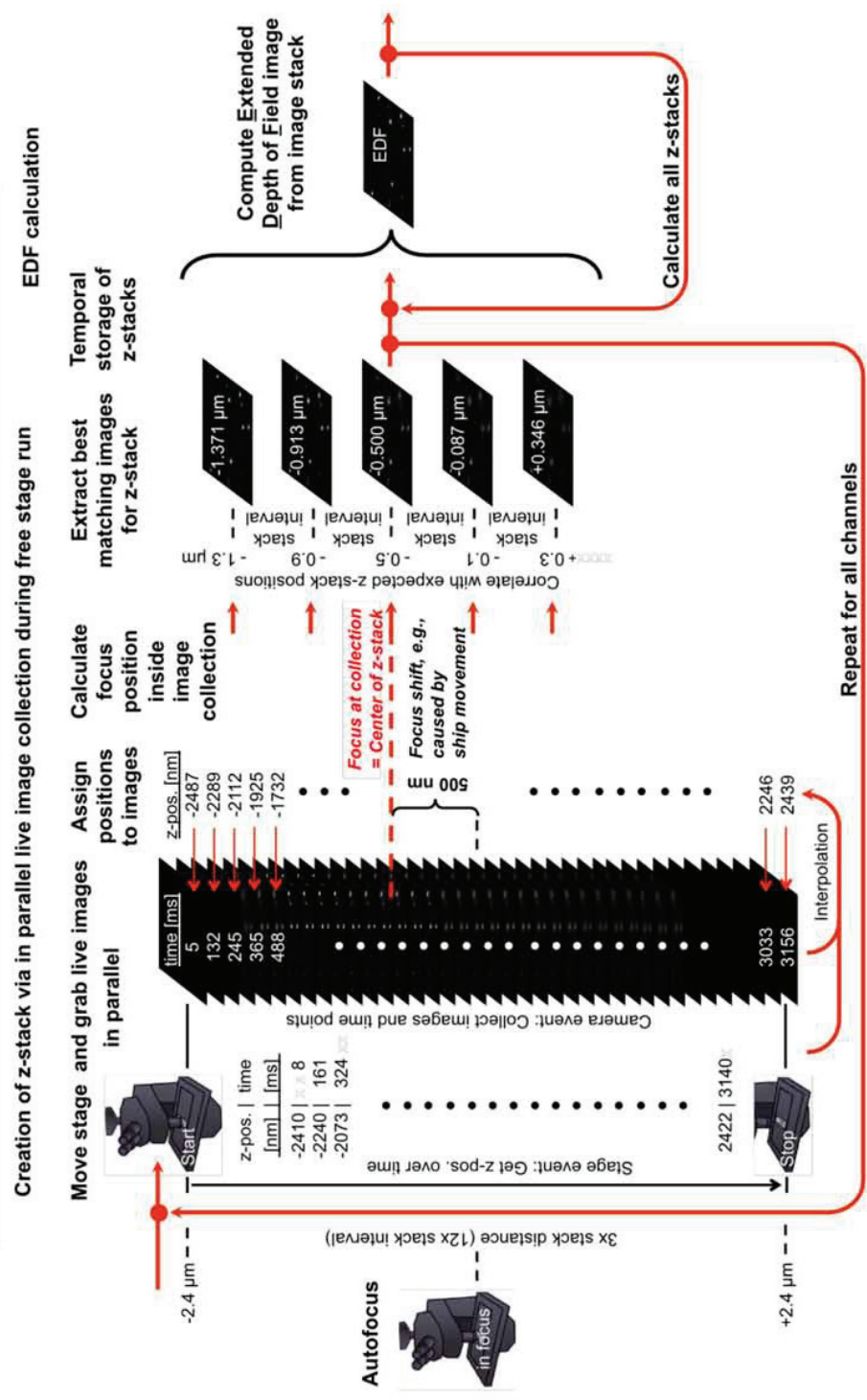
Appendix Figures and Tables

the cell analysis with the ACMETool2.0 (H-L). The first image (A) depicts the whole microscopic set up and when starting the image acquisition at first an overview image (B) has to be acquired. This is followed by the selection of the object slide position (C) and a slide overview image is obtained (D) with the 1 c objective. In a next step (E) samples have to be labelled and the number of FOV's is defined. Then channels are chosen (F) and the image acquisition (G) can start. When acquisition is done, images are imported into the ACMETool2.0 software. Within ACMETool2.0, at first image quality control (H) is done and with the remaining high quality images the metafile is calculated (I), which is then analysed for cell enumeration (K). As a result ACMETool is giving a tab-delimited report file (M) which then can be used to graphically show the cell numbers (L).



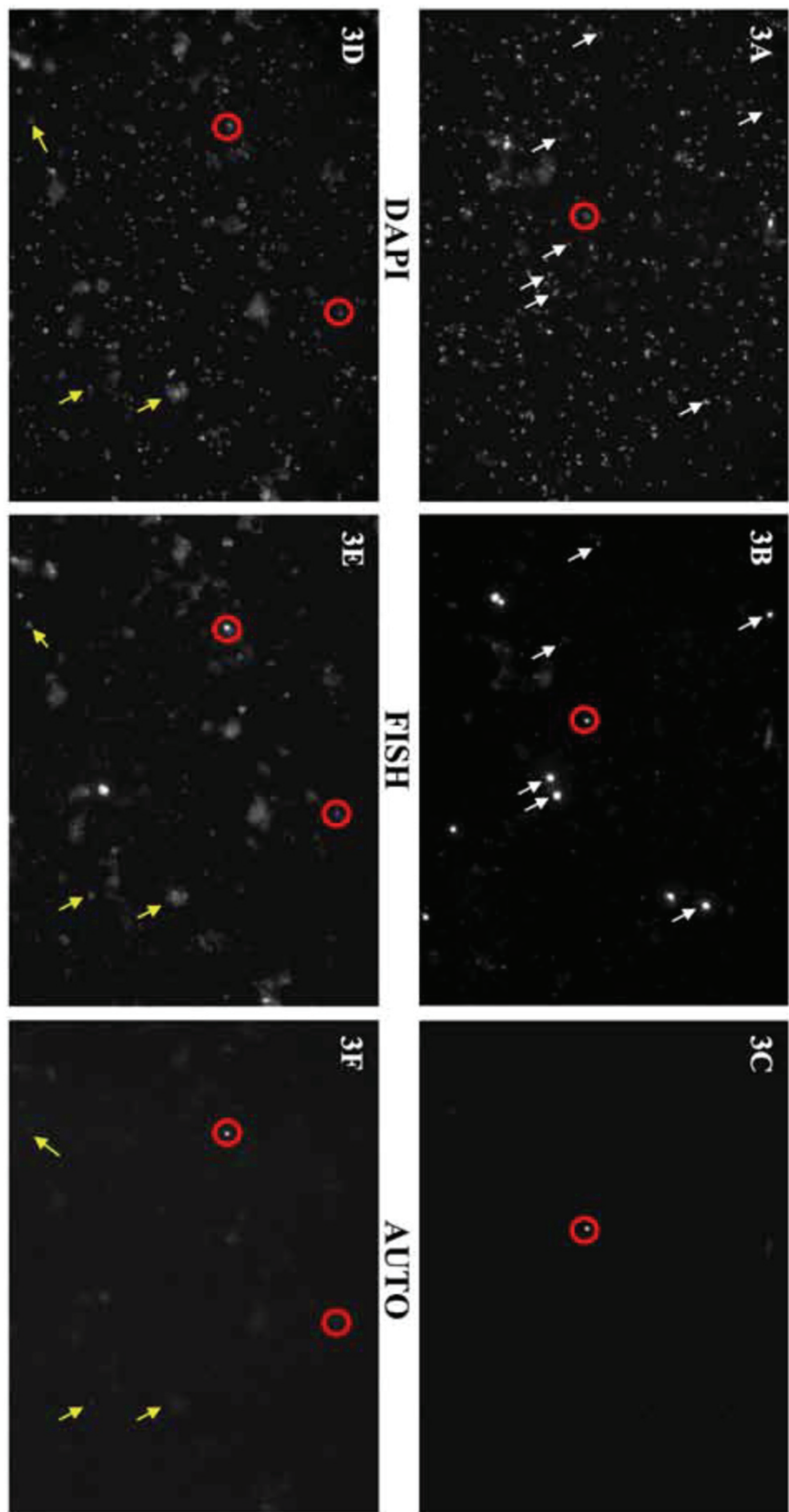
2C

FQEDF: Focused quick stack image acquisition for extended depth of field calculation



Chapter 1 Supplementary Figure 2 A-C. A) EDF- Flow chart of sequential z-stack image acquisition for extended depth of field calculation. The scheme shows exemplary a z-stack with five images and a stack interval of $0.4\ \mu\text{m}$. B) QEDF- Flow chart of quick stack image acquisition for extended depth of field calculation. The scheme shows exemplary a z-stack with five images, a stack interval of $0.4\ \mu\text{m}$ and a stage z-speed of $1\ \mu\text{m}$ per second. C) FQEDF- Flow chart of focused quick stack image acquisition for extended depth of field

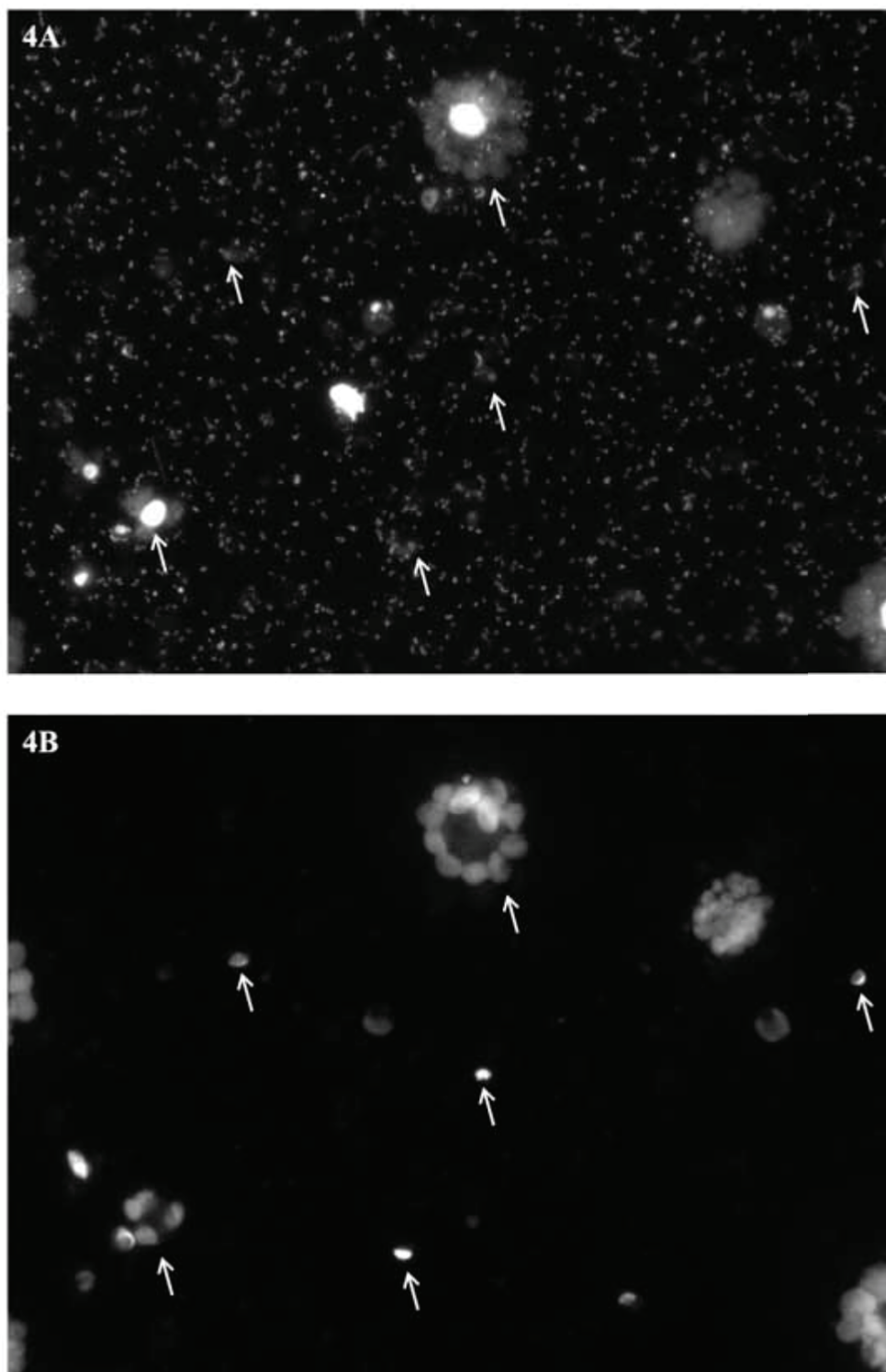
calculation. The scheme shows exemplary a z-stack with five images, a stack interval of $0.4\mu\text{m}$ and a stage z-speed of $1\mu\text{m}$ per second.



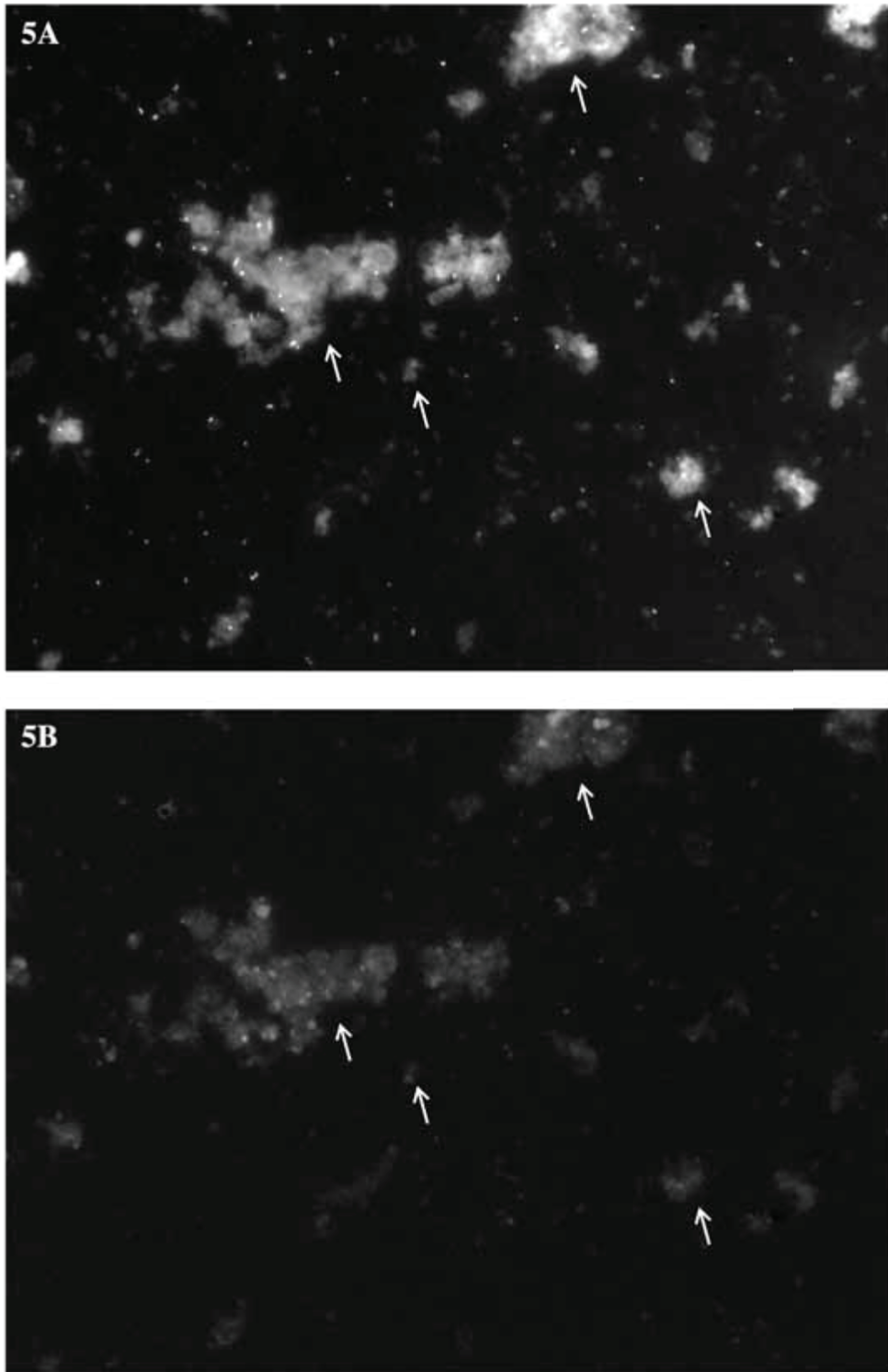
Chapter 1 Supplementary Figure 3 Gray-scale micrographs show auto-fluorescent signals (red circles) detected in both, the channel for FISH signals as well as the channel for auto-

Appendix Figures and Tables

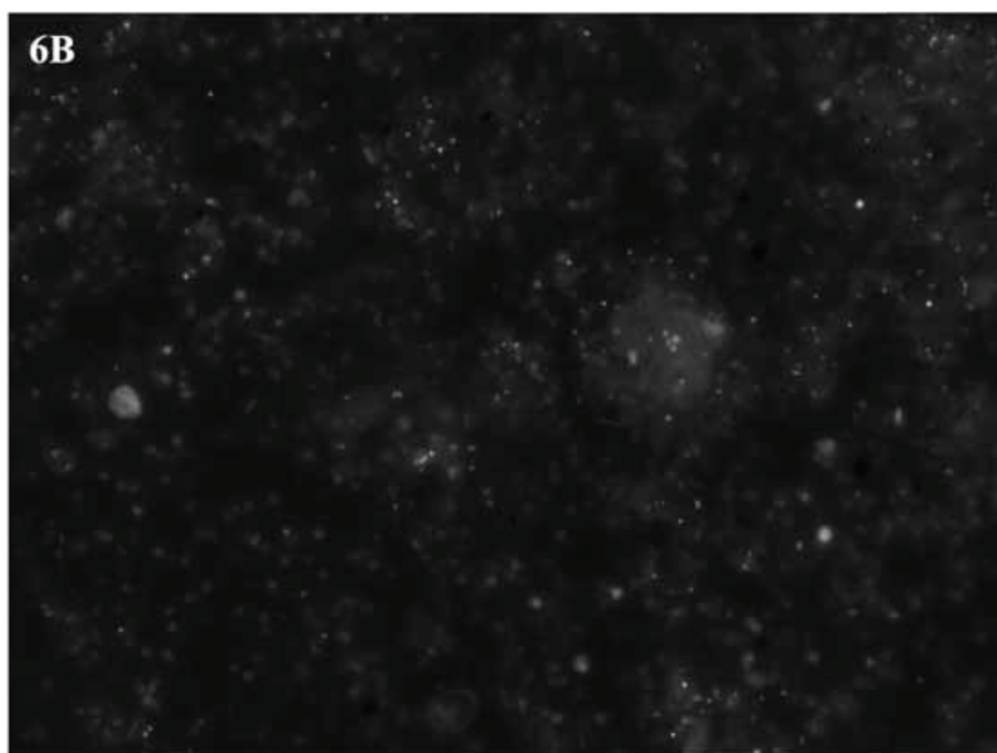
fluorescent signals. A/D: EDF stack image of DAPI-stained cells under UV illumination. B/E: EDF stack image of FISH signals under blue excitation. C/F: EDF stack image of auto-fluorescent signals under red excitation. White arrows on micrographs 3A-C show FISH-positive signals, since they possess a DAPI signal and a FISH signal, but no AUTO signal. Yellow arrows on micrographs 3D-F show debris of cells and other auto-fluorescent signals.

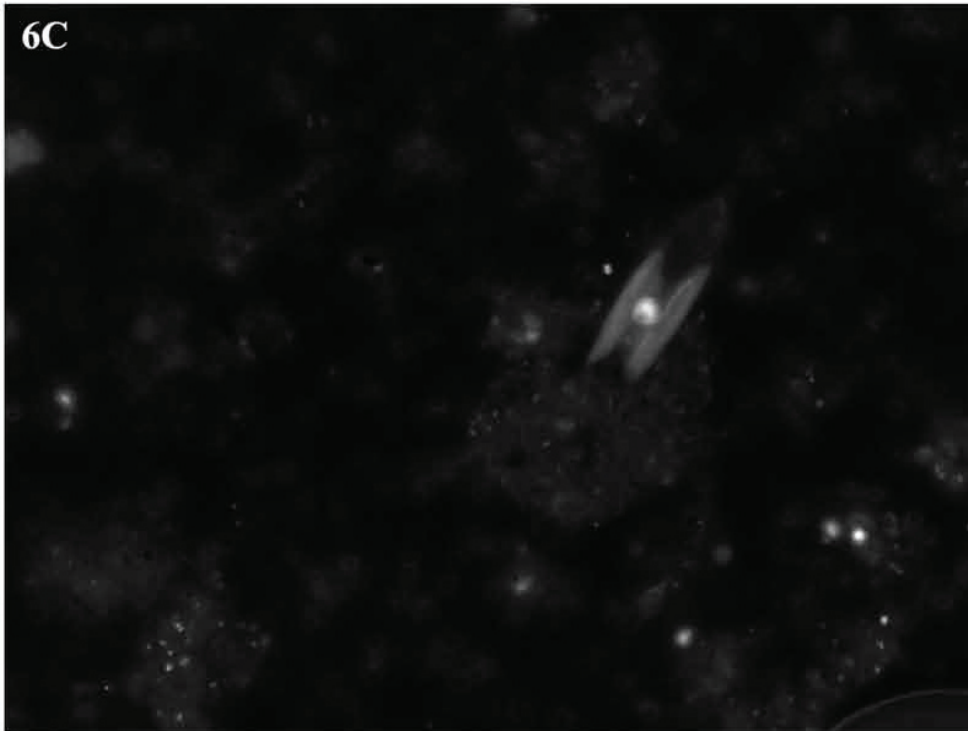


Chapter 1 Supplementary Figure 4 Grey-scale micrographs show images with small and large phytoplankton cells, indicated by white arrows. A: EDF stack image of DAPI-stained cells under UV illumination. B: EDF stack image auto-fluorescent signals under red excitat



Chapter 1 Supplementary Figure 5 Grey-scale micrographs show images with cell debris, indicated by white arrows. A: EDF stack image of DAPI-stained cells under UV illumination. B: EDF stack image auto-fluorescent image auto fluorescent signals under red excitation.





Chapter 1 Supplementary Figure 6 Grey-scale micrographs show images with small and large phytoplankton, cell debris and areas out-of-focus A: air bubble in the mounting media between membrane filter and cover slide. B: due to aggregates and cell debris the whole image is out-of-focus. C/D: due to phytoplankton cells and cell debris the whole images is out of focus.

Stack image acquisition with subsequent EDF calculation												Movement of the ship during automated image acquisition					
n	Station	Channel	Number of FOV tried to image	Number of high quality images obtained	Percent high quality images obtained	Period of image acquisition	Average of absolute roll angle [degree]	Max roll angle ^a [degree]	Average of absolute pitch [degree]	Max pitch ^b [degree]	Average of absolute heave [meter]	Max heave ^c [meter]					
1	Stat2-S	DAPI	55	2	4	15th Oct. 2012, - 00:27:22 02:18:14	1.79	-7.22	0.79	-2.95	0.49	-2.29					
2		FISH	55	5	9								4.89	2.40	2.40		
3	Stat2-D	DAPI	55	0	0	15th Oct. 2012, - 02:19:38 04:13:27	1.28	-6.31	0.80	-3.66	0.44	-2.11					
4		FISH	55	6	11								4.64	2.27	1.94		
5	Stat3-S	DAPI	55	8	15	15th Oct. 2012, - 04:14:13 06:11:29	1.63	-6.05	0.80	-3.37	0.43	-2.05					
6		FISH	55	14	25								6.52	2.26	1.95		
7	Stat3-D	DAPI	55	11	20	15th Oct. 2012, - 06:12:16 08:09:05	1.23	-5.85	0.80	-3.26	0.43	-1.99					
8		FISH	55	8	15								5.03	1.63	2.38		
9	Stat4-S	DAPI	55	2	4	15th Oct. 2012, - 08:09:52 10:02:50	1.12	-5.95	0.79	-2.99	0.42	-1.93					
10		FISH	55	4	7								4.36	1.59	1.74		
11	Stat4-D	DAPI	55	10	18	15th Oct. 2012, - 10:03:38 12:01:52	1.07	-4.96	0.78	-2.61	0.39	-1.77					
12		FISH	55	5	9								4.08	1.15	1.83		
13	Stat4-DCM	DAPI	91	11	12	21st Oct. 2012, - 06:23:47 08:26:58	0.76	-3.37	0.56	-1.80	0.28	-1.29					
14		FISH	91	12	13								3.63	0.75	1.27		
15	Stat2-20m	DAPI	91	6	7	21st Oct. 2012, - 12:11:14 14:17:54	0.96	-4.46	0.55	-2.37	0.29	-1.28					
16		FISH	91	12	13								5.21	1.35	1.36		
17	Stat2	DAPI	55	3	5	15th Oct. 2012, - 22:51:38 00:15:54	1.41	-6.53	0.78	-2.54	0.43	-1.91					
18		FISH	55	3	5								4.57	1.14	1.83		
19	Stat3	DAPI	55	5	9	16th Oct. 2012, - 00:18:06 01:42:26	1.40	-7.22	0.80	-2.80	0.42	-1.91					
20		FISH	55	4	7								5.20	1.39	1.92		
21	Stat3	DAPI	55	7	13	16th Oct. 2012, - 01:44:00 03:10:26	1.32	-5.82	0.80	-4.01	0.40	-1.58					
22		FISH	55	2	4								4.29	2.43	1.86		
23	Stat5	DAPI	55	4	7	16th Oct. 2012, - 03:12:02 04:37:52	0.51	-2.23	0.94	-3.97	0.37	-1.83					
24		FISH	55	2	4								2.77	3.26	1.84		
25	Stat2	DAPI	55	7	13	16th Oct. 2012, - 04:39:40 05:56:36	1.47	-5.89	0.94	-4.22	0.43	-1.97					
26		FISH	55	3	5								3.86	3.05	1.90		

27	Stat3	DAPI	55	3	5	16th Oct. 2012, - 05:59:30 07:19:02	1.93	-7.67	0.81	-3.01	0.56	-2.47
28		FISH	55	8	15			4.71		1.18		2.52
29	Stat3	DAPI	55	3	5	16th Oct. 2012, - 07:21:16 08:45:18	2.00	-9.45	0.79	-2.88	0.56	-2.47
30		FISH	55	3	5			6.85		1.16		2.76
31	Stat5	DAPI	55	7	13	16th Oct. 2012, - 08:46:54 10:14:02	2.20	-8.82	0.78	-2.62	0.60	-2.43
32		FISH	55	3	5			5.52		1.21		2.38
		Average:	60	6								
		Total:	1904	183								
Performance yield [Percent high quality images of total]:					9.6							
Number tests with >= 10 high quality images:					6							
Percent tests with >= 10 high quality images of n:					18.8							

QEDF												
n	Station	Channel	Movement of the ship during automated image acquisition			Period of image acquisition	Average of absolute roll angle [degree]	Max roll angle [degree]	Average of absolute pitch [degree]	Max pitch [degree]	Average of absolute heave [meter]	Max heave [meter]
1	Stat6-150m	DAPI	91	4	4	9th Nov. 2012, 15:27:54 - 16:47:30	0.68	-2.52	0.95	-4.11	0.44	-1.88
2	Stat7-150m	DAPI	91	6	7	9th Nov. 2012, 16:54:08 - 18:15:43	0.62	-2.54	0.95	-5.03	0.42	-2.28
3		FISH	91	5	5		1.56	3.36	2.13			
4	Stat8-150m	DAPI	91	7	8	9th Nov. 2012, 18:10:39 - 19:29:35	0.49	-2.29	0.91	-4.40	0.40	-1.87
5		FISH	91	7	8		1.59	1.59	2.94	2.00		
6	Stat9-150m	DAPI	91	8	9	6th Nov. 2012, 21:43:50 - 23:04:36	0.93	-3.61	0.43	-2.47	0.24	-0.98
7		FISH	91	14	15		1.60	1.60	1.92	1.04		
8	Stat10-20m	DAPI	91	14	15	7th Nov. 2012, 00:28:34 - 01:49:26	0.88	-3.38	0.53	-3.33	0.25	-1.14
9		FISH	91	10	11		1.67	1.67	2.41	1.06		
10	Stat10-DCM	DAPI	91	9	10	6th Nov. 2012, 23:05:58 - 00:27:07	1.05	-3.84	0.47	-1.88	0.23	-1.14
11		FISH	91	20	22		2.58	2.58	1.47	0.99		
12	Stat11-20m	DAPI	91	17	19	7th Nov. 2012, 01:50:56 - 03:11:36	0.93	-3.16	0.54	-2.52	0.21	-0.91
13		FISH	91	21	23		1.14	1.14	1.89	0.93		
14	Stat11-DCM	DAPI	91	13	14	7th Nov. 2012, 03:13:04 - 04:31:10	0.98	-2.66	0.52	-2.17	0.20	-0.82
15		FISH	91	10	11		1.39	1.39	1.67	0.87		
16	Stat11-150m	DAPI	91	16	18	7th Nov. 2012, 04:32:39 - 05:51:47	0.78	-3.02	0.51	-2.42	0.22	-0.90
17		FISH	91	11	12		1.56	1.56	1.56	0.94		
18	Stat12-20m	DAPI	91	11	12	7th Nov. 2012, 05:53:15 - 07:11:20	0.78	-2.75	0.47	-1.95	0.24	-1.02
19		FISH	91	7	8		1.48	1.48	1.50	1.06		
20	Stat4-150m	DAPI	91	24	26	7th Nov. 2012, 07:12:56 - 08:33:28	0.78	-3.33	0.47	-2.05	0.22	-0.97
21		FISH	91	16	18		1.91	1.91	1.66	0.92		
Average:			91	12								
Total:			1911	250								
Performance yield [Percent high quality images of total]:					13.1							
Number tests with >= 10 high quality images:					13							
Percent tests with >= 10 high quality images of n:					61.9							

n	Station	Channel	Number of FOV tried to image	Number of high quality images obtained	Percent high quality images obtained	Period of automated image acquisition	Movement of the ship during image acquisition						
							Average of absolute roll [degree]	Max roll angle [degree]	Average of absolute pitch [degree]	Max pitch [degree]	Average of absolute heave [meter]	Max heave [meter]	
1	Stat2-20m	DAPI	78	10	13	7th Nov. 2012, 16:47:21 - 18:04:52	0.73	-2.49	0.52	-2.05	0.22	-0.90	
2	Stat2-20m	FISH	78	21	27			0.94		1.57		0.99	
3	Stat2-DCM	DAPI	78	31	40	8th Nov. 2012, 12:19:52 - 13:55:04	0.47	-2.37	0.57	-2.22	0.22	-0.93	
4	Stat2-DCM	FISH	78	35	45			1.76		1.08		1.01	
5	Stat3-DCM	DAPI	78	32	41	8th Nov. 2012, 13:55:44 - 15:31:35	0.70	-2.29	0.44	-1.33	0.23	-0.96	
6	Stat3-DCM	FISH	78	41	53			2.82		0.55		0.99	
7	Stat2-150m	DAPI	65	18	28	6th Nov. 2012, 13:39:18 - 14:58:49	1.21	-4.11	0.45	-1.93	0.27	-1.19	
8	Stat2-150m	FISH	65	20	31			1.94		1.28		1.31	
9	Stat5-20m	DAPI	23	9	39	7th Nov. 2012, 09:28:29 - 09:55:45	0.70	-2.77	0.40	-2.03	0.23	-0.96	
10	Stat5-20m	FISH	23	12	52			2.01		1.40		0.91	
11	Stat3-20m	DAPI	91	24	26	6th Nov. 2012, 15:21:13 - 17:12:26	0.83	-3.79	0.52	-2.66	0.24	-1.04	
12	Stat3-20m	FISH	91	33	36			2.40		1.96		1.16	
13	Stat3-150m	DAPI	91	30	33	6th Nov. 2012, 17:13:08 - 19:04:11	0.93	-3.95	0.50	-2.14	0.23	-1.18	
14	Stat3-150m	FISH	91	22	24			2.29		1.81		1.09	
15	Stat20-D	DAPI	91	11	12	19th Nov. 2012, 00:32:10 - 02:21:08	1.28	-3.02	0.76	-3.55	0.29	-1.36	
16	Stat20-D	FISH	91	11	12			0.40		2.23		1.51	
17	Sta55-D	DAPI	91	18	20	14th Nov. 2012, 09:56:57 - 11:43:23	1.53	-6.26	1.13	-5.07	0.62	-2.65	
18	Sta55-D	FISH	91	15	16			4.93		4.38		3.07	
19	Stat56-20m	DAPI	60	10	17	15th Nov. 2012, 15:36:18 - 16:49:31	0.52	-2.03	0.71	-3.01	0.30	-1.25	
20	Stat56-20m	FISH	60	18	30			2.33		1.46		1.30	
21	Stat56-DCM	DAPI	91	12	13	14th Nov. 2012, 13:26:11 - 15:16:23	1.31	-5.48	1.15	-5.20	0.50	-2.46	
22	Stat56-DCM	FISH	91	16	18			3.40		3.75		2.46	
23	Stat56-D	DAPI	70	11	16	15th Nov. 2012, 17:18:52 - 18:44:17	0.55	-2.06	0.70	-2.79	0.32	-1.51	
24	Stat56-D	FISH	70	15	21			2.29		1.85		1.53	
25	Stat57-20m	DAPI	91	10	11	15th Nov. 2012, 21:58:08 - 23:48:27	0.47	-1.43	0.65	-2.52	0.27	-1.26	
26	Stat57-20m	FISH	91	13	14			2.03		1.51		1.35	
27	Stat57-DCM	DAPI	91	20	22	15th Nov. 2012, 23:49:07 - 01:39:24	0.36	-1.65	0.62	-2.43	0.25	-1.35	
28	Stat57-DCM	FISH	91	22	24			1.67		1.51		1.25	
29	Stat57-D	DAPI	59	12	20	16th Nov. 2012, 05:07:02 - 06:17:41	0.85	-1.87	0.57	-2.26	0.23	-1.06	
30	Stat57-D	FISH	59	13	22			2.81		1.09		1.09	

31	Stat58-20m	DAPI	91	22	24	16th Nov. 2012, 07:12:33	-	0.47	-1.90	0.60	-2.27	0.23	-1.19
32		FISH	91	34	37		09:04:22		1.09		1.04		1.13
33	Stat58-DCM	DAPI	73	8	11	16th Nov. 2012, 09:05:04	-	0.61	-3.11	0.60	-2.22	0.22	-1.00
34		FISH	73	18	25		10:34:58		1.77		1.25		0.97
35	Stat58-DCM	DAPI	62	26	42	16th Nov. 2012, 12:31:05	-	0.84	-2.64	0.62	-2.35	0.26	-1.06
36		FISH	62	18	29		13:44:05		0.91		1.20		1.08
37	Stat59-20m	DAPI	91	11	12	16th Nov. 2012, 15:09:38	-	1.05	-3.04	0.62	-2.49	0.25	-1.18
38		FISH	91	17	19		16:57:32		1.14		1.31		1.06
40	Stat59-D	DAPI	91	34	37	16th Nov. 2012, 22:33:28	- 00:08:46	1.23	0.80	0.59	1.43	0.19	1.19
41		FISH	78	16	21				-2.64		-2.09		-0.81
49	Stat4-20m	DAPI	78	13	17	7th Nov. 2012, 18:08:20	-	0.80	-2.16	0.50	-2.52	0.23	-1.02
50		FISH	78	17	22		19:35:58		0.66		1.51		1.06
51	Stat4-DCM	DAPI	48	18	38	8th Nov. 2012, 15:32:16	-	0.42	-2.10	0.55	-2.10	0.22	-0.95
52		FISH	48	19	40		16:31:04		1.34		1.08		0.90
53	Stat5-DCM	DAPI	50	13	26	9th Nov. 2012, 12:11:36	-	0.76	-2.74	0.99	-4.32	0.49	-2.04
54		FISH	50	12	24		13:12:49		1.17		2.90		2.23
55	Stat6-D	DAPI	91	19	21	20th Nov. 2012, 11:59:54	-	0.79	-3.58	0.73	-1.86	0.14	-0.69
56		FISH	91	37	41		13:49:03		4.49		0.55		0.67
57	Stat22-150m	DAPI	91	16	18	7th Nov. 2012, 14:21:17	-	0.84	-2.59	0.39	-1.88	0.21	-1.02
58		FISH	91	29	32		16:13:18		3.24		1.29		1.06
		Average:	76	19									
		Total:	3815	962									
Performance yield (Percent high quality images of total):					25.2								
Number tests with >= 10 high quality images:					56								
Percent tests with >= 10 high quality images of n:					96.6								

Chapter 1 Supplementary Table 1 On-board performance test of the three different methods for stack image acquisition with extended depth of focus calculation.

Appendix Figures and Table for Chapter 2

On-site microbial diversity and abundance analysis in the remotest part of the world's oceans, the South Pacific Gyre

Greta Reintjes, Halina Tegetmeyer, Jörg Wulf, Miriam Bürgisser, Christian
Quast, Frank-Oliver Glöckner, Bernhard M. Fuchs, Rudolf Amann

Manuscript in prep.

Appendix Figures and Tables

Chapter 2 Supplementary Table 1 Latitude and longitude of stations sampled along SO245 “Ultracpac” cruise including depths of individual samples from each station.

<i>Station type</i>	<i>Station number</i>	<i>Station ID</i>	<i>Date</i>	<i>Latitude [degree north]</i>	<i>Longitude [degree east]</i>	<i>Depth [m]</i>
<i>Intermediate 1</i>	1	SO245-01-08	2015/12/25	-23,30186	-84,3374	20
<i>Intermediate 1</i>	1	SO245-01-07	2015/12/25	-23,30186	-84,3374	50
<i>Intermediate 1</i>	1	SO245-01-06	2015/12/25	-23,30186	-84,3374	75
<i>Intermediate 1</i>	1	SO245-01-05	2015/12/25	-23,30186	-84,3374	100
<i>Intermediate 1</i>	1	SO245-01-04	2015/12/25	-23,30186	-84,3374	125
<i>Intermediate 1</i>	1	SO245-01-03	2015/12/25	-23,30186	-84,3374	150
<i>Intermediate 1</i>	1	SO245-01-02	2015/12/25	-23,30186	-84,3374	400
<i>Intermediate 1</i>	1	SO245-01-01	2015/12/25	-23,30186	-84,3374	500
<i>Main 1</i>	2	SO245-02-12	2015/12/27	-23,31035	-90,1767	20
<i>Main 1</i>	2	SO245-02-12	2015/12/27	-23,31035	-90,1767	50
<i>Main 1</i>	2	SO245-02-12	2015/12/27	-23,31035	-90,1767	100
<i>Main 1</i>	2	SO245-02-10	2015/12/27	-23,31033	-90,1766	125
<i>Main 1</i>	2	SO245-02-10	2015/12/27	-23,31033	-90,1766	150
<i>Main 1</i>	2	SO245-02-10	2015/12/27	-23,31033	-90,1766	175
<i>Main 1</i>	2	SO245-02-10	2015/12/27	-23,31033	-90,1766	200
<i>Main 1</i>	2	SO245-02-10	2015/12/27	-23,31033	-90,1766	250
<i>Main 1</i>	2	SO245-02-10	2015/12/27	-23,31033	-90,1766	300
<i>Main 1</i>	2	SO245-02-05	2015/12/27	-23,29502	-90,1763	500
<i>Main 1</i>	2	SO245-02-05	2015/12/27	-23,29502	-90,1763	1000
<i>Main 1</i>	2	SO245-02-02	2015/12/27	-23,29502	-90,1762	1500
<i>Main 1</i>	2	SO245-02-02	2015/12/27	-23,29502	-90,1762	2200

Appendix Figures and Tables

Main 1	2	SO245-02-02	2015/12/27	- 23,29502	-90,1762	3500
Intermediate 2	2	SO245-03-01	2015/12/29	- 23,29968	-95,17727	50
Intermediate 2	3	SO245-03-01	2015/12/29	- 23,29968	-95,17727	100
Intermediate 2	3	SO245-03-01	2015/12/29	- 23,29968	-95,17727	125
Intermediate 2	3	SO245-03-01	2015/12/29	- 23,29968	-95,17727	150
Intermediate 2	3	SO245-03-01	2015/12/29	- 23,29968	-95,17727	170
Intermediate 2	3	SO245-03-01	2015/12/29	- 23,29968	-95,17727	200
Intermediate 2	3	SO245-03-01	2015/12/29	- 23,29968	-95,17727	300
Intermediate 2	3	SO245-03-01	2015/12/29	- 23,29968	-95,17727	500
Main 2	4	SO245-04-13	2015/12/31	- 23,30054	-99,59499	50
Main 2	4	SO245-04-13	2015/12/31	- 23,30054	-99,59499	100
Main 2	4	SO245-04-11	2015/12/31	- 23,30057	-99,59498	150
Main 2	4	SO245-04-11	2015/12/31	- 23,30057	-99,59498	175
Main 2	4	SO245-04-11	2015/12/31	- 23,30057	-99,59498	200
Main 2	4	SO245-04-11	2015/12/31	- 23,30057	-99,59498	225
Main 2	4	SO245-04-11	2015/12/31	- 23,30057	-99,59498	250
Main 2	4	SO245-04-11	2015/12/31	- 23,30057	-99,59498	300
Main 2	4	SO245-04-07	2015/12/31	- 23,30005	-100,0001	500
Main 2	4	SO245-04-07	2015/12/31	- 23,30005	-100,0001	1000
Main 2	4	SO245-04-01	2015/12/30	- 23,29996	-100,0001	2250
Main 2	4	SO245-04-01	2015/12/30	- 23,29996	-100,0001	3500
Main 2	4	SO245-04-01	2015/12/30	- 23,29996	-100,0001	3900
Intermediate 3	5	SO245-05-01	2016/1/2	- 23,29842	-107,0102	50
Intermediate 3	5	SO245-05-01	2016/1/2	- 23,29842	-107,0102	100
Intermediate	5	SO245-05-01	2016/1/2	-	-107,0102	150

Appendix Figures and Tables

3				23,29842		
Intermediate 3	5	SO245-05-01	2016/1/2	-	-107,0102	175
Intermediate 3	5	SO245-05-01	2016/1/2	23,29842	-107,0102	200
Intermediate 3	5	SO245-05-01	2016/1/2	23,29842	-107,0102	225
Intermediate 3	5	SO245-05-01	2016/1/2	23,29842	-107,0102	250
Intermediate 3	5	SO245-05-01	2016/1/2	23,29842	-107,0102	300
Intermediate 3	5	SO245-05-01	2016/1/2	23,29842	-107,0102	500
Main 3	6	SO245-06-11	2016/1/4	-	-110,2953	20
Main 3	6	SO245-06-11	2016/1/4	23,30003	-110,2953	40
Main 3	6	SO245-06-11	2016/1/4	23,30003	-110,2953	60
Main 3	6	SO245-06-11	2016/1/4	23,30003	-110,2953	80
Main 3	6	SO245-06-11	2016/1/3	23,29422	-110,2337	100
Main 3	6	SO245-06-11	2016/1/3	23,29422	-110,2337	125
Main 3	6	SO245-06-08	2016/1/3	23,29422	-110,2337	150
Main 3	6	SO245-06-08	2016/1/3	23,29422	-110,2337	175
Main 3	6	SO245-06-08	2016/1/3	23,29422	-110,2337	200
Main 3	6	SO245-06-08	2016/1/3	23,29422	-110,2337	225
Main 3	6	SO245-06-08	2016/1/3	23,29422	-110,2337	250
Main 3	6	SO245-06-08	2016/1/3	23,29422	-110,2337	275
Main 3	6	SO245-06-08	2016/1/3	23,29422	-110,2337	300
Intermediate 4	7	SO245-07-04	2016/1/6	-	-114,0559	20
Intermediate 4	7	SO245-07-04	2016/1/6	25,58913	-114,0559	50
Intermediate 4	7	SO245-07-04	2016/1/6	25,58913	-114,0559	125
Intermediate 4	7	SO245-07-04	2016/1/6	25,58913	-114,0559	150
Intermediate 4	7	SO245-07-04	2016/1/6	25,58913	-114,0559	175

Appendix Figures and Tables

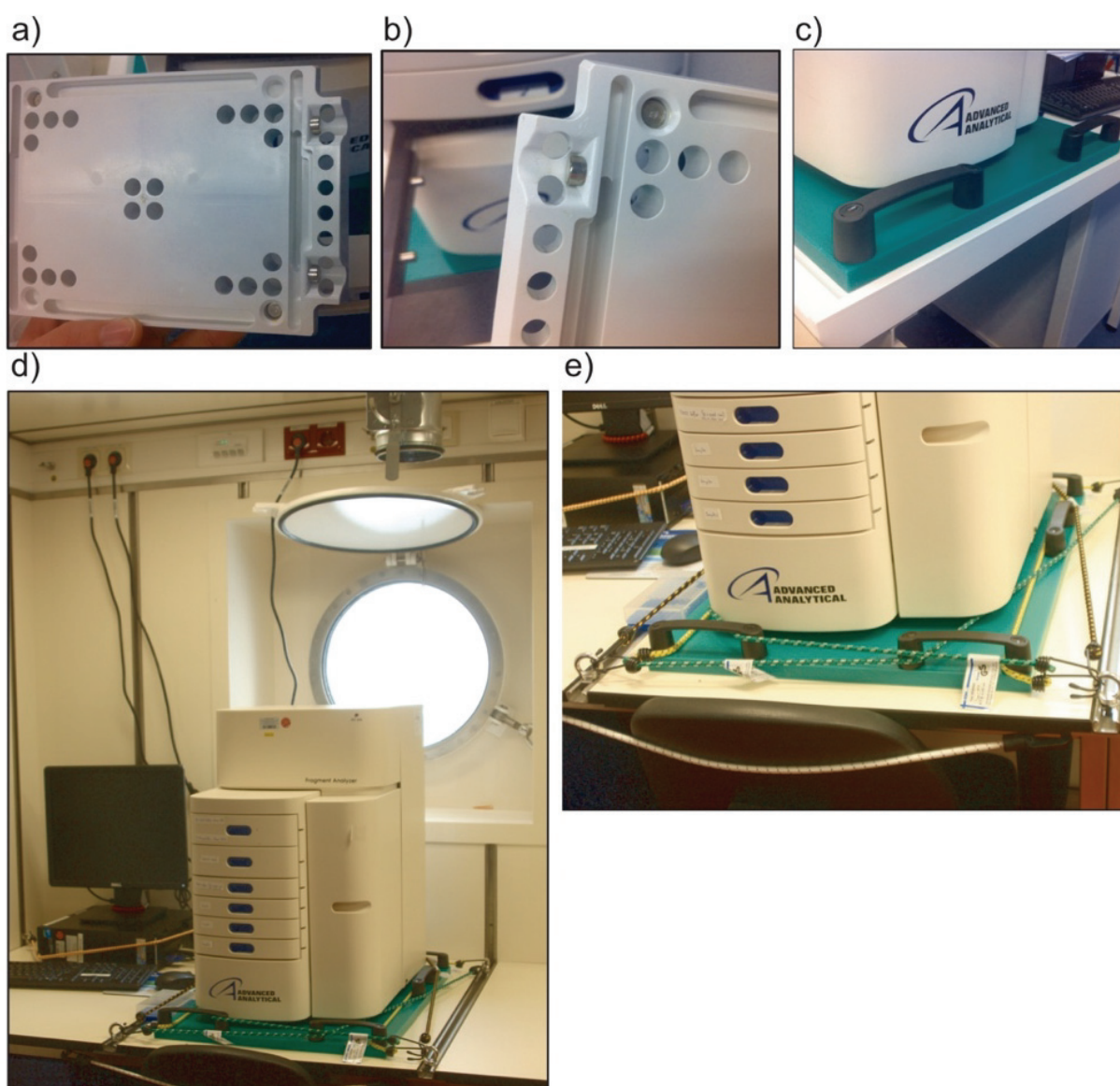
<i>Intermediate 4</i>	7	SO245-07-04	2016/1/6	- 25,58913	-114,0559	200
<i>Intermediate 4</i>	7	SO245-07-04	2016/1/6	- 25,58913	-114,0559	250
<i>Intermediate 4</i>	7	SO245-07-04	2016/1/6	- 25,58913	-114,0559	300
<i>Main 4</i>	8	SO245-08-10	2016/1/8	- 27,44496	-117,37212	20
<i>Main 4</i>	8	SO245-08-10	2016/1/8	- 27,44496	-117,37212	60
<i>Main 4</i>	8	SO245-08-10	2016/1/8	- 27,44496	-117,37212	100
<i>Main 4</i>	8	SO245-08-10	2016/1/8	- 27,44496	-117,37212	150
<i>Main 4</i>	8	SO245-08-10	2016/1/8	- 27,44496	-117,37212	175
<i>Main 4</i>	8	SO245-08-10	2016/1/8	- 27,44496	-117,37212	200
<i>Main 4</i>	8	SO245-08-10	2016/1/8	- 27,44496	-117,37212	250
<i>Main 4</i>	8	SO245-08-10	2016/1/8	- 27,44496	-117,37212	500
<i>Main 4</i>	8	SO245-08-19	2016/1/8	- 27,44496	-117,37212	1500
<i>Main 4</i>	8	SO245-08-05	2016/1/8	- 27,44496	-117,37212	2250
<i>Main 4</i>	8	SO245-08-01	2016/1/8	- 27,44496	-117,37212	3615
<i>Intermediate 5</i>	9	SO245-09-01	2016/1/9	-30,379	-121,45804	25
<i>Intermediate 5</i>	9	SO245-09-01	2016/1/9	-30,379	-121,45804	150
<i>Intermediate 5</i>	9	SO245-09-01	2016/1/9	-30,379	-121,45804	175
<i>Intermediate 5</i>	9	SO245-09-01	2016/1/9	-30,379	-121,45804	200
<i>Intermediate 5</i>	9	SO245-09-01	2016/1/9	-30,379	-121,45804	225
<i>Intermediate 5</i>	9	SO245-09-01	2016/1/9	-30,379	-121,45804	250
<i>Intermediate 5</i>	9	SO245-09-01	2016/1/9	-30,379	-121,45804	300
<i>Intermediate 5</i>	9	SO245-09-01	2016/1/9	-30,379	-121,45804	500
<i>Main 5</i>	10	SO245-10-10	2016/1/10	- 33,30205	-126,0458	20
<i>Main 5</i>	10	SO245-10-10	2016/1/10	- 33,30205	-126,0458	60
<i>Main 5</i>	10	SO245-10-10	2016/1/10	-	-126,0458	100

Appendix Figures and Tables

				33,30205		
Main 5	10	SO245-10-10	2016/1/10	-	-126,0458	125
				33,30205		
Main 5	10	SO245-10-10	2016/1/10	-	-126,0458	150
				33,30205		
Main 5	10	SO245-10-10	2016/1/10	-	-126,0458	175
				33,30205		
Main 5	10	SO245-10-10	2016/1/10	-	-126,0458	200
				33,30205		
Main 5	10	SO245-10-10	2016/1/10	-	-126,0458	250
				33,30205		
Main 5	10	SO245-10-10	2016/1/10	-	-126,0458	300
				33,30205		
Main 5	10	SO245-10-10	2016/1/10	-	-126,0458	500
				33,30205		
Main 5	10	SO245-10-06	2016/1/10	-	-125,59995	1000
				33,29996		
Main 5	10	SO245-10-06	2016/1/10	-	-125,59995	1500
				33,29996		
Main 5	10	SO245-10-03	2016/1/10	-33,3	-126,0007	2000
Main 5	10	SO245-10-01	2016/1/10	-	-125,59994	2800
				33,30002		
Main 5	10	SO245-10-01	2016/1/10	-	-125,59994	3970
				33,30002		
Main 6	12	SO245-12-14	2016/1/16	-	-139,48606	20
				39,18613		
Main 6	12	SO245-12-14	2016/1/16	-	-139,48606	40
				39,18613		
Main 6	12	SO245-12-14	2016/1/16	-	-139,48606	60
				39,18613		
Main 6	12	SO245-12-14	2016/1/16	-	-139,48606	80
				39,18613		
Main 6	12	SO245-12-14	2016/1/16	-	-139,48606	100
				39,18613		
Main 6	12	SO245-12-14	2016/1/16	-	-139,48606	150
				39,18613		
Main 6	12	SO245-12-14	2016/1/16	-	-139,48606	200
				39,18613		
Main 6	12	SO245-12-14	2016/1/16	-	-139,48606	300
				39,18613		
Main 6	12	SO245-12-14	2016/1/16	-	-139,48606	500
				39,18613		
Main 6	12	SO245-12-10	2016/1/16	-	-139,48607	1000
				39,18613		
Main 6	12	SO245-12-06	2016/1/15	-	-139,48605	2500
				39,18617		
Main 6	12	SO245-12-02	2016/1/15	-	-139,4859	5230
				39,18603		

Appendix Figures and Tables

Chapter 2 Supplementary Figure 1 Images of the alterations of Ion Torrent PGM (Thermo Fisher), Ion Torrent OT2 (Thermo Fisher) and Fragment analyser (AATI) to enable on-board use. a & b) Images of the fragment analyser sampling trays with attached magnets to prevent accidental dropping. c) Image of 2 cm thick polyethylene base plate (green) with handles for secure placement and easy transport. d & e) Images of fragment analyser securely attached to ship working surface using bungee cords to prevent accidental movement during ship pitch and roll movements. f –h) Images of secured Ion Torrent PGM, Ion Torrent OT2 and ES with attached 2 cm thick polyethylene base plate (green) with handles for secure placement and easy transport.



f)



g)



h)



Chapter 2 Supplementary Table 2 "Lab on a ship" server pipeline commands and time required for each step to process 330,000 sequences.

Initialize SilvaNGS (3 min for 330000 sequences)

silva_submit --config <FILENAME.conf> init

Check status of initialization or any other step, see above for details.

silva_submit --config=<FILENAME.conf> status

Import files (3 min for 330000 sequences)

silva_submit --config <FILENAME.conf> import

Cluster (10 min for 330000 sequences)

silva_submit --config <FILENAME.conf> cluster

Align (8 min for 330000 sequences)

silva_submit --config <FILENAME.conf> align

Classify (100 min for 330000 sequences)

silva_submit --config <FILENAME.conf> classify

Rarefaction (10 min for 330000 sequences)

silva_submit --config <FILENAME.conf> rarefaction

Stats (5 min for 330000 sequences)

silva_submit --config <FILENAME.conf> stats

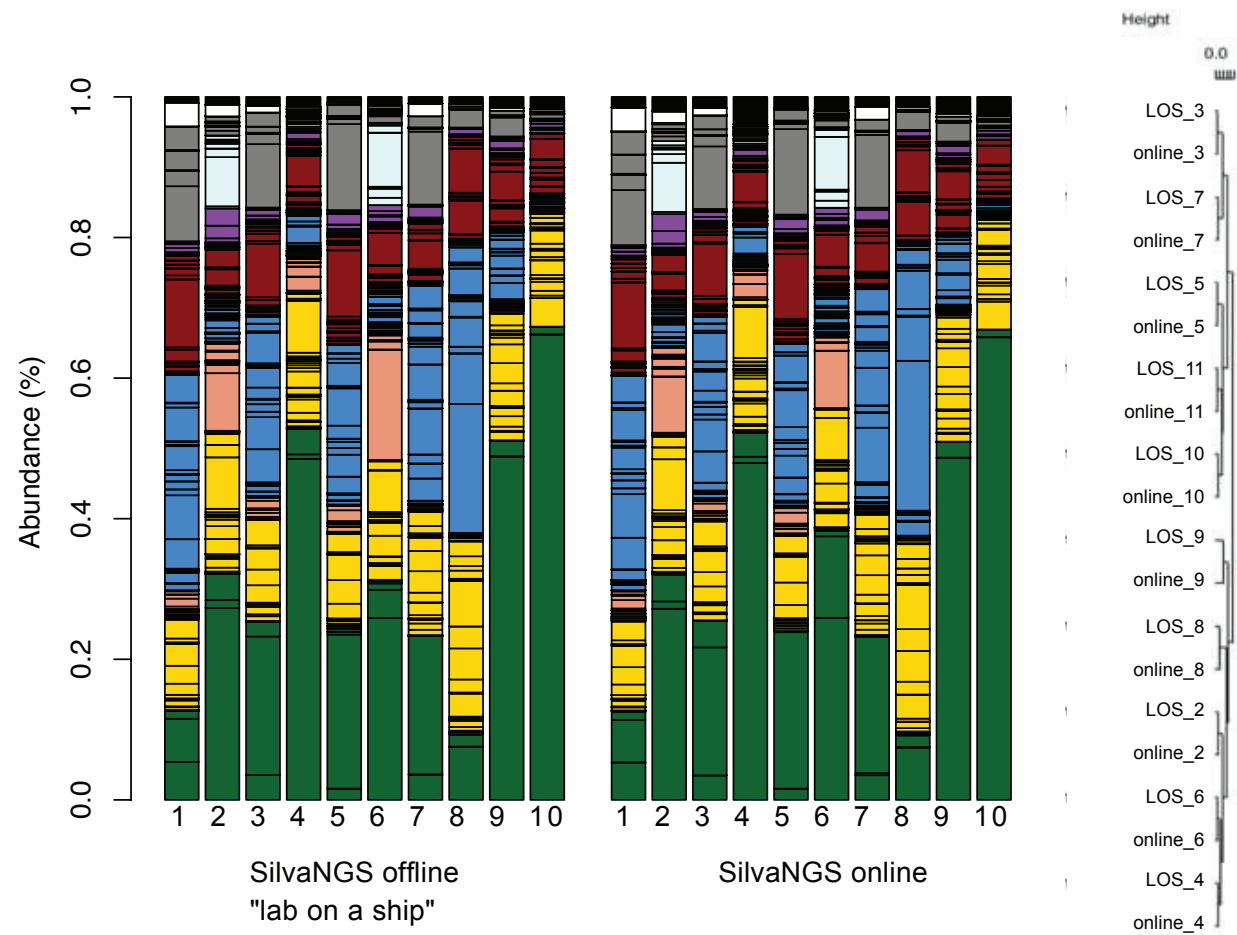
Taxplot (5 min for 330000 sequences)

silva_submit --config <FILENAME.conf> taxplot

Exports (10 min for 330000 sequences)

silva_submit --config <FILENAME.conf> export

Chapter 2 Supplementary Figure 2 Bar chart and cluster analysis of the bacterial community composition obtained from the analysis of ten samples (labelled 1-10) on two versions of the SilvaNGS pipeline (online and offline “lab on a ship”). The first ten samples are the results from the offline “lab on a ship” server, the second ten samples are the results from the online SilvaNGS server. Sequences were classified to genus level and colour coded at the phylum level.



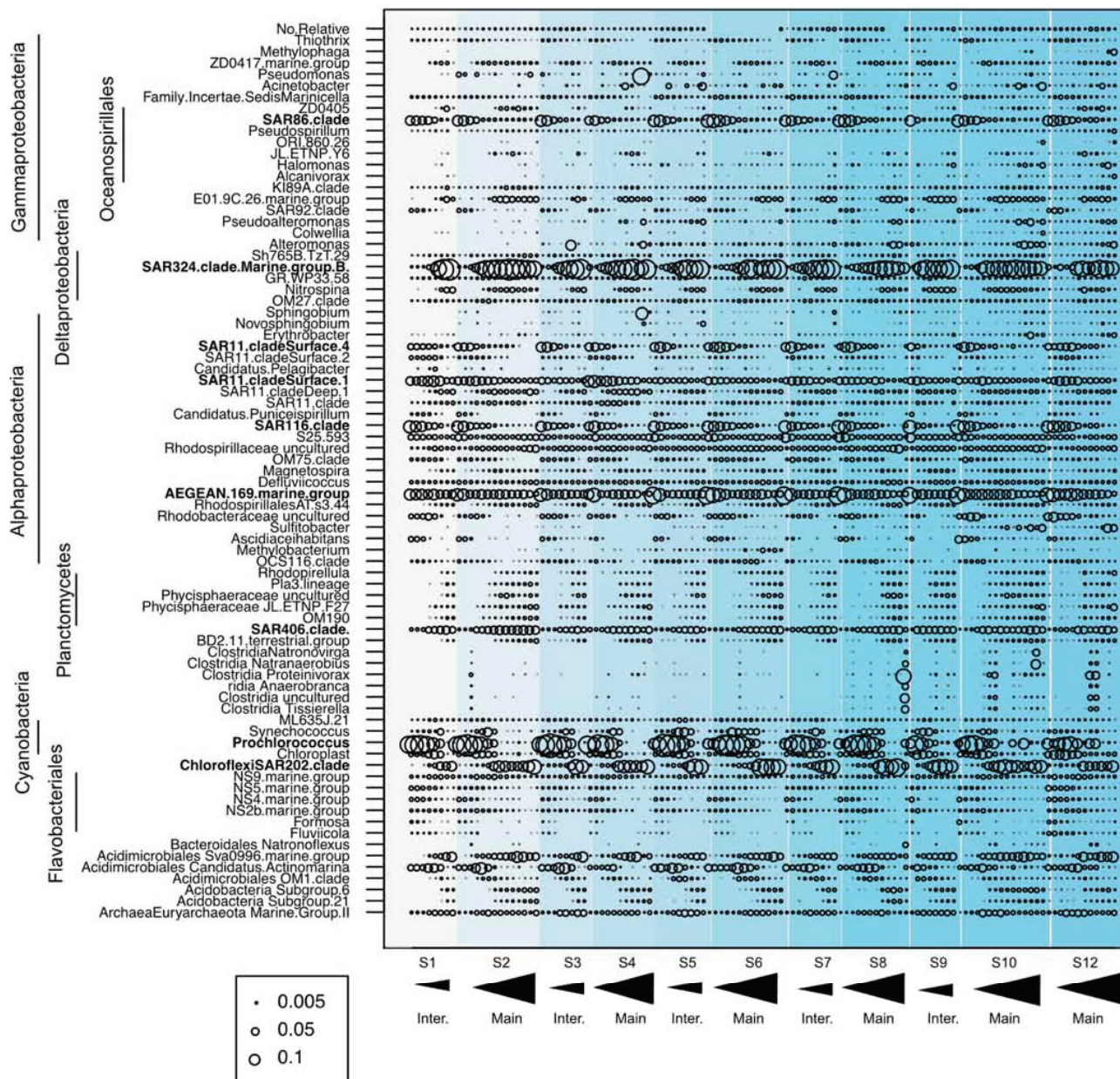
Appendix Figures and Tables

Chapter 2 Supplementary Table 3 Statistical analysis of bacteria richness and diversity across various depth ranges calculated from relative read abundances. Samples were taken along the SO245 “Ultramac” cruise.

<i>Depth (m)</i>	<i>Richness (Genus)</i>	<i>Shannon- Index</i>	<i>Simpson</i>	<i>Inverse Simpson</i>	<i>Evenness</i>
<i>20 to 100</i>	149	2.83	0.89	9.66	0.58
<i>100-200</i>	170	2.99	0.88	9.50	0.59
<i>200-500</i>	218	3.12	0.88	9.17	0.58
<i>1000-5000</i>	242	3.17	0.89	10.16	0.58

Appendix Figures and Tables

Chapter 2 Supplementary Figure 3 Bubble plot of bacterial and archaeal genera with a minimum relative read abundance of 0.001%. The size of the bubbles indicates the average relative read abundance (%) of each genus normalised against the total abundance. Each vertical row of bubbles shows the microbial composition of a sample from a specific station at a specific depth. The station names (S1 –S12) are located under the sections and each station is coloured in a different blue tone. Main (20 – 5000 m) and intermediate (20 – 500 m) station are indicated by large and small black triangles, respectively. The triangles thickness indicates an increase in depth (shallow to deep).



On-Board Sequencing Time Table		
Time for analysis of 11 samples		
	Ion314chip time (min)	Ion318 chip time (min)
Filtration	180	180
DNA extraction	90	90
DNA quantification (Fragment Analyser)	60	60
PCR	12	12
PCR clean up and size selection	60	60
Amplicon quantification (Fragment Analyser)	60	60
Pool calculation and preparation	60	60
OT2	480	480
ES	60	60
Sequencing	240	420
Ion torrent suite	120	240
Offline Server Analysis (for 300,000 reads)		
Import	3	3
Cluster	10	10
Align	8	8
Classify	100	100
Export (rarefaction, stats, taxplots)	20	20
Plotting results	30	60
	1593	1923
	27 hours	32 hours

Appendix Figures and Table for Chapter 3

Free-living and particle-associated bacteria exist as an interactive assemblage.

Greta Reintjes, Cheng Wang, Jörg Wulf, Bernhard Fuchs, Rudolf Amann

Manuscript in prep.

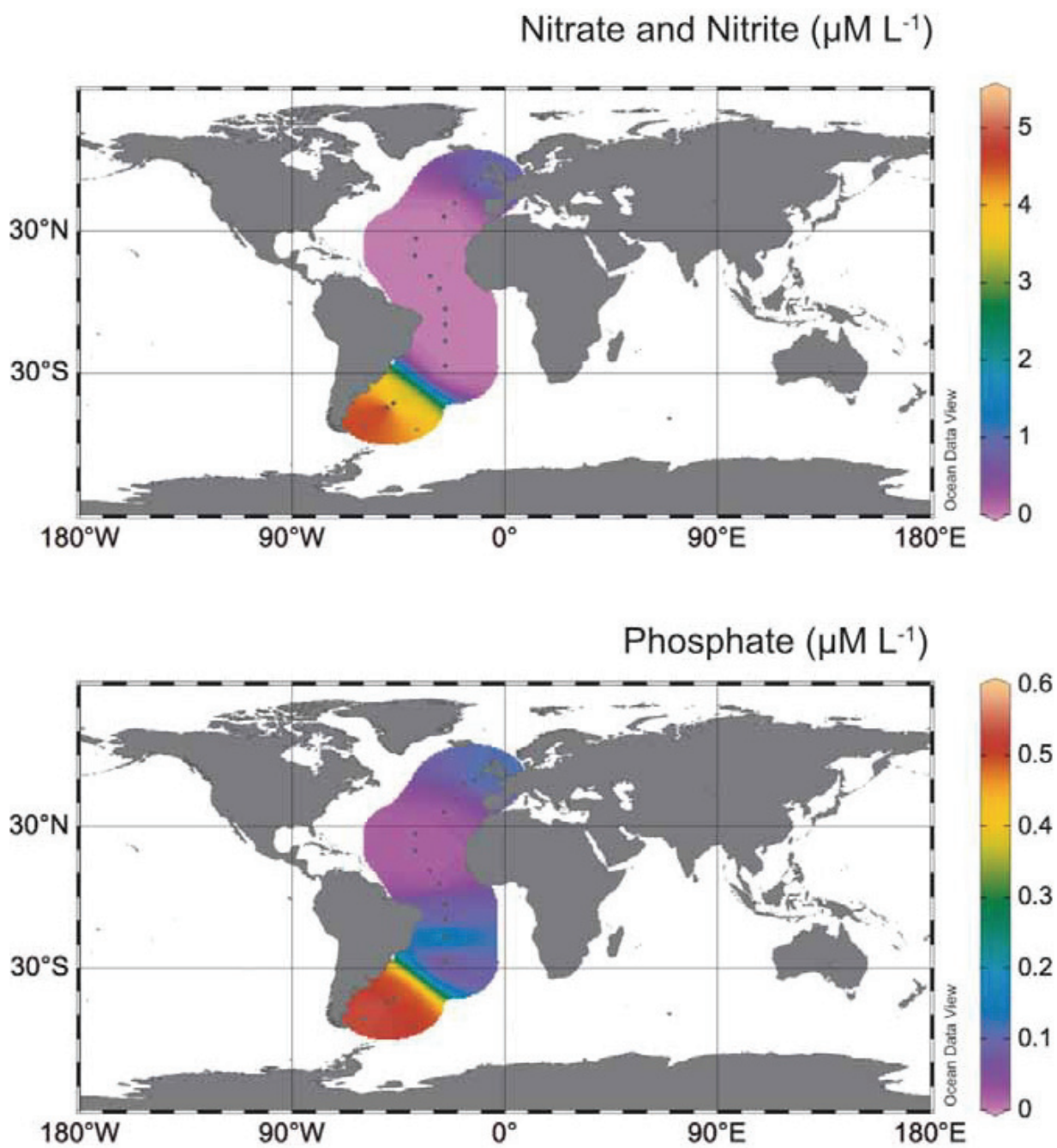
Appendix Figures and Tables

Chapter 3 Supplementary Table 1 PCR reaction mix and thermocycler conditions applied in Chapter 3

<i>PCR Reaction</i>	<i>Volume</i>	<i>Thermocycler conditions</i>
<i>Molecular grade H₂O</i>	28 µl	1 cycle:
<i>5 x HF buffer</i>	10 µl	94°C for 5 min
<i>dNTPs mix (2,5 mM)</i>	1 µl	35 cycles:
<i>Forward Primer (100 µM)</i>	0.5 µl	94°C for 30 sec
<i>Reverse Primer (100 µM)</i>	0.5 µl	55°C for 30 sec
<i>Phusion Polymerase (0,02 units µl⁻¹)</i>	0.5 µl	72°C for 30 sec
<i>DNA (10 ngµL⁻¹)</i>	1 µl	1 cycle:
<i>DMSO</i>	1 µl	72°C for 5 min

Appendix Figures and Tables

Chapter 3 Supplementary Figure 1 Geographic surface contour plots showing the measured surface nitrate and nitrite (combined) and phosphate concentrations ($\mu\text{M L}^{-1}$) along the AMT22. Black dots indicate points of sampling



Appendix Figures and Tables

Chapter 3 Supplementary Table 2 Averaged total abundance (cell ml⁻¹) of Bacteria (EUB I-III) Bacteroidetes (CF319a), Gammaproteobacteria (GAM42) and Cyanobacteria (CYA664) within different size fractions (FL, small-PA, large-PA) enumerated by FISH

	<i>EUB I-III</i>	<i>CF319a</i>	<i>GAM42</i>	<i>CYA664</i>
<i>FL</i>	7.62E+05	5.66E+04	1.09E+04	1.53E+05
<i>small PA</i>	1.53E+03	2.07E+02	6.70E+01	5.90E+01
<i>large PA</i>	3.15E+02	7.58E+01	4.00E+01	2.32E+01

Appendix Figures and Table for Chapter 4

An alternative polysaccharide uptake mechanism of marine bacteria

Greta Reintjes, Carol Arnosti, Bernhard M. Fuchs, Rudolf Amann

Manuscript published: ISME Journal March 2017
DOI: 10.1038/ismej.2017.26

Appendix Figures and Tables

Chapter 4 Supplementary Table 1 FISH probes used in this study

Probe Name	Sequence 5' - 3'	FA%	Reference
CF319a	TGGTCCGTGTCTCAGTAC	35	Manz et al. (1992)
PLA46	GACTTGCATGCCTAATCC	30	Neef et al. (1998)
CAT653	CCCCCTCTCCCTTACTCT	25	This study

**FA corresponds to the formamide concentration using in the hybridisation buffer.*

Appendix Figures and Tables

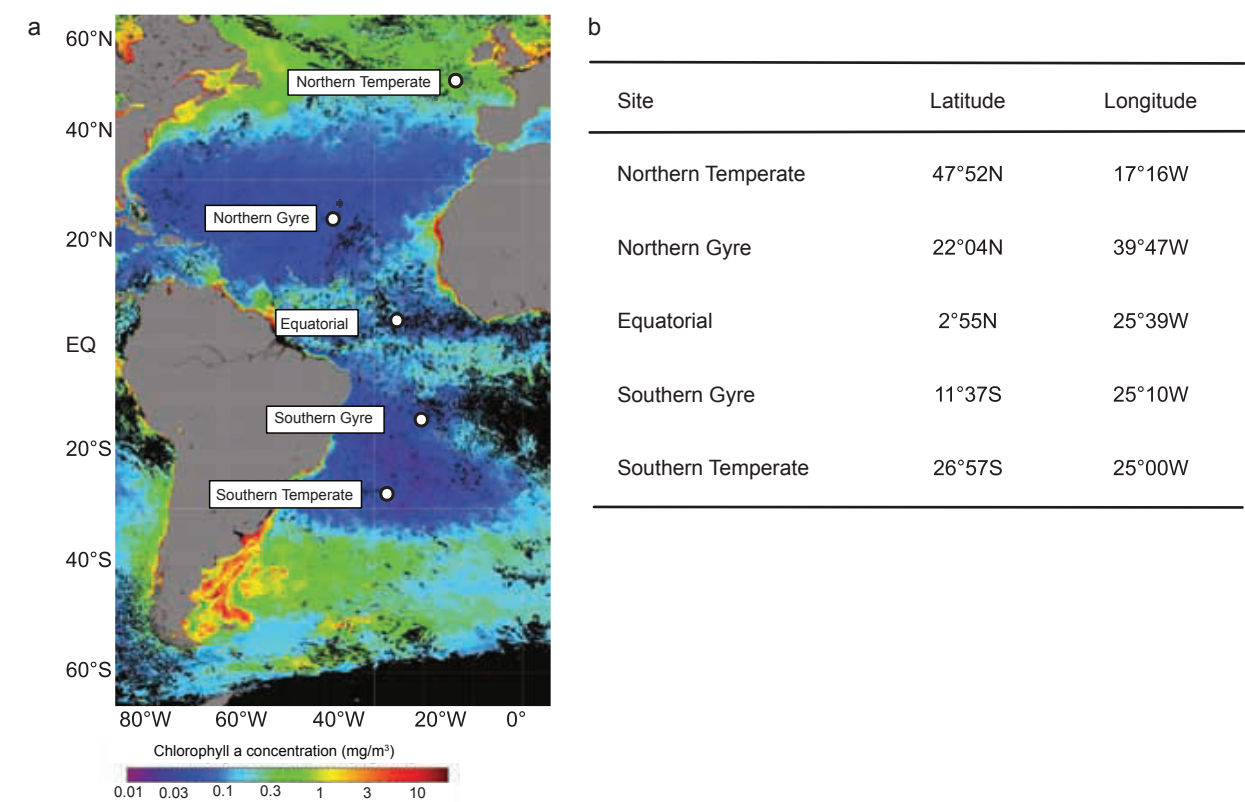
Chapter 4 Supplementary Table 2 Carbon source and concentration added to individual media

Medium	Substrate	Stock concentration	Volume added [ml] to 1L
HaHa high carbon	Glucose, cellobiose, yeast extract, peptone and casamino acids	100 g l ⁻¹	2 ml
Ha Ha minimal	Glucose, cellobiose, yeast extract, peptone and casamino acids	1 g l ⁻¹	1.2 ml
HaHa Laminarin	Yeast extract and laminarin	1 g l ⁻¹ and 50g l ⁻¹	1.2 ml and 1 ml
HaHa FLA-Laminarin 3.5µM	FLA-Laminarin	16.6 mM monomer l ⁻¹	0.021 ml
HaHa FLA-Laminarin 35µM	FLA-Laminarin	16.6 mM monomer l ⁻¹	0.210 ml

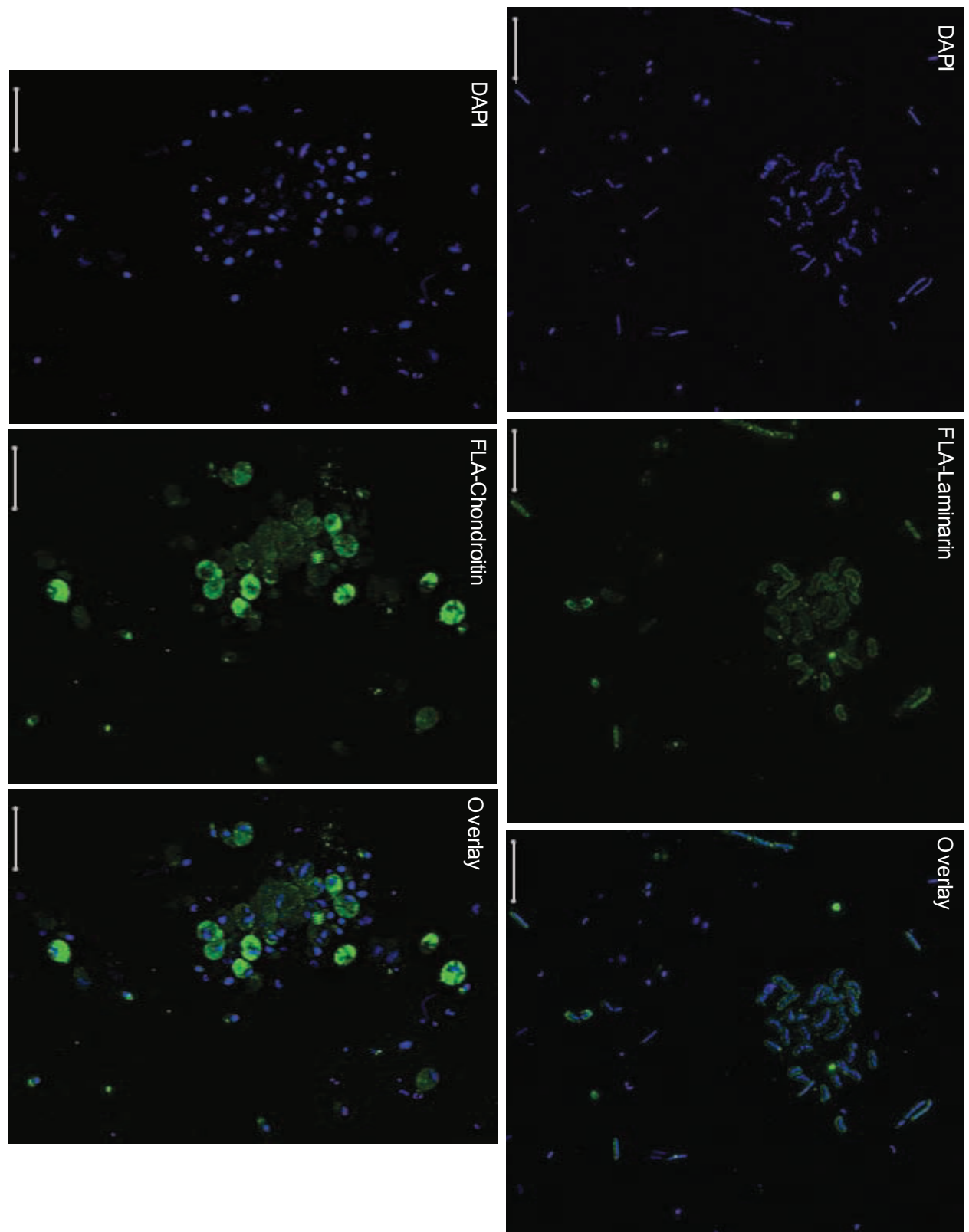
Appendix Figures and Tables

Chapter 4 Supplementary Table 3 Flow cytometry results showing signal intensities (FL1 533/30.H) from cells incubated with varying FLA-laminarin concentrations over time (5 - 100 min). Background shows the FL1 signal intensity of G. forsetii without the addition of FLA-laminarin. The substrate loss signal indicates the reduction of the FL1 signal after 1 day after inoculation (1:10) into HaHa laminarin medium.

Substrate Concentration (μM)	Incubation time (min)					Substrate Loss
	5	20	40	60	100	1260
35	2373	2194	2107	2061	1919	501
15	1670	1462	1420	1363	1325	
5	1178	1005	942	894	819	
3.5	1108	916	876	814	759	
1	803	579	525	473	426	
0.5	371	254	241	232	219	
0.05	291	218	211	207	203	
0 (Background)	179					



Chapter 4 Supplementary Figure 1 Sampling sites in the Atlantic Ocean. (a) Sites shown by white dots; background colours indicate the average chlorophyll *a* concentration (mg m^{-3}) during the sampling period (map obtained from MODIS, Ocean Biology Processing Group (2014)). (b) Latitude and longitude of each sampling site

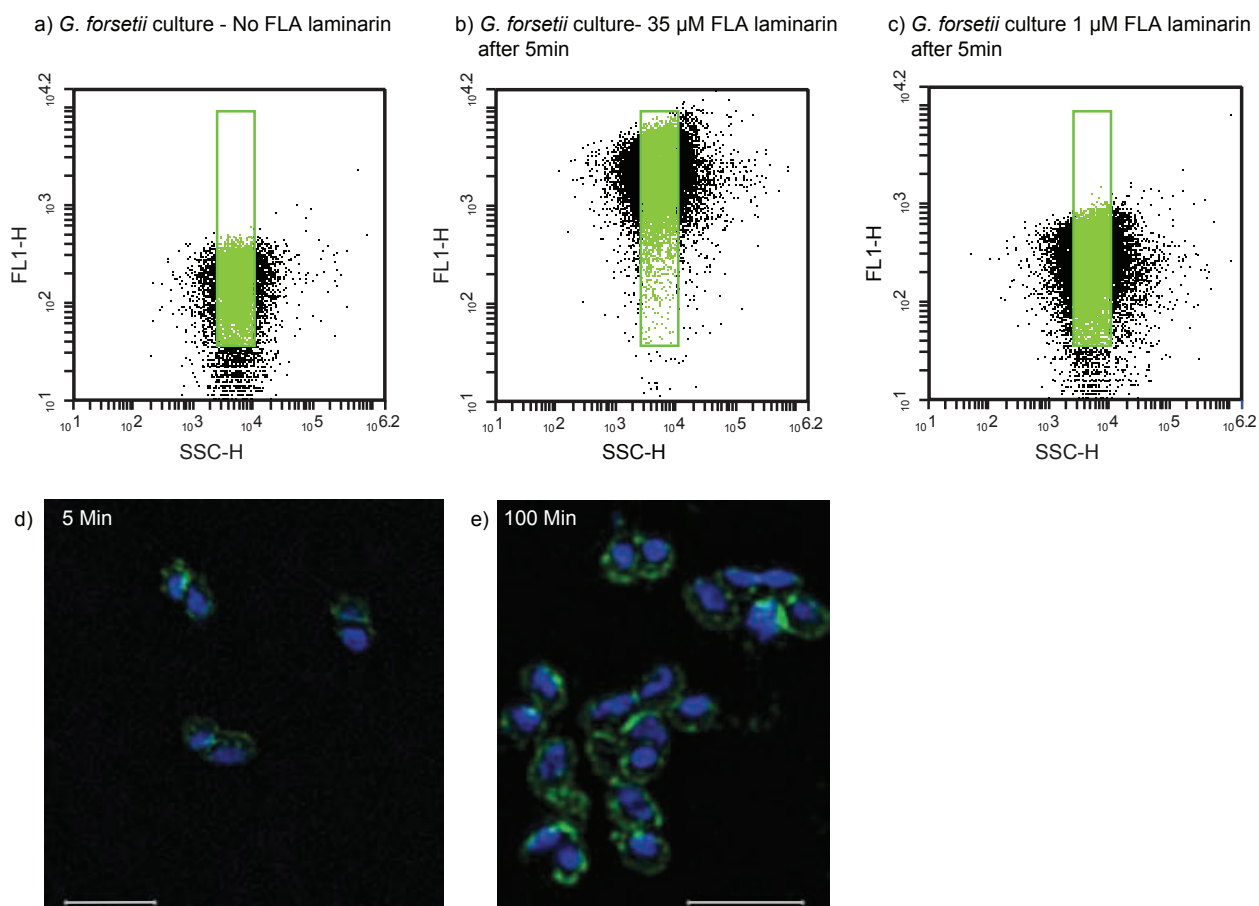


Chapter 4 Supplementary Figure 2 Epifluorescence microscopy images showing the morphological variability of substrate stained cells. Images were taken from the laminarin incubation of the Northern Temperate station after 3 days (above) and the chondroitin

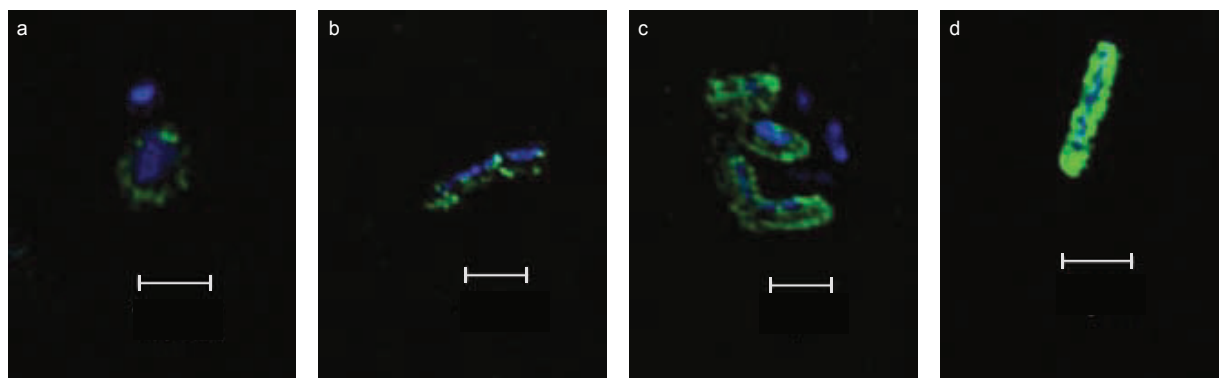
Appendix Figures and Tables

sulphate incubation of the Southern Temperate station after 6 days (below). Cells were stained by DAPI to visualise the DNA (left, blue) and show FLA- laminarin or FLA-chondroitin sulphate specific staining (middle, green). Scale bar = 5 μ m

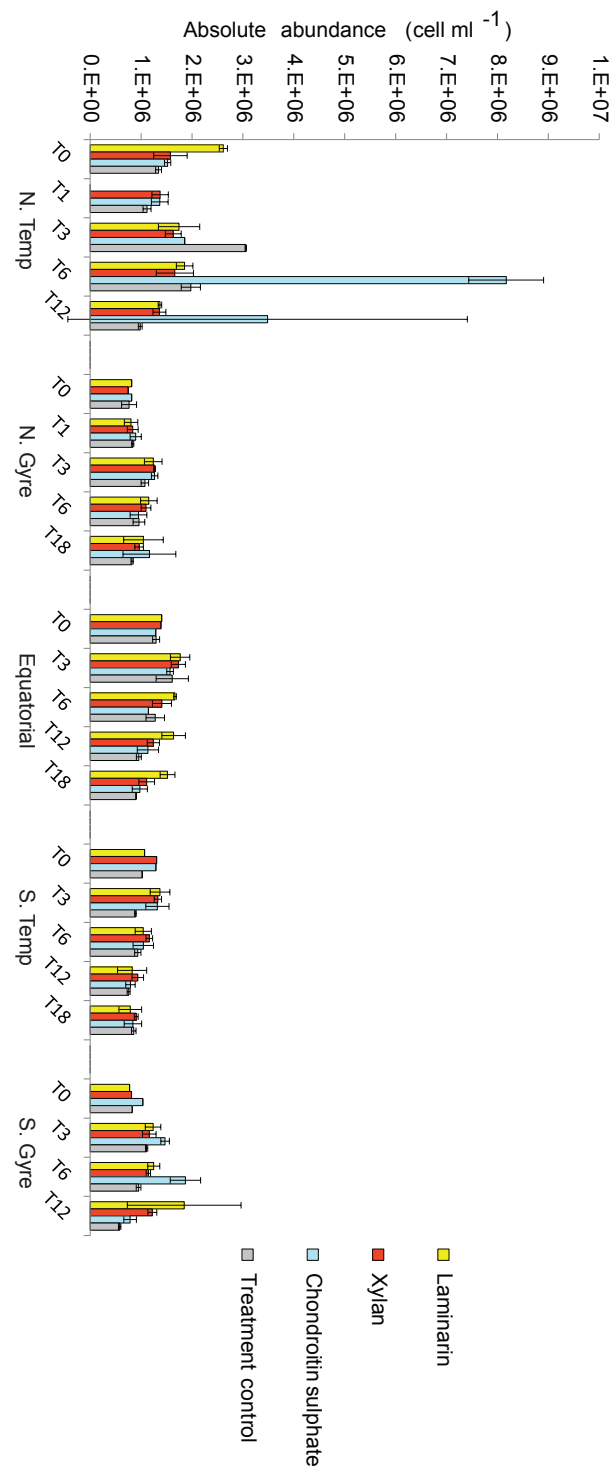
Appendix Figures and Tables



Chapter 4 Supplementary Figure 3 Detection of FLA-laminarin uptake by *G. forsetii* over time using flow cytometry. (a) Untreated control culture of *G. forsetii* showing background FL1-H signal (green gating). (b) *G. forsetii* incubated with 35 μ M FLA-laminarin showing high FL1-H signal (green gating) after just 5 min. (c) *G. forsetii* incubation with 1 μ M FLA laminarin showing low FLA signal after 5 min. (d and e) Substrate uptake by *G. forsetii* over time. SR-SIM images showing FLA-laminarin uptake by *G. forsetii* after 5 min and 100 min. Scale bar = 5 μ m

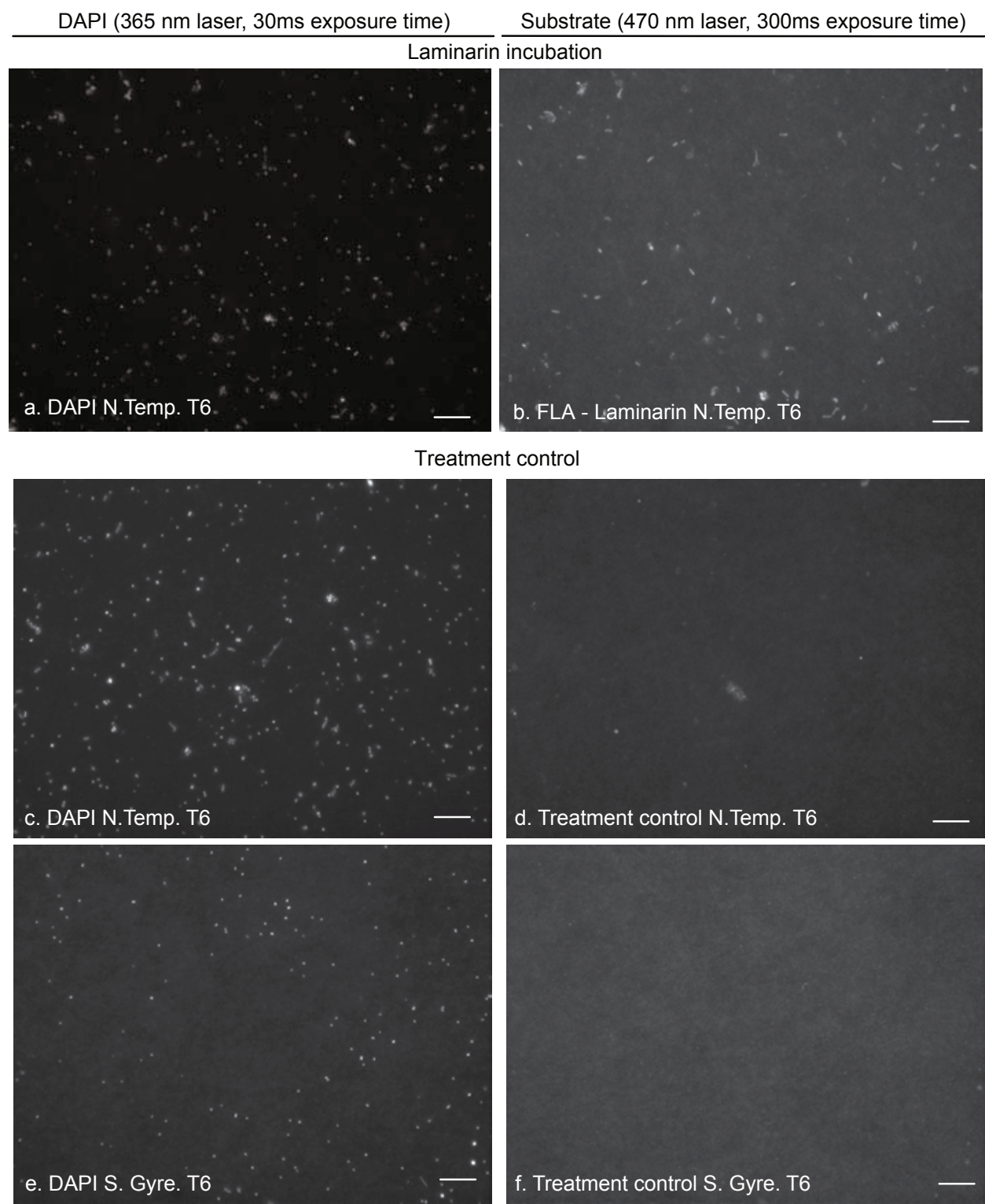


Chapter 4 Supplementary Figure 4 Change in substrate staining of cells over time. (a-d) Two colour (blue = DAPI, green = FLA-laminarin) super-resolution structured illumination microscopy images of cells from the Northern Temperate station incubated with fluorescently labelled laminarin. Time series incubation after (a) 30 min, (b) 3 days, (c) 6 days, and (d) 12 days. Intensity of staining increased over time. Scale bar = 1 μ m

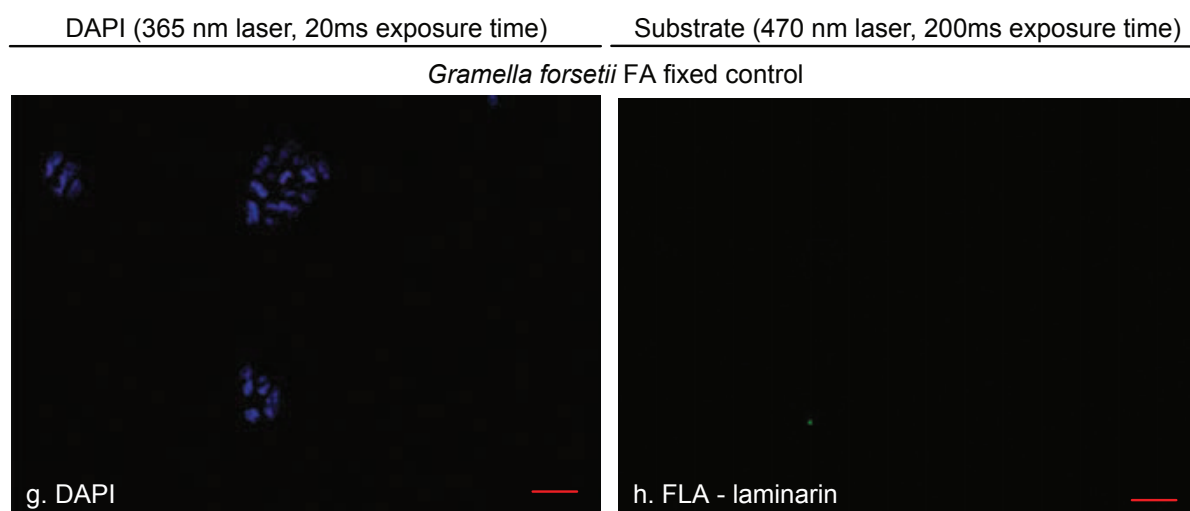


Chapter 4 Supplementary Figure 5 Change in absolute cellular abundance (cell ml⁻¹) during each substrate incubation (laminarin, xylan, chondroitin) and unamended treatment control over time in the Northern Temperate, Northern Gyre, Equatorial, Southern Gyre, and Southern Temperate station. The error bars indicate the total range of triplicate incubations

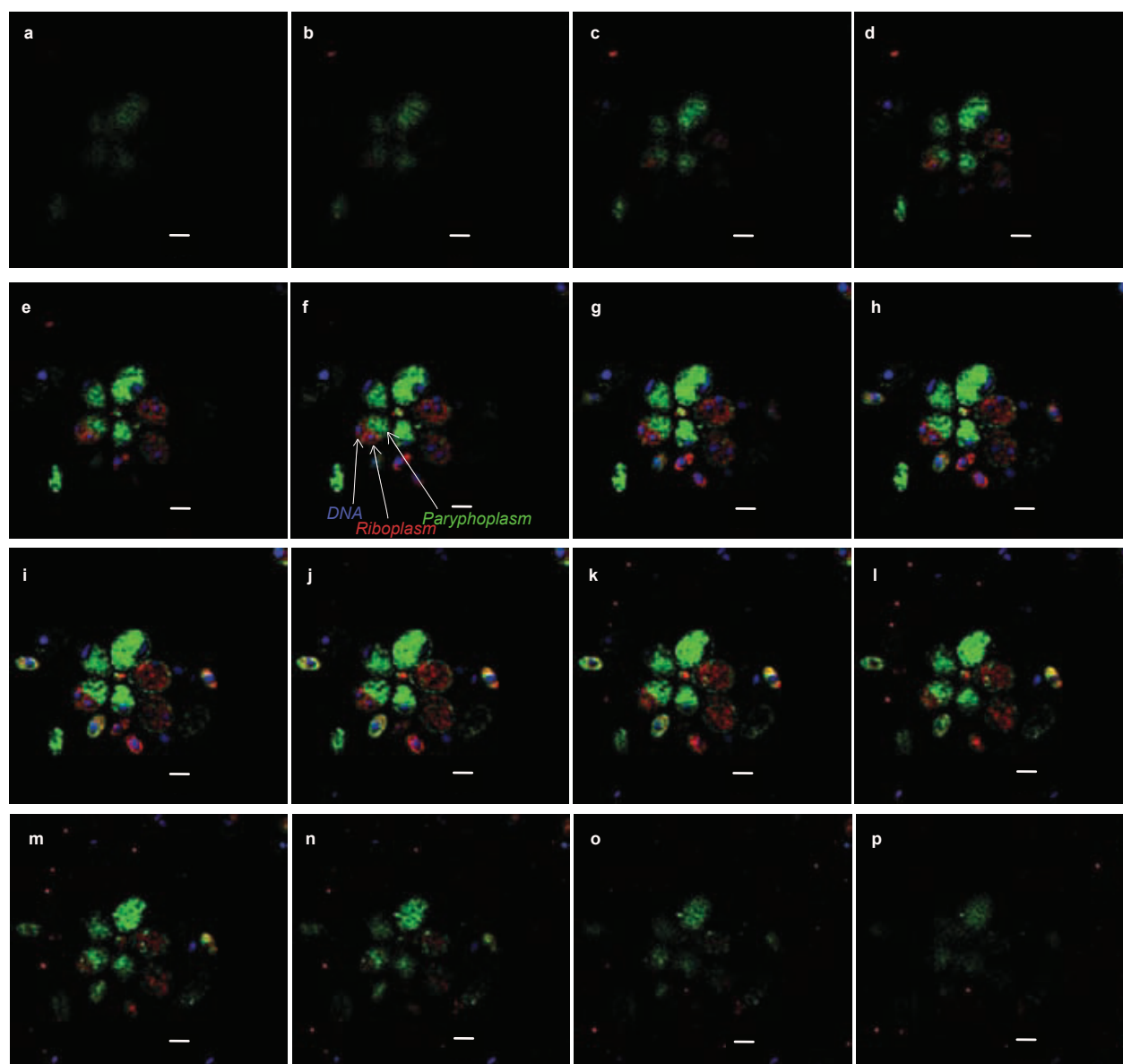
Appendix Figures and Tables



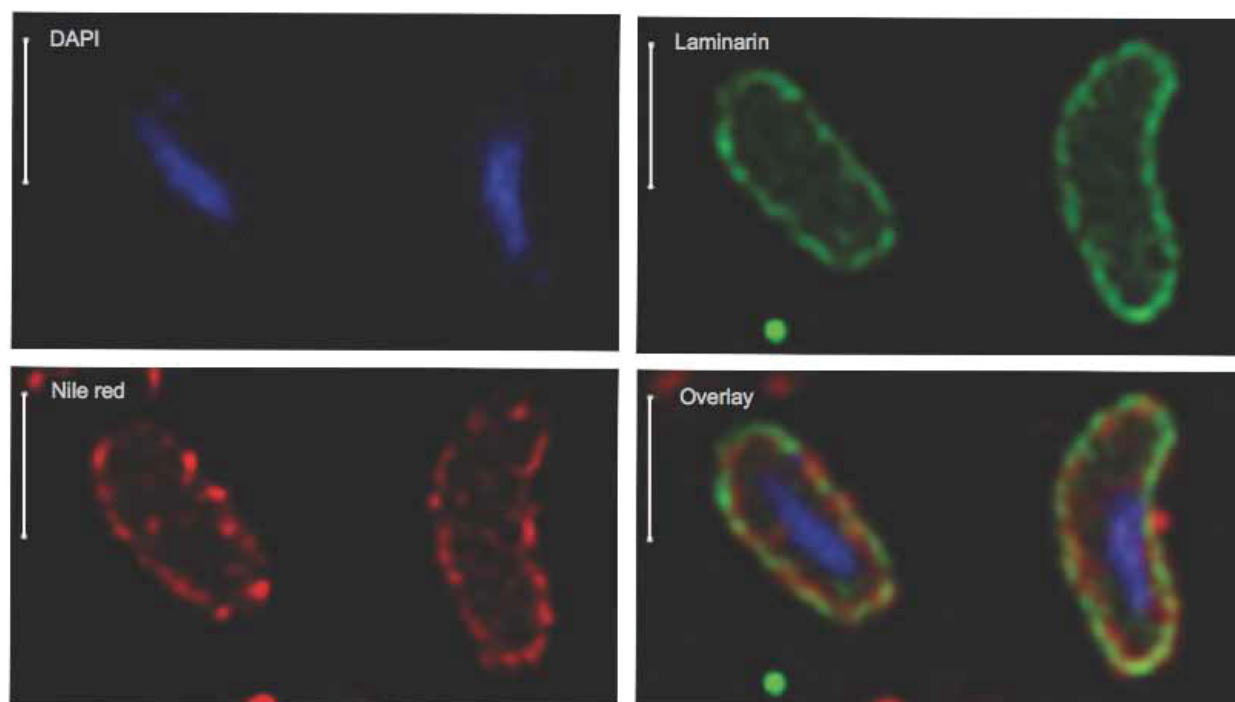
Appendix Figures and Tables



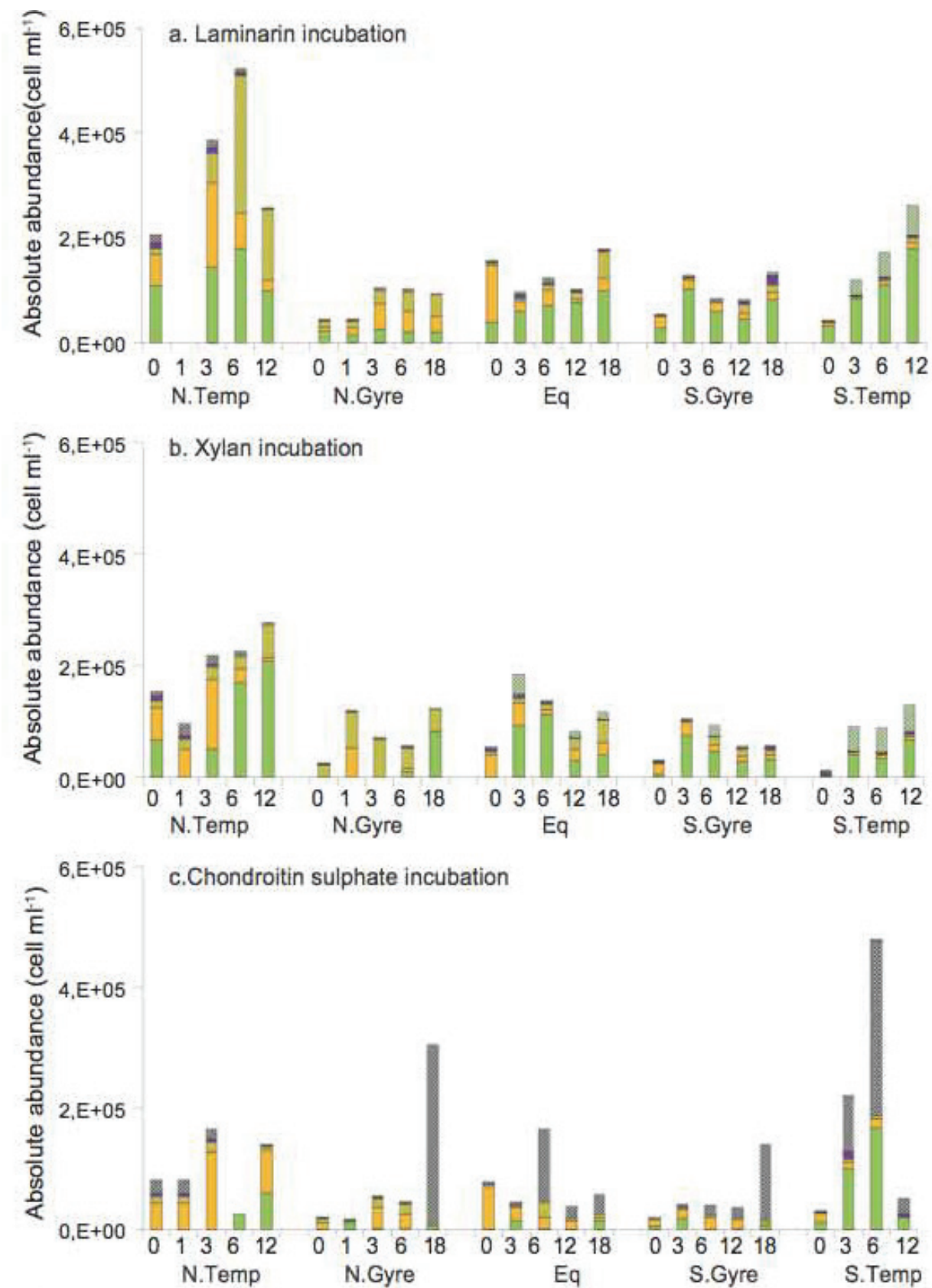
Chapter 4 Supplementary Figure 6 Panels (a) – (h) show epifluorescence microscopy images of DAPI stained cells excited by 365 nm with a constant exposure time of 30 ms (left side), and corresponding image of the same field of view excited by 488 nm at constant exposure of 300 ms (right side). Cells excited by 488 nm show in panel (b) positive FLA-laminarin signal in the Northern Temperate Station at T6, in panels (d) and (f) treatment control of the Northern Temperate and Southern Gyre station at T6. White scale bar = 10 μ m. Image (g) shows DAPI stained *G. forsetii* cell after fixation in 2% formaldehyde (FA) for 2 h and subsequent addition to FLA-laminarin medium for 2 h. Panel (h) is the corresponding image excited by 488 nm showing no unspecific substrate staining of cells. Red scale bar = 2 μ m

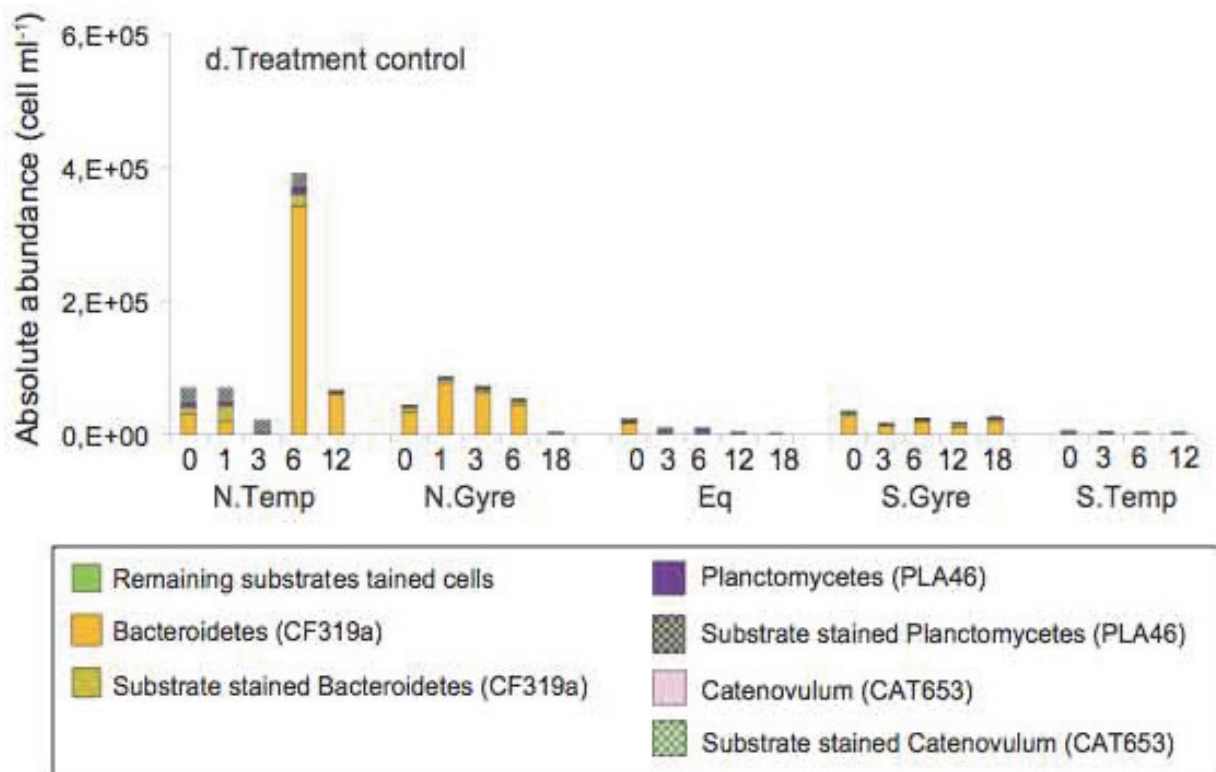


Chapter 4 Supplementary Figure 7 SR-SIM Z-stack of cells incubated with chondroitin sulphate. Images (a-p) show horizontal slices of the cells at $0.2\mu\text{m}$ intervals. Chondroitin (green) is in the paryphoplasm; FISH signal (red, Pla46) is in the riboplasm, and DNA is stained by DAPI (blue). Scale bar = $1\mu\text{m}$



Chapter 4 Supplementary Figure 8 *Sus*-like uptake of FLA-PS by *Bacteroidetes*. SR-SIM images of halo-like substrate staining (FLA-laminarin; green) in the Northern Temperate station after 6 days. Cell was counter stained using Nile red (red) and DAPI (blue) to visualise the membranes and DNA, respectively. Scale bar = 0.5 μm





Chapter 4 Supplementary Figure 9 Absolute abundance of Bacteroidetes, Planctomycetes, and Catenovulum during substrate incubations and treatment control (a) laminarin, (b) xylan, (c) chondroitin sulphate, (d) treatment control) of the Northern Temperate, Northern Gyre, Equatorial, Southern Gyre, and Southern Temperate stations. The absolute abundance was determined by using group specific FISH probes CF319a (orange), PLA46 (purple) and CAT653 (pink) for Bacteroidetes, Planctomycetes, and Catenovulum respectively. Also shown is the percentage of Bacteroidetes (orange with green strips), Planctomycetes (purple with green strips) and Catenovulum (pink with green strips) showing substrate stained

Appendix Figures and Table for Chapter 5

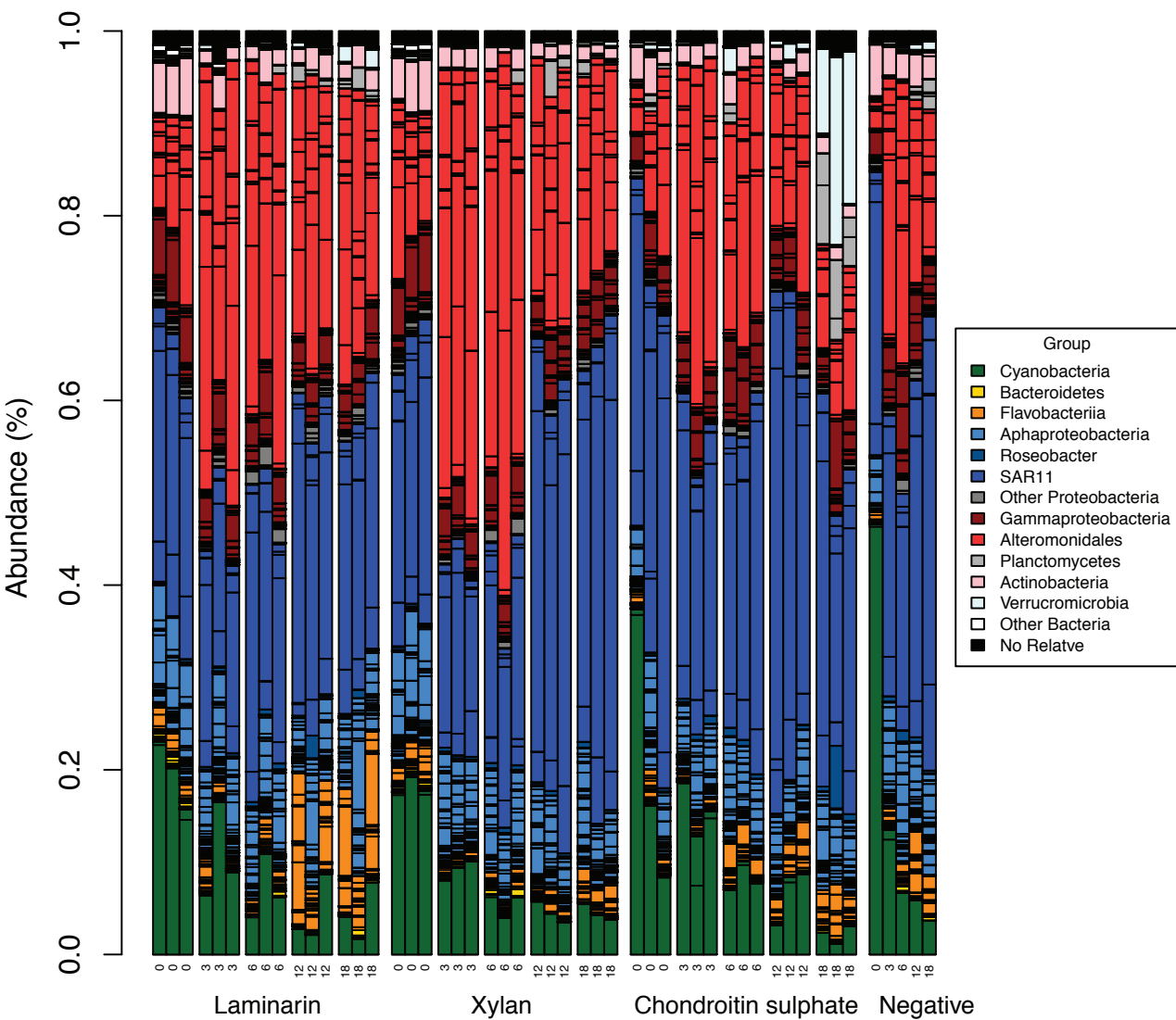
Tracking bacterial community dynamics in polysaccharide incubations along an Atlantic Meridional Transect.

Greta Reintjes, Carol Arnosti, Bernhard M. Fuchs, Rudolf Amann

Manuscript: In preparation

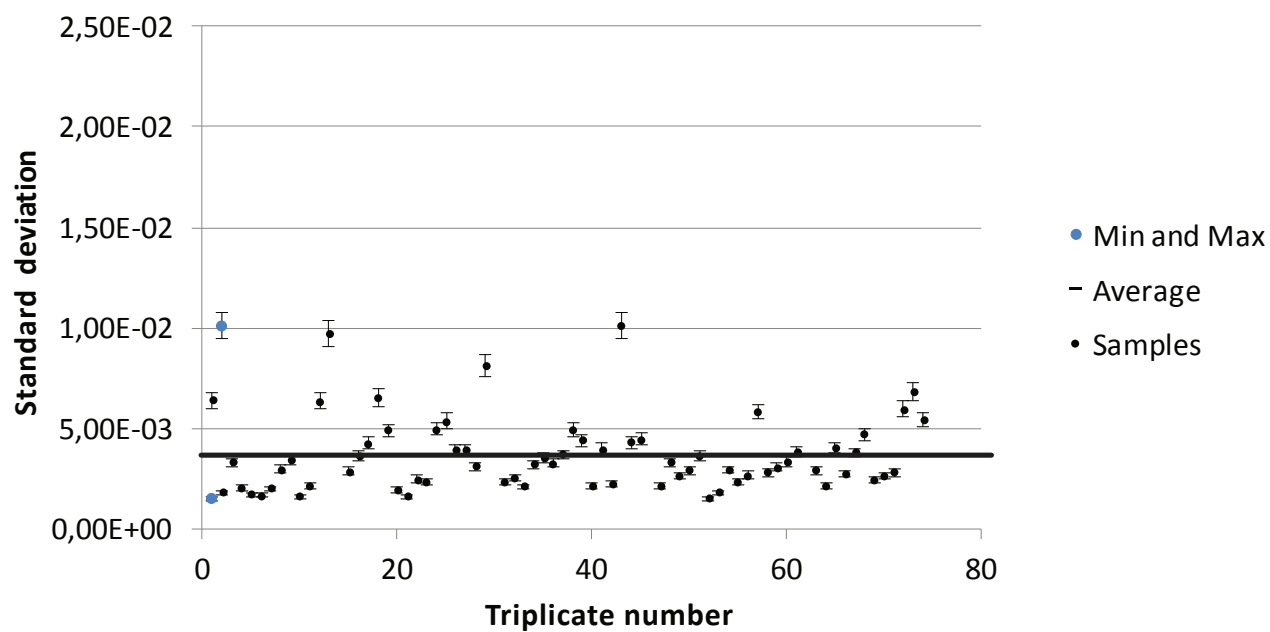
Appendix Figures and Tables

Chapter 5 Supplementary Figure 1 Bar chart showing the bacterial community composition across biological triplicates substrate incubations (laminarin, xylan, chondroitin sulphate) and a treatment control (not in triplicate) of the *S. Gyre* (N). All incubations were sampled after 0, 3, 6, 12 and 18 days.



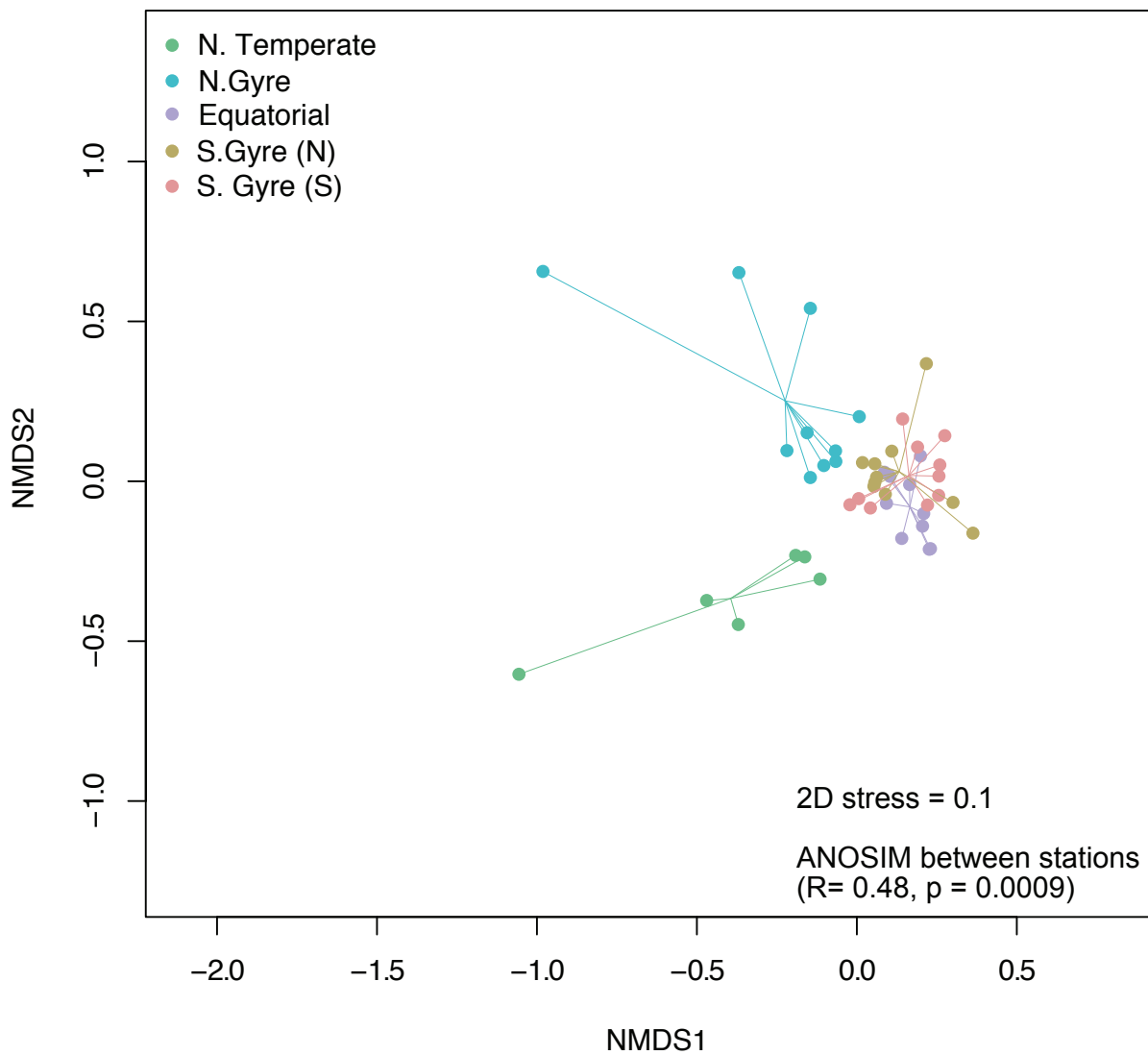
Appendix Figures and Tables

Chapter 5 Supplementary Figure 2 Standard deviation and 95% confidence intervals of the relative read abundance within biological triplicates. Samples were obtained from substrate incubations along the AMT22.



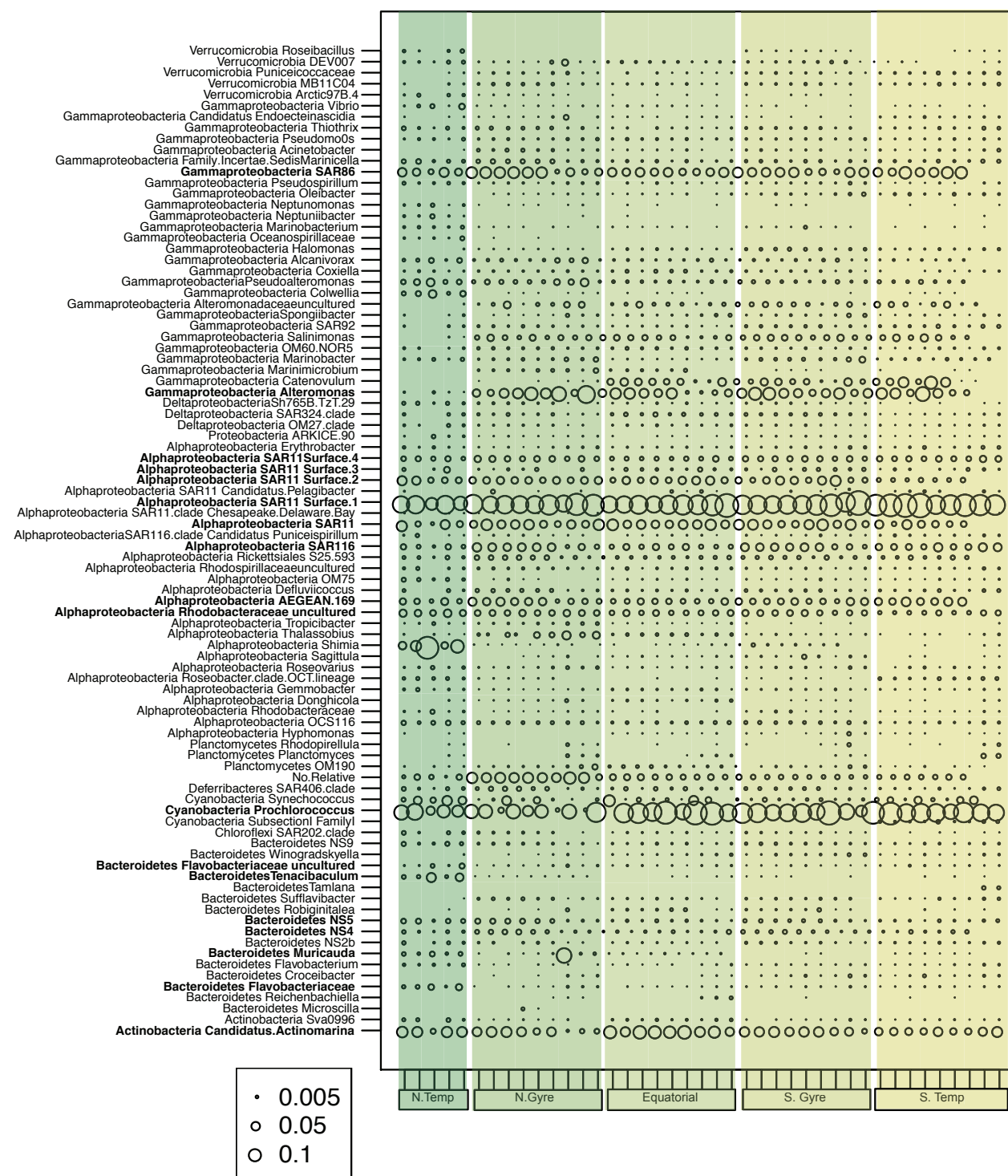
Appendix Figures and Tables

Chapter 5 Supplementary Figure 3 NMDS plot showing Bray Curtis dissimilarity between the initial (T0) bacterial community composition at each station (N. Temperate, N. Gyre, Equatorial, S. Gyre (N), S. Gyre (S)) along the AMT22.



Appendix Figures and Tables

Chapter 5 Supplementary Figure 4 Bubble plot of bacterial genera with a minimum relative read abundance of 0.005% in all initial (T0) samples of the N. Temperate, N. Gyre, Equatorial, S. Gyre (N) and S. Gyre (S) stations (depicted by green boxes). The size of the bubbles indicates the average relative abundance (%) of each genus. The dominant genera are highlighted in bold font.



References

- Abdullahi AS, Underwood GJC, Gretz MR (2006). Extracellular Matrix Assembly in Diatoms (Bacillariophyceae). V. Environmental Effects on Polysaccharide Synthesis in the Model Diatom, *Phaeodactylum Tricornutum*1 *Journal of Phycology* **42**: 363-378.
- Acinas SG, Antón J, Rodríguez-Valera F (1999). Diversity of Free-Living and Attached Bacteria in Offshore Western Mediterranean Waters as Depicted by Analysis of Genes Encoding 16S rRNA. *Appl Environ Microbiol* **65**: 514-522.
- Agogué H, Lamy D, Neal PR, Sogin ML, Herndl GJ (2011). Water mass-specificity of bacterial communities in the North Atlantic revealed by massively parallel sequencing. *Molecular Ecology* **20**: 258-274.
- Alderkamp A-C, Van Rijssel M, Bolhuis H (2007). Characterization of marine bacteria and the activity of their enzyme systems involved in degradation of the algal storage glucan laminarin. *FEMS Microbiology Ecology* **59**: 108-117.
- Allredge AL, Passow U, Logan BE (1993). The abundance and significance of a class of large, transparent organic particles in the ocean. *Deep Sea Research Part I: Oceanographic Research Papers* **40**: 1131-1140.
- Allen LZ, Allen EE, Badger JH, McCrow JP, Paulsen IT, Elbourne LD *et al* (2012). Influence of nutrients and currents on the genomic composition of microbes across an upwelling mosaic. *The ISME journal* **6**: 1403-1414.

References

- Allers E, Gómez-Consarnau L, Pinhassi J, Gasol JM, Šimek K, Pernthaler J (2007). Response of Alteromonadaceae and Rhodobacteriaceae to glucose and phosphorus manipulation in marine mesocosms. *Environmental Microbiology* **9**: 2417-2429.
- Allison SD (2005). Cheaters, diffusion and nutrients constrain decomposition by microbial enzymes in spatially structured environments. *Ecology Letters* **8**: 626-635.
- Alonso-Sáez L, Díaz-Pérez L, Morán XAG (2015). The hidden seasonality of the rare biosphere in coastal marine bacterioplankton. *Environmental Microbiology* **17**: 3766-3780.
- Aluwihare LI, Repeta DJ (1999). A comparison of the chemical characteristics of oceanic DOM and extracellular DOM produced by marine algae. *Marine Ecology Progress Series* **186**: 105-117.
- Aluwihare LI, Repeta DJ, Chen RF (2002). Chemical composition and cycling of dissolved organic matter in the Mid-Atlantic Bight. *Deep Sea Research Part II: Topical Studies in Oceanography* **49**: 4421-4437.
- Amado AM, Cotner JB, Cory RM, Edhlund BL, McNeill K (2015). Disentangling the Interactions Between Photochemical and Bacterial Degradation of Dissolved Organic Matter: Amino Acids Play a Central Role. *Microbial ecology* **69**: 554-566.
- Amann R, Fuchs BM, Behrens S (2001). The identification of microorganisms by fluorescence in situ hybridisation. *Current Opinion in Biotechnology* **12**: 231-236.
- Anderson TR, Tang KW (2010). Carbon cycling and POC turnover in the mesopelagic zone of the ocean: Insights from a simple model. *Deep Sea Research Part II: Topical Studies in Oceanography* **57**: 1581-1592.
- Anderson TR, Christian JR, Flynn KJ (2015). Chapter 15 - Modeling DOM Biogeochemistry A2 - Hansell, Dennis A. In: Carlson CA (ed). *Biogeochemistry of Marine Dissolved Organic Matter (Second Edition)*. Academic Press: Boston. pp 635-667.
- Antranikian G, Vorgias CE, Bertoldo C (2005). Extreme Environments as a Resource for Microorganisms and Novel Biocatalysts. In: Ulber R, Le Gal Y (eds). *Marine Biotechnology I*. Springer Berlin Heidelberg: Berlin, Heidelberg. pp 219-262.
- Arnosti C (2003). Fluorescent derivatization of polysaccharides and carbohydrate-containing biopolymers for measurement of enzyme activities in complex media. *Journal of Chromatography B* **793**: 181-191.
- Arnosti C (2004). Speed bumps and barricades in the carbon cycle: substrate structural effects on carbon cycling. *Marine Chemistry* **92**: 263-273.

References

- Arnosti C (2011). Microbial extracellular enzymes and the marine carbon cycle. *Annual Review of Marine Science* **3**: 401-425.
- Arnosti C, Steen AD, Ziervogel K, Ghobrial S, Jeffrey WH (2011). Latitudinal Gradients in Degradation of Marine Dissolved Organic Carbon. *PLoS ONE* **6**: e28900.
- Arnosti C, Fuchs BM, Amann R, Passow U (2012). Contrasting extracellular enzyme activities of particle-associated bacteria from distinct provinces of the North Atlantic Ocean. *Frontiers in microbiology* **3**: 425.
- Azam F, Fenchel T, Field JG, Gray J, Meyer-Reil L, Thingstad F (1983). The ecological role of water-column microbes in the sea. *Estuaries* **50**: 2.
- Azam F (1998). Microbial control of oceanic carbon flux: the plot thickens. *Science* **280**: 694-695.
- Azam F, Malfatti F (2007). Microbial structuring of marine ecosystems. *Nature Reviews Microbiology* **5**: 782-791.
- Baker BJ, Banfield JF (2003). Microbial communities in acid mine drainage. *FEMS Microbiology Ecology* **44**: 139-152.
- Baldwin AJ, Moss JA, Pakulski JD, Catala P, Joux F, Jeffrey WH (2005). Microbial diversity in a Pacific Ocean transect from the Arctic to Antarctic circles. *Aquat Microb Ecol* **41**: 91-102.
- Bauer M, Kube M, Teeling H, Richter M, Lombardot T, Allers E *et al* (2006). Whole genome analysis of the marine Bacteroidetes ‘Gramella forsetii’ reveals adaptations to degradation of polymeric organic matter. *Environmental Microbiology* **8**: 2201-2213.
- Becker S, Scheffel A, Polz MF, Hehemann J-H (2017). Accurate quantification of laminarin in marine organic matter with enzymes from marine microbes. *Appl Environ Microbiol*: 03389.
- Behrenfeld MJ, Falkowski PG (1997). Photosynthetic rates derived from satellite-based chlorophyll concentration. *Limnol Oceanogr* **42**: 1-20.
- Behrens S, Lösekann T, Pett-Ridge J, Weber PK, Ng W-O, Stevenson BS *et al* (2008). Linking Microbial Phylogeny to Metabolic Activity at the Single-Cell Level by Using Enhanced Element Labeling-Catalyzed Reporter Deposition Fluorescence In Situ Hybridization (EL-FISH) and NanoSIMS. *Appl Environ Microbiol* **74**: 3143-3150.

References

- Béjà O, Aravind L, Koonin EV, Suzuki MT, Hadd A, Nguyen LP *et al* (2000). Bacterial Rhodopsin: Evidence for a New Type of Phototrophy in the Sea. *Science* **289**: 1902-1906.
- Bengtsson MM, Øvreås L (2010). Planctomycetes dominate biofilms on surfaces of the kelp *Laminaria hyperborea*. *BMC Microbiology* **10**: 261.
- Benner R, Pakulski JD, Mc Carthy M, Hedges JI, Hatcher PG (1992). Bulk Chemical Characteristics of Dissolved Organic Matter in the Ocean. *Science* **255**: 1561-1564.
- Bennke CM, Neu TR, Fuchs BM, Amann R (2013). Mapping glycoconjugate-mediated interactions of marine Bacteroidetes with diatoms. *Systematic and Applied Microbiology* **36**: 417-425.
- Bennke CM, Reintjes G, Schattenhofer M, Ellrott A, Wulf J, Zeder M *et al* (2016). Modification of a high- throughput automatic microbial cell enumeration system for ship board analyses. *Appl Environ Microbiol* **82**: 3289-3296.
- Berlemont R, Martiny AC (2016). Glycoside Hydrolases across Environmental Microbial Communities. *PLOS Computational Biology* **12**: e1005300.
- Biddanda B, Benner R (1997). Carbon, nitrogen, and carbohydrate fluxes during the production of particulate and dissolved organic matter by marine phytoplankton. *Limnol Oceanogr* **42**: 506-518.
- Biers EJ, Sun S, Howard EC (2009). Prokaryotic Genomes and Diversity in Surface Ocean Waters: Interrogating the Global Ocean Sampling Metagenome. *Appl Environ Microbiol* **75**: 2221-2229.
- Biersmith A, Benner R (1998). Carbohydrates in phytoplankton and freshly produced dissolved organic matter. *Marine Chemistry* **63**: 131-144.
- Bjursell MK, Martens EC, Gordon JI (2006). Functional genomic and metabolic studies of the adaptations of a prominent adult human gut symbiont, bacteroides thetaiotaomicron, to the suckling period. *Journal of biological chemistry* **281**: 36269-36279.
- Bondoso J, Godoy-Vitorino F, Balagué V, Gasol JM, Harder J, Lage OM (2017). Epiphytic Planctomycetes communities associated with three main groups of macroalgae. *FEMS Microbiology Ecology* **fiw255**.
- Bray JR, Curtis JT (1957). An Ordination of the Upland Forest Communities of Southern Wisconsin. *Ecological Monographs* **27**: 325-349.

References

- Broecker WS (1997). Thermohaline Circulation, the Achilles Heel of Our Climate System: Will Man-Made CO₂ Upset the Current Balance? *Science* **278**: 1582-1588.
- Brown MV, Ostrowski M, Grzymski JJ, Lauro FM (2014). A trait based perspective on the biogeography of common and abundant marine bacterioplankton clades. *Marine Genomics* **15**: 17-28.
- Buchan A, LeClerc GR, Gulvik CA, Gonzalez JM (2014). Master recyclers: features and functions of bacteria associated with phytoplankton blooms. *Nature Reviews Microbiology* **12**: 686-698.
- Bunse C, Pinhassi J (2016). Marine Bacterioplankton Seasonal Succession Dynamics. *Trends in Microbiology*: In Press.
- Calvo-Díaz A, Díaz-Pérez L, Suárez LÁ, Morán XAG, Teira E, Maraño E (2011). Decrease in the Autotrophic-to-Heterotrophic Biomass Ratio of Picoplankton in Oligotrophic Marine Waters Due to Bottle Enclosure. *Appl Environ Microbiol* **77**: 5739-5746.
- Cameron EA, Kwiatkowski KJ, Lee B-H, Hamaker BR, Koropatkin NM, Martens EC (2014). Multifunctional Nutrient-Binding Proteins Adapt Human Symbiotic Bacteria for Glycan Competition in the Gut by Separately Promoting Enhanced Sensing and Catalysis. *mBio* **5**.
- Campbell BJ, Yu L, Heidelberg JF, Kirchman DL (2011). Activity of abundant and rare bacteria in a coastal ocean. *Proceedings of the National Academy of Sciences* **108**: 12776-12781.
- Canfield DE, Stewart FJ, Thamdrup B, De Brabandere L, Dalsgaard T, Delong EF *et al* (2010). A Cryptic Sulfur Cycle in Oxygen-Minimum-Zone Waters off the Chilean Coast. *Science* **330**: 1375-1378.
- Chitsaz H, Yee-Greenbaum JL, Tesler G, Lombardo M-J, Dupont CL, Badger JH *et al* (2011). De novo assembly of bacterial genomes from single cells. *Nature biotechnology* **29**: 915-921.
- Cho BC, Azam F (1988). Major role of bacteria in biogeochemical fluxes in the ocean's interior. *Nature* **332**: 441-443.
- Cho I, Blaser MJ (2012). The human microbiome: at the interface of health and disease. *Nature Review Genetics* **13**: 260-270.

References

- Chróst RJ (1992). Significance of bacterial ectoenzymes in aquatic environments. *Hydrobiologia* **243**: 61-70.
- Ciais P, Sabine C, Bala G, Bopp L, Brovkin V, Canadell J *et al* (2013). Carbon and other biogeochemical cycles. *Climate change 2013: The Physical Science Basis. Contribution of Working Group I to the Fifth Assessment Report of the Intergovernmental Panel on Climate Change* Cambridge University Press: Cambridge, United Kingdom and New York, NY, USA. pp 465-570.
- Ciais P, Sabine C, Bala G, Bopp L, Brovkin V, Canadell J *et al* (2014). Carbon and other biogeochemical cycles. *Climate change 2013: the physical science basis. Contribution of Working Group I to the Fifth Assessment Report of the Intergovernmental Panel on Climate Change*. Cambridge University Press. pp 465-570.
- Cloern JE (1996). Phytoplankton bloom dynamics in coastal ecosystems: a review with some general lessons from sustained investigation of San Francisco Bay, California. *Reviews of Geophysics* **34**: 127-168.
- Cordero OX, Ventouras L-A, DeLong EF, Polz MF (2012). Public good dynamics drive evolution of iron acquisition strategies in natural bacterioplankton populations. *Proceedings of the National Academy of Sciences* **109**: 20059-20064.
- Cram JA, Chow C-ET, Sachdeva R, Needham DM, Parada AE, Steele JA *et al* (2015). Seasonal and interannual variability of the marine bacterioplankton community throughout the water column over ten years. *The ISME Journal* **9**: 563-580.
- Crespo BG, Pommier T, Fernández-Gómez B, Pedrós-Alió C (2013). Taxonomic composition of the particle-attached and free-living bacterial assemblages in the Northwest Mediterranean Sea analyzed by pyrosequencing of the 16S rRNA. *Microbiology Open* **2**: 541-552.
- Cuskin F, Lowe EC, Temple MJ, Zhu Y, Cameron EA, Pudlo NA *et al* (2015). Human gut *Bacteroidetes* can utilize yeast mannan through a selfish mechanism. *Nature* **517**: 165-169.
- D'Elia JN, Salyers AA (1996). Effect of regulatory protein levels on utilization of starch by *Bacteroides thetaiotaomicron*. *Journal of Bacteriology* **178**: 7180-7186.
- Dabney J, Meyer M, Pääbo S (2013). Ancient DNA Damage. *Cold Spring Harbor Perspectives in Biology* **5**: a012567.
- Dang H, Lovell CR (2000). Bacterial Primary Colonization and Early Succession on Surfaces in Marine Waters as Determined by Amplified rRNA Gene Restriction

References

- Analysis and Sequence Analysis of 16S rRNA Genes. *Appl Environ Microbiol* **66**: 467-475.
- Datta MS, Sliwerska E, Gore J, Polz MF, Cordero OX (2016). Microbial interactions lead to rapid micro-scale successions on model marine particles. *Nature Communications* **7**: 11965.
- De Vargas C, Audic S, Henry N, Decelle J, Mahé F, Logares R *et al* (2015). Eukaryotic plankton diversity in the sunlit ocean. *Science* **348**: 1261605.
- Decad GM, Nikaido H (1976). Outer membrane of gram-negative bacteria. XII. Molecular-sieving function of cell wall. *Journal of Bacteriology* **128**: 325-336.
- DeLong EF, Preston CM, Mincer T, Rich V, Hallam SJ, Frigaard N-U *et al* (2006). Community Genomics Among Stratified Microbial Assemblages in the Ocean's Interior. *Science* **311**: 496-503.
- DeLong EF (2009). The microbial ocean from genomes to biomes. *Nature* **459**: 200-206.
- Driskill LE, Bauer MW, Kelly RM (1999). Synergistic interactions among β -laminarinase, β -1, 4-glucanase, and β -glucosidase from the hyperthermophilic archaeon *Pyrococcus furiosus* during hydrolysis of β -1, 4-, β -1, 3-, and mixed-linked polysaccharides. *Biotechnology and bioengineering* **66**: 51-60.
- Ducklow HW (1999). The bacterial component of the oceanic euphotic zone. *FEMS Microbiology Ecology* **30**: 1-10.
- Dumitriu S (2010). *Polysaccharides: structural diversity and functional versatility*. CRC Press.
- Dupont CL, Rusch DB, Yooseph S, Lombardo M-J, Alexander Richter R, Valas R *et al* (2012). Genomic insights to SAR86, an abundant and uncultivated marine bacterial lineage. *The ISME Journal* **6**: 1186-1199.
- El-Swaiss H, Dunn KA, Bielawski JP, Li WKW, Walsh DA (2014). Seasonal assemblages and short-lived blooms in coastal northwest Atlantic Ocean bacterioplankton. *Environmental Microbiology* **17**: 3642-3661.
- Elifantz H, Malmstrom RR, Cottrell MT, Kirchman DL (2005). Assimilation of Polysaccharides and Glucose by Major Bacterial Groups in the Delaware Estuary. *Appl Environ Microbiol* **71**: 7799-7805.

References

- Elifantz H, Dittel AI, Cottrell MT, Kirchman DL (2007). Dissolved organic matter assimilation by heterotrophic bacterial groups in the western Arctic Ocean. *Aquat Microb Ecol* **50**: 39-49.
- Emerson S, Hedges J (2008). *Chemical oceanography and the marine carbon cycle*. Cambridge University Press.
- Falkowski P, Scholes RJ, Boyle E, Canadell J, Canfield D, Elser J *et al* (2000). The Global Carbon Cycle: A Test of Our Knowledge of Earth as a System. *Science* **290**: 291-296.
- Faust K, Lahti L, Gonze D, de Vos WM, Raes J (2015). Metagenomics meets time series analysis: unraveling microbial community dynamics. *Current Opinion in Microbiology* **25**: 56-66.
- Fernández-Gómez B, Richter M, Schuler M, Pinhassi J, Acinas SG, González JM *et al* (2013). Ecology of marine Bacteroidetes: a comparative genomics approach. *The ISME Journal* **7**: 1026-1037.
- Field CB, Behrenfeld MJ, Randerson JT, Falkowski P (1998). Primary Production of the Biosphere: Integrating Terrestrial and Oceanic Components. *Science* **281**: 237-240.
- Finkel ZV (2014). Marine Net Primary Production. In: Freedman B (ed). *Global Environmental Change*. Springer Netherlands: Dordrecht. pp 117-124.
- Flombaum P, Gallegos JL, Gordillo RA, Rincón J, Zabala LL, Jiao N *et al* (2013). Present and future global distributions of the marine Cyanobacteria *Prochlorococcus* and *Synechococcus*. *Proceedings of the National Academy of Sciences* **110**: 9824-9829.
- Foley MH, Cockburn DW, Koropatkin NM (2016). The Sus operon: a model system for starch uptake by the human gut Bacteroidetes. *Cellular and Molecular Life Sciences* **73**: 2603-2617.
- Follett CL, Repeta DJ, Rothman DH, Xu L, Santinelli C (2014). Hidden cycle of dissolved organic carbon in the deep ocean. *Proceedings of the National Academy of Sciences* **111**: 16706-16711.
- Franzosa EA, Hsu T, Sirota-Madi A, Shafquat A, Abu-Ali G, Morgan XC *et al* (2015). Sequencing and beyond: integrating molecular 'omics' for microbial community profiling. *Nature Reviews Microbiology* **13**: 360-372.

References

- Friedline CJ, Franklin RB, McCallister SL, Rivera MC (2012). Bacterial assemblages of the eastern Atlantic Ocean reveal both vertical and latitudinal biogeographic signatures. *Biogeosciences* **9**: 2177-2193.
- Fuerst JA, Sagulenko E (2011). Beyond the bacterium: *planctomycetes* challenge our concepts of microbial structure and function. *Nature Reviews Microbiology* **9**: 403-413.
- Fuhrman JA, Comeau DE, Hagström Å, Chan AM (1988). Extraction from Natural Planktonic Microorganisms of DNA Suitable for Molecular Biological Studies. *Appl Environ Microbiol* **54**: 1426-1429.
- Ganesh S, Parris DJ, DeLong EF, Stewart FJ (2014). Metagenomic analysis of size-fractionated picoplankton in a marine oxygen minimum zone. *The ISME journal* **8**: 187-211.
- Geider RJ, MacIntyre HL, Kana TM (1997). Dynamic model of phytoplankton growth and acclimation: responses of the balanced growth rate and the chlorophyll a:carbon ratio to light, nutrient-limitation and temperature. *Marine Ecology Progress Series* **148**: 187-200.
- Ghai R, Mizuno CM, Picazo A, Camacho A, Rodriguez-Valera F (2013). Metagenomics uncovers a new group of low GC and ultra-small marine Actinobacteria. *Nature Scientific Reports* **3**: 2471.
- Ghiglione JF, Mevel G, Pujo-Pay M, Mousseau L, Lebaron P, Goutx M (2007). Diel and Seasonal Variations in Abundance, Activity, and Community Structure of Particle-Attached and Free-Living Bacteria in NW Mediterranean Sea. *Microbial Ecology* **54**: 217-231.
- Gilbert JA, Field D, Swift P, Thomas S, Cummings D, Temperton B *et al* (2010). The Taxonomic and Functional Diversity of Microbes at a Temperate Coastal Site: A 'Multi-Omic' Study of Seasonal and Diel Temporal Variation. *PLoS ONE* **5**: e15545.
- Giovannoni SJ, Bibbs L, Cho J-C, Stapels MD, Desiderio R, Vergin KL *et al* (2005). Proteorhodopsin in the ubiquitous marine bacterium SAR11. *Nature* **438**: 82-85.
- Giovannoni SJ, Stingl U (2005). Molecular diversity and ecology of microbial plankton. *Nature* **437**: 343-348.
- Giovannoni SJ, Vergin KL (2012). Seasonality in Ocean Microbial Communities. *Science* **335**: 671-676.

References

- Glenwright AJ, Pothula KR, Bhamidimarri SP, Chorev DS, Baslé A, Firbank SJ *et al* (2017). Structural basis for nutrient acquisition by dominant members of the human gut microbiota. *Nature* **541**: 407-411.
- Glöckner FO, Kube M, Bauer M, Teeling H, Lombardot T, Ludwig W *et al* (2003). Complete genome sequence of the marine planctomycete *Pirellula* sp. strain 1. *Proceedings of the National Academy of Sciences* **100**: 8298-8303.
- Gómez-Pereira PR (2010). Marine Bacteroidetes: distribution patterns and role in the degradation of organic matter. PhD thesis.
- Gómez-Pereira PR, Hartmann M, Grob C, Tarran GA, Martin AP, Fuchs BM *et al* (2012a). Comparable light stimulation of organic nutrient uptake by SAR11 and *Prochlorococcus* in the North Atlantic subtropical gyre. *The ISME Journal* **7**: 603-614.
- Gómez-Pereira PR, Schüler M, Fuchs BM, Bennke C, Teeling H, Waldmann J *et al* (2012b). Genomic content of uncultured *Bacteroidetes* from contrasting oceanic provinces in the North Atlantic Ocean. *Environmental Microbiology* **14**: 52-66.
- González JM, Fernández-Gómez B, Fernández-Guerra A, Gómez-Consarnau L, Sánchez O, Coll-Lladó M *et al* (2008). Genome analysis of the proteorhodopsin-containing marine bacterium *Polaribacter* sp. MED152 (Flavobacteria). *Proceedings of the National Academy of Sciences* **105**: 8724-8729.
- Green JL, Bohannan BJM, Whitaker RJ (2008). Microbial Biogeography: From Taxonomy to Traits. *Science* **320**: 1039-1043.
- Grondin JM, Tamura K, Déjean G, Abbott DW, Brumer H (2017). Polysaccharide Utilization Loci: Fuelling microbial communities. *Journal of Bacteriology*: JB-00860.
- Grossart H-P, Simon M (1993). Limnetic macroscopic organic aggregates (lake snow): occurrence, characteristics, and microbial dynamics in Lake Constance. *Limnol Oceanogr* **38**: 532-546.
- Grossart H-P, Riemann L, Azam F (2001). Bacterial motility in the sea and its ecological implications. *Aquat Microb Ecol* **25**: 247-258.
- Grossart H-P (2010). Ecological consequences of bacterioplankton lifestyles: changes in concepts are needed. *Environmental Microbiology Reports* **2**: 706-714.
- Gupta RS, Lorenzini E (2007). Phylogeny and molecular signatures (conserved proteins and indels) that are specific for the Bacteroidetes and Chlorobi species. *BMC Evolutionary Biology* **7**: 71-71.

References

- Hainfeld JF, Powell RD (2000). New Frontiers in Gold Labeling. *Journal of Histochemistry & Cytochemistry* **48**: 471-480.
- Halm H, Lam P, Ferdelman TG, Lavik G, Dittmar T, LaRoche J *et al* (2012). Heterotrophic organisms dominate nitrogen fixation in the South Pacific Gyre. *The ISME Journal* **6**: 1238-1249.
- Hammes F, Vital M, Egli T (2010). Critical Evaluation of the Volumetric “Bottle Effect” on Microbial Batch Growth. *Appl Environ Microbiol* **76**: 1278-1281.
- Hansel C (2017). Small but mighty: how minor components drive major biogeochemical cycles. *Environmental Microbiology Reports* **9**: 8-10.
- Hansell DA, Carlson CA (1998). Net community production of dissolved organic carbon. *Global Biogeochemical Cycles* **12**: 443-453.
- Hansell DA (2013). Recalcitrant dissolved organic carbon fractions. *Annual Review of Marine Science* **5**: 421-445.
- Hanson CA, Fuhrman JA, Horner-Devine MC, Martiny JBH (2012). Beyond biogeographic patterns: processes shaping the microbial landscape. *Nature Reviews Microbiology* **10**: 497-506.
- He W, Chen M, Schlautman MA, Hur J (2016). Dynamic exchanges between DOM and POM pools in coastal and inland aquatic ecosystems: A review. *Science of The Total Environment* **551–552**: 415-428.
- Head SR, Komori HK, LaMere SA, Whisenant T, Van Nieuwerburgh F, Salomon DR *et al* (2014). Library construction for next-generation sequencing: Overviews and challenges. *BioTechniques* **56**: 61-68.
- Hecky RE, Mopper K, Kilham P, Degens ET (1973). The amino acid and sugar composition of diatom cell-walls. *Mar Biol* **19**: 323-331.
- Hedges JI (1992). Global biogeochemical cycles: progress and problems. *Marine Chemistry* **39**: 67-93.
- Helbert W (2017). Marine Polysaccharide sulfatases. *Frontiers in Marine Science* **4**.
- Hewson I, Steele JA, Capone DG, Fuhrman JA (2006). Remarkable heterogeneity in meso- and bathypelagic bacterioplankton assemblage composition. *Limnol Oceanogr* **51**: 1274-1283.

References

- Hollibaugh JT, Wong PS, Murrell MCM (2000). Similarity of particle-associated and free-living bacterial communities in northern san francisco bay, california. *Aquat Microb Ecol* **21**: 103-114.
- Howarth RW (1988). Nutrient Limitation of Net Primary Production in Marine Ecosystems. *Annual Review of Ecology and Systematics* **19**: 89-110.
- Huston AL, Deming JW (2002). Relationships between microbial extracellular enzymatic activity and suspended and sinking particulate organic matter: seasonal transformations in the North Water. *Deep Sea Research Part II: Topical Studies in Oceanography* **49**: 5211-5225.
- Ishizaka J, Takahashi M, Ichimura S (1983). Evaluation of coastal upwelling effects on phytoplankton growth by simulated culture experiments. *Mar Biol* **76**: 271-278.
- Iverson V, Morris RM, Frazar CD, Berthiaume CT, Morales RL, Armbrust EV (2012). Untangling Genomes from Metagenomes: Revealing an Uncultured Class of Marine Euryarchaeota. *Science* **335**: 587-590.
- Jiao N, Herndl GJ, Hansell DA, Benner R, Kattner G, Wilhelm SW *et al* (2010). Microbial production of recalcitrant dissolved organic matter: long-term carbon storage in the global ocean. *Nature Reviews Microbiology* **8**: 593-599.
- Jiao N, Zheng Q (2011). The Microbial Carbon Pump: from Genes to Ecosystems. *Appl Environ Microbiol* **77**: 7439-7444.
- Juggins S (2016-07-13). Rioja: Analysis of Quaternary Science Data. In: Juggins S (ed), 0.9-9 edn: Cran. pp Functions for the analysis of Quaternary science data, including constrained clustering, WA, WAPLS, IKFA, MLRC and MAT transfer functions, and stratigraphic diagrams.
- Kabisch A, Otto A, König S, Becher D, Albrecht D, Schüler M *et al* (2014). Functional characterization of polysaccharide utilization loci in the marine Bacteroidetes ‘*Gramella forsetii*’ KT0803. *The ISME Journal* **8**: 1492-1502.
- Kaiser C, Franklin O, Richter A, Dieckmann U (2015). Social dynamics within decomposer communities lead to nitrogen retention and organic matter build-up in soils. *Nature Communications* **6**: 8960.
- Karunatilaka KS, Cameron EA, Martens EC, Koropatkin NM, Biteen JS (2014). Superresolution Imaging Captures Carbohydrate Utilization Dynamics in Human Gut Symbionts. *mBio* **5**: e02172.

References

- Kellogg CTE, Deming JW (2014). Particle-associated extracellular enzyme activity and bacterial community composition across the Canadian Arctic Ocean. *FEMS Microbiology Ecology* **89**: 360-375.
- KerheRvé P, Charrière B, Gadel F (1995). Determination of marine monosaccharides by high-pH anion-exchange chromatography with pulsed amperometric detection. *Journal of Chromatography A* **718**: 283-289.
- Kjørboe T, Andersen KP, Dam HG (1990). Coagulation efficiency and aggregate formation in marine phytoplankton. *Mar Biol* **107**: 235-245.
- Kjørboe T, Grossart H-P, Ploug H, Tang K (2002). Mechanisms and Rates of Bacterial Colonization of Sinking Aggregates. *Appl Environ Microbiol* **68**: 3996-4006.
- Kjørboe T, Tang K, Grossart H-P, Ploug H (2003). Dynamics of Microbial Communities on Marine Snow Aggregates: Colonization, Growth, Detachment, and Grazing Mortality of Attached Bacteria. *Appl Environ Microbiol* **69**: 3036-3047.
- Kirchman DL, Meon B, Ducklow HW, Carlson CA, Hansell DA, Steward GF (2001). Glucose fluxes and concentrations of dissolved combined neutral sugars (polysaccharides) in the Ross Sea and Polar Front Zone, Antarctica. *Deep Sea Research Part II: Topical Studies in Oceanography* **48**: 4179-4197.
- Klindworth A, Pruesse E, Schweer T, Peplies J, Quast C, Horn M *et al* (2013). Evaluation of general 16S ribosomal RNA gene PCR primers for classical and next-generation sequencing-based diversity studies. *Nucleic Acids Research* **41**: e1.
- Koebnik R, Locher KP, Van Gelder P (2000). Structure and function of bacterial outer membrane proteins: barrels in a nutshell. *Molecular Microbiology* **37**: 239-253.
- Lage OM, Bondoso J (2014). Planctomycetes and macroalgae, a striking association. *Frontiers in microbiology* **5**: 133.
- Lam P, Lavik G, Jensen MM, van de Vossenberg J, Schmid M, Woebken D *et al* (2009). Revising the nitrogen cycle in the Peruvian oxygen minimum zone. *Proceedings of the National Academy of Sciences* **106**: 4752-4757.
- Landa M, Blain S, Christaki U, Monchy S, Obernosterer I (2016). Shifts in bacterial community composition associated with increased carbon cycling in a mosaic of phytoplankton blooms. *The ISME Journal* **10**: 39-50.

References

- Lee S, Fuhrman JA (1991). Species composition shift of confined bacterioplankton studies at the level of community DNA. *Marine ecology progress series* **79**: 195-201.
- Legendre L, Rivkin RB, Weinbauer M, Guidi L, Uitz J (2015). The microbial carbon pump concept: Potential biogeochemical significance in the globally changing ocean. *Progress in Oceanography* **134**: 432-450.
- Letscher RT, Knapp AN, James AK, Carlson CA, Santoro AE, Hansell DA (2015). Microbial community composition and nitrogen availability influence DOC remineralization in the South Pacific Gyre. *Marine Chemistry* **177**: 325-334.
- Levin PA, Angert ER (2015). Small but Mighty: Cell Size and Bacteria. *Cold Spring Harbor Perspectives in Biology* **7**: a019216.
- Li D-Q, Zhou Y-X, Liu T, Chen G-J, Du Z-J (2015). *Catenovulum maritimus* sp. nov., a novel agarolytic gammaproteobacterium isolated from the marine alga *Porphyra yezoensis* Ueda (AST58-103), and emended description of the genus *Catenovulum*. *Antonie van Leeuwenhoek* **108**: 427-434.
- Litchfield CD (1998). Survival strategies for microorganisms in hypersaline environments and their relevance to life on early Mars. *Meteoritics & Planetary Science* **33**: 813-819.
- Logan BE, Passow U, Alldredge AL, Grossart H-P, Simont M (1995). Rapid formation and sedimentation of large aggregates is predictable from coagulation rates (half-lives) of transparent exopolymer particles (TEP). *Deep Sea Research Part II: Topical Studies in Oceanography* **42**: 203-214.
- Lombard V, Golaconda Ramulu H, Drula E, Coutinho PM, Henrissat B (2014). The carbohydrate-active enzymes database (CAZy) in 2013. *Nucleic Acids Research* **42**: D490-D495.
- Longhurst AR (2007). Chapter 9 - The Atlantic Ocean. *Ecological Geography of the Sea (Second Edition)*. Academic Press: Burlington. pp 131-273.
- López-Pérez M, Kimes NE, Haro-Moreno JM, Rodriguez-Valera F (2016). Not All Particles Are Equal: The Selective Enrichment of Particle-Associated Bacteria from the Mediterranean Sea. *Frontiers in Microbiology* **7**: 996.
- Luca P, Sevrine S, Darren C, Aditee M, J Icarus A (2016). Biological or microbial carbon pump? The role of phytoplankton stoichiometry in ocean carbon sequestration. *Journal of Plankton Research*: 1-7

References

- Luo H, Moran MA (2015). How do divergent ecological strategies emerge among marine bacterioplankton lineages? *Trends in Microbiology* **23**: 577-584.
- Lyons M, Dobbs F (2012). Differential utilization of carbon substrates by aggregate-associated and water-associated heterotrophic bacterial communities. *Hydrobiologia* **686**: 181-193.
- Maier-Reimer E, Hasselmann K (1987). Transport and storage of CO₂ in the ocean—an inorganic ocean-circulation carbon cycle model. *Climate Dynamics* **2**: 63-90.
- Malmstrom RR, Rodrigue S, Huang KH, Kelly L, Kern SE, Thompson A *et al* (2013). Ecology of uncultured Prochlorococcus clades revealed through single-cell genomics and biogeographic analysis. *The ISME Journal* **7**: 184-198.
- Marañón E, Holligan PM, Varela M, Mouriño B, Bale AJ (2000). Basin-scale variability of phytoplankton biomass, production and growth in the Atlantic Ocean. *Deep Sea Research Part I: Oceanographic Research Papers* **47**: 825-857.
- Mardis ER (2008). The impact of next-generation sequencing technology on genetics. *Trends in Genetics* **24**: 133-141.
- Mardis ER (2013). Next-Generation Sequencing Platforms. *Annual Review of Analytical Chemistry* **6**: 287-303.
- Martens EC, Koropatkin NM, Smith TJ, Gordon JI (2009). Complex glycan catabolism by the human gut microbiota: the Bacteroidetes Sus-like paradigm. *Journal of Biological Chemistry* **284**: 24673-24677.
- Martens EC, Kelly AG, Tauzin AS, Brumer H (2014). The devil lies in the details: How variations in polysaccharide fine-structure impact the physiology and evolution of gut microbes. *Journal of Molecular Biology* **426**: 3851-3865.
- Martin W, Baross J, Kelley D, Russell MJ (2008). Hydrothermal vents and the origin of life. *Nat Rev Micro* **6**: 805-814.
- Martiny JBH, Bohannan BJ, Brown JH, Colwell RK, Fuhrman JA, Green JL *et al* (2006). Microbial biogeography: putting microorganisms on the map. *Nature Reviews Microbiology* **4**: 102-112.
- Massana R, PedrósttAlió C, Casamayor EO, Gasol JM (2001). Changes in marine bacterioplankton phylogenetic composition during incubations designed to measure biogeochemically significant parameters. *Limnol Oceanogr* **46**: 1181-1188.

References

- McCarren J, Becker JW, Repeta DJ, Shi Y, Young CR, Malmstrom RR *et al* (2010). Microbial community transcriptomes reveal microbes and metabolic pathways associated with dissolved organic matter turnover in the sea. *Proceedings of the National Academy of Sciences* **107**: 16420-16427.
- McCarter L (1999). The multiple identities of *Vibrio parahaemolyticus*. *Journal of molecular microbiology and biotechnology* **1**: 51-57.
- McCarthy M, Hedges J, Benner R (1996). Major biochemical composition of dissolved high molecular weight organic matter in seawater. *Marine Chemistry* **55**: 281-297.
- Mestre M, Borrull E, Sala M, Gasol JM (2017). Patterns of bacterial diversity in the marine planktonic particulate matter continuum. *The ISME Journal* **11**: 999-1010.
- Milici M, Vital M, Tomasch J, Badewien TH, Giebel H-A, Plumeier I *et al* (2017). Diversity and community composition of particle-associated and free-living bacteria in mesopelagic and bathypelagic Southern Ocean water masses: Evidence of dispersal limitation in the Bransfield Strait. *Limnol Oceanogr*: In Press.
- Millero FJ (1996). *Chemical Oceanography, Fourth Edition*. CRC Press.
- Molloy S (2012). Marine microbiology: SAR86: streamlined for success. *Nature Reviews Microbiology* **10**: 82-83.
- Montesano-Roditis L, Glitz DG, Traut RR, Stewart PL (2001). Cryo-electron Microscopic Localization of Protein L7/L12 within the Escherichia coli 70 S Ribosome by Difference Mapping and Nanogold Labeling. *Journal of Biological Chemistry* **276**: 14117-14123.
- Moore LR, Rocap G, Chisholm SW (1998). Physiology and molecular phylogeny of coexisting *Prochlorococcus* ecotypes. *Nature* **393**: 464-467.
- Moran MA, Kujawinski EB, Stubbins A, Fatland R, Aluwihare LI, Buchan A *et al* (2016). Deciphering ocean carbon in a changing world. *Proceedings of the National Academy of Sciences* **113**: 3143-3151.
- Morel A, Gentili B, Claustre H, Babin M, Bricaud A, Ras J *et al* (2007). Optical properties of the “clearest” natural waters. *Limnol Oceanogr* **52**: 217-229.
- Morris JJ, Lenski RE, Zinser ER (2012). The black queen hypothesis: Evolution of dependencies through adaptive gene loss. *mBio* **3**: e00036.

References

- Morris RM, Rappé MS, Connon SA, Vergin KL, Siebold WA, Carlson CA *et al* (2002). SAR 11 clade dominates ocean surface bacterioplankton communities. *Nature* **420**: 806-810.
- Morris RM, Rappé MS, Urbach E, Connon SA, Giovannoni SJ (2004). Prevalence of the Chloroflexi-Related SAR202 Bacterioplankton Cluster throughout the Mesopelagic Zone and Deep Ocean. *Appl Environ Microbiol* **70**: 2836-2842.
- Musat N, Foster R, Vagner T, Adam B, Kuypers MM (2012). Detecting metabolic activities in single cells, with emphasis on nanoSIMS. *Fems Microbiol Rev* **36**: 486-511.
- Mykkestad SM (1995). Release of extracellular products by phytoplankton with special emphasis on polysaccharides. *Science of The Total Environment* **165**: 155-164.
- Ndeh D, Rogowski A, Cartmell A, Luis AS, Baslé A, Gray J *et al* (2017). Complex pectin metabolism by gut bacteria reveals novel catalytic functions. *Nature*: In Press.
- Neugebauer H, Herrmann C, Kammer W, Schwarz G, Nordheim A, Braun V (2005). ExbBD-Dependent Transport of Maltodextrins through the Novel MalA Protein across the Outer Membrane of *Caulobacter crescentus*. *Journal of Bacteriology* **187**: 8300-8311.
- Neumann AM, Balmonte JP, Berger M, Giebel H-A, Arnosti C, Voget S *et al* (2015). Different utilization of alginate and other algal polysaccharides by marine *Alteromonas macleodii* ecotypes. *Environmental Microbiology* **17**: 3858-3868.
- Novelli G, Predazzi I, Mango R, Romeo F, Mehta J (2010). Role of genomics in cardiovascular medicine. *World Journal of Cardiology* **2(12)**: 428-436.
- Ocean Biology Processing Group (2014). Moderate-resolution Imaging Spectroradiometer (MODIS) Terra Ocean Color Data. NASA Goddard Space Flight Center, Ocean Ecology Laboratory: NASA OB.DAAC, Greenbelt, MD, USA.
- Oksanen J, Blanchet FG, Kindt R, Legendre P, Minchin PR, O'Hara RB *et al* (2013). vegan: Community Ecology Package. R package version 2.0-10.
- Osterholz H, Niggemann J, Giebel H-A, Simon M, Dittmar T (2015). Inefficient microbial production of refractory dissolved organic matter in the ocean. *Nature Communications* **6**: 7422.
- Pace NR (1997). A Molecular View of Microbial Diversity and the Biosphere. *Science* **276**: 734-740.

References

- Padilla CC, Ganesh S, Gantt S, Huhman A, Parris DJ, Sarode N *et al* (2015). Standard filtration practices may significantly distort planktonic microbial diversity estimates. *Frontiers in Microbiology* **6**: 547.
- Pakulski JD, Benner R (1994). Abundance and distribution of carbohydrates in the ocean. *Limnol Oceanogr* **39**: 930-940.
- Paparoditis P, Västermark Å, Le AJ, Fuerst JA, Saier Jr MH (2014). Bioinformatic analyses of integral membrane transport proteins encoded within the genome of the planctomycetes species, *Rhodopirellula baltica*. *Biochimica et Biophysica Acta (BBA) - Biomembranes* **1838**: 193-215.
- Partensky F, Hoepffner N, Li W, Ulloa O, Vaultot D (1993). Photoacclimation of *Prochlorococcus* sp. (Prochlorophyta) Strains Isolated from the North Atlantic and the Mediterranean Sea. *Plant Physiology* **101**: 285-296.
- Partensky F, Hess WR, Vaultot D (1999). *Prochlorococcus*, a marine photosynthetic prokaryote of global significance. *Microbiology and Molecular Biology Reviews* **63**: 106-127.
- Pedersen MF, Borum J (1996). Nutrient control of algal growth in estuarine waters. Nutrient limitation and the importance of nitrogen requirements and nitrogen storage among phytoplankton and species of macroalgae. *Marine Ecology Progress Series* **142**: 261-272.
- Pilskaln CH, Lehmann C, Paduan JB, Silver MW (1998). Spatial and temporal dynamics in marine aggregate abundance, sinking rate and flux: Monterey Bay, central California. *Deep Sea Research Part II: Topical Studies in Oceanography* **45**: 1803-1837.
- Pilson MEQ (2012). *An Introduction to the Chemistry of the Sea*. Cambridge University Press: New York, USA.
- Pinti DL (2014). Oxygen-Minimum Zone. In: Amils R, Gargaud M, Cernicharo Quintanilla J, Cleaves HJ, Irvine WM, Pinti D *et al* (eds). *Encyclopedia of Astrobiology*. Springer Berlin Heidelberg: Berlin, Heidelberg. pp 1-2.
- Piontek J, Lunau M, Handel N, Borchard C, Wurst M, Engel A (2010). Acidification increases microbial polysaccharide degradation in the ocean. *Biogeosciences* **7**: 1615-1624.
- Piontek J, Händel N, De Bodt C, Harlay J, Chou L, Engel A (2011). The utilization of polysaccharides by heterotrophic bacterioplankton in the Bay of Biscay (North Atlantic Ocean). *Journal of Plankton Research* **33**: 1719-1735.

References

- Piontek J, Sperling M, Nöthig E-M, Engel A (2014). Regulation of bacterioplankton activity in Fram Strait (Arctic Ocean) during early summer: The role of organic matter supply and temperature. *Journal of Marine Systems* **132**: 83-94.
- Polovina JJ, Howell EA, Abecassis M (2008). Ocean's least productive waters are expanding. *Geophysical Research Letters* **35**.
- Pomeroy LR (1974). The Ocean's Food Web, A Changing Paradigm. *BioScience* **24**: 499-504.
- Props R, Kerckhof F-M, Rubbens P, De Vrieze J, Hernandez Sanabria E, Waegeman W *et al* (2017). Absolute quantification of microbial taxon abundances. *The ISME Journal* **11**: 584-587.
- Prosser JI (2010). Replicate or lie. *Environmental microbiology* **12**: 1806-1810.
- Pruzzo C, Huq A, Colwell RR, Donelli G (2005). Pathogenic Vibrio Species in the Marine and Estuarine Environment. In: Belkin S, Colwell RR (eds). *Oceans and Health: Pathogens in the Marine Environment*. Springer US: Boston, MA. pp 217-252.
- Quast C, Pruesse E, Yilmaz P, Gerken J, Schweer T, Yarza P *et al* (2013). The SILVA ribosomal RNA gene database project: improved data processing and web-based tools. *Nucleic Acids Research* **41**: D590-D596.
- Quince C, Curtis TP, Sloan WT (2008). The rational exploration of microbial diversity. *The ISME Journal* **2**: 997-1006.
- Raimbault P, Garcia N, Cerutti F (2008). Distribution of inorganic and organic nutrients in the South Pacific Ocean − evidence for long-term accumulation of organic matter in nitrogen-depleted waters. *Biogeosciences* **5**: 281-298.
- Rakoff-Nahoum S, Coyne MJ, Comstock LE (2014). An ecological network of polysaccharide utilization among human intestinal symbionts. *Current Biology* **24**: 40-49.
- Rakoff-Nahoum S, Foster KR, Comstock LE (2016). The evolution of cooperation within the gut microbiota. *Nature* **533**: 255-259.
- Rappé MSS, Giovannoni SJ (2003). The Uncultured Microbial Majority. *Annual Review of Microbiology* **57**: 369-394.
- Rappe' MS, Cannon SA, Vergin KL, Giovannoni SJ (2002). Cultivation of the ubiquitous SAR 11 marine bacterioplankton clade. *Nature* **418**: 630-633.

References

- Ras J, Claustre H, Uitz J (2008). Spatial variability of phytoplankton pigment distributions in the Subtropical South Pacific Ocean: comparison between in situ and predicted data. *Biogeosciences* **5**: 353-369.
- Raven JA, Evans MC, Korb RE (1999). The role of trace metals in photosynthetic electron transport in O₂-evolving organisms. *Photosynthesis Research* **60**: 111-150.
- Raven JA, Falkowski PG (1999). Oceanic sinks for atmospheric CO₂. *Plant, Cell & Environment* **22**: 741-755.
- Reeves AR, Wang GR, Salyers AA (1997). Characterization of four outer membrane proteins that play a role in utilization of starch by *Bacteroides thetaiotaomicron*. *Journal of Bacteriology* **179**: 643-649.
- Reintjes G, Arnosti C, Fuchs BM, Amann R (2017). An alternative polysaccharide uptake mechanism of marine bacteria. *The ISME Journal*: In Press.
- Rieck A, Herlemann D, Jürgens K, Grossart H-P (2015). Particle -Associated differ from free-living bacteria in surface waters of the baltic sea *Frontiers in microbiology* **6**.
- Riesenfeld CS, Schloss PD, Handelsman J (2004). Metagenomics: Genomic Analysis of Microbial Communities. *Annual Review of Genetics* **38**: 525-552.
- Rinta-Kanto JM, Sun S, Sharma S, Kiene RP, Moran MA (2012). Bacterial community transcription patterns during a marine phytoplankton bloom. *Environmental Microbiology* **14**: 228-239.
- Robinson C, Williams PJIB (2007). Respiration and its measurement in surface marine waters. In: del Giorgio P, Williams P (eds). *Respiration in Aquatic Ecosystems*. Oxford University Press.
- Rogers TE, Pudlo NA, Koropatkin NM, Bell JSK, Moya Balasch M, Jasker K *et al* (2013). Dynamic responses of *Bacteroides thetaiotaomicron* during growth on glycan mixtures. *Molecular Microbiology* **88**: 876-890.
- Rooney-Varga JN, Giewat MW, Savin MC, Sood S, LeGresley M, Martin J (2005). Links between phytoplankton and bacterial community dynamics in a coastal marine environment. *Microbial ecology* **49**: 163-175.
- Rösel S, Allgaier M, Grossart H-P (2012). Long-Term Characterization of Free-Living and Particle-Associated Bacterial Communities in Lake Tiefwaren Reveals Distinct Seasonal Patterns. *Microbial ecology* **64**: 571-583.

References

- Rusch DB, Halpern AL, Sutton G, Heidelberg KB, Williamson S, Yooseph S *et al* (2007). The Sorcerer II Global Ocean Sampling Expedition: Northwest Atlantic through Eastern Tropical Pacific. *PLOS Biology* **5**: e77.
- Sabine CL, Feely RA, Gruber N, Key RM, Lee K, Bullister JL *et al* (2004). The Oceanic Sink for Anthropogenic CO₂. *Science* **305**: 367-371.
- Sambrotto RN, Niebauer HJ, Goering JJ, Iverson RL (1986). Relationships among vertical mixing, nitrate uptake, and phytoplankton growth during the spring bloom in the southeast Bering Sea middle shelf. *Continental Shelf Research* **5**: 161-198.
- Sarmiento H, Gasol JM (2012). Use of phytoplankton-derived dissolved organic carbon by different types of bacterioplankton. *Environmental Microbiology* **14**: 2348-2360.
- Sarmiento JL, Le Quéré C (1996). Oceanic Carbon Dioxide Uptake in a Model of Century-Scale Global Warming. *Science* **274**: 1346-1350.
- Schattenhofer M, Fuchs BM, Amann R, Zubkov MV, Tarran GA, Pernthaler J (2009). Latitudinal distribution of prokaryotic picoplankton populations in the Atlantic Ocean. *Environmental Microbiology* **11**: 2078-2093.
- Schloss PD, Westcott SL, Ryabin T, Hall JR, Hartmann M, Hollister EB *et al* (2009). Introducing mothur: Open-Source, Platform-Independent, Community-Supported Software for Describing and Comparing Microbial Communities. *Appl Environ Microbiol* **75**: 7537-7541.
- Seymour JR, Marcos, Stocker R (2009). Resource Patch Formation and Exploitation throughout the Marine Microbial Food Web. *The American Naturalist* **173**: E15-E29.
- Shade A, Jones SE, Caporaso JG, Handelsman J, Knight R, Fierer N *et al* (2014). Conditionally Rare Taxa Disproportionately Contribute to Temporal Changes in Microbial Diversity. *mBio* **5**: e01371-01314.
- Shan D, Li X, Gu Z, Wei G, Gao Z, Shao Z (2014). Draft Genome Sequence of the Agar-Degrading Bacterium *Catenovulum* sp. Strain DS-2, Isolated from Intestines of *Halotis diversicolor*. *Genome Announcements* **2**: e00144-00114.
- Sheik CS, Jain S, Dick GJ (2014). Metabolic flexibility of enigmatic SAR324 revealed through metagenomics and metatranscriptomics. *Environmental Microbiology* **16**: 304-317.

References

- Simon HM, Smith MW, Herfort L (2014). Metagenomic insights into particles and their associated microbiota in a coastal margin ecosystem. *Frontiers in microbiology* **5**: 466.
- Simon M, Grossart H-P, Schweitzer B, Ploug H (2002). Microbial ecology of organic aggregates in aquatic ecosystems. *Aquat Microb Ecol* **28**: 175-211.
- Sinsabaugh RS (1994). Enzymic analysis of microbial pattern and process. *Biol Fert Soils* **17**: 69-74.
- Sison-Mangus MP, Jiang S, Kudela RM, Mehic S (2016). Phytoplankton-Associated Bacterial Community Composition and Succession during Toxic Diatom Bloom and Non-Bloom Events. *Frontiers in Microbiology* **7**: 1433.
- Smith M, Zeigler Allen L, Allen A, Herfort L, Simon H (2013). Contrasting genomic properties of free-living and particle-attached microbial assemblages within a coastal ecosystem. *Frontiers in Microbiology* **4**: 120.
- Smith SV (1984). Phosphorus versus nitrogen limitation in the marine-environment *Limnol Oceanogr* **29**: 1149-1160.
- Sogin ML, Morrison HG, Huber JA, Welch DM, Huse SM, Neal PR *et al* (2006). Microbial diversity in the deep sea and the underexplored “rare biosphere”. *Proceedings of the National Academy of Sciences* **103**: 12115-12120.
- Sunagawa S, Coelho LP, Chaffron S, Kultima JR, Labadie K, Salazar G *et al* (2015). Structure and function of the global ocean microbiome. *Science* **348**: 1261359.
- Suzuki S, Kaneko R, Kodama T, Hashihama F, Suwa S, Tanita I *et al* (2017). Comparison of community structures between particle-associated and free-living prokaryotes in tropical and subtropical Pacific Ocean surface waters. *Journal of Oceanography*: 1-13.
- Swan BK, Martinez-Garcia M, Preston CM, Sczyrba A, Woyke T, Lamy D *et al* (2011). Potential for Chemolithoautotrophy Among Ubiquitous Bacteria Lineages in the Dark Ocean. *Science* **333**: 1296-1300.
- Swan BK, Tupper B, Sczyrba A, Lauro FM, Martinez-Garcia M, González JM *et al* (2013). Prevalent genome streamlining and latitudinal divergence of planktonic bacteria in the surface ocean. *Proceedings of the National Academy of Sciences* **110**: 11463-11468.

References

- Tada Y, Taniguchi A, Nagao I, Miki T, Uematsu M, Tsuda A *et al* (2011). Differing growth responses of major phylogenetic groups of marine bacteria to natural phytoplankton blooms in the western North Pacific Ocean. *Appl Environ Microbiol* **77**: 4055-4065.
- Tang JK-H, You L, Blankenship RE, Tang YJ (2012). Recent advances in mapping environmental microbial metabolisms through ^{13}C isotopic fingerprints. *Journal of The Royal Society Interface* **9**: 2767-2780.
- Tarran GA, Heywood JL, Zubkov MV (2006). Latitudinal changes in the standing stocks of nano- and picoeukaryotic phytoplankton in the Atlantic Ocean. *Deep Sea Research Part II: Topical Studies in Oceanography* **53**: 1516-1529.
- Taylor JD, Cunliffe M (2017). Coastal bacterioplankton community response to diatom-derived polysaccharide microgels. *Environmental Microbiology Reports* **9**: 151-157.
- Teeling H, Fuchs BM, Becher D, Klockow C, Gardebrecht A, Bennke CM *et al* (2012). Substrate-controlled succession of marine bacterioplankton populations induced by a phytoplankton bloom. *Science* **336**: 608-611.
- Teeling H, Fuchs BM, Bennke CM, Krüger K, Chafee M, Kappelmann L *et al* (2016). Recurring patterns in bacterioplankton dynamics during coastal spring algae blooms. *eLife* **5**: e11888.
- Teira E, José Pazó M, Serret P, Fernández E (2001). Dissolved organic carbon production by microbial populations in the Atlantic Ocean. *Limnol Oceanogr* **46**: 1370-1377.
- Teira E, Abalde J, Álvarez-Ossorio MT, Bode A, Cariño C, Cid Á *et al* (2003). Plankton carbon budget in a coastal wind-driven upwelling station off A Coruña (NW Iberian Peninsula). *Marine Ecology Progress Series* **265**: 31-43.
- Teira E, Gasol JM, Aranguren-Gassis M, Fernández A, González J, Lekunberri I *et al* (2008). Linkages between bacterioplankton community composition, heterotrophic carbon cycling and environmental conditions in a highly dynamic coastal ecosystem. *Environmental Microbiology* **10**: 906-917.
- Thomas F, Hehemann J-H, Rebuffet E, Czjzek M, Michel G (2011). Environmental and Gut Bacteroidetes: The Food Connection. *Frontiers in Microbiology* **2**: 93.
- Thornton DCO (2014). Dissolved organic matter (DOM) release by phytoplankton in the contemporary and future ocean. *European Journal of Phycology* **49**: 20-46.

References

- Traving SJ, Thygesen UH, Riemann L, Stedmon CA (2015). A model of extracellular enzymes in free-living microbes: which strategy pays off? *Appl Environ Microbiol* **81**: 7385-7393.
- Travisano M, Velicer GJ (2004). Strategies of microbial cheater control. *Trends in Microbiology* **12**: 72-78.
- Tripp HJ (2013). The unique metabolism of SAR11 aquatic bacteria. *Journal of Microbiology* **51**: 147-153.
- Turner JT (2015). Zooplankton fecal pellets, marine snow, phytodetritus and the ocean's biological pump. *Progress in Oceanography* **130**: 205-248.
- van den Burg B (2003). Extremophiles as a source for novel enzymes. *Current Opinion in Microbiology* **6**: 213-218.
- Van Dongen-Vogels V, Seymour JR, Middleton JF, Mitchell JG, Seuront L (2012). Shifts in picophytoplankton community structure influenced by changing upwelling conditions. *Estuarine, Coastal and Shelf Science* **109**: 81-90.
- Van Wambeke F, Obernosterer I, Moutin T, Duhamel S, Ulloa O, Claustre H (2008). Heterotrophic bacterial production in the eastern South Pacific: longitudinal trends and coupling with primary production. *Biogeosciences* **5**: 157-169.
- Vaulot D, Marie D, Olson RJ, Chisholm SW (1995). Growth of *Prochlorococcus*, a photosynthetic prokaryote, in the equatorial Pacific Ocean. *Science* **268**: 1480.
- Venter JC, Remington K, Heidelberg JF, Halpern AL, Rusch D, Eisen JA *et al* (2004). Environmental Genome Shotgun Sequencing of the Sargasso Sea. *Science* **304**: 66-74.
- Vetter YA, Deming JW, Jumars PA, Krieger-Brockett BB (1998). A Predictive Model of Bacterial Foraging by Means of Freely Released Extracellular Enzymes. *Microbial ecology* **36**: 75-92.
- Volk T, Hoffert MI (1985). *Ocean carbon pumps: analysis of relative strengths and efficiencies in ocean-driven atmospheric CO₂ changes*. American Geophysical Union; Geophysical Monograph 32.
- Wagner M, Haider S (2012). New trends in fluorescence in situ hybridization for identification and functional analyses of microbes. *Current Opinion in Biotechnology* **23**: 96-102.

References

- Walsh EA, Smith DC, Sogin ML, D'Hondt S (2015). Bacterial and archaeal biogeography of the deep chlorophyll maximum in the South Pacific Gyre. *Aquat Microb Ecol* **75**: 1-13.
- Wegner C-E, Richter-Heitmann T, Klindworth A, Klockow C, Richter M, Achstetter T *et al* (2013). Expression of sulfatases in *Rhodopirellula baltica* and the diversity of sulfatases in the genus *Rhodopirellula*. *Marine Genomics* **9**: 51-61.
- Weiss P, Schweitzer B, Amann R, Simon M (1996). Identification in situ and dynamics of bacteria on limnetic organic aggregates (lake snow). *Appl Environ Microbiol* **62**: 1998-2005.
- Wells ML, Goldberg ED (1991). Occurrence of small colloids in sea water. *Nature* **353**: 342-344.
- Wemheuer B, Wemheuer F, Hollensteiner J, Meyer F-D, Voget S, Daniel R (2015). The green impact: bacterioplankton response towards a phytoplankton spring bloom in the southern North Sea assessed by comparative metagenomic and metatranscriptomic approaches. *Frontiers in Microbiology* **6**: 805.
- West NJ, Schönhuber WA, Fuller NJ, Amann RI, Rippka R, Post AF *et al* (2001). Closely related *Prochlorococcus* genotypes show remarkably different depth distributions in two oceanic regions as revealed by in situ hybridization using 16S rRNA-targeted oligonucleotides. *Microbiology* **147**: 1731-1744.
- West SA, Diggle SP, Buckling A, Gardner A, Griffin AS (2007). The Social Lives of Microbes. *Annual Review of Ecology, Evolution, and Systematics* **38**: 53-77.
- Westberry T, Behrenfeld MJ, Siegel DA, Boss E (2008). Carbon-based primary productivity modeling with vertically resolved photoacclimation. *Global Biogeochemical Cycles* **22**: GB2024.
- Whitman WB, Coleman DC, Wiebe WJ (1998). Prokaryotes: The unseen majority. *Proceedings of the National Academy of Sciences* **95**: 6578-6583.
- Wietz M, Wemheuer B, Simon H, Giebel H-A, Seibt MA, Daniel R *et al* (2015). Bacterial community dynamics during polysaccharide degradation at contrasting sites in the Southern and Atlantic Oceans. *Environmental Microbiology* **17**: 3822-3831.
- Wunsch C (2002). What Is the Thermohaline Circulation? *Science* **298**: 1179-1181.

References

- Xing P, Hahnke RL, Unfried F, Markert S, Huang S, Barbeyron T *et al* (2015). Niches of two polysaccharide-degrading *Polaribacter* isolates from the North Sea during a spring diatom bloom. *The ISME Journal* **9**: 1410-1422.
- Yan S, Yu M, Wang Y, Shen C, Zhang X-H (2011). *Catenovulum agarivorans* gen. nov., sp. nov., a peritrichously flagellated, chain-forming, agar-hydrolysing gammaproteobacterium from seawater. *International Journal of Systematic and Evolutionary Microbiology* **61**: 2866-2873.
- Yang S-J, Kang I, Cho J-C (2016). Expansion of Cultured Bacterial Diversity by Large-Scale Dilution-to-Extinction Culturing from a Single Seawater Sample. *Microbial ecology* **71**: 29-43.
- Yilmaz P, Iversen MH, Hankeln W, Kottmann R, Quast C, Glöckner FO (2012). Ecological structuring of bacterial and archaeal taxa in surface ocean waters. *FEMS Microbiology Ecology* **81**: 373-385.
- Zhang R, Liu B, Lau SC, Ki JS, Qian PY (2007). Particle-attached and free-living bacterial communities in a contrasting marine environment: Victoria Harbor, Hong Kong. *FEMS Microbiology Ecology* **61**: 496-508.
- Zielinski O, Henkel R, Voff D, Ferdelman TG (2017). Physical oceanography during SONNE cruise SO245 (UltraPac). PANGAEA.
- Zinger L, Amaral-Zettler LA, Fuhrman JA, Horner-Devine MC, Huse SM, Welch DBM *et al* (2011). Global Patterns of Bacterial Beta-Diversity in Seafloor and Seawater Ecosystems. *PLoS ONE* **6**: e24570.
- Zubkov MV, Sleigh MA, Burkill PH, Leakey RJG (2000). Picoplankton community structure on the Atlantic Meridional Transect: a comparison between seasons. *Progress in Oceanography* **45**: 369-386.